VOLUME 32 | SUPPLEMENT 2 | MARCH 2019

MODERN PATHOLOGY

USCAP 2019

ABSTRACTS

GYNECOLOGIC AND OBSTETRIC PATHOLOGY (993-1161)

USCAP 108TH ANNUAL MEETING

UNLOCKING YOUR INGENUITY

MARCH 16-21, 2019

National Harbor, Maryland
Gaylord National Resort & Convention Center

Published by
SPRINGER NATURE
www.ModernPathology.org

USCAP Creating a Better Pathologist
AN OFFICIAL JOURNAL OF THE UNITED STATES AND CANADIAN ACADEMY OF PATHOLOGY

EDUCATION COMMITTEE

Jason L. Hornick, Chair
Rhonda K. Yantiss, Chair, Abstract Review Board and Assignment Committee
Laura W. Lamps, Chair, CME Subcommittee
Steven D. Billings, Interactive Microscopy Subcommittee
Shree G. Sharma, Informatics Subcommittee
Raja R. Seethala, Short Course Coordinator
Ilan Weinreb, Subcommittee for Unique Live Course Offerings
David B. Kaminsky (Ex-Officio)
Aleodor (Doru) Andea
Zubair Baloch
Olca Basturk
Gregory R. Bean, Pathologist-in-Training
Daniel J. Brat
Ashley M. Cimino-Mathews
James R. Cook
Sarah M. Dry
William C. Faquin
Carol F. Farver
Yuri Fedoriw
Meera R. Hameed
Michelle S. Hirsch
Lakshmi Priya Kunju
Anna Marie Mulligan
Rish Pai
Vinita Parkash
Anil Parwani
Deepa Patil
Kwun Wah Wen, Pathologist-in-Training

ABSTRACT REVIEW BOARD

Benjamin Adam
Michelle Afkhami
Narasimhan (Narsi) Agaram
Rouba Ali-Fehmi
Ghassan Allo
Isabel Alvarado-Cabrero
Christina Arnold
Rohit Bhargava
Justin Bishop
Jennifer Boland
Elena Brachtel
Marilyn Bui
Shelley Caltharp
Joanna Chan
Jennifer Chapman
Hui Chen
Yingbei Chen
Benjamin Chen
Rebecca Chernock
Beth Clark
James Conner
Alejandro Contreras
Claudiu Cotta
Timothy D'Alfonso
Farbod Darvishian
Jessica Davis
Heather Dawson
Elizabeth Demicco
Suzanne Dintzis
Michelle Downes
Daniel Dye
Andrew Evans
Michael Feely
Dennis Firchau
Larissa Furtado
Anthony Gill
Ryan Gill
Paula Ginter
Tamara Giorgadze
Raul Gonzalez
Purva Gopal
Anuradha Gopalan
Jennifer Gordetsky
Rondell Graham
Alejandro Gru
Nilesh Gupta
Mamta Gupta
Krisztina Hanley
Douglas Hartman
Yael Heher
Walter Henricks
John Higgins
Mai Hoang
Mojgan Hosseini
Aaron Huber
Peter Illei
Doina Ivan
Wei Jiang
Vickie Jo
Kirk Jones
Neerja Kambham
Chiah Sui (Sunny) Kao
Dipti Karamchandani
Darcy Kerr
Ashraf Khan
Rebecca King
Michael Kluk
Kristine Konopka
Gregor Krings
Asangi Kumarapeli
Alvaro Laga
Cheng-Han Lee
Zaibo Li
Haiyan Liu
Xiuli Liu
Yen-Chun Liu
Tamara Lotan
Anthony Magliocco
Kruti Maniar
Jonathan Marotti
Emily Mason
Jerri McLemore
Bruce McManus
David Meredith
Anne Mills
Neda Moatamed
Sara Monaco
Atis Muehlenbachs
Bita Naini
Dianna Ng
Tony Ng
Ericka Olgaard
Jacqueline Parai
Yan Peng
David Pisapia
Alexandros Polydorides
Sonam Prakash
Manju Prasad
Peter Pytel
Joseph Rabban
Stanley Radio
Emad Rakha
Preetha Ramalingam
Priya Rao
Robyn Reed
Michelle Reid
Natasha Rekhtman
Michael Rivera
Michael Roh
Andres Roma
Avi Rosenberg
Esther (Diana) Rossi
Peter Sadow
Safia Salaria
Steven Salvatore
Souzan Sanati
Sandro Santagata
Anjali Saqi
Frank Schneider
Jeanne Shen
Jiaqi Shi
Wun-Ju Shieh
Gabriel Sica
Deepika Sirohi
Kalliopi Siziopikou
Lauren Smith
Sara Szabo
Julie Teruya-Feldstein
Gaetano Thiene
Khin Thway
Rashmi Tondon
Jose Torrealba
Evi Vakiani
Christopher VandenBussche
Sonal Varma
Endi Wang
Christopher Weber
Olga Weinberg
Sara Wobker
Mina Xu
Shaofeng Yan
Anjana Yeldandi
Akihiko Yoshida
Gloria Young
Minghao Zhong
Yaolin Zhou
Hongfa Zhu
Debra Zynger

To cite abstracts in this publication, please use the following format: **Author A, Author B, Author C, et al. Abstract title (abs#). In "File Title."** ***Modern Pathology*** **2019; 32 (suppl 2): page#**

993 SOX2 and Claudin-4 Are Useful Marker for Differentiating the Undifferentiated Uterine Carcinoma From the Recently Recognized SMARCA4 (BRG1)-Deficient Malignant Rhabdoid Tumor of Uterus

Nfn Aakash[1], Bihong Zhao[2], Hui Zhu[1], Jamie Buryanek[1], Jianmin Ding[1], Qigang Sun[3], Songlin Zhang[4]
[1]The University of Texas Health Science Center at Houston, Houston, TX, [2]UTHealth, McGovern Medical School, Houston, TX, [3]UT Health Science Center at Houston, Houston, TX, [4]The University of Texas at Houston, Houston, TX

Disclosures: Nfn Aakash: None; Bihong Zhao: None; Hui Zhu: None; Jamie Buryanek: None; Jianmin Ding: None; Qigang Sun: None; Songlin Zhang: None

Background: Small cell carcinoma of ovary of hypercalcemia type (SCCOHT) is characterized by germline or somatic mutation in *SMACAR4 (BRG1)*, and SCCOHT is now considered as a mesenchymal malignant tumor with rhabdoid morphology. Recently, SMARCA4-deficient undifferentiated uterine sarcoma (malignant rhabdoid tumor of uterus, MRTU) has been recognized as a distinct entity that shows histomorphologic similarity to uterine undifferentiated carcinoma. Distinguishing SMACAR4 and/or SMARCB1(INI1)-deficient tumor from undifferentiated and dedifferentiated endometrial carcinoma is important for identifying the most appropriate treatment strategy for individual patient.

Design: A large panel of antibodies for immunohistochemistry was performed on 4 cases including one SCCOHT, one recently encountered MRTU, and 2 uterine undifferentiated carcinomas. The antibodies included AE1/AE3, pankeratin, CAM5.2, EMA, PAX-8, SALL4, OCT4, SOX2, Nanog, CD44, INI1, BRG1, claudin-4, EZH2 and MSI panels (MSH2, MSH6, MLH1 and PMS2).

Results: The 2 undifferentiated uterine carcinomas showed intact INI1 and BRG1, and both SCCOHT and MRTU cases had intact INI1 but complete BRG1 loss. All 4 tumors were positive for SALL4, a commonly used marker for germ cell tumor and have intact MSI expression. The undifferentiated uterine carcinomas were focally positive for caludin-4, but both SCCOHT and MRTU were negative for claudin-4. SOX2 was strongly positive in the 2 undifferentiated uterine carcinomas (Figure 1) and complete negative for SCCOHT and MRTU (Figure 2). EZH2, Enhancer of Zeste Homologue 2, was highly expressed by all 4 tumors. All other tested antibodies showed no significant difference between undifferentiated uterine carcinoma and SCCOHT and MRTU.

Figure 1 - 993

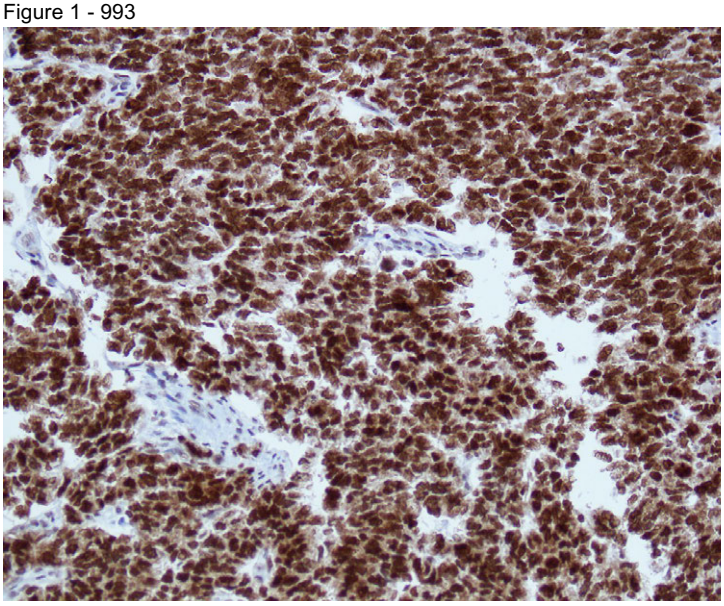

Figure 2 - 993

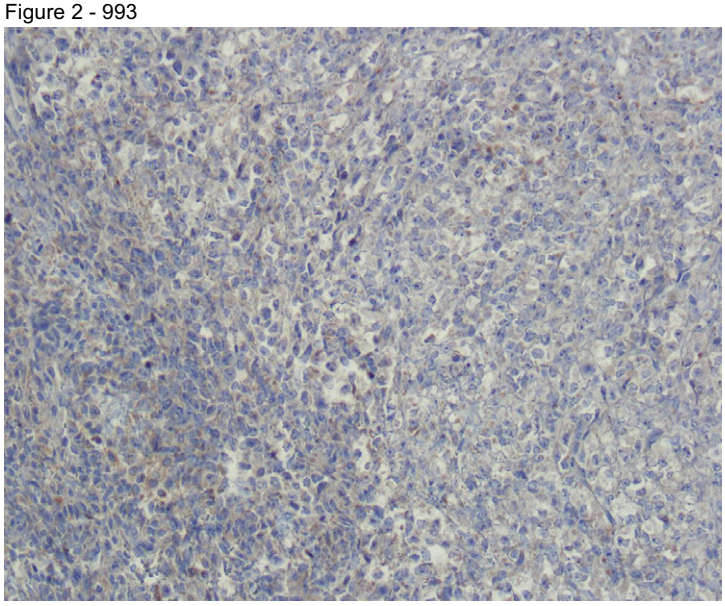

Conclusions: SMARCAR4 loss is the characteristic feature for SCCOHT and the recently recognized MRTU. SCCOHT has a very aggressive clinical behavior, and MRTU has similar poor prognosis as SCCOHT based on the very limited current knowledge (only few proved cases). Our study showed the useful value of SOX2 and claudin-4 in differentiating undifferentiated uterine carcinoma from SCCOHT and MRTU. Also, the high EZH2 expression in these tumors may be useful information for searching the targeted chemotherapy.

994 Claudin-4, INI1 and SMARCA4 Expression in Anaplastic Carcinomas Arising in Mucinous Tumors of the Ovary

Kristine Albin[1], Melinda Lerwill[1], Marina Kem[1], Robert Young[2], Mari Mino-Kenudson[1], Esther Oliva[1]
[1]Massachusetts General Hospital, Boston, MA, [2]Harvard Medical School, Boston, MA

Disclosures: Kristine Albin: None; Melinda Lerwill: None; Marina Kem: None; Robert Young: None; Mari Mino-Kenudson: *Consultant*, Merrimack Pharmaceuticals; *Consultant*, H3 Biomedicine; Esther Oliva: None

Background: Anaplastic carcinoma arising in mucinous tumors of the ovary (AC-MTO) is an uncommon tumor showing a varied histopathologic spectrum including rhabdoid, sarcomatoid and pleomorphic morphologies. It has previously been shown that some sarcomas and carcinomas with rhabdoid morphology show inactivation of the SWI/SNF (switch/sucrose non-fermentable) chromatin remodeling complex, which has been associated with poor outcomes. Given the rhabdoid morphology of some AC-MTOs, we aimed to explore whether this subset could be associated with inactivation of any of the SWI/SNF complex components, specifically SMARCB1 (INI1) and SMARCA4 (BRG1). Additionally, claudin-4, a tight junction associated protein, is considered a marker for epithelial differentiation. While its expression has been shown to be lost in many sarcomatoid carcinomas of multiple organs, a recent study has reported retained expression of claudin-4 in most SWI/SNF complex-deficient undifferentiated carcinomas. Given the sarcomatoid and pleomorphic morphology of some AC-MTOs, further characterization with claudin-4 in these tumors may provide insights regarding the nature of these components.

Design: Immunohistochemistry for SMARCB1, SMARCA4 and claudin-4 was performed on 13 AC-MTOs (5 pleomorphic, 4 rhabdoid and 4 sarcomatoid) and one sarcoma-like mural nodule.

Results: Loss of claudin-4 expression was observed in 7 of 13 tumors (54%) including 1/4 rhabdoid, 2/5 pleomorphic and 4/4 sarcomatoid, with one sarcomatoid tumor showing focal loss. Additionally, claudin-4 membranous staining was observed in the mucinous component in all tumors (13/13). SMARCB1 expression was lost in 1 of 13 tumors (8%) and showed rhabdoid morphology, while SMARCA4 expression was retained in all. The sarcoma-like mural nodule also showed loss of claudin-4 and retained expression of SMARCA4 and SMARCB1.

Conclusions: The marked loss of expression of claudin-4 seen in the sarcomatoid and pleomorphic components of these tumors with retained expression in the mucinous component, is a novel finding not previously described. Loss of claudin-4 expression in this study may indicate an epithelial to mesenchymal transition of these tumors from carcinoma to sarcoma. The loss of INI1 in one tumor with rhabdoid morphology is also a novel finding, although its association with prognosis requires further evaluation.

995 Expression of SMAD4 is Retained in Gynecologic Neoplasms

Sarah Alghamdi[1], Andre Pinto[2], Khaled Algashaamy[3]
[1]University of Miami/Jackson Memorial Hospital, Miami, FL, [2]University of Miami, Miami Beach, FL, [3]Miami, FL

Disclosures: Sarah Alghamdi: None; Andre Pinto: None; Khaled Algashaamy: None

Background: *SMAD4* (*DPC4*) is a mediator of the transforming growth factor-beta (TGF-?)/SMAD4 signaling pathway, which is responsible for multiple cellular functions including tumorigenesis and cancer progression. Mutations in SMAD4 although not specific, are seen in approximately 55% of pancreatic adenocarcinomas, and to a lesser extent, in colorectal and lung carcinomas. A few studies have explored the value of immunohistochemistry (IHC) for SMAD4 in gynecological neoplasms (mainly in the ovary), and have shown retained expression of this marker. However, literature is sparse when it comes to other sites such as endometrium and cervix, as well as in benign ovarian mucinous neoplasms. The aim of this study is to assess the expression of SMAD4 in various gynecologic tumors.

Design: We retrospectively selected primary tumors of endometrial, ovarian and cervical origin. The cases were chosen in order to obtain a spectrum of neoplasms having mucinous differentiation. Few cases of metastatic tumors involving the ovary were also included. IHC for SMAD4 was performed using whole tissue sections, and designated as positive (normal; retained) or negative (abnormal; lost).

Results: A total of 85 cases were retrieved. Ovarian tumors included 13 primary mucinous adenocarcinomas, 9 mucinous borderline tumors (8 of intestinal and 1 of endocervical types), 19 mucinous cystadenomas, 1 Brenner tumor and 6 metastatic adenocarcinomas (3 of which were of pancreatobiliary origin, and the remainder of unknown origin). Endometrial tumors corresponded to 16 endometrioid adenocarcinomas with mucinous differentiation and 13 mucinous adenocarcinomas. Finally, cervical tumors consisted of 8 cases of invasive endocervical adenocarcinomas (7 of usual type and 1 of gastric type). SMAD4 IHC showed retained (positive) nuclear expression in almost all primary gynecological cases (78/79), with the exception of 1 gastric-type cervical adenocarcinoma. Of the 6 metastatic cases, 4 showed loss of nuclear expression (4/6), 3 of which being of pancreatobiliary origin.

Conclusions: Retained nuclear expression of SMAD4 was seen in 98.7% of primary gynecologic neoplasms in our study, corresponding to tumors arising from uterine cervix, endometrium and ovary. As metastatic carcinomas can occasionally simulate primary tumors, these results can be of utility when dealing with mucinous lesions on which metastatic origin is suspected. Abnormal (loss of) SMAD4 expression virtually excludes a primary gynecologic neoplasm.

996 Does the Measurement of Circumferential Extent (Width) Have Prognostic Significance in Early Cervical Carcinoma?

Hussein Alnajar[1], Anna-Lee Clarke[2], William Watkin[3]
[1]University of Chicago (NorthShore) Pathology, Evanston, IL, [2]University of Chicago (Evanston-Northshore), Evanston, IL, [3]NorthShore University HealthSystem, Evanston, IL

Disclosures: Hussein Alnajar: None; Anna-Lee Clarke: None; William Watkin: None

Background: In patients presumed to have clinically low stage cervical carcinoma, treatment options depend on accurate pathological assessment of depth of stromal invasion(DI) and horizontal extent(HE) of tumor. In addition to the standard measurements of DI&HE, the most recent revision of the CAP protocol for reporting cervical cancer requires the assessment of circumferential extent /width(CE). If the tumor involves 1 block, the circumferential extent(width) will be 2.5 mm to 3 mm(thickness of 1 block). When more than 1 block is involved, it is the product of the number of consecutive blocks with tumor and thickness of a block. In this study, we evaluate whether the CE measurement adds prognostic value to the standard staging measurements(DI, HE).

Design: Patients with invasive cervical cancer on cervical LEEP/conization or hysterectomy samples between 2010 and 2018 were identified from the pathology files.DI, HE and T stage were gleaned from the pathology reports. Slides were reviewed to determine CE, measured by multiplying the number of consecutive slides involved by both 2.5 mm and 3 mm. Data was analyzed using Pearson correlation coefficient. Final pathological stage and residual disease status was determined in patients who had subsequent procedures(Table1).

Results: 40 patients with slides available for review were identified. The mean age was 45(range 27-69). 26(65%) had squamous cell carcinoma,12(30%) adenocarcinoma and 2(5%) adenosquamous carcinoma. AJCC staging:55% stage pT1a, 37.5% stage pT1b and 7.5% with higher stages. 8 cases(20%) had a gross lesion(in these cases the measured circumference was more than the gross measurement). 18 cases had a follow-up procedure, conization or hysterectomy. 6 had residual disease. All 6 had positive endocervical margins.CE was positively correlated with both DI&HE(fig.1) using either the 2.5 or 3 mm estimate(p=0.01). CE also correlated T stage although there were 2 outliers(fig.2). There was no correlation between CE and the presence of residual disease in follow-up specimens. The only significant predictor of residual disease in a subsequent procedure was positive margins.

Case number	Age	Procedure	Diagnosis	Gross lesion	Subsequent procedure	Residual disease
1	55	Conization	Adeno	No	Hysterectomy	Yes
2	45	Conization	SCC	Yes	Hysterectomy	No
3	50	Conization	SCC	No	Hysterectomy	No
4	28	Conization	Adeno	No	Hysterectomy	Yes
5	52	Conization	SCC	No	Hysterectomy	Yes
6	47	Hysterectomy	Adeno	No	No	N/A
7	38	Hysterectomy	Adeno	No	No	N/A
8	42	Conization	Adeno	No	Hysterectomy	No
9	33	Conization	Adeno	No	No	N/A
10	37	Conization	SCC	No	Hysterectomy	No
11	60	Hysterectomy	SCC	Yes	No	N/A
12	63	Conization	SCC	No	Hysterectomy	No
13	29	Conization	SCC	No	No	N/A
14	36	Hysterectomy	SCC	Yes	No	N/A
15	50	LEEP	SCC	No	Hysterectomy	No
16	37	LEEP	SCC	No	Hysterectomy	No
17	45	Hysterectomy	Adeno	No	No	N/A
18	37	LEEP	SCC	No	Hysterectomy	Yes
19	40	LEEP	SCC	No	Conization	Yes
20	42	LEEP	SCC	No	LEEP	No
21	39	Hysterectomy	Adenosquamous	Yes	No	N/A
22	34	Conization	SCC	No	No	N/A
23	48	Hysterectomy	SCC	No	No	N/A
24	53	Hysterectomy	Adeno	No	No	N/A
25	63	Hysterectomy	Adeno	Yes	No	N/A
26	30	Conization	SCC	No	Conization	No
27	36	Hysterectomy	SCC	No	No	N/A
28	67	LEEP	SCC	No	No	N/A
29	65	Hysterectomy	Adeno	Yes	No	N/A
30	69	Hysterectomy	SCC	No	No	N/A
31	44	Hysterectomy	Adeno	No	No	N/A
32	54	Conization	Adenosquamous	No	Hysterectomy	Yes
33	59	Hysterectomy	SCC	No	No	N/A
34	43	Hysterectomy	SCC	Yes	No	N/A
35	49	Hysterectomy	SCC	Yes	No	N/A
36	39	Hysterectomy	Adeno	No	No	N/A
37	29	Conization	SCC	No	Conization	No
38	55	LEEP	SCC	No	Hysterectomy	No
39	36	Hysterectomy	SCC	No	No	N/A
40	27	LEEP	SCC	No	LEEP	No

Figure 1 - 996

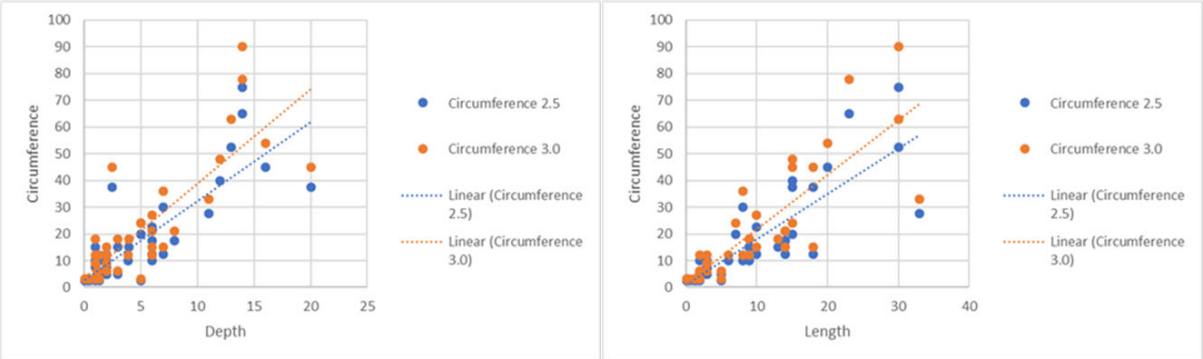

Figure 2 - 996

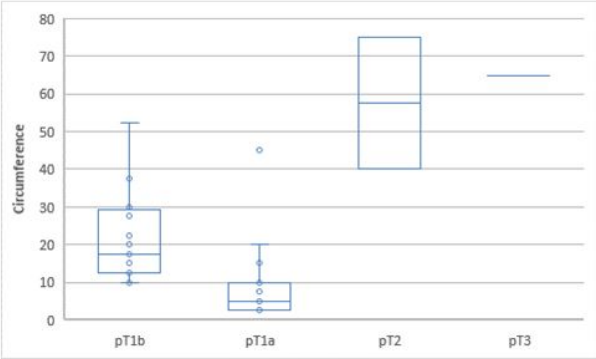

Conclusions: In our study, CE correlated with standard staging parameters of DI&HE and provided no additional prognostic information. Positive margins in the LEEP/cone were the only significant predictor of residual disease in a subsequent procedure. Further studies with larger number of patients with long term follow-up will be needed to assess the importance of the CE measurement.

997 Malignant Melanoma of the Vulva: A Clinicopathologic Review and Survival Outcomes Analysis

Isabel Alvarado-Cabrero[1], Maria Delia Perez Montiel[2], Denisse Ramírez-González[3], Rafael Estevez-Castro[4], Raquel Valencia-Cedillo[5]

[1]Mexican Oncology Hospital IMSS, Mexico, MEX, Mexico, [2]Mexico City, DF, Mexico, [3]Hospital de Especialidades, Centro Médico Nacional, IMSS, Mexico City, DF, Mexico, [4]Laboratorio de Patologia Dra. Rosario Castro, Santiago, Dominican Republic, [5]Mexican Oncology Hospital IMSS, Cd Mexico, MEX, Mexico

Disclosures: Isabel Alvarado-Cabrero: None; Maria Delia Perez Montiel: None; Denisse Ramírez-González: None; Rafael Estevez-Castro: None; Raquel Valencia-Cedillo: None

Background: Malignant Melanoma of the Vulva (MMV) is an uncommon tumor representing <1% of all female genital tract malignancies.

Design: We performed a clinicopathological review of 226 cases to identify potential clinical and/or morphologic predictors of outcome. Retrospective review of all cases of MMV were identified by an inpatient database during the period 1999-2017 at two Oncology Centers. We reviewed the clinical and histologic characteristics of all cases and determined associations between these parameters and survival

Results: We performed a clinicopathological review of 226 cases to identify potential clinical and/or morphologic predictors of outcome. Retrospective review of all cases of MMV were identified by an inpatient database during the period 1999-2017 at two Oncology Centers. We reviewed the clinical and histologic characteristics of all cases and determined associations between these parameters and survival.

Median age was 71 years (55 to 88). The presenting symptoms included mass (82%), bleeding (36%), pain or discomfort (22%). Median diameter of tumor was 3.8 cm (1 to 6.5 cm). 145 cases represented nodular melanoma (64%) while superficial spreading comprised 81 cases (36%). Mean Breslow thickness was 3.9 mm (1 to 12 mm), mean number of mitoses/mm^2 was 4 (1-10). Ulceration and lymphovascular invasion were seen in 59% and 56% tumors, respectively. Using 8th edition AJCC staging system, 52 patients were stage I, 117 stage II, 49 stage III, and 8 patients were stage IV.

176 patients had radical vulvectomy with lymph node dissection, 8 had biopsy and palliative treatment, and the remaining 42 patients had local excision only.

The median disease-free survival was 10 months and the 5-year overall survival rate was 45%. Tumor ulceration, greater tumor thickness, higher mitotic rate, lymphovascular invasion, positive lymph nodes and surgical staging were the most important prognostic factors.

Conclusions: In this series, the survival rate is poor as the lesions occurred in elderly women and the melanomas were thick at presentation. MMV had a high tendency towards regional and distant recurrences

998 Malignant Uterine PEComas: A Molecular Analysis of 8 Cases by Next-Generation Sequencing

William Anderson[1], Michelle Hirsch[2], Fei Dong[2], Marisa Nucci[1]
[1]Brigham and Women's Hospital, Harvard Medical School, Boston, MA, [2]Brigham and Women's Hospital, Boston, MA

Disclosures: William Anderson: None; Michelle Hirsch: None; Fei Dong: None; Marisa Nucci: None

Background: Perivascular epithelioid cell tumors (PEComas) are a distinctive group of mesenchymal neoplasms that demonstrate both smooth muscle and melanocytic differentiation. Relatively few genetic events are recognized in uterine PEComas, including inactivation of *TSC1/TSC2* and rearrangements of *TFE3* and *RAD51B* that were recently described in tumors of varying biologic potential. In a proportion of uterine cases, oncogenic drivers have not been identified. In uterine leiomyosarcoma (ULMS), a tumor which shows significant overlap with PEComas, alternative lengthening of telomeres (ALT) was recently identified through *ATRX* mutation. We therefore sought to establish whether similar mechanisms are active in a series of malignant PEComas, by more completely characterizing their mutational profile using next-generation sequencing (NGS).

Design: 8 malignant uterine PEComas with available material were identified from the files at our institution from 2013-2018 and the diagnoses were confirmed based on existing criteria. A targeted NGS panel including the coding regions of 447 genes was performed on each case to identify underlying molecular events.

Results: The mean patient age was 57 (ra: 37–74) years. None had a history of tuberous sclerosis complex. Histologic features of malignancy included large size (mean: 8.6 cm; ra: 4.5-12.5 cm), high-grade atypia (8/8), increased mitotic activity (mean: 138 per 50 high-power fields), necrosis (7/8), and lymphovascular invasion (4/8). Molecular testing revealed inactivating *TP53* (5/8) and *ATRX* (5/8) mutations, frequently occurring together (4/8), to be the most common events. A subset showed inactivation of *TSC1/TSC2* (3/8). Additional genes showing recurrent copy loss included *RB1* and *CDKN2A*. In cases with available material, *ATRX* and *TP53* alterations were found to correlate with immunohistochemistry: *ATRX* showed loss of nuclear expression (1/1) while p53 was diffusely positive/mutated (2/2).

Clinical follow-up was available for all cases and ranged from 5 to 93 (median: 25) months. All except one patient developed metastases with the most common site being lung (4/7). The majority had received mTOR inhibitor therapy (7/8). Three patients died of disease, while the remaining five were all alive with disease.

Figure 1 - 998

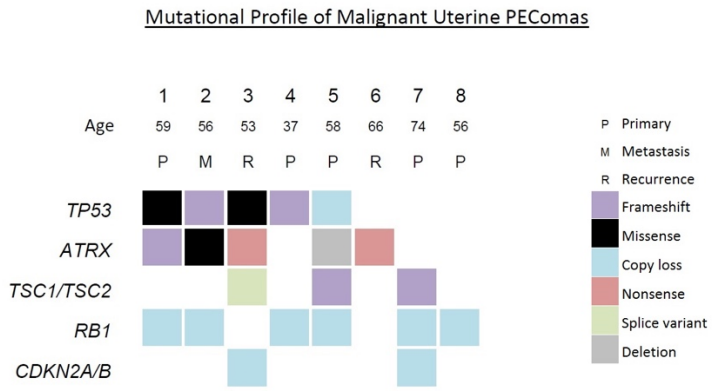

Conclusions: This study has expanded the spectrum of molecular events identified in malignant uterine PEComas. The finding of recurrent *ATRX* mutations is similar to recent studies of ULMS and supports a shared pathobiology including the importance of ALT.

999 Immunophenotypic Classification of Endocervical Adenocarcinoma in situ Based on Comprehensive Immunohistochemical Markers: Gastric-Type, Gastrointestinal-Type, Intestinal-Type, and Müllerian-Type

Shiho Asaka[1], Tomoyuki Nakajima[2], Takeshi Uehara[3], Hiroyoshi Ota[4]
[1]Johns Hopkins University School of Medicine, Baltimore, MD, [2]Shinshu University Hospital, Matsumoto, Japan, [3]Shinshu University School of Medicine, Matsumoto, Japan, [4]Shinshu University School of Health Sciences, Matsumoto, Japan

Disclosures: Shiho Asaka: None; Tomoyuki Nakajima: None; Takeshi Uehara: None; Hiroyoshi Ota: None

Background: As per the International Endocervical Adenocarcinoma Criteria and Classification (IECC) 2017, the three major subtypes of invasive endocervical adenocarcinoma are usual, gastric, and intestinal types. However, their precursor lesions have not been fully described yet. We investigated the histopathology and immunophenotype of, and human papillomavirus (HPV) infection in, endocervical adenocarcinoma in situ (AIS) and lobular endocervical glandular hyperplasia (LEGH).

Design: AIS, LEGH, and normal endocervical mucosa (NEM) samples (N=28, 23, 34, respectively) were immunohistochemically analyzed using lineage markers (claudin 18 (CLDN18), gastric cells; cadherin 17 (CDH17), intestinal cells; PAX8, Müllerian epithelial cells). High-risk HPV RNA-ISH (RNAscope system) was performed in AISs.

Results: AISs were immunophenotypically subclassified as gastric-type (G) (N=2, 7%), diffuse (≥50%) CLDN18 expression and negative or focal (<50%) CDH17 expression; gastrointestinal-type (GI) (N=3, 10%), diffuse CLDN18 and CDH17 expression; intestinal-type (I) (N=8, 29%), diffuse CDH17 expression and negative or focal (<50%) CLDN18 expression; Müllerian-type (M) (N=14, 50%), diffuse PAX8 expression and negative or focal (<50%) CLDN18 and/or CDH17 expression, and AIS, not otherwise specified (N=1, 4%). All the LEGHs were of the gastric type. NEMs were negative for neither CLDN18 nor CDH17. PAX8 was diffusely positive in one (50%) G-, two (67%) GI-, five (63%) I-, and 14 (100%) M-AISs, 15 (65%) LEGHs, and all the NEMs. Histopathologically, G-AIS shows columnar cells with pale eosinophilic cytoplasm and a variable amount of apical mucin. I-AIS shows either columnar cells with amphophilic cytoplasm and a variable amount of apical mucin or predominant goblet cells. GI-AIS shows a close admixture of G-AIS and I-AIS. M-AIS shows tumor cells with cytological features of usual-type endocervical adenocarcinoma: columnar cells with amphophilic to pale eosinophilic cytoplasm with little apical mucin and occasionally with apical cytoplasmic snouts. One (50%) G-AIS was associated with LEGH. One (33%) GI-, seven (88%) I-, and six (43%) M-AISs occurred with either LSIL/HSIL or squamous cell carcinoma. High-risk HPV was detected in three (100%) GI-, eight (100%) I-, and 13 (93%) M-AISs, but not in G-AISs.

Conclusions: AISs were classified into putative precursor types corresponding to the endocervical adenocarcinoma subtypes. Frequent PAX8 expression in each AIS type suggests a common Müllerian duct origin of AIS.

1000 Telomere Length in Precancerous Lesions of Ovarian Cancer Including p53 Signature and Incidental Serous Tubal Intraepithelial Carcinoma

Shiho Asaka[1], Christine Davis[2], Shiou-Fu Lin[3], Tian-Li Wang[2], Christopher Heaphy[1], Ie-Ming Shih[4]
[1]Johns Hopkins University School of Medicine, Baltimore, MD, [2]Johns Hopkins Medical Institutions, Baltimore, MD, [3]Taipei Medical University-Shuang Ho Hospital, New Taipei City, Taiwan, [4]Johns Hopkins Hospital, Baltimore, MD

Disclosures: Shiho Asaka: None; Christine Davis: None; Shiou-Fu Lin: None; Tian-Li Wang: None; Christopher Heaphy: None; Ie-Ming Shih: None

Background: Telomere shortening represents one of the key molecular characteristics in the development of human cancer. We have previously demonstrated that most serous tubal intraepithelial carcinomas (STIC), the precursors of ovarian high-grade serous carcinoma (HGSC), that are associated with HGSC have shorter telomeres than normal fallopian tubal epithelium (NFT) and concurrent HGSC. Since all STICs analyzed were associated with HGSC, it remains unknown if a similar telomere length abnormality occurs in “p53 signatures”, histologically unremarkable epithelial lesions with p53 overexpression that have been proposed as precursors of STIC, and incidental STICs without concurrent HGSC.

Design: In this study, we quantitatively measured telomere lengths by performing telomere-specific FISH with combined p53 immunofluorescence in 15 p53 signatures, 30 STICs without HGSC, 6 STICs with HGSC, 2 HGSCs, and 44 adjacent NFTs. We also compared these new results to our prior telomere length data in 22 STICs with HGSC and 12 HGSCs.

Results: Similar to STICs with or without concurrent cancer, the majority of p53 signatures (87%) exhibited significant telomere shortening (as compared to NFTs). Notably, among the STICs analyzed, the incidental STICs without HGSC tended to have longer telomere lengths than those with HGSC ($p = 0.0005$). Incidental STICs and p53 signatures showed significantly less cell-to-cell heterogeneity in telomere lengths compared to the STICs with concurrent HGSC ($p = 0.0009$ and $p = 0.0041$, respectively). In general, ovarian HGSCs tended to have longer telomere lengths and increased heterogeneity compared to STICs and p53 signatures. Interestingly, several HGSC cases (36%) displayed longer telomere lengths, compared to NFTs, highlighting a phenomenon which was rarely observed in STICs (10%) and not at all in the p53 signatures.

Conclusions: In conclusion, incidental STICs without concurrent ovarian HGSC are molecularly different from STICs with concurrent HGSC; these lesions are more similar to p53 signatures and, while still displaying some degree of telomere shortening, are characterized by longer telomeres and less cell-to-cell heterogeneity in telomere lengths when directly compared to STICs with concurrent HGSC.

1001 Long Interspersed Element-1 Expression in Ovarian Cancers and Precancerous Lesions Including Serous Tubal Intraepithelial Carcinomas and p53 Signatures

Shiho Asaka[1], Thomas Pisanic[2], Jeff Wang[3], Kathleen Burns[1], Tian-Li Wang[4], Ie-Ming Shih[5]
[1]Johns Hopkins University School of Medicine, Baltimore, MD, [2]Johns Hopkins University, Baltimore, MD, [3]Johns Hopkins Institute for NanoBioTechnology, Baltimore, MD, [4]Johns Hopkins Medical Institutions, Baltimore, MD, [5]Johns Hopkins Hospital, Baltimore, MD

Disclosures: Shiho Asaka: None; Thomas Pisanic: None; Jeff Wang: None; Kathleen Burns: *Primary Investigator*, EMD Biosciences; *Primary Investigator*, JUNO Therapeutics; Tian-Li Wang: None; Ie-Ming Shih: None

Background: Long interspersed element-1 (LINE-1) is a mobile DNA sequence known as a retrotransposon that uses RNA intermediates to copy itself throughout the genome. This activity is known to create genetic heterogeneity due to retrotransposon insertions in the human genome and has been implicated in the pathogenesis of various human diseases and cancer, in particular. Although increased LINE-1 expression is observed in many types of advanced cancers including ovarian high-grade serous carcinoma (HGSC), its expression has not been fully evaluated in precancerous lesions, such as serous tubal intraepithelial carcinoma (STIC) and “p53 signatures” which are histologically unremarkable fallopian tube epithelium foci exhibiting p53 overexpression.

Design: We performed immunohistochemical staining to assess LINE-1 open reading frame 1 protein (ORF1p) expression in 112 various types of ovarian cancers (45 HGSCs, 37 clear cell carcinomas, and 30 endometrioid carcinomas), 32 STICs, 12 p53 signatures, and 33 adjacent, normal-appearing fallopian tube epithelium (NFT). We also examined LINE-1 promoter methylation in seven representative STIC cases with adjacent NFTs and 12 fallopian tube samples from healthy women as controls.

Results: Overall, 75% of ovarian carcinomas exhibited overexpression of LINE-1 ORF1p, including 42 (93%) HGSCs, 24 (65%) clear cell carcinomas, and 18 (60%) endometrioid carcinomas. We found that 22 (69%) of STICs exhibited intense LINE-1 immunoreactivity compared to adjacent NFTs, with a higher prevalence among patients with concurrent HGSC (78%) than in those without (57%). Hypomethylation of the LINE-1 promoter was found in all seven STICs exhibiting LINE-1 overexpression. None of the 12 p53 signatures demonstrated significant LINE-1 expression.

Conclusions: Our results indicate that LINE-1 retrotransposons often become derepressed during the progression of putative ovarian cancer precursor lesions from the p53 signature to STIC stages and that LINE-1 remain highly expressed in carcinoma. LINE-1 expression and activity could be important in the initiation and development of ovarian cancers.

1002 Mismatch Repair Deficiency Secondary to MLH1 Methylation is Associated with Worse Recurrence-Free and Overall Survival in Endometrioid-Type Endometrial Cancer

Monica Avila[1], Bryan Fellman[2], Russell Broaddus[2]
[1]The University of Texas MD Anderson Cancer Center, Bellaire, TX, [2]The University of Texas MD Anderson Cancer Center, Houston, TX

Disclosures: Monica Avila: None; Bryan Fellman: None; Russell Broaddus: None

Background: Beyond advanced stage and grade at time of presentation, there are few reliable biomarkers that identify patients with endometrioid-type endometrial cancer at higher risk for recurrence or that impact overall survival. The detection of mismatch repair deficiency secondary to *MLH1* gene methylation and subsequent loss of MLH1 protein is one of the most common molecular events in endometrioid carcinomas, occurring in 15-20% of cases. There is conflicting evidence on the effect of mismatch repair loss on clinical outcome. The objective of this study was to determine if *MLH1* hypermethylation has an impact on recurrence and survival.

Design: Clinical and pathological variables for 615 endometrial carcinoma patients were extracted from pathology reports and the electronic medical record. Tumors were screened via immunohistochemistry for the presence of the mismatch repair proteins MLH1, MSH2, MSH6, and PMS2, with testing of *MLH1* methylation when there was loss of MLH1. Patients were then divided into 3 groups: mismatch repair deficient-probable Lynch (dMMR-L), sporadic mismatch repair deficient with *MLH1* methylation (dMMR-S), and mismatch repair intact (iMMR).

Results: 515 patients had endometrioid carcinomas, and 100 had non-endometrioid carcinomas. Of those with endometrioid-type carcinoma, 44 were dMMR-L, 86 were dMMR-S and 385 were iMMR (Table 1). Both the dMMR-S (24%) and dMMR-L (27%) groups had a higher incidence of presentation at stage III or IV compared to the iMMR patients (13%; p=0.012). Sites of recurrence (abdominal, extra-abdominal, local) did not differ between the 3 groups. Multivariate analysis showed that the dMMR-S group had significantly worse

recurrence-free [p<0.001; HR 2.58 (1.52-4.38)] and overall [p<0.001; HR 3.76(2.07-6.83)] survival (Figure 1). This effect was especially pronounced in Stage I endometrioid patients (n=355) . Mismatch repair deficiency had no impact on survival in the patients with non-endometrioid cancers.

Table 1. Clinical and Pathologic Characteristics Associated with Endometrioid Endometrial Adenocarcinoma

	MMR Intact (iMMR)		MLH1 Methylation (dMMR-S)		Probable Lynch (dMMR-L)		
Variable	**N**	**%**	**N**	**%**	**N**	**%**	**p-value**
N	385		86		44		
Mean Age (SD)	57.44 (12.08)		64.65 (9.50)		58.53 (11.47)		0.000
Mean BMI (SD)	36.08 (10.66)		35.18 (9.16)		31.14 (8.99)		0.009
Stage							0.012
I	268	82.97	57	67.06	30	68.18	
II	14	4.33	7	8.24	2	4.55	
III	33	10.22	16	18.82	10	22.73	
IV	8	2.48	5	5.88	2	4.55	
Recurrence Site							0.893
Abdomen	10	35.71	8	42.11	2	28.57	
Extra-Abdominal	11	39.29	6	31.58	2	28.57	
Local	7	25	5	26.32	3	42.86	

Figure 1 - 1002

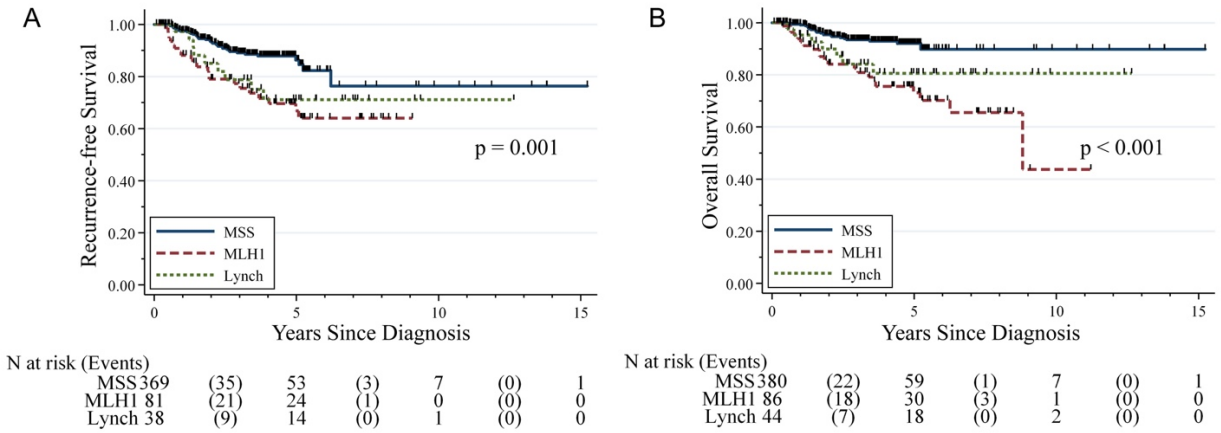

Conclusions: Patients with endometrioid carcinomas with MLH1 loss due to *MLH1* methylation more often present with advanced stage disease and have decreased recurrence-free and overall survival compared to patients with mismatch repair intact tumors. This is in sharp contrast to the effect of mismatch repair deficiency in colorectal cancer. *MLH1* methylation provides prognostic value in early stage disease and should be taken into account in stage I patients for whom adjuvant therapy is a consideration.

1003 Expression of Bile Acid Receptors TGR5 and FXR in Adnexal High Grade Serous Carcinoma: Possible New Therapeutic Targets

Ryan Bemke[1], Christopher Flynn[2]
[1]University of Wisconsin School of Medicine and Public Health, Madison, WI, [2]University of Wisconsin, Madison, WI

Disclosures: Ryan Bemke: None; Christopher Flynn: None

Background: Obesity is associated with a higher incidence of ovarian cancer, possibly by increasing circulating levels of as yet unidentified hormones. We propose bile acids (BAs) as the hormones influencing the incidence of ovarian cancer in this population.

BAs are typically recognized for their role in digestion. However, they are also hormones with roles in endocrine signaling and regulation of lipid and glucose metabolism, insulin sensitivity, and metabolic syndrome. In addition, different BAs are known to have cancer-promoting and protective roles in gastrointestinal cancers.

A potential role for BAs in gynecologic cancers has also been established. A metabolomics analysis of serum from patients with epithelial ovarian cancers identified an association with high levels of CPG, a byproduct of cholic acid (CA), a primary BA, production. In the same analysis there was also a trend for increased glycocholic acid, a conjugated form of CA. Chenodeoxycholic acid, the other primary bile acid, promotes proliferation of an endometrial cancer cell line through a transmembrane BA receptor, TGR5. Additionally, the enzymes which produce BAs as well as BA nuclear receptors (FXR, etc.), are located in granulosa cells and oocytes. Bile acids are also identified in follicular fluid.

Design: To further elucidate the potential role for BAs in ovarian cancer, 100 adnexal high grade serous carcinomas (AHGSCs) from patients who did not receive neo-adjuvant therapy were stained with antibodies for TGR5 and FXR. The slides were scored semi-quantitatively by stain intensity (negative, weak, moderate, or strong) and percent of stain-positive cells (0-100%) by visual observation. Stain results were compared to patient characteristics (disease stage, recurrence free survival, overall survival, etc.).

Results: TGR5 showed moderate to strong staining in 88/89 (99%) of tumors. FXR had moderate to strong positivity in 36/89 (40%) of tumors. Patients with moderate/strong FXR staining tumors were more likely to have disease recurrence than patients with negative/weak staining tumors (94% vs 84%) and were more likely to die from their disease (88% vs 79%).

Conclusions: The high levels of expression of these BA receptors suggests a possible role in the development of AHGSC. Additionally, as TGR5 is found in almost all tumors and FXR is strongly expressed in 40% of cases and is correlated with worse prognosis, they could be an avenue for possible new therapies in a disease with few therapeutic options and poor prognosis.

1004 Evaluation of SWI/SNF Complex Proteins in Ovarian Clear Cell Carcinoma

Jennifer Bennett[1], Ricardo Lastra[2], Esther Oliva[3]
[1]University of Chicago Medical Center, Chicago, IL, [2]University of Chicago, Chicago, IL, [3]Massachusetts General Hospital, Boston, MA

Disclosures: Jennifer Bennett: None; Ricardo Lastra: None; Esther Oliva: None

Background: The SWI/SNF complex is a group of proteins including SMARCA2, SMARCA4, SMARCB1, and ARID1A that functions in chromatin remodeling. SMARCA4 mutations have been detected in several gynecologic malignancies including dedifferentiated endometrial carcinoma and small cell carcinoma of the ovary, hypercalcemic type. Recent studies have reported SMARCA4 and SMARCA2 mutations in a small subset of ovarian clear cell carcinomas (OCCC), but studies evaluating their overall incidence and potential prognostic significance are limited.

Design: We evaluated a tissue microarray consisting of 66 OCCCs (3 cores per tumor) for SMARCA2, SMARCA4, SMARCB1, and ARID1A expression by immunohistochemistry, and compared the findings with various clinicopathologic features.

Results: Patients ranged from 31 to 82 (mean 55) years and tumors from 2 to 32 (mean 12) cm with 65% stage I, 5% II, 23% III, and 8% IV. Follow-up was available for all patients and ranged from 3 to 265 (mean 60) months with 50% alive and well, 44% dead from disease, and 6% dead from other causes. Recurrences occurred in 32% of patients.

Loss of ARID1A immunohistochemical expression was noted in 42% and loss of SMARCA2 in 14%. No loss of expression was identified for SMARCA4 or SMARCB1. Neither loss of SMARCA2 nor ARID1A expression was predictive of survival (p=0.47 and p=0.84, respectively). No associations were detected between SMARCA2 and age, size, stage, predominant growth pattern, background precursor, oxyphilic subtype, nuclear atypia, or mitotic activity. Although patients with loss of ARID1A were younger (50 vs 58 years, p=0.02), no other clinicopathologic feature reached statistical significance (Table). Sections of the metastatic carcinoma were available for 5 patients and showed 100% concordance for ARID1A, SMARCA4, and SMARCB1 expression, but 80% for SMARCA2 (expressed in the primary tumor, but lost in the metastasis).

Clinicopathologic Features and Associated P-Values		
Clinicopathologic Feature	**SMARCA2**	**ARID1A**
Age	0.43	0.02
Size	0.35	0.93
Stage (I vs II-IV)	0.48	0.30
Predominant Pattern	0.64	0.23
Endometriosis/Adenofibroma	1.00	0.25
Oxyphilic Subtype	0.68	0.76
Nuclear Atypia	0.47	0.79
Mitoses/10 High-Power Fields	0.11	0.98

Conclusions: Loss of expression for SMARCA4 and SMARCB1 by immunohistochemistry is an infrequent occurrence in OCCCs. While loss of ARID1A and SMARCA2 were detected in 42% and 14% of tumors, respectively, they do not carry any prognostic significance.

Limitations to this study include evaluation based on microarray cores, which could potentially result in a false negative due to tumor heterogeneity, as well as unknown mutational status of these proteins.

1005 Female Adnexal Tumors of Probable Wolffian Origin (FATWO): A Morphological, Immunohistochemical, and Molecular Analysis

Jennifer Bennett[1], Lauren Ritterhouse[1], Ricardo Lastra[2], Anna Pesci[3], Jordan Newell[4], Eike-Christian Burandt[5], Loes Kooreman[6], Koen Van de Vijver[7], Ana Félix[8], Gian Franco Zannoni[9], Robert Young[10], Esther Oliva[11]
[1]University of Chicago Medical Center, Chicago, IL, [2]University of Chicago, Chicago, IL, [3]IRCCS Ospedale Sacro Cuore Don Calabria, Negrar, Verona, Italy, [4]Penn State Health, Hershey, PA, [5]University Medical Center Hamburg-Eppendorf, Hamburg, Germany, [6]MUMC, Maastricht, Netherlands, [7]University Hospital Ghent, Ghent, Belgium, [8]Instituto Portugues de Oncologia de Lisboa/CEDOC, Lisboa, Portugal, [9]Catholic University of Sacred Heart, Rome, Italy, [10]Harvard Medical School, Boston, MA, [11]Massachusetts General Hospital, Boston, MA

Disclosures: Jennifer Bennett: None; Lauren Ritterhouse: None; Ricardo Lastra: None; Anna Pesci: None; Jordan Newell: None; Eik; Christian Burandt: None; Loes Kooreman: None; Koen Van de Vijver: None; Ana Félix: None; Gian Franco Zannoni: None; Robert Young: None; Esther Oliva: None

Background: FATWOs share morphological and immunohistochemical features with certain other adnexal tumors, often presenting a diagnostic challenge. Mutational analysis, although limited, has identified *KMT2D* mutations in 37% (4/11) and *STK11* in 18% (2/11).

Design: We evaluated the morphology, immunoprofile, and molecular phenotype of 13 FATWOs using a 1213 gene next generation sequencing panel.

Results: Patients ranged from 32 to 66 (mean 45) years and tumors from 1.8 to 30 (mean 10) cm. Metastatic disease at diagnosis was present in 2. Follow-up was available in 4 (range 3 to 14 years). No recurrences or tumor related deaths occurred (Table). A tubular pattern was predominant in 7, solid in 3, and sieve-like in 3. All had low-grade nuclei with rare to absent mitoses, and necrosis in 2. Both metastatic FATWOs lacked necrosis with one being tubular-dominant (70%) and the other primarily sieve-like (90%). EMA, PAX8, GATA3, and TTF1 were universally negative, pankeratin and vimentin diffusely positive, and CK7, ER, PR, CD10, WT1, calretinin, and inhibin variably expressed. p53 was wildtype.

Sufficient DNA was isolated in 6 tumors resulting in detection of 95 single nucleotide variants (SNV) in 83 genes. These mutations were missense in 77, splicing in 11, frameshift in 4, in-frame deletions in 2, and nonsense in 1. Pathogenic mutations included *STK11* (3/6), *APC* (1/6), and *MBD4* (1/6). Although *KMT2D* mutations were detected in 4 FATWOs, they have been previously classified as benign germline variants. Additional recurrent mutations are highlighted in Figure 1. Copy number variations (CNV) were noted in 3 (Figure 2), all of which had *STK11* mutations. While a *SMARCA4* splicing mutation was noted in one tumor, *KRAS, NRAS, PIK3A, PTEN, CTNNB1, TP53, BRCA1/2, FOXL2, DICER1*, and *ARID1A/1B* mutations were not detected.

Clinical Features of Patients with FATWOs

Case	Age (years)	Size (cm)	Location	Metastases at Diagnosis	Recurrences	Follow-Up (years)	Status
FWO1	38	12	Adnexal	None	None	14	NED
FWO2	41	8	Adnexal	None	N/A	N/A	LTFU
FWO3	32	N/A	Adnexal	Omentum	None	3	DOC
FWO4	48	4.5	Mesosalpinx	None	N/A	N/A	LTFU
FWO5	66	4.5	Paratubal	Sigmoid peritoneum, omentum	None	3	DOC
FWO6	32	N/A	Broad ligament	None	N/A	N/A	N/A
FWO7	37	6	Paratubal	None	N/A	N/A	LTFU
FWO8	58	8.5	Broad ligament	None	N/A	N/A	LTFU
FWO9	56	30	Broad ligament	None	None	11	NED
FWO10	48	11.3	Ovary	None	N/A	N/A	LTFU
FWO11	N/A	9	N/A	N/A	N/A	N/A	LTFU
FWO12	37	14	Paratubal	None	N/A	N/A	LTFU
FWO13	41	1.8	Paratubal	None	None	9	NED

NED=no evidence of disease; N/A=not available; LTFU=lost to follow-up; DOC=dead from other causes

Figure 1 - 1005

Recurrent Single Nucleotide Variants in FATWOs

Gene	FWO1	FWO3	FWO5	FWO7	FWO12	FWO13	Previous Studies
KMT2D							N=4
PTCH1							N=2
RNF213							NT
SPECC1							NT
STK11							N=2
SYNE1							NT

Case #

Missense
Nonsense
Frameshift
Splicing

NT=not tested

Figure 2 - 1005

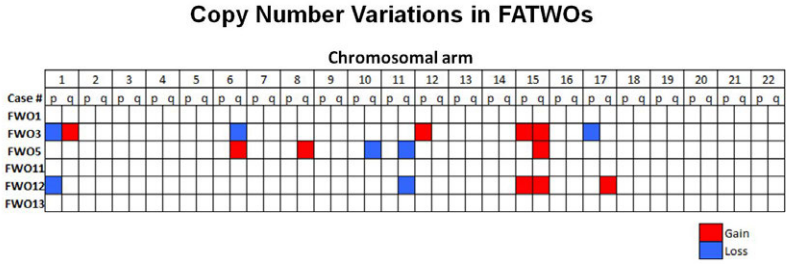

Conclusions: Overall, based upon previous studies and the data herein, recurrent mutations are uncommon in FATWOs, with *KMT2D* and *STK11* being the most frequent (54%, 8/14 and 29%, 5/17, respectively). However, FATWOs consistently lack mutations typical of morphologic mimics (sex cord stromal tumors, endometrioid/serous carcinoma) and other wolffian-derived tumors (mesonephric carcinoma). Interestingly, in this study, metastatic tumors had both CNVs and *STK11* mutations, suggesting the possibility that these alterations may be associated with aggressive behavior. Additional studies are warranted to further characterize the molecular spectrum of these unusual tumors.

1006 Type of TP53 mutation is not prognostic in high grade serous ovarian carcinoma, but presence is prognostic in endometriosis-associated carcinomas

Mary Anne Brett[1], Susan Ramus[2], James Brenton[3], Martin Kobel[1]
[1]University of Calgary, Calgary, AB, [2]University of New South Wales, Sydney, NSW, Australia, [3]University of Cambridge, Cambridge, United Kingdom

Disclosures: Mary Anne Brett: None; Susan Ramus: None; James Brenton: None; Martin Kobel: None

Background: To validate whether p53 expression status is associated with survival in women diagnosed with high-grade serous ovarian carcinoma and to explore this relationship in other ovarian carcinoma histotypes.

Design: p53 expression was assessed on 3612 high-grade serous, 742 endometrioid, and 531 clear cell ovarian carcinomas represented on tissue microarrays from 27 study sites participating in the Ovarian Tumor Tissue Analysis (OTTA) consortium using a previously validated immunohistochemical assay accurately predicting the type of *TP53* mutation. Three abnormal expression patterns, which correlate with types of *TP53* mutations (overexpression/missense, complete absence, and cytoplasmic/loss of function) and the normal (wildtype) pattern were recorded. Overall survival analyses were performed for each histotype.

Results: Type of *TP53* mutation inferred by p53 immunohistochemistry does not correlate with overall survival in high-grade serous carcinoma (p=0.94). The presence of abnormal p53 expression was significantly associated with overall survival in endometrioid and clear

cell carcinoma (p<0.0001 and p=0.0015, respectively). Abnormal, mutant-type p53 expression was present in 9.6% of ovarian endometrioid carcinomas (Fig 1.) and 11.1% of ovarian clear cell carcinomas.

Figure 1 - 1006

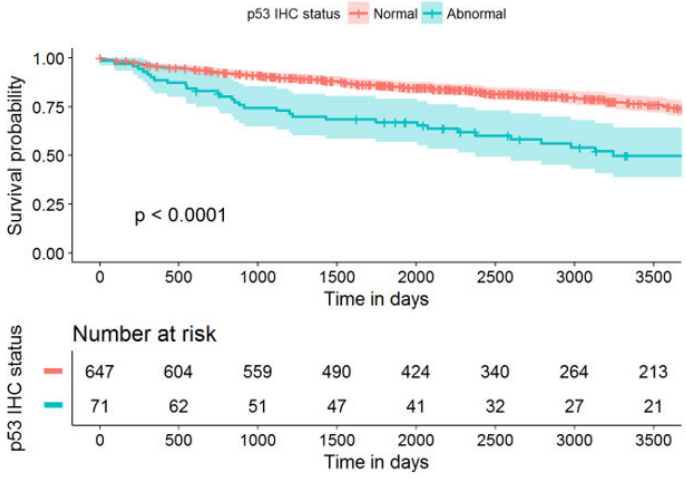

Conclusions: This study provides definitive evidence that the type of *TP53* mutation is not associated with outcome in high-grade serous carcinomas suggesting an equivalent impact of underlying *TP53* mutations. Abnormal/mutant type p53 expression in endometriosis-associated endometrioid and clear cell carcinomas is a strong poor prognostic marker, which could be used to identify patients that require additional therapy.

1007 Optimized molecular risk stratification for ovarian endometrioid carcinomas

Mary Anne Brett[1], Evan Cairns[2], Derek Chiu[3], Pauline Haag[4], David Farnell[5], Jana Pasternak[6], Marcel Grube[4], Janine Senz[2], Annette Staebler[7], Sara Brucker[6], Jessica McAlpine[8], Stefan Kommoss[4], Aline Talhouk[9], Martin Kobel[1], Michael Anglesio[2]
[1]University of Calgary, Calgary, AB, [2]University of British Columbia, Vancouver, BC, [3]BC Cancer Research Centre, Vancouver, BC, [4]Tuebingen University Hospital, Tuebingen, Germany, [5]Vancouver, BC, [6]Tuebingen University Hospital, Tübingen, Germany, [7]University of Tuebingen, Tuebingen, Germany, [8]University of British Columbia and BC Cancer Agency, Vancouver, BC, [9]University of British Columbia and British Columbia Cancer Agency, Vancouver, BC

Disclosures: Mary Anne Brett: None; Evan Cairns: None; Derek Chiu: None; Pauline Haag: None; David Farnell: None; Jana Pasternak: None; Marcel Grube: None; Janine Senz: None; Annette Staebler: None; Sara Brucker: None; Jessica McAlpine: None; Stefan Kommoss: None; Aline Talhouk: None; Martin Kobel: None; Michael Anglesio: None

Background: Endometrioid ovarian carcinoma (ENOC) accounts for greater than 10% of ovarian carcinomas and is typically associated with a favorable prognosis compared to other histotypes. Prognostication is important for patient management. Our group has previously derived a validated and clinically relevant prognostic tool, ProMisE, as a surrogate to classify the four TCGA molecular subtypes of endometrial carcinoma. Our aim was to validate the prognostic associations of ProMisE in ENOC.

Design: 218 ENOC cases from the COEUR cohort were subjected to sequencing of POLE exonuclease domain hotspot mutations, and immunohistochemistry for the four MMR proteins and p53 using tissue microarrays. Cases were assigned into four groups following the process outlined for endometrial cancers: (1) mismatch repair deficient if any of the four MMR proteins were absent (MMRd), (2) POLE exonuclease domain mutated as per sequencing (POLE), (3) p53 mutant (p53abn) or (4) p53 wild type (p53wt) based on immunohistochemistry. Kaplan-survival analysis were performed; outcomes and proportions of each class was compared to their endometrial cancer counterparts.

Results: The majority of cases were p53wt (77%), followed by MMRd (13%), p53abn (7%) and POLE mutated (3%). Compared to p53wt, p53abn cases had the highest risk of recurrence (HR=3.5, 95%, CI 1.60-6.99). The risk of recurrence was reduced for POLE exonuclease domain mutated cases (HR=0.47), and there was no difference for MMR deficient cases (HR=1.13, CI 0.41-2.50).

Conclusions: ProMisE stratification of ENOC was highly similar to their uterine carcinoma counterparts with only moderate shifts in the proportions of each class. Our data are consistent with a strong etiological and biological link between these cancers.

1008 Undifferentiated Endometrial Carcinoma Arising in the Background of High grade Endometrial Carcinoma – Proposed Update in the Definition of Dedifferentiated Endometrial Carcinoma

Aurelia Busca[1], Carlos Parra-Herran[1], Jelena Mirkovic[1]
[1]Sunnybrook Health Sciences Centre - University of Toronto, Toronto, ON

Disclosures: Aurelia Busca: None; Carlos Parra-Herran: None; Jelena Mirkovic: None

Background: Dedifferentiated endometrial adenocarcinoma (DEC) is currently defined by the coexistence of an undifferentiated carcinoma with a low-grade (LG; FIGO grade 1 or 2) endometrioid carcinoma. A few DEC with a high grade (HG) carcinoma have been mentioned in the literature, however this phenomenon is still poorly characterized and currently not recognized in the WHO classification. We aim to describe the morphologic and immunohistochemical characteristics of DEC with HG carcinoma (HG-DEC) and compare them with DEC associated with LG endometrial carcinoma (LG-DEC).

Design: DEC diagnosed between 2008 and 2018 were reviewed using strict morphologic criteria: the undifferentiated carcinoma was defined as a monotonous population of cells growing in a sheet-like pattern and showing lack of cohesion, squamous or mucinous differentiation, and spindled growth pattern. Immunohistochemistry for pankeratin, CK8/18, EMA, E-cadherin, p53, ER and MMR proteins was done.

Results: We identified a total of 13 DECs. In 8 cases (61.5%) the undifferentiated component was associated with a HG carcinoma (4 endometrioid FIGO grade 3, 2 with ambiguous features, 1 with mixed serous/endometrioid carcinoma). The remaining 5 (38.5%, control group) had a LG component (3 FIGO grade 1 and 2 FIGO grade 2). All LG-DEC and 4 of the HG-DEC (50%) were confined to the uterus (stage pT1); conversely 4 (50%) HG-DEC (50%) were stage pT2 or higher. On follow up, 2 HG-DEC died of disease, both with minor amount of undifferentiated carcinoma (10%). One additional HG-DEC had recurrence at the vaginal vault 52 days after surgery (undifferentiated component - 2% of tumor volume). There was only one recurrence in the LG-DEC group, 6 months post-surgery. The undifferentiated component in both groups showed patchy or complete loss of keratins, EMA, E-cadherin and ER staining. P53 was normal in 12/13 cases. Loss of MLH1 and PMS2 was observed in 4/8 (50%) cases in HG-DEC and 3/4 (75%) cases in LG-DEC.

Conclusions: We characterize DEC arising in HG carcinoma, a previously under-recognized phenomenon. The undifferentiated component of HG-DEC has morphologic and immunophenotypic similarities to LG-DEC, including MMR loss. However, in this small cohort HG-DEC appears to have higher prevalence of advanced stage, recurrence and mortality, independent of the amount of undifferentiated component. We propose updating the current definition of dedifferentiated carcinoma to include cases arising in the background of HG endometrial carcinoma.

1009 Prognostic Value of Grading of Primary Ovarian Mucinous Carcinoma - a Comparative Analysis of Silverberg, FIGO and WHO Systems

Aurelia Busca[1], Sharon Nofech-Mozes[1], Ekaterina Olkhov-Mitsel[2], Dina Bassiouny[1], Nadia Ismiil[1], Bojana Djordjevic[3], Carlos Parra-Herran[1]
[1]Sunnybrook Health Sciences Centre - University of Toronto, Toronto, ON, [2]Sunnybrook Health Sciences Centre, Toronto, ON, [3]University of Toronto, Scarborough, ON

Disclosures: Aurelia Busca: None; Sharon Nofech-Mozes: None; Ekaterina Olkhov-Mitsel: None; Dina Bassiouny: None; Nadia Ismiil: None; Bojana Djordjevic: None; Carlos Parra-Herran: None

Background: Grading of primary ovarian mucinous carcinoma (POMC) is not consistent among practices. Options include Silverberg, FIGO and a vague three-tier system proposed in the WHO classification (well- G1, moderate-G2, poorly differentiated-G3) which lacks clear definitions for each grade. POMC is underrepresented in studies comparing grading systems. In addition, the growth pattern (expansile vs infiltrative) is currently not taken into account in any system. Thus, we herein analyze the prognostic value of various grading methods in a well-annotated cohort of POMC.

Design: Institutional POMCs (2000-2018) were identified. Only tumors confirmed as POMC through morphology, immunohistochemistry and clinical correlation were included; those of uncertain origin, metastases, with mixed histology and only microinvasion or intraepithelial carcinoma were excluded. POMCs were graded by Silverberg and FIGO following standard criteria. Definitions for WHO grading terminology were established as follows: G1 (expansile growth only), G2 (infiltrative growth <50% tumor) and G3 (infiltrative growth ≥50% tumor). Outcome events (tumor-related death or recurrence) were recorded.

Results: Of a total of 46 POMCs, 37 (80%) were stage 1, 5 (11%) stage 2 and 4 (9%) stage 3. On follow-up (mean 52 months, range 1-190) a total of 5 patients (11%) had adverse events (3 recurrences and 4 deaths), all occurring within 2 years from surgery. There was concordance amongst three systems in 17 cases (37%), and between FIGO and Silverberg in 38 cases (82.6%). On univariate analysis stage (p=0.01, Cox proportional analysis), Silverberg grade (p=0.01), WHO grading (p=0.03) and presence of infiltrative growth (p=0.008) correlated with outcome. FIGO showed no significant correlation. Increased survival was seen in patients with Silverberg grade 1 vs 2 (p=0.001, log rank) and patients with WHO G1 and G2 vs G3 (p=0.005), with similar survival curves for WHO G1 and WHO G2 (Figure 1).

Figure 1 - 1009

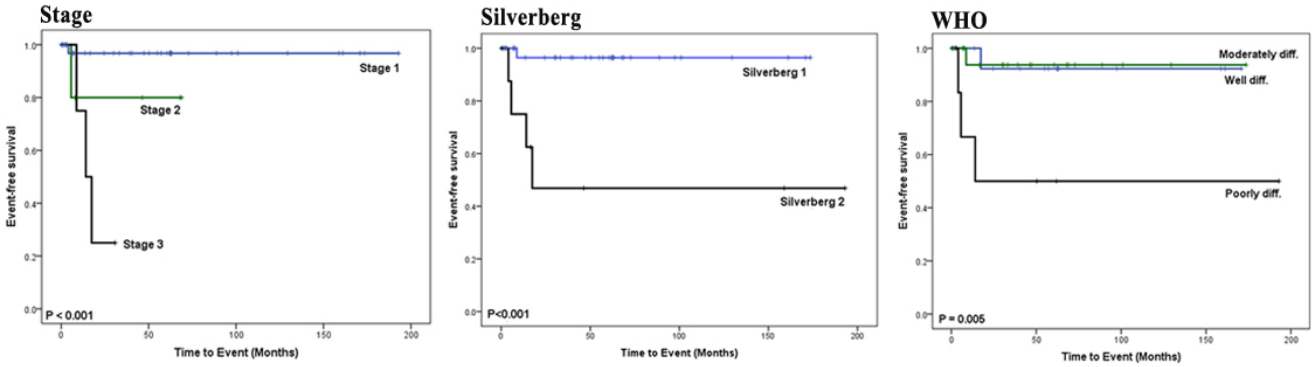

Conclusions: We propose clear definitions for the WHO grading terminology of POMC, which incorporate growth pattern and correlate with patient outcome. Furthermore, the proposed WHO system can be simplified in a two tier system consisting of low-grade (G1 and G2) and high grade (G3), which may be more appropriate for patient risk stratification. Silverberg also appears to be prognostically significant, unlike FIGO. Further evaluation of POMC grade and its relationship with other prognostic variables is warranted.

1010 MELF-Like Pattern in Myoinvasive Clear Cell and Serous Endometrial Carcinoma

Alain Cagaanan[1], Jin Xu[2], Paul Weisman[3], Stephanie McGregor[3]
[1]Madison, WI, [2]Memorial Sloan Kettering Cancer Center, New York, NY, [3]University of Wisconsin, Madison, WI

Disclosures: Alain Cagaanan: None; Jin Xu: None; Paul Weisman: None; Stephanie McGregor: None

Background: Endometrioid carcinoma can have a distinct pattern of myoinvasion known as MELF (microcystic, elongated, and fragmented) that has been associated with lymphovascular invasion (LVI) and other prognostic significance. To date these changes have not been studied extensively in other histologic types of endometrial carcinomas. We studied MELF-like histologic changes and prognostic factors in serous and clear cell endometrial carcinoma.

Design: Myoinvasive endometrial clear cell (n=9) and serous carcinoma (n=22) cases were retrieved from archives. Hematoxylin and eosin-stained slides were reviewed. Only unequivocal cases of clear cell carcinoma were chosen. Cases of serous carcinoma were confirmed by immunohistochemistry for p53, p16, and ER. The presence of a MELF-like pattern was recorded according to the presence of classic architectural features, fibromyxoid and/or lymphocytic stromal reaction, histiocytoid morphology in lymphatics, neutrophilic infiltrate/accumulation, and attenuated eosinophilic epithelium. The presence of LVI and lymph node metastasis were also recorded. Chi square analyses were used to assess for significance.

Results: A MELF-like pattern was present in 4 of 9 cases of clear cell carcinoma (44%) and in 8 of 22 cases of serous carcinoma (36%), with changes being slightly more extensive in clear cell carcinoma and more focal in serous carcinoma. In clear cell carcinoma, LVI was present in nearly all cases (8/9) irrespective of the presence of a MELF-like pattern. In serous carcinoma on the other hand, LVI was more common when a MELF-like pattern was present (8/8 with MELF-like pattern versus 2/14 without, p<0.001). Lymph node metastasis were also more frequent in cases of serous carcinoma with a MELF-like pattern but did not reach significance (3/5 versus 3/12 without, p=0.17).

Conclusions: Though MELF-pattern invasion is currently regarded as a feature of endometrioid histology, a MELF-like pattern can also be observed in myoinvasive endometrial serous and clear cell carcinomas. As in endometrioid carcinoma, the presence of a MELF-like pattern in serous carcinoma appears associated with an increased propensity for lymphatic spread. Additional study is necesary in larger series to corroborate the significance of these findings.

1011 5-Hydroxymethylcytosine (5-hmC) Is a Novel Prognostic Marker in Ovarian Clear Cell Carcinoma

David Chapel[1], Ricardo Lastra[1], Ernst Lengyel[1], Esther Oliva[2], Jennifer Bennett[3]
[1]University of Chicago, Chicago, IL, [2]Massachusetts General Hospital, Boston, MA, [3]University of Chicago Medical Center, Chicago, IL

Disclosures: David Chapel: None; Ricardo Lastra: None; Ernst Lengyel: None; Esther Oliva: None; Jennifer Bennett: None

Background: Clear cell carcinoma of the ovary is an aggressive malignancy that arises in women across a wide age range, but up to date, no reliable prognostic markers or morphologic features have been reported. 5-Hydroxymethylcytosine (5-hmC) is an epigenetic marker involved in DNA demethylation. Published studies have reported pathobiologic, diagnostic, and prognostic roles of 5-hmC in various

malignancies. We studied the potential prognostic impact of nuclear 5-hmC expression in survival in patients with ovarian clear cell (OCCC), endometrioid (OEC), and high-grade serous (HGSC) carcinomas.

Design: Tissue microarrays consisting of 69 OCCCs, 62 OECs, and 57 HGSCs were stained for 5-hmC. Nuclear 5-hmC expression was scored semi-quantitatively by two pathologists (<1%, 1-10%, 11-25%, 26-75%, and >75%), with discrepancies settled by consensus. Loss of 5-hmC was defined by staining in <10% of tumor nuclei, as previously reported. Univariate (log-rank test) and multivariate (proportional hazards regression) were performed for disease-specific survival (DSS) and progression-free survival (PFS).

Results: Eight OCCCs (12%; 2 stage IA, 1 stage II, 3 stage III, 2 stage IV), 13 OECs (21%), and 16 HGSCs (28%) showed loss of 5-hmC with good interobserver agreement (kappa = 0.70). Loss of 5-hmC was significantly associated with shorter DSS (p=0.0009), shorter PFS (p=0.0002), and extra-ovarian spread (p=0.02) in OCCC. There was no relationship between 5-hmC loss in OCCC and age at diagnosis, endometriosis, or adenofibromatous background. No association was detected between nuclear 5-hmC and DSS or PFS in OEC or HGSC. On multivariate analysis, extra-pelvic spread and 5-hmC loss were both independent predictors of shorter DSS.

Figure 1 - 1011

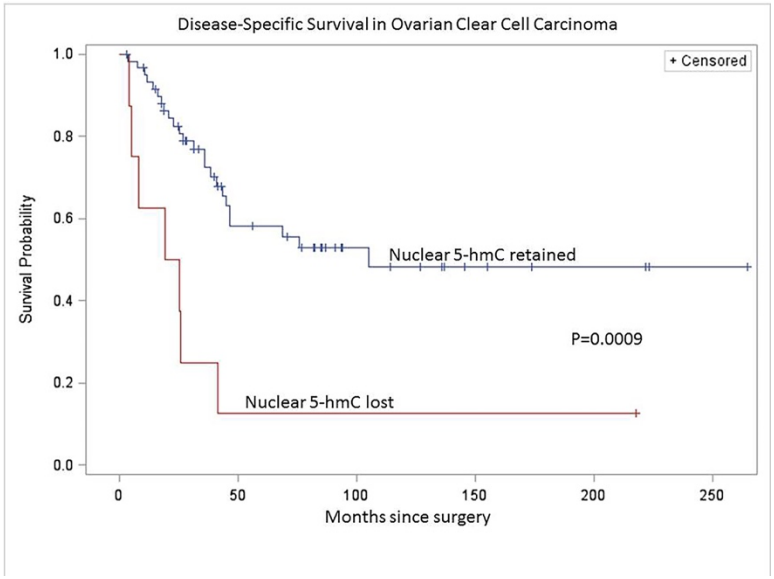

Conclusions: Our data indicate that semi-quantitative assessment of nuclear 5-hmC in OCCC stratifies patients for both DSS and PFS. Loss of 5-hmC remains an independent predictor of shorter DSS after correcting for tumor stage. As immunohistochemistry is a widely available and low-cost test, with assessment of nuclear 5-hmC staining showing good interobserver concordance herein, it potentially represents a promising biomarker. Next steps include multivariate modeling of nuclear 5-hmC alongside additional clinical and morphologic factors in OCCC, as well as application of molecular assays to more precisely characterize epigenetic alterations in OCCC.

1012 Quantitative Next-Generation Sequencing-Based Analysis Indicate Progressive Accumulation of Microsatellite Instability between Atypical Hyperplasia / Endometrial Intraepithelial Neoplasia and Paired Endometrioid Endometrial Carcinoma

David Chapel[1], Sushant Patil[1], Andrei Plagov[2], Sabah Kadri[3], Ricardo Lastra[1], Jeremy Segal[4], Lauren Ritterhouse[5]
[1]University of Chicago, Chicago, IL, [2]University of Illinois Hospitals and Health Sciences System, Chicago, IL, [3]Ann & Robert H. Lurie Children's Hospital of Chicago, Chicago, IL, [4]University of Chicago, Riverside, IL, [5]University of Chicago Medical Center, Chicago, IL

Disclosures: David Chapel: None; Sushant Patil: None; Andrei Plagov: None; Sabah Kadri: None; Ricardo Lastra: None; Jeremy Segal: None; Lauren Ritterhouse: None

Background: Atypical hyperplasia / endometrial intraepithelial neoplasia (AH/EIN) is a precursor lesion to endometrial endometrioid carcinoma (EEC), distinguished principally by the lesser architectural abnormalities in AH/EIN. Because EEC is frequently seen in women with Lynch syndrome (LS), many institutions routinely screen all EECs for LS, either by immunohistochemistry (IHC) for mismatch repair proteins (MMRPs) or by molecular testing for microsatellite instability (MSI). Although the relationship between AH/EIN and EEC is well established, studies examining molecular and clonal evolution in cases with MSI are limited.

Design: Seven paired AH/EIN and EEC samples with known MMRP deficiency by IHC were subject to a next-generation sequencing (NGS) assay (OncoPlus, 1213 genes) to detect mutations, copy number variations, MSI, and tumor mutational burden. A laboratory-developed MSI module was applied, assessing stability of 336 microsatellite loci by comparing the homopolymer length distribution to a baseline distribution for each locus. Clonal evolution of molecular alterations and MSI loci were compared between AH/EIN and paired EEC.

Results: Of the 7 EECs, 6 were deficient for MLH1 and PMS2, and 1 for MSH2 and MSH6. All 7 AH/EIN showed the same MMRP loss pattern as their paired EEC. Compared to paired EEC specimens, AH/EIN harbored on average one-third the number of mutations, across recurrently mutated genes including *PTEN*, *PIK3CA*, *ARID1A*, *CTNNB1*, *KRAS*, and *PIK3R1*. In all 7 cases, the EEC samples harbored a higher proportion of microsatellite-unstable loci (mean, 38%) compared to the paired AH/EIN sample (mean, 16%). While all 7 EEC cases were called MSI-H by NGS, only 3 AH/EIN samples met the NGS criteria for MSI-H. The majority of individual microsatellite loci showed progression of instability in the transition from AH/EIN to paired EEC.

Conclusions: This study provides evidence for increasing levels of MSI from AH/EIN to EECs and sheds light on the clonal evolution of type 1 endometrial neoplasia. We observed good concordance between AH/EIN and paired EEC at the level of MMRP IHC, despite more than twofold difference in the quantity of accrued microsatellite-unstable loci between AH/EIN-EEC pairs. These findings suggest that MMRP loss is an early neoplastic event, followed by accumulation of microsatellite changes. Attention to morphology is critical in selecting foci for NGS-based MSI testing, as errant selection of AH/EIN-dominant areas may yield a false-negative MSI-low result.

1013 BCOR Rearrangement High Grade Endometrial Stromal Sarcoma, a Potential for Misdiagnosis

Yufan Cheng[1], Xiaoyu Tu[1]
[1]*Fudan University Shanghai Cancer Center, Shanghai, China*

Disclosures: Yufan Cheng: None; Xiaoyu Tu: None

Background: Endometrial stromal sarcomas (ESS) are genetically heterogeneous uterine tumors. The most recent World Health Organization classification describes YWHAE–NUTM2 HGESS. More recently, ZC3H7B-BCOR gene fusion ESS was identified as a genetic subset of high grade ESS (HGESS). Till now, only 17 cases were reported. We herein investigate the clinicopathologic features and the differential diagnoses of this tumor.

Design: 5 cases of BCOR rearrangement HGESS were collected from consultant files of Fudan University Shanghai Cancer Center. Interphase FISH was carried out using a BCOR(Xp11.4) dual color break-apart probe. The clinical data, histologic features, immunohistochemical findings were analyzed.

Results: All of the cases occurred in adult women with a median age of 48 (range, 45–55) years. Abdominal pain and abnormal vaginal bleeding were the most common symptoms. Microscopically, they predominantly presented as tongue-like and/or intersecting myometrial invasion. Stomal myxoid matrix and/or collagen plaques were prominent in all the cases. Most displayed uniform haphazard fascicles of short spindle cells with mild to moderate nuclear atypia. Mitotic figures and necrosis are easily identified. No remarkable nuclear pleomorphism was noted. Most tumors are in rich of thick-walled small blood vessels. No prominent perivascular tumor cell whorling of conventional low-grade endometrial stromal sarcoma were seen. All tumors expressed CD10 with only limited or absent desmin, SMA and/or h-caldesmon staining. ER or PR expression was seen in 4 tumors and both marker expression was seen in 1 tumor. Diffuse cyclin D1 was present in 2 tumors. BCOR immunoreactivity was present in 4 tumors with strong staining in 3 and moderate staining in 1 respectively. Ki-67 index were from 10 to 30%. Fluorescence in situ hybridization confirmed chromosomal aberration of BCOR gene in all tumors, including 2 previously diagnosed as myxoid leiomyosarcoma, 1 as spindle cell uterine sarcoma and 1 as low-grade endometrial stromal sarcoma. Limited follow-up information revealed that 60% (3/5) patients underwent tumor recurrence, metastasis or death in one year.

Figure 1 - 1013

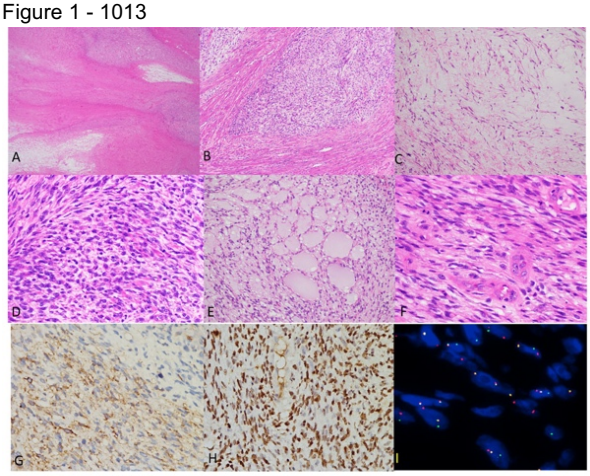

Hypercelluar and hypocellular area (A), tongue-like, infiltrative growth patterns (B), prominent myxoid stroma (C), tumor cells with haphazard fascicular architecture, moderate atypia and brisk mitoses (D), pneumonedema-like change (E), thick-walled blood vessels without perivascular whorling (F), strong and diffuse reactivity for CD10 (G) and BCOR (H). Tumor cells comprised a pair of split signals, indicating a rearrangement involving the SYT gene (I).

Conclusions: This report, as well as the prior studies, indicates that BCOR rearrangement HGESS have distinct morphological features and aggressive clinical behavior. As there are overlapping morphologic features between BCOR rearrangement HGESS and other myxoid uterine mesenchymal tumors, especially myxoid leiomyosarcoma, molecular analysis is essential for differe

1014 Multiplexed Immunoflourescence Analysis of Immune Microenvironments in Ovarian Tumors

Curtis Chin[1], Maira Campos[1], Itsushi Shintaku[2], Yunfeng Li[1], Gottfried Konecny[1], Jianyu Rao[3]
[1]David Geffen School of Medicine at UCLA, Los Angeles, CA, [2]University of California, Los Angeles, Los Angeles, CA, [3]Los Angeles, CA

Disclosures: Curtis Chin: None; Itsushi Shintaku: None; Yunfeng Li: None; Jianyu Rao: None

Background: Therapies inhibiting immune checkpoints such as PD-1/PD-L1 are approved or in development for a wide range of cancers, including ovarian cancer. Determining which patients will benefit from PD-1/PD-L1 directed therapy remains an important clinical question. Immunohistochemistry (IHC) has been a mainstay for determining level of PD-L1 expression in tumors, however multiple issues remain, including determining an appropriate PD-L1 cutoff value, and differentiating staining of tumor versus immune cells.

Recently, we studied the association between PD-L1 IHC reactivity with molecular classifications of ovarian tumors using mRNA expression with NanoString technology across a patient cohort with varying clinical and tumor histopathologic characteristics. Here we compare multiplexed immunofluorescence (MIF)-based versus traditional IHC-based PD-L1 analysis in these ovarian tumors.

Design: MIF staining and miRNA expression were performed on formalin-fixed paraffin embedded tissue across 81 patients enrolled in a Phase II trial for primary ovarian cancer (TRIO14 trial). IF staining was performed using multicolor probes for PD-L1 (SP142, Abcam), CD8 (C8/144B, Dako), and pan-keratin (AE1/3, Dako).

Results: The imaging platform demonstrated an ability to resolve, at high resolution, heterogeneous PD-L1 expression on tumor versus PD-L1 expression on lymphocytes and macrophages by signal co-localization (Figures 1-2). Preliminary analysis showed in general a strong concordance with PD-L1 expression in tumor cells measured by MIF and IHC. However, MIF allows more precise separation of the PD-L1 in tumor infiltrating lymphocytes (CD8+) and tumor cells (pan-keratin+).

Figure 1 - 1014

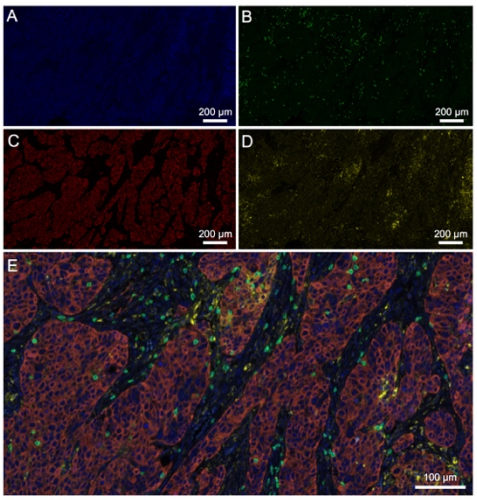

Figure 1: Multiplexed immunofluorescence for studying ovarian tumor immunoreactivity and microenvironment. Images acquired using different dye-probe conjugates for DAPI nuclear stain (A), FITC CD8 (B), Cy5 pan-keratin AE1/3 (C), and Cy3 PD-L1 (D). Overlaying images (E) demonstrates co-localization of PD-L1 with tumor epithelial cells versus tumor immune cells such as lymphocytes and macrophages.

Figure 2 - 1014

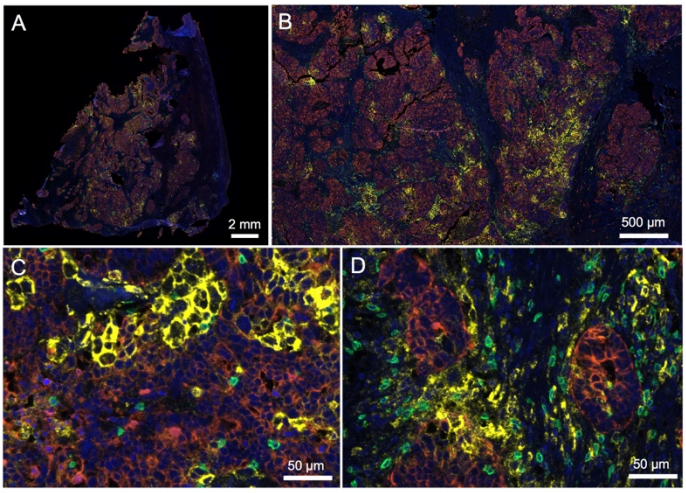

Figure 2: Multiplexed immunofluorescence of a primary ovarian carcinoma with immunoreactive transcriptional subtype. Image overlays taken at 0.57x (A, whole slide), 4x (B), and 40x (C-D), demonstrate heterogeneous PD-L1 expression across the tumor, with presence of tumor infiltrating lymphocytes, some of which express PD-L1.

Conclusions: Multiplexed IF may provide a more precise and granular level of analysis to complement molecular classification in predicting response to immunotherapy in the future.

1015 Correlating PD-L1 Expression with Transcriptional Profiles of Ovarian Tumors with Various Clinical and Histopathologic Characteristics

Curtis Chin[1], Maira Campos[1], Itsushi Shintaku[2], Gottfried Konecny[1], Jianyu Rao[3]
[1]David Geffen School of Medicine at UCLA, Los Angeles, CA, [2]University of California, Los Angeles, Los Angeles, CA, [3]Los Angeles, CA

Disclosures: Curtis Chin: None; Itsushi Shintaku: None; Jianyu Rao: None

Background: Determining which patients will benefit from PD-L1 directed therapy remains an important clinical question. In ovarian cancer, nearly all patients experience a relapse with median progression-free survival of 18 months. While no FDA-approved PD-L1 immunotherapy exists for ovarian cancer, interim results of a Phase II trial of pembrolizumab monotherapy showed modest antitumor efficacy, with an optimal PD-L1 expression combined positive score (CPS) cutoff point of 10%.

Recent genomic studies investigated whether gene expression subtypes associated with distinct tumor biology are predictive of clinical prognosis. High-grade serous ovarian carcinoma has four gene transcriptional subtypes: immunoreactive, differentiated, proliferative, and mesenchymal. When applied to well-annotated patient cohorts, the transcriptional subtypes show significant differences in overall survival, with immunoreactive subtype as most favorable.

We studied the association between PD-L1 immunohistochemistry (IHC) reactivity with the aforementioned molecular classification using mRNA expression with NanoString technology across a patient cohort with varying clinical and tumor histopathologic characteristics. Our ultimate goal will be to determine if the molecular classification combined with PD-L1 expression will allow us to better predict response to immunotherapy in the future.

Design: PD-L1 staining and miRNA expression was performed on formalin-fixed paraffin embedded tissue across 93 patients enrolled in a Phase II trial for primary ovarian cancer (TRIO14). IHC staining was performed using PD-L1 monoclonal antibody (SP142 clone, Ventana) and scored using CPS. Non-parametric statistical analysis was performed using Kruskal-Wallis and Dunn's multiple comparison test.

Results: There was higher PD-L1 expression in immunoreactive transcriptional subtype (Figs 1-2), with significant mean rank differences between immunoreactive *vs* differentiated (33.39, $p < 0.001$), *vs* mesenchymal (39.63, $p < 0.001$), but not *vs* proliferative (20.34, $p = 0.098$). IHC scoring with tumor-only expression showed similar trends. There were no significant differences across different histological types, grades, and levels of CA-125 (Table 1).

ID	PD-L1 positivity (%) Tumor cells	PD-L1 Combined Positive Score (CPS) Immune cells	Molecular subtype	Histological subtype	Histological grade	CA-125	
10006	5	10	10	IMM	papillary serous	moderately differentiated	elevated
10007	5	5	6	MES	papillary serous	not graded	elevated
10009	4	20	8	PRO	papillary serous	poorly differentiated	normal
10014	10	15	15	PRO	endometrioid	poorly differentiated	elevated
10015	1	15	8	PRO	papillary serous	poorly differentiated	elevated
10020	15	20	25	PRO	papillary serous	poorly differentiated	elevated
10021	2	8	5	MES	papillary serous	not graded	elevated
10028	3	15	5	PRO	papillary serous	poorly differentiated	elevated
10029	10	10	20	DIF	other	poorly differentiated	normal
10033	0	2	1	MES	papillary serous	moderately differentiated	elevated
10040	5	8	7	DIF	papillary serous	poorly differentiated	normal
10044	3	10	8	DIF	papillary serous	poorly differentiated	elevated
10046	8	10	10	IMM	endometrioid	poorly differentiated	elevated
10052	0	2	1	PRO	papillary serous	poorly differentiated	elevated
10053	5	5	6	PRO	papillary serous	moderately differentiated	elevated
10054	20	25	40	IMM	papillary serous	poorly differentiated	elevated
10057	20	20	40	IMM	papillary serous	poorly differentiated	elevated
10058	10	30	25	PRO	endometrioid	poorly differentiated	elevated
10063	25	20	40	IMM	papillary serous	poorly differentiated	elevated
10068	8	10	15	IMM	endometrioid	moderately differentiated	elevated
10069	5	8	7	MES	papillary serous	moderately differentiated	elevated
10073	2	2	3	DIF	papillary serous	moderately differentiated	elevated
10083	5	8	8	DIF	papillary serous	poorly differentiated	elevated
10084	0	0	0	MES	papillary serous	poorly differentiated	elevated
10086	2	5	5	PRO	papillary serous	not graded	normal
10087	1	10	3	MES	papillary serous	poorly differentiated	elevated
10089	2	5	3	DIF	papillary serous	moderately differentiated	elevated
10094	5	5	7	MES	papillary serous	poorly differentiated	elevated
10095	5	10	8	MES	papillary serous	moderately differentiated	elevated
10096	8	5	15	IMM	papillary serous	poorly differentiated	normal
10099	8	10	15	IMM	papillary serous	poorly differentiated	elevated
10100	3	2	5	DIF	papillary serous	poorly differentiated	elevated
10101	3	5	5	DIF	papillary serous	poorly differentiated	elevated
10102	0	3	1	DIF	papillary serous	poorly differentiated	elevated
10103	3	5		DIF	papillary serous	poorly differentiated	elevated
10105	0	2	1	DIF	papillary serous	moderately differentiated	elevated
10108	1	2	2	DIF	papillary serous	moderately differentiated	normal
10117	0	5	2	DIF	other	moderately differentiated	elevated
10118	0	0	0	MES	papillary serous	poorly differentiated	elevated
10120	1	2	3	MES	papillary serous	moderately differentiated	elevated
10121	3	5	5	PRO	papillary serous	poorly differentiated	elevated
10127	0	3	1	MES	papillary serous	moderately differentiated	elevated
10132	3	5	5	DIF	other	poorly differentiated	elevated
10134	1	5	3	PRO	papillary serous	poorly differentiated	elevated
10135	5	5	8	DIF	papillary serous	poorly differentiated	elevated
10136	5	8	8	PRO	papillary serous	poorly differentiated	elevated
10139	0	0	0	MES	endometrioid	moderately differentiated	elevated
10140	1	3	2	IMM	papillary serous	poorly differentiated	elevated
10143	0	3	2	MES	mixed	moderately differentiated	elevated
10145	30	20	40	IMM	papillary serous	poorly differentiated	elevated
10146	0	10	5	MES	papillary serous	poorly differentiated	elevated
10147	8	10	10	PRO	papillary serous	moderately differentiated	elevated
10148	0	2	1	DIF	papillary serous	poorly differentiated	normal
10150	1	3	3	PRO	papillary serous	poorly differentiated	elevated
10154	1	2	2	MES	papillary serous	poorly differentiated	elevated
10155	5	2	8	IMM	papillary serous	poorly differentiated	elevated
10156	10	10	15	IMM	papillary serous	poorly differentiated	elevated
10160	2	5	5	IMM	papillary serous	poorly differentiated	elevated
10162	5	3	7	PRO	papillary serous	poorly differentiated	elevated
10163	1	3	2	PRO	papillary serous	not graded	elevated
10165	1	3	2	PRO	mixed	poorly differentiated	elevated
10169	2	2	3	DIF	papillary serous	moderately differentiated	elevated
10171	3	5	7	DIF	mixed	poorly differentiated	elevated
10179	0	2	2	DIF	papillary serous	poorly differentiated	normal
10181	0	2	1	MES	papillary serous	poorly differentiated	elevated
10182	5	10	8	DIF	papillary serous	moderately differentiated	normal
10185	1	5	3	DIF	papillary serous	moderately differentiated	elevated
10188	8	12	10	DIF	papillary serous	poorly differentiated	normal
10189	3	5	10	IMM	other	poorly differentiated	elevated
10190	0	2	1	DIF	papillary serous	moderately differentiated	elevated
10196	1	2	2	DIF	papillary serous	poorly differentiated	elevated
10197	3	3	5	PRO	papillary serous	poorly differentiated	elevated
10198	5	3	6	MES	papillary serous	poorly differentiated	elevated
10199	2	5	3	PRO	papillary serous	poorly differentiated	elevated
10200	3	2	5	DIF	papillary serous	moderately differentiated	elevated
10202	6	20	20	PRO	papillary serous	poorly differentiated	elevated
10205	6	5	10	IMM	papillary serous	poorly differentiated	elevated
10207	5	8	7	DIF	papillary serous	poorly differentiated	elevated
10208	1	2	2	MES	papillary serous	poorly differentiated	elevated
10213	15	10	15	MES	papillary serous	poorly differentiated	elevated
10214	2	3	5	PRO	papillary serous	poorly differentiated	elevated
10217	1	2	2	MES	papillary serous	well differentiated	elevated
10218	0	1	1	MES	papillary serous	moderately differentiated	elevated
10220	2	2	5	MES	papillary serous	moderately differentiated	elevated
10221	2	5	5	MES	Clear cell	poorly differentiated	elevated
10223	2	2	3	IMM	papillary serous	poorly differentiated	elevated
10225	1	2	2	MES	papillary serous	poorly differentiated	elevated
10226	2	3	3	MES	papillary serous	poorly differentiated	elevated
10227	1	3	2	MES	papillary serous	poorly differentiated	elevated
10228	25	10	30	IMM	papillary serous	poorly differentiated	elevated
10229	8	7	15	IMM	papillary serous	poorly differentiated	normal
10230	4	5	8	MES	papillary serous	poorly differentiated	elevated
10231	1	2	2	DIF	papillary serous	well differentiated	elevated

Figure 1 - 1015

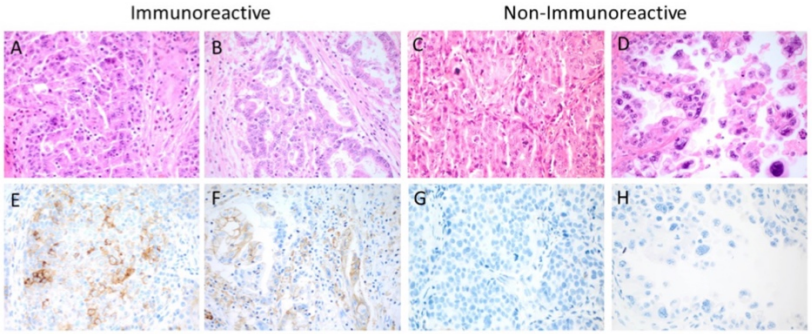

Figure 1: PD-L1 expression across different histopathological and molecular transcriptional subtypes of ovarian tumors. Representative H&E (A-D) and corresponding PD-L1 IHC (E-H) images of ovarian tumors classified as immunoreactive (*left*) and non-immunoreactive (*right*) molecular transcriptional subtypes. Histological subtypes of tumors were serous (A, C), endometrioid (B), and clear cell (D).

Figure 2 - 1015

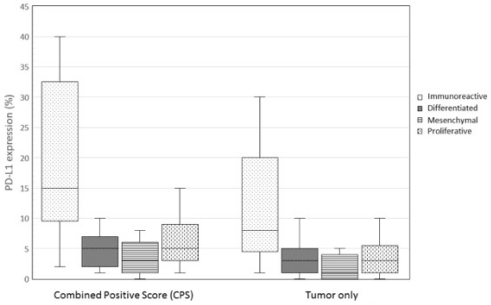

Figure 2: Box and whisker plot of PD-L1 expression scored using CPS (left) and tumor only metrics (right) for 93 ovarian tumors. These tumors wee characterized as immunoreactive (light dots, N=18), differentiated (dark dots, N=27), mesenchymal (horizontal lines, N=27), or proliferative (vertical dashes, N=21) molecular transcriptional subtypes.

Conclusions: Ovarian tumors with increased PD-L1 expression tend to have immunoreactive gene expression profiles. Use of an immunoreactive multigene signature may allow broader assessment of immunoreactivity when compared to use of a single biomarker such as PD-L1 and warrants further clinical exploration

1016 Uterine and Vaginal Sarcomas Resembling Fibrosarcoma: A Clinicopathological and Molecular Analysis of 13 Cases Showing Common NTRK-Rearrangements and the Description of a COL1A1-PDGFB Fusion Novel to Uterine Neoplasms

Sabrina Croce[1], Isabelle Hostein[1], Teri Longacre[2], Anne Mills[3], Gaëlle Pérot[4], Mojgan Devouassoux-Shisheboran[5], Valérie Velasco[1], Anne Floquet[6], Frédéric Guyon[1], Camille Chakiba[1], Denis Querleu[1], Emmanuel Khalifa[1], Laetitia Mayeur[1], Flora Rebier[1], Sophie Le Guellec[7], Isabelle Soubeyran[1], W Glenn McCluggage[8]

[1]Institut Bergonié, Bordeaux, France, [2]Stanford University, Stanford, CA, [3]University of Virginia, Charlottesville, VA, [4]Inserm U1218, Institut Bergonié, Toulouse, France, [5]University Hospital Lyon, Pierre-Bénite, France, [6]Institut Bergonié, Bordeaux, Gabon, [7]Institut Claudius Regaud, Toulouse, France, [8]The Royal Hospitals, Belfast, United Kingdom

Disclosures: Sabrina Croce: None; Isabelle Hostein: None; Teri Longacre: None; Anne Mills: None; Denis Querleu: None; Emmanuel Khalifa: None; Sophie Le Guellec: None; W Glenn McCluggage: None

Background: Mesenchymal neoplasms of the uterus (corpus and cervix) encompass a heterogeneous group of tumors with differing morphologies, immunophenotypes and molecular alterations. The most common malignant mesenchymal neoplasms are leiomyosarcoma, low-grade and high-grade endometrial stromal sarcoma (*YWHAE or BCOR* rearranged), and undifferentiated sarcoma. A variety of other malignant mesenchymal neoplasms occur rarely within the uterus, including fibroblastic malignant peripheral nerve sheath tumors (neurofibrosarcoma) which are most common in the cervix.

Design: Targeted RNA-sequencing (ArcherDx®), dual FISH fusion, array-CGH and Trk immunohistochemistry analysis were performed on a series of 13 spindle cell sarcomas of the uterus and vagina (10 cervix, 2 corpus, 1 vagina) with features resembling fibrosarcoma. Morphologic and molecular data were integrated with clinical follow up.

Results: Seven of 13 tumors exhibited *NTRK* rearrangements (6 *TMP3-NTRK1* and 1 *EML4-NTRK3*) and 3 a *COL1A1-PDGFB* fusion; in the other 3 neoplasms, all of which were positive with S100 (2 diffuse, 1 focal), we identified no rearrangement. All the *NTRK* fusion-positive sarcomas were located in the cervix and exhibited diffuse staining with Trk while all the other neoplasms were negative. CD34 was diffusely positive in all 3 of the *COL1A1-PDGFB* fusion sarcomas. The latter molecular abnormality is identical to that commonly found in dermatofibrosarcoma protuberans and has not been reported previously in uterine mesenchymal neoplasms. We suggest that uterine sarcomas with a morphology resembling fibrosarcoma (and in which leiomyosarcoma and the known molecularly confirmed high-grade endometrial stromal sarcomas have been excluded) can be divided into 3 groups:- an *NTRK* fusion group (Figure 1), a *COL1A1-PDGFB*fusion group (which could be termed dermatofibrosarcoma of the uterus) (Figure 2) and a group containing neither of these molecular abnormalities which, on the basis of positive staining with S100, we suggest to currently classify as malignant peripheral nerve sheath tumor, although additional molecular studies may identify specific genetic alterations necessitating a nomenclature change. We suggest a diagnostic algorithm when reporting such neoplasms.

Table. Clinico-pathological, Immunohistochemical, RNA-Sequencing and Genomic Data

Case	Age (years)	Size (cm)	Follow up (months)	Tumor Location	CD34	S100	Trk	Cyclin D1	BCOR	Translocation frequency	ArrayCGH GI	9p21.3 deletion (CDKN2A)
1	32	5.5	AWD 19	Cervix	N	D	N	80%	<5%	No	21.4	homozygous 1.3 MB
2	47	5	DOD 11	Corpus/LUS	D	F	N	90%	<5%	No	12.5	no
3	39	NA	NA	Cervix	D	D	D	80%	0	*TPM3/NTRK1* 59%	2	heterogyzous 0.5 MB
4	44	4.5	NED 2	Cervix	D	D	D	90%	0	*TPM3/NTRK1* 80%	5.3	homozygous 0.1 MB
5	26	12	AWD 52	Cervix	D	D	D	30%	0	*EML4/NTRK3* 90%	21.3	Homozygous 0.3 MB
6	82	8.2	NED 10	Cervix	D	N	N	15%	0	*COLA1A/PDGFB* 56%	9.14	no
7	50	9	DOD 34	Vagina	N	D	N	80%	0	No	5.3	heterogyzous 1.6 MB
8	23	3	NED 33	Cervix	D	D	D	90%	0	*TPM3/NTRK1* 84%	12.25	Heterozygous 1.6 MB
9	30	2.5	NED 12	Cervix	F	D	D	90%	<5%	*TPM3/NTRK1* 87%	8.3	Homozygous 0.5 MB
10	60	5.8	DOD 60	Cervix	D	N	N	10%	0	*TPM3/NTRK1* 6%* *COLA1A/PDGFB* 86%	16.2	no
10				Recurrence case 10			N	75%	0	*COLA1A/PDGFB* 86%	NI	NI
11	33	5	NED 108	Cervix	D	D	D	80%	0	*TPM3/NTRK1* 57%	NI	NI
12	23	2.8	AWD 30	Cervix	D	F and weak	D	20%	0	*TPM3/NTRK1* 86%	6.25	heterozygous 1 MB
12				Recurrence case 12			D	30%	0	*TPM3/NTRK1* 85%	20.5	homozygous, 0.9 MB
13	48	12	NA-Recent case	Corpus	D	N	N	90%	0	*COLA1A/PDGFB* 74%	ND	ND

MB: Megabase; ER: Estrogen Receptor; PR: Progesterone Receptor; CGH: comparative genomic hybridization; ND: not done, F: Focal <50% of tumor cells; D: Diffuse, >50% of tumor cells; N: Negative; NI: Not Interpretable; NED: no evidence of disease; AWD: alive with disease; DOD: dead of disease; LUS: lower uterine segment.

Other immunohistochemical markers were performed in many of the cases.

*** Case 10 harbored the *TPM3-NTRK1* fusion in a small percentage (6%) only in the primary tumor and not in the recurrence. As such, it was considered negative for *NTRK* rearrangement.**

Figure 1 - 1016

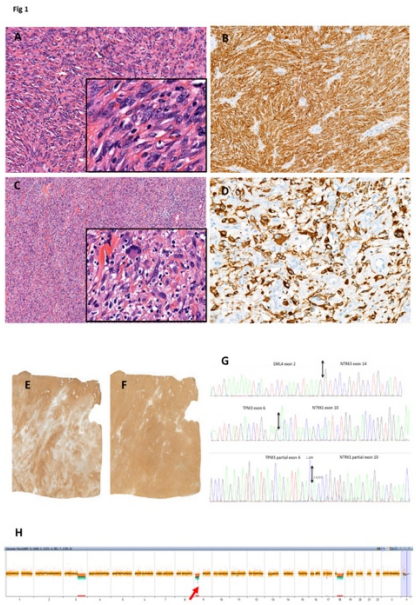

Figure 2 - 1016

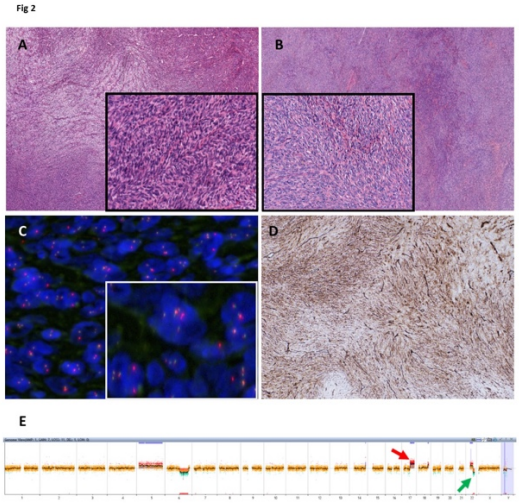

Conclusions: Identification of these newly described fusion-associated sarcomas is important given the potential for targeted treatments.

1017 NanoCind®, the CINSARC signature applied to FFPE samples, predicts clinical outcome of patients with uterine smooth muscle tumors. A French GYN-Sarcoma Group study

Sabrina Croce[1], Tom Lesluyes[2], Carine Valle[3], Loubna M'hamdi[4], Gaëlle Pérot[5], Eberhard Stoeckle[1], Jean-Christophe Noël[6], Quitterie Fontanges[6], Denis Querleu[1], Frédéric Guyon[1], Anne Floquet[7], Camille Chakiba[1], Laetitia Mayeur[1], Flora Rebier[1], Sophie Le Guellec[8], Frédéric Chibon[9]

[1]Institut Bergonié, Bordeaux, France, [2]CRCT Toulouse, Toulouse, France, [3]Inserm U1037, Toulouse, France, [4]IUCT Oncopole, Toulouse, France, [5]Inserm U1037 CRCT/IUCT, Toulouse, France, [6]Hopital Erasme, Bruxelles, Belgium, [7]Institut Bergonié, Bordeaux, Gabon, [8]Institut Claudius Regaud, Toulouse, France, [9]Inserm U1037 CRCT/ICR, Toulouse, France

Disclosures: Sabrina Croce: None; Carine Valle: None; Gaëlle Pérot: None; Denis Querleu: None; Sophie Le Guellec: None; Frédéric Chibon: None

Background: The diagnosis of uterine smooth muscle lesions, based on the Stanford criteria, is straightforward in the majority of the cases. However, the morphology is sometimes not clear and introduces a degree of subjectivity in the interpretation of these criteria. In such cases, a STUMP (smooth muscle tumors with uncertain malignant potential) diagnosis is made. Genomic Index (GI) assessment by array-CGH has been shown to divide the STUMP tumors into two groups: benign leiomyoma tumors (LM) and malignant tumors similar to leiomyosarcoma (LMS).

Bizarre Nuclei-Leiomyomas (BN-LM) represent a diagnostic challenge especially when the Bizarre Nuclei are diffused throughout the tumor at a high density. Genomic profile analysis is not always informative because BN-LM show genomic profiles of intermediate complexity with GI often higher than the LMS diagnostic threshold.

Uterine LMS is a clinically very aggressive disease with challenging outcome prediction, especially for FIGO stage I tumors which relapse in half of cases.

Among sarcomas, the 67 gene signature CINSARC (Complexity INdex in SARComas) has demonstrated significant prognostic value in 17 tumor types. Now NanoCind® is applicable to formalin-fixed, paraffin-embedded (FFPE) samples, we tested whether it predicts clinical outcome in uterine smooth muscle tumors.

Design: In a series of 78 FFPE uterine smooth muscle tumors (45 LMS, 5 STUMP, 19 LM and 9 BN-LM) NanoCind® (the CINSARC signature by NanoString) was evaluated and compared to other current prognostic markers.

Results: The CINSARC signature splits LMS and STUMP (with GI>10) into two groups with significantly different prognoses as demonstrated by different overall survival (OS) (*P*=0.014, HR=4) and progression-free survival (PFS) (*P*=0.022, HR=2.66).

As expected, NanoCind® clearly stratifies LMS from conventional LM. Interestingly, it clusters BN-LM with benign tumors, which was not previously possible by applying GI (Figure 1).

Figure 1 - 1017

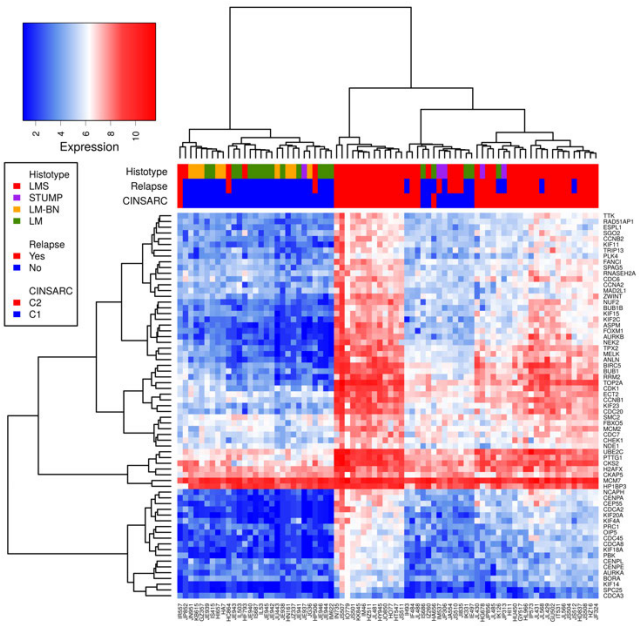

Conclusions: The CINSARC signature (NanoCind®), on FFPE blocks, improves morphological and genomic classification of uterine smooth muscle tumors both at the diagnostic level, identifying BN-LM, and at the prognostic level identifying poor prognosis patients even in those with low stage (I and II) tumors. We therefore propose that NanoCind® should now be prospectively tested to optimize clinical management of patients with uterine sarcoma.

1018 Expression of the Immune Checkpoint TIM-3 in Cervical and Vulvar Squamous Neoplasia

Jacob Curley[1], Anne Mills[2]
[1]University of Virginia Health System, Coleman, VA, [2]University of Virginia, Charlottesville, VA

Disclosures: Jacob Curley: None; Anne Mills: None

Background: Immunotherapies targeting the PD-1/PD-L1 pathway have shown some success in cervical and vulvar cancers, but little is known about the vulnerability of these tumors to other checkpoint inhibitors. TIM-3 is a checkpoint molecule with similar immune inhibitory function to PD-1/PD-L1. Furthermore, there are currently drugs in clinical trials designed to target TIM-3 in a variety of tumor types. To date however, TIM-3 expression has not been well-investigated in cervical and vulvar epithelial neoplasms.

Design: Sixty-three cases of cervical Squamous cell carcinoma (SCC) (n=15), HPV-associated vulvar SCC (n=16), differentiated vulvar intraepithelial neoplasia (dVIN)-associated vulvar SCC (n=3), dVIN (n=2), VIN 3 (n=15), and CIN3 (n=14) were collected from the archival pathology files and reviewed. TIM-3 immunohistochemical staining was performed and scored in the tumor cells based on staining extent as 0%, 1-5%, 6-10%, 11-25%, 26-50%, or >50%.

Results: Tumoral TIM-3 expression was seen in two-thirds of the cervical SCCs (67%, 10/15) and the majority of the vulvar SCCs (84%, 16/19) (**Fig 1-2**). In contrast, TIM-3 expression was rare in cases of isolated CIN3 and VIN3 (14%, 2/14 and 13%, 2/15 respectively) (**Fig 1-2**). Furthermore, the intraepithelial lesions which were TIM-3 positive exhibited only focal expression with just a single case of VIN3 exhibiting greater than 5% positivity in tumor cells. In contrast, TIM-3 expression in the invasive tumors ranged from 1-5% positivity up to >50% positivity in tumor cells with the median expression level lying between 11-25%. There was no significant difference in expression levels of TIM-3 between vulvar and cervical lesions.

Figure 1 - 1018

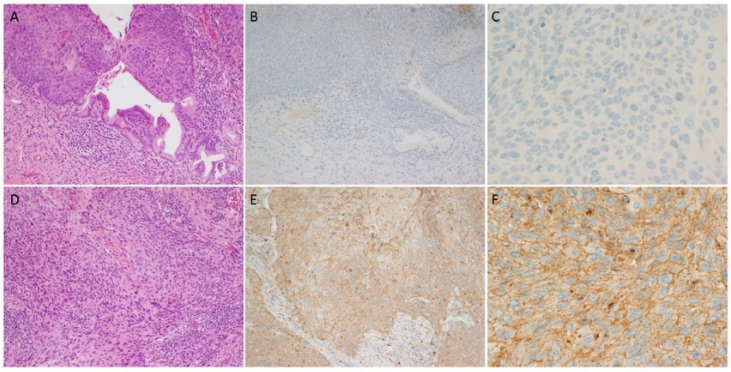

Figure 1. H&E section of CIN III (A) with corresponding negative TIM-3 IHC staining, at low (B) and high (C) magnification. H&E section of invasive cervical squamous cell carcinoma (D) with corresponding diffusely positive staining with TIM-3 IHC, at low (E) and high (F) magnification.

Figure 2 - 1018

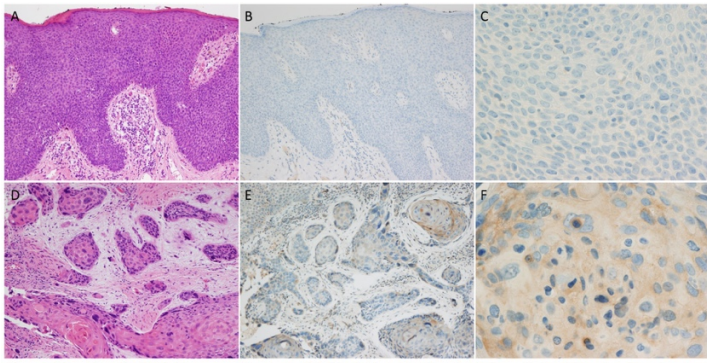

Figure 2. H&E section of VIN III (A) with corresponding negative TIM-3 IHC staining, at low (B) and high (C) magnification. H&E section of invasive vulvar squamous cell carcinoma (D) with corresponding faint, focal positive staining with TIM-3 IHC, at low (E) and high (F) magnification.

Conclusions: TIM-3 is expressed in vulvar and cervical invasive squamous cell carcinomas at varying levels while it is only minimally expressed in vulvar and cervical *in situ* lesions. These findings suggest that TIM-3 may play a key role in invasive cervical and vulvar squamous cell carcinomas. Further investigation should be performed to elucidate the role of TIM-3 in invasive vulvar and cervical lesions and to determine its potential as a target for immunotherapy.

1019 Uterine Rhabdomyosarcomas: Targeted Capture and RNA Sequencing Analyses of Three Cases

Arnaud Da Cruz Paula[1], Charles Ashley[1], Rodrigo Gularte-Mérida[1], Ana Paula Martins Sebastiao[1], David Brown[1], Fresia Pareja[1], Darya Buehler[2], Sarah Chiang[1], Jorge Reis-Filho[1], Paul Weisman[3], Britta Weigelt[1]
[1]Memorial Sloan Kettering Cancer Center, New York, NY, [2]University of Wisconsin, Madison, Madison, WI, [3]University of Wisconsin, Madison, WI

Disclosures: Arnaud Da Cruz Paula: None; Charles Ashley: None; Rodrigo Gularte-Mérida: None; Ana Paula Martins Sebastiao: None; David Brown: None; Fresia Pareja: None; Darya Buehler: None; Sarah Chiang: None; Jorge Reis-Filho: *Advisory Board Member*, Voltion Rx; *Advisory Board Member*, Paige.AI; *Consultant*, Goldman Sachs; Paul Weisman: None; Britta Weigelt: None

Background: Uterine rhabdomyosarcoma (URMS) is an extremely rare and aggressive mesenchymal tumor. Little is known about the genetics of URMS. Here, we sought to characterize the genetic alterations underpinning primary pure URMSs.

Design: DNA samples from tumor and matched normal tissue from three non-alveolar URMSs were subjected to massively parallel sequencing targeting 468 cancer-related genes (MSK-IMPACT). One of these cases (RMS1) was heterogeneous and two components, displaying low and high levels of mitotic activity, were microdissected and subjected separately to MSK-IMPACT and RNA-sequencing for fusion gene discovery. Somatic mutations, copy number alterations and fusion genes were defined using state-of-the-art bioinformatics algorithms.

Results: The three URMSs included in this study expressed desmin and myogenin by immunohistochemistry, confirming heterologous rhabdomyoblastic differentiation. Massively parallel sequencing analysis revealed the presence of somatic *TP53* mutations and high levels of gene copy number alterations including recurrent gains/amplifications of 8q, 18q and 19q, and recurrent losses of 6p and 16q in two URMSs (RMS2 and RMS3). Amplifications included *CCNE1* (RMS2, RMS3), *MYOD1* (RMS2), *MYCN* (RMS2) and *BCL2* (RMS3) and homozygous deletions of *FOXO1* and *RB1* (RMS2), amongst others. Consistent with their clonal relatedness, the low and high proliferation components of the heterogeneous URMS shared a clonal *KMT2A* missense mutation (p.F9C) associated with loss of heterozygosity of the wild-type allele, a clonal *MET* (p.I735V) mutation and similar patterns of gene copy number alterations, including 1q gains, and 11q, 19p and 22q losses. Whilst the copy number profile of the high-proliferation component was more complex, the low-proliferation component harbored an amplification on 19p13, encompassing *NOTCH3* and *DNMT1*. The high-proliferation component harbored an in-frame, expressed *PTK2-WHSC1L1* chimeric transcript resulting in the fusion of exon 1 of *PTK2* and exons 2-24 of *WHSC1L1*, a histone methyltransferase involved as a fusion gene partner in other malignancies. RMS2 had a *MYOD1* gene amplification, recently reported in non-uterine spindle cell RMSs, however none of the URMSs studied here harbored somatic mutations affecting *DICER1*, *MYOD1, PIK3CA, NRAS* or *KRAS*.

Conclusions: URMSs are genetically heterogenous and appear to be underpinned by genetic alterations regulating histone methylation genes, including *KMT2A, DNMT1* and *WHSC1L1*.

1020 Are Endometrial Cancers Arising in BRCA1/BRCA2 Germline Mutations Carriers True BRCA1/BRCA2 Cancers?

Arnaud Da Cruz Paula[1], Evan Smith[1], Karen Cadoo[1], Nadeem Abu-Rustum[1], Xin Pei[1], Nadeem Riaz[1], Mark Robson[1], Jorge Reis-Filho[1], Diana Mandelker[1], Britta Weigelt[1]
[1]Memorial Sloan Kettering Cancer Center, New York, NY

Disclosures: Arnaud Da Cruz Paula: None; Evan Smith: *Consultant*, Best Doctors; Karen Cadoo: None; Nadeem Abu-Rustum: *Grant or Research Support*, GRAIL; *Speaker*, prIME Oncology; *Grant or Research Support*, Stryker/Novadaq; *Grant or Research Support*, Olympus; Xin Pei: None; Nadeem Riaz: *Speaker*, Illumina; *Grant or Research Support*, Pfizer; Mark Robson: *Advisory Board Member*, McKesson; *Advisory Board Member*, AstraZeneca; *Advisory Board Member*, Pfizer; *Grant or Research Support*, AstraZeneca; *Grant or Research Support*, Myriad; Jorge Reis-Filho: *Advisory Board Member*, Volition Rx; *Advisory Board Member*, Paige.AI; *Consultant*, Goldman Sachs; Diana Mandelker: None; Britta Weigelt: None

Background: *BRCA1* and *BRCA2* (*BRCA1/2*) pathogenic germline mutations are causative of the Hereditary Breast and Ovarian Cancer Syndrome. The role of *BRCA1/2* germline mutations in the development of endometrial cancer (EC) is still a matter of controversy. Bi-allelic but not mono-allelic *BRCA1/2* alterations have been shown to be associated with genomic features of homologous recombination DNA (HRD) repair deficiency. Here we sought to define if ECs arising in *BRCA1/2*germline mutation carriers harbor bi-allelic alterations and/or genomics features of HR deficiency.

Design: Sequencing data of ECs from patients with *BRCA1/2* germline mutations subjected to massively parallel sequencing targeting 410 cancer-related genes under an IRB-approved protocol at Memorial Sloan Kettering Cancer Center (n=7) and to whole-exome sequencing (WES) by The Cancer Genome Atlas (n=3) were analyzed. Somatic mutations, copy number alterations, loss of heterozygosity (LOH) and microsatellite instability (MSI) were defined. In ECs subjected to WES, genomic features of HRD were investigated.

Results: Six ECs were from *BRCA1* and four from *BRCA2* germline pathogenic mutation carriers. The median age at EC diagnosis was 60 years (range 44-78). The histologic types varied, and included 5 FIGO grade II/III endometrioid carcinomas, 2 serous/clear cell carcinomas and 2 carcinosarcomas. Bi-allelic alterations through LOH of the wild-type allele of *BRCA1* or *BRCA2* were found in 5 (83%) *BRCA1* and 1 (25%) *BRCA2* ECs, respectively. Somatic *TP53* mutations were found in all ECs, irrespective of the presence of mono- or bi-allelic *BRCA1/2* alterations. Two ECs lacking LOH of the *BRCA1/2* wild-type allele (i.e. mono-allelic alterations) were MSI-high by MSIsensor, had a high mutational burden and an MSI-related mutational signature. The three ECs subjected to WES harbored *BRCA1* bi-allelic alterations, were of endometrioid type, and displayed genomic features of HRD, including high large-scale transition scores and a dominant HRD mutational signature (i.e. signature 3).

Conclusions: A subset of *BRCA1/2*-associated ECs harbors bi-allelic *BRCA1/2* alterations and genomics features of HRD, establishing a causal link between the *BRCA1/2* pathogenic germline mutations and the development of ECs. A subset of ECs arising in the context of *BRCA1/2* germline pathogenic mutations lacking LOH of the wild-type allele were found to be MSI-high and likely constituted sporadic cancers.

1021 Comprehensive Morphological and Molecular Analyses Establish Germline BRCA-Associated Endometrial Carcinoma as a Distinct Entity

Marthe de Jonge[1], Lauren Ritterhouse[2], Cor de Kroon[1], Maaike Vreeswijk[1], Jeremy Segal[3], Rutika Puranik[4], Christi van Asperen[5], Vincent Smit[1], Brooke Howitt[6], Tjalling Bosse[5]
[1]Leiden University Medical Center, Leiden, Netherlands, [2]University of Chicago Medical Center, Chicago, IL, [3]University of Chicago, Riverside, IL, [4]UChicago Medicine, Chicago, IL, [5]LUMC, Leiden, Netherlands, [6]Stanford University School of Medicine, Stanford, CA

Disclosures: Marthe de Jonge: None; Lauren Ritterhouse: None; Cor de Kroon: None; Maaike Vreeswijk: None; Jeremy Segal: None; Rutika Puranik: None; Christi van Asperen: None; Vincent Smit: None; Brooke Howitt: None; Tjalling Bosse: None

Background: Distinct histopathological characteristics, such as recognized for *BRCA*-associated adnexal high grade serous carcinoma (HGSC), have not been studied in endometrial carcinoma (EC). We comprehensively evaluate the molecular and morphologic features of EC occurring in patients with germline *BRCA1/2* mutations (g*BRCA*).

Design: EC were selected from the nationwide cohort study on Hereditary Breast and Ovarian Cancer in the Netherlands (HEBON). 19 morphologic features were scored and histotype was determined by three expert gynecologic pathologists, blinded for subsequent molecular analyses consisting of next generation sequencing (1212 gene panel “OncoPlus” assay). EC with loss of heterozygosity (LOH) for the *BRCA*-wildtype allele (g*BRCA*/LOHpos) were defined g*BRCA*-associated, those without LOH (g*BRCA*/LOHneg) were defined ‘sporadic’ EC not associated to the g*BRCA* mutation. All cases were classified into one of the four TCGA molecular subgroups: *POLE*, MSI, *TP53*/copy number high (*TP53*/CN-H) or copy number low (CN-L).

Results: In total, 40 EC were included (30 g*BRCA1,* 10 g*BRCA2*). 24 (60%) EC were gBRCA/LOHpos and 16 (40%) g*BRCA*/LOHneg. g*BRCA*/LOHpos EC were associated with non-endometrioid (58%, *P*=0.001), grade 3 histology (79%, *P*<0.001) and all but one were of the *TP53*/CN-H subgroup (96%, *P*<0.001). 50% of g*BRCA*/LOHpos EC showed a Solid, pseudoEndometrioid and/or Transitional carcinoma-like morphology (SET) in >25% of the tumor (typical of *BRCA*-associated HGSC). In contrast, g*BRCA*/LOHneg EC were mainly grade 1 endometrioid EC (94%) without SET morphology (0%) and showed a heterogeneous distribution of molecular subgroups: *POLE* (6.3%), MSI (25%), CN-L (62.5%) and *TP53*/CN-H (6.3%). In addition, g*BRCA*/LOHpos EC were associated with destructive invasion pattern (82% vs 27%, *P*=0.002*)*, desmoplasia (85% vs 46%, *P*=0.04), trabecular growth (44% vs 0%, *P*=0.002), high nuclear grade (79% vs 6.3%, <0.001), tumor giant cells (46% vs 6.3%, *P*=0.012), and a higher mitotic index (*P*<0.001). g*BRCA*/LOHpos EC had fewer pathogenic variants in *PTEN* (17% vs 94%, *P<0.001), PIK3CA* (17% vs 56%, *P*=0.015), *ARID1A (*4% vs 44%, *P=0.004), PIK3R1* (4% vs 44%, *P=0.004*) and *CTNNB1* (0% vs 38%, *P=0.002)* as compared to g*BRCA*/LOHneg EC.

Figure 1 - 1021

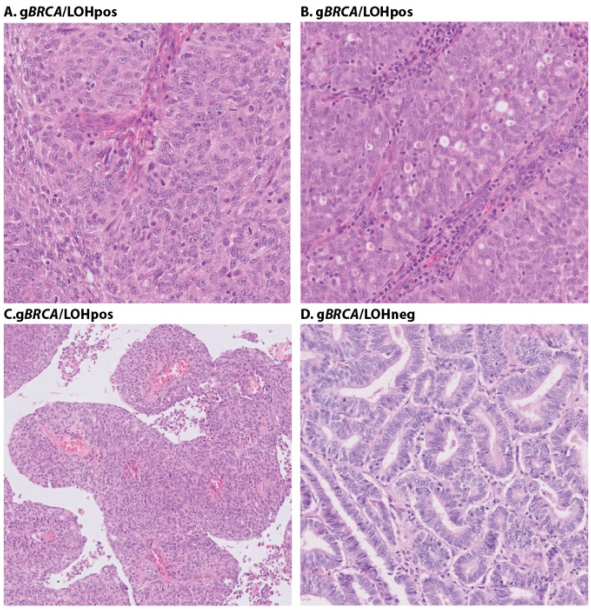

Figure 1: Example of a g*BRCA*/LOHpos EC showing Solid (A), pseudoEndometrioid (B) and Transitional carcinoma-like (C) (SET)-features.
Glandular (D) growth pattern as observed in most g*BRCA*/LOHneg EC.

Conclusions: This study comprises the largest cohort of EC occurring in g*BRCA* patients to date. We found that g*BRCA*-associated EC have morphologic and molecular features unlike typical EC, and likely represent a distinct entity characterized by high grade, *TP53* mutations (CN-H) and frequent SET morphology.

1022 BRCA and High-Grade Serous Carcinoma: a Morphological, Immunohistochemical and Genetic Study

Antonio De Leo[1], Giacomo Santandrea[1], Roberta Zuntini[1], Barbero Giovanna[2], Daniela Turchetti[1], Barbara Corti[1], Daniela Rubino[1], Giulia Dondi[3], Giulia Borghese[1], Anna Nunzia Della Gatta[1], Anna Myriam Perrone[1], Pierandrea De Iaco[1], Claudio Ceccarelli[1], Donatella Santini[1]
[1]S.Orsola-Malpighi Hospital, University of Bologna, Bologna, Italy, [2]University of Bologna, Bologna, Italy, [3]S. Orsola-Malpighi Hospital, University of Bologna, Modena, Italy

Disclosures: Antonio De Leo: None; Giacomo Santandrea: None; Roberta Zuntini: None; Barbero Giovanna: None; Daniela Turchetti: None; Barbara Corti: None; Daniela Rubino: None; Giulia Dondi: None; Giulia Borghese: None; Anna Nunzia Della Gatta: None; Anna Myriam Perrone: None; Pierandrea De Iaco: None; Claudio Ceccarelli: None; Donatella Santini: None

Background: Solid-pseudoendometrioid-transitional (SET) variant of high grade serous carcinoma (HGSC) has been recently described in BRCA 1/2 mutated patients. The aim of the study was to investigate the correlation between BRCA mutational status, age, peritoneal cancer index (PCI), tumor morphology, serous tubal intraepithelial carcinoma (STIC), tumor infiltrating lymphocytes (TILs) and peritoneal invasion patterns.

Design: 59 consecutive patients with HGSC (mean age 64 years) were collected. Tumor histological features, STIC, TILs and peritoneal invasion patterns were evaluated without knowledge of BRCA mutation status and classified as previously described. Immunohistochemical characterization of HGSC and TILs were performed. BRCA mutational status was tested both on formalin-fixed

paraffin-embedded (FFPE) tissue samples and blood. To assess the extent of peritoneal cancer throughout the peritoneal cavity, PCI score was determined for all patients.

Results: BRCA1/2 mutations were found in 41% of cases (88.9% germline mutation and 11.1% somatic mutation). Morphologically, 52.5 of cases were classified as usual HGSC and 47.5% as SET variant. BRCA-associated HGSCs were statistically correlated with SET morphology (p=0.0002), but not with age. Compared with the usual HGSC, the SET tumors were strongly associated with pushing pattern of peritoneal invasion (p=0.0002) and high density of TILs (p=0.0002), while the correlation with PCI was not relevant. Furthermore, the hot-spot CD8+ TIL enumeration (>100/10 HPFs) was significantly higher in SET tumors (p=0.004). STIC was found in 62.7% of cases, and tended to show a lower association with the SET variant compared to the usual HGSC.

Conclusions: In the present study, SET-HGSCs showed a statistically significant association with BRCA mutation, TILs with high number of CD8+ lymphocytes, and a pushing pattern of peritoneal invasion. Conversely, STIC was significantly more frequent in HGSC with classic morphology. These pathologic differences among the usual HGSC and the SET variant and their different relations to BRCA mutations allow to identify two possible separable entities, thus supporting the hypotesis of a dualistic model of HGSC.

1023 Integrated Assessment of ATRX Mutation Status and Protein Expression by IHC in Uterine Mesenchymal Tumors

Walter Devine[1], Karuna Garg[2], Joseph Rabban[3], Charles Zaloudek[4], James Grenert[2], Rebecca Wolsky[2]
[1]University of California, San Francisco, Berkeley, CA, [2]University of California, San Francisco, San Francisco, CA, [3]UCSF Pathology, San Francisco, CA, [4]UCSF Medical Center at Mission Bay, San Francisco, CA

Disclosures: Walter Devine: None; Karuna Garg: None; Joseph Rabban: *Employee*, Merck & Co., Inc.; Charles Zaloudek: None; James Grenert: None; Rebecca Wolsky: None

Background: A subset of uterine mesenchymal tumors show overlapping morphologic and immunophenotypic features of PEComa and leiomyosarcoma (LMS). This distinction has treatment implications as many PEComas show TSC gene alterations making them potentially targetable with mTOR inhibitors. Alpha-Thalassemia/Mental Retardation Syndrome X-linked (ATRX) encodes a member of the SWI/SNF family of chromatin remodeling proteins and is associated with alternative lengthening of telomeres. Recent studies have found that inactivating mutations in ATRX are frequently observed in uterine LMS. This study compares the frequency of inactivating ATRX mutations in uterine LMS and PEComas by next generation sequencing (NGS) and correlates mutation status with ATRX protein expression by immunohistochemistry (IHC).

Design: Next generation sequencing (NGS) and ATRX IHC were performed on 20 uterine LMS (10 with epithelioid features) and 11 uterine PEComas. Complete loss of ATRX nuclear staining with appropriate internal controls was considered a positive test result. The IHC and NGS results were interpreted blinded to each other and to the original diagnosis.

Results: Mutations in the ATRX gene were identified in 50% of LMS but none of the PEComas (55% of which had a TSC mutation). Of the 10 ATRX mutations in LMS, 8 were inactivating mutations classified as pathogenic and 2 were missense variants classified as variants of uncertain significance (VUS). ATRX IHC demonstrated loss of nuclear expression in all 8 LMS with pathogenic mutations and retained nuclear expression in the 2 cases with ATRX VUS. Three additional LMS showed loss of ATRX IHC expression in the absence of any demonstrable mutation. None of the PEComas showed loss of ATRX by IHC.

ATRX IHC	Leiomyosarcoma (n=20)	PEComa (n=11)
Wildtype	9 (none with ATRX mutation)	11 (none with ATRX mutation)
Loss	11 (8 with inactivating ATRX mutations)	0

Conclusions: Mutations in ATRX appear to be highly specific for uterine LMS as compared to PEComa. The data suggests that ATRX IHC can be used as an adjunct tool to distinguish the two entities in diagnostically difficult cases. All inactivating ATRX gene mutations (8/8) were associated with a loss of ATRX protein expression by IHC. An additional 3 LMS demonstrated loss of ATRX IHC expression in the absence of any demonstrable mutation, suggesting alternative mechanisms of ATRX inactivation such as epigenetic silencing, large scale deletions, or structural rearrangements. The oncogenic mechanism of ATRX remains to be elucidated. In summary, our limited data suggests ATRX mutation status and IHC may be useful in the distinction between uterine LMS and PEComa.

1024 A Screening Study Reveals Genetic Alterations of Fumarate Hydratase in Uterine Leiomyomas from Young Patients

Jessica Dillon[1], Chengbao Liu[2], Deyin Xing[1]
[1]Johns Hopkins Hospital, Baltimore, MD, [2]Dallas, TX

Disclosures: Jessica Dillon: None; Chengbao Liu: None; Deyin Xing: None

Background: Hereditary leiomyomatosis and renal cell cancer (HLRCC) syndrome is an autosomal dominant condition caused by germline mutations in the fumarate hydratase (FH) gene. Patients with HLRCC are predisposed to developing aggressive type 2 papillary renal cell carcinomas and cutaneous leiomyomas. In young women, the syndrome often presents with symptomatic uterine leiomyomas, leading to myomectomy or hysterectomy. As such, early identification and triage of syndromic patients allows for clinical surveillance and presents an opportunity for timely detection of renal cell carcinoma.

Design: In this study, we screened 153 cases of uterine leiomyomas from women up to 30 years old for loss of fumarate hydratase protein expression by immunohistochemical staining. Three gynecologic pathologists separately reviewed each tumor for morphologic features that have been described in FH deficient leiomyomas, including staghorn vessels, hypercellularity, alveolar edema, cytologic atypia, nucleoli, and perinucleolar halos. Mutational analysis of tumors with loss of FH were investigated by PCR amplification of 10 exons within the FH gene and subsequent Sanger sequencing. The status of promoter methylation was assessed by bisulfite sequencing.

Results: Loss of FH protein expression was detected in 7 (4.6%) of 153 screened uterine leiomyomas from young patients, 10 times higher than the general population. Of the 7 cases with FH loss, 4 women were Caucasian and 3 were African American, ranging in age from 26 to 30 years old. All FH-deficient leiomyomas displayed at least 3 of the commonly described morphologic features and all 7 tumors contained staghorn vasculature and perinucleolar halos. Nine mutations were identified in 6/7 (86%) tumors with FH loss of expression. The mutations are currently being investigated as somatic or germline. Promoter methylation was not present in any of the 7 tumors.

Conclusions: Our data showed immunohistochemical staining provides a valuable tool to screen uterine leiomyomas for mutational changes in the FH gene. While genetic mutations confer a loss of expression, promoter methylation of the FH gene appears to be unrelated to protein expression.

1025 Transcriptome Alterations in Low Grade Endometrial Neoplasia Associated with Progestin Therapy Correlate with Histologic Measures of Response

Bojana Djordjevic[1], Ekaterina Olkhov-Mitsel[2], Yutaka Amemiya[3], Carlos Parra-Herran[4], Arun Seth[4]
[1]University of Toronto, Scarborough, ON, [2]Sunnybrook Health Sciences Centre, Toronto, ON, [3]Sunnybrook Research Institute, Toronto, ON, [4]Sunnybrook Health Sciences Centre - University of Toronto, Toronto, ON

Disclosures: Bojana Djordjevic: None; Ekaterina Olkhov-Mitsel: None; Yutaka Amemiya: None; Carlos Parra-Herran: None; Arun Seth: None

Background: Cellular mechanisms underlying lack of response to progestin therapy in low grade endometrial neoplasia are poorly understood. We have previously examined the pre-treatment genomic profile of atypical endometrial hyperplasia (AH) and FIGO grade 1 endometrioid carcinomas (ECs) that exhibited complete (CR), partial (PR) or no response (NR) to progestin therapy. *PTEN* truncation mutations predominated in CR (78%) compared to PR and NR (33%, 20%) cases. Mutations unique to CR were largely in DNA repair genes (*ATR, BRCA1*), while mutations unique to NR primarily occurred in the PI3K-AKT/MAPK pathway (*KDR, NF1*). We now surveyed the transcriptome landscape of AH and EC before and after progestin treatment.

Design: Pre- and post-treatment paraffin-embedded endometrial biopsy samples of 20 AH (n=14) and FIGO grade 1 EC (n=6) from patients who received ≥ 6 months of oral progestin treatment underwent whole transcriptome RNA sequencing for global gene expression using Ion AmpliSeq™ Transcriptome Human Gene Expression Kit. CR (n=9), was characterized by resolution of architectural complexity and cytologic atypia, PR (n=6) by resolution of cytologic atypia only, and NR (n=5) by persistence of the original lesion.

Results: By unsupervised analysis, CR and PR, but not NR cases, showed similar trend changes in the global transcriptome profile between pre- and post-progestin-treatment samples. The top 10 altered gene transcripts in CR and PR (IGFBP1, GNLY, SCARA5, PRL, PAEP, TIMP3, ZBTB16, ITGAD, CTSW, GAS1) were similarly altered in NR, but to a much lesser extent. Notably, the majority of these transcripts are functionally associated with the PI3K-AKT/MAPK pathway. In one case, the initial post-treatment sample contained areas of CR and PR, but a follow-up sample progressed to NR and showed expression alterations mirroring the differences between CR/PR and NR seen in the whole study cohort.

Conclusions: This is the first comprehensive transcriptome study of low grade endometrial neoplasia with a uniform minimum progestin treatment period and strictly defined histological outcomes.CR and NR cases are characterized by different genomic and transcriptomic profiles. Similarity of changes in gene expression in response to progestin treatment in CR and PR, but not NR cases, suggests that PR

cases may be better managed clinically as CR rather than as NR. Accrual of mutations and mRNA level alterations within the PI3K-AKT/MAPK pathway may be related to progestin resistance in NR cases.

1026 Mutations in the PI3K-AKT/MAPK Signaling Pathway and upregulation of CYP17A1 are Associated with Progesterone Therapy Resistance in Low Grade Endometrial Neoplasia

Bojana Djordjevic[1], Ekaterina Olkhov-Mitsel[2], Yutaka Amemiya[3], Carlos Parra-Herran[4], Arun Seth[4]
[1]University of Toronto, Scarborough, ON, [2]Sunnybrook Health Sciences Centre, Toronto, ON, [3]Sunnybrook Research Institute, Toronto, ON, [4]Sunnybrook Health Sciences Centre - University of Toronto, Toronto, ON

Disclosures: Bojana Djordjevic: None; Ekaterina Olkhov-Mitsel: None; Yutaka Amemiya: None; Carlos Parra-Herran: None; Arun Seth: None

Background: Progestin is increasingly favored as an alternative to surgical treatment of atypical endometrial hyperplasia (AH) and FIGO grade 1 endometrioid carcinoma (EC), but is ineffective in ~ 30% of patients with no reliable predictive biomarkers. The objective of this study was to identify genomic and transcriptome changes within the progesterone pathway, as well as potential biomarkers of progestin response or resistance.

Design: 20 pre- and post- treatment endometrial biopsies from AH (n=14) and FIGO grade 1 EC (n=6) patients who received ≥6 months of oral progestin treatment were analyzed. Complete response (CR) (n=9), was characterized by resolution of architectural complexity and cytologic atypia, partial response (PR) (n=6) by resolution of cytologic atypia only, and no response (NR) (n=5) by persistence of the original lesion. Formalin fixed paraffin embedded lesional tissue underwent targeted sequencing of 161 genes Ion Torrent Oncomine comprehensive V3 panel and whole transcriptome RNA sequencing for global gene expression. Bioinformatics analysis focused on progesterone action pathways.

Results: We identified mutations in 2 progesterone-mediated genes PIK3CA (5/20, CR, PR and NR samples) and PIK3R1 (4/20, CR and PR samples). Additional mutations (*KDR, NF1*) in PI3K-AKT/MAPK pathways were found solely in NR patients. *CYP17A1* was the only transcript significantly upregulated in NR vs. CR and PR pre-treatment samples. The enzyme CYP17A1 is involved in progesterone metabolism, and is frequently upregulated during neoplastic transformation of hormone-mediated cancers; inhibitors CYP17A1 have shown therapeutic significance for prostate cancer. In post vs. pre-treatment samples, expression of 11 transcripts (up-regulation of CAV1, CD38, FOXO1, PIK3CD, PIK3R1, PTGER2, PTN, TXNIP and downregulation of DSG2, PIK3R3, SRD5A2) was altered in CR but not in NR cases. Of these, 3 (FOXO1, PTGER2 and TXNIP) were also altered in PR post-treatment samples.

Conclusions: In this multiplatform profiling study of progesterone action pathways in low grade endometrial neoplasia, upregulation of CYP17A1 appears to be predictive of progestin therapy resistance. Lack of significant alterations in progesterone pathway genes NR cases following progestin therapy suggests that other pathways, particularly the PI3K-AKT/MAPK pathway, may be independent drivers of cellular proliferation.

1027 Epithelial-Mesenchymal-Transition status in high grade serous carcinoma of the ovary and outcome on prognosis

Reza Eshraghi[1], Sara Javidiparsijani[2], Yihong Ma[3], Oluwatobi Odetola[1], Xiuzhen Duan[1], Stefan Pambuccian[1]
[1]Loyola University Medical Center, Maywood, IL, [2]Loyola University Hospital, Maywood, IL, [3]Loyola University Medical Center, Hinsdale, IL

Disclosures; Reza Eshraghi: None; Sara Javidiparsijani: None; Yihong Ma: None; Oluwatobi Odetola: None; Xiuzhen Duan: None; Stefan Pambuccian: None

Background: The epithelial-mesenchymal-transition (EMT) is considered important for invasive and metastatic potential of many cancers, including ovarian carcinoma. The aim of this study was to evaluate the prognostic impact of the expression of markers of epithelial (E-cadherin, EMA and CD138) and mesenchymal (Vimentin and SOX9) differentiation in high grade serous carcinomas of the ovary.

Design: An immunohistochemical analysis was conducted using tissue microarray samples of 24 ovarian high grade serous carcinomas, and the relationships between the predominant expression of epithelial or mesenchymal markers and outcomes was investigated. For each of the five markers used we evaluated the intensity (0-3+) and percent of tumor cells stained and obtained a score by multiplying the two. Finally, we added the scores for the two mesenchymal markers and subtracted the scores of the three epithelial markers, thus obtaining a combined EMT expression score. Based on the mean of this EMT expression score, we divided the tumors into two groups: low EMT score and high EMT score. All patients were treated surgically and received post-operative chemotherapy. We compared the number of patients who recurred or died within a 6-60 months interval between the two groups (high and low EMT score) using Fisher exact test.

Results: The 5 markers showed different expression scores in the tumors analyzed (Table). Based on the mean EMT scores ranging from -660 to 100, with a mean score of -275. Significantly more patients in the high EMT score group recurred or died during the follow-up period (8/11, 73% vs. 3/13, 23%, p <0.05).

	E-Cad	EMA	vim	CD138	SOX 9	EP	MES	MES-EP	EMT SCORE	STATUS	Months
case1	60	300	30	0	160	360	190	-170	HIGH	DIED	13
case 2	140	100	30	40	120	280	150	-130	HIGH	RECURRED	19
case 3	160	300	20	30	270	490	290	-200	HIGH	RECURRED	20
case 4	240	20	0	150	300	410	300	-110	HIGH	DIED	11
case 5	160	140	0	0	270	300	270	-30	HIGH	AWOD	25
case 6	180	30	0	30	210	240	210	-30	HIGH	RECURRED	26
case 7	300	300	160	0	150	600	310	-290	LOW	AWOD	18
case 8	300	300	100	100	150	700	250	-450	LOW	AWOD	18
case 9	100	120	100	30	210	250	310	60	HIGH	RECURRED	16
case 10	300	200	270	270	40	770	310	-460	LOW	AWOD	6
case 11	300	270	60	240	270	810	330	-480	LOW	AWOD	4
case 12	80	300	15	300	240	680	255	-425	LOW	AWOD	13
case 13	300	200	20	300	270	800	290	-510	LOW	AWOD	15
case 14	180	300	0	270	210	750	210	-540	LOW	RECURRED	18
case 15	300	200	240	120	60	620	300	-320	LOW	AWOD	1
case 16	150	100	0	0	150	250	150	-100	HIGH	DIED	60
case 17	300	300	90	150	0	750	90	-660	LOW	AWOD	67
case 18	300	0	0	0	200	300	200	-100	HIGH	AWOD	19
case 19	300	300	60	0	200	600	260	-340	LOW	AWOD	29
case 20	300	300	0	30	0	630	0	-630	LOW	AWOD	20
case 21	60	300	10	0	80	360	90	-270	LOW	DIED	48
case 22	20	160	100	0	180	180	280	100	HIGH	AWOD	4
case 23	180	240	20	0	270	420	290	-130	HIGH	RECURRED	60
case 24	150	300	0	30	120	480	120	-360	LOW	RECURRED	12

Conclusions: These data indicate that the EMT status is significantly associated with outcome in patients with ovarian high grade serous carcinomas. Therefore, the EMT score may be an important prognostic factor and targeting EMT may be a promising approach to therapy for ovarian cancer.

1028 Role of matrix metalloproteinases in immunohistochemical assessment of the invasiveness potential of extragenital endometriosis

Cazacu Eugeniu, Chisinau, Moldova, Republic of

Disclosures: Cazacu Eugeniu: None

Background: Matrix metalloproteinases are proteolytic zinc enzymes responsible for the degradation of extracellular matrix modelig of endometrisis lesions and their involvement in the invasivenes ov these lesions.The purpose of this study was to evaluate the expression of matrix metalloproteinases MMP1, MMP2, MMP9, MMP14 in extragenital endometriosis.

Design: From 2010 to 2018, 42 cases of endometriosis were identified in our institution's pathology file. Histochemical stains for Masson's trichrome and immunohistochemical stains for matrix metalloproteinases MMP1, MMP2, MMP9, MMP14 antibodies ware performed. Evaluation of the aggressive potential of extragenital endometriosis lesions by investigating the expression of markers involved in the extracellular matrix both at the endometriosis sites and in the endometrium of the control group obtained after hysterectomy with diagnoses of leiomyoma. The staining was evaluated with the Immuno Reactive Score (IRS) [Remmele & Stegner, 1987.].

Results: The patient group consist 42 women with endometriosis, age range of 21-63 years (median 40). Location included: the anterior abdominal wall after caesarean operation- 27, umbilical hernia- 4, perineal region- 1, appendix- 4, colon- 5, ileum- 1case. The reactivity of

MMP2, MMP9 and MMP14 metalloproteinase in endometriotic lesions was higher than in eutopic endometrium. MMP2 and MMP9 IHC staining were performed, and endometriosis – associated fibrosis and lymphocytic infiltrate evaluated with MMP1. Nuclear staining of MMP2 for glands and both membranous and cytoplasmic staining of MMP9 for stroma were considered positive. In cases with intestinal endometriosis staining was diffuse and intensity was strong (3+), in abdominal wall endometriosis intensity was moderate (2+) while eutopic endometrium staining was diffuse and intensity was weak to moderate (1-2+) in all cases. MMP14 was positiv and intensity was moderate in both cases.The expression of MMP1 on the examined tissues, was absent.

Conclusions: Expression of MMP2, MMP9, MMP14 matrix metalloproteinases was greater at the endometriosis sites than at the normal endometrium, which would confer greater invasive potential to endometriotic lesions. The existence of different expression patterns of the 3 matrix metalloproteinases in the ectopic endometrial tissue and the adjacent stroma, respectively, suggests a reciprocal interaction of these two components to facilitate the expansion of endometriotic lesions.

1029 Low Grade Endometrial Endometrioid Carcinoma Invading Into the Outer Myometrium from Tumor-Colonized Adenomyosis, Is It Equivalent to FIGO Stage IA or IB Disease?

Elizabeth Euscher[1], Stephen Gruschkus[1], Roland Bassett[1], Preetha Ramalingam[2], Anais Malpica[1]
[1]The University of Texas MD Anderson Cancer Center, Houston, TX, [2]Houston, TX

Disclosures: Elizabeth Euscher: None; Stephen Gruschkus: None; Roland Bassett: None; Preetha Ramalingam: None; Anais Malpica: None

Background: The presence of myometrial invasion (MI) into the outer myometrial half (OMH) arising from tumor (tu)-colonized adenomyosis (cAM) has been considered to be equivalent to FIGO stage IA disease; however, some believe that cases of this type should be regarded as FIGO stage IB. In this study, we ascertained the behavior of low grade endometrial endometrioid carcinomas (LGEECas) with invasion into the OMH arising from tu-CAM (cohort 1). For comparison, we also reviewed LGEECas with invasion into either the inner MH (IMH) or OMH unassociated with tu-cAM (cohorts 2 and 3, respectively).

Design: Cohorts 1-3 (2005 to 2015) were evaluated for patient (pt) age, tu size, lymphovascular invasion (LVI), cervical stroma invasion (CxSInv), FIGO stage, treatment (tx) and follow up (f/u).Cohorts 2 and 3 were selected from consecutive accessions blinded to stage and outcome.

Results: A summary of results is presented in Table 1. A 3-way comparison showed no statistically significant differences between cohorts with respect to pt age, tu size or CxSInv. A 3-way comparison of the rates of LVI was statistically significant (p=0.017), but pairwise comparisons of Cohort 1 vs 2 (p=0.32) or Cohort 1 vs 3 (p=0.411) were not.18 (14.9%) pts were FIGO Stage III: Cohort 1, 1 pt (7.7%); Cohort 2, 4 pts (7.0%); Cohort 3, 13 pts (25.5%). A univariable logistic regression model using Cohort 3 as the reference group showed Cohorts 1 and 2 less likely to have advanced stage disease relative to Cohort 3 (p=0.019). Recurrence status was known for 113 (93.3%) pts and unknown for 4 pts in Cohorts 1 and 3 each. None of the 9 Cohort 1 pts with f/u recurred while 3 (5.3%) and 5 (10.6%) pts in Cohorts 2 and 3 respectively recurred. A comparison of Cohorts 1-3 showed no statistically significant relationship with respect to recurrence (p=0.525). Tx differed by cohort: 91.7% of Cohort 3 pts had adjuvant tx vs. 58.3% of Cohort 1 pts and 36.8% of Cohort 2 pts (p<0.0001). Of the 5 Cohort 1 pts without adjuvant tx, 3 had f/u and are free of tu.

Data Summary for Cohorts 1-3

	Overall (n=121)	Cohort 1 (n=13)	Cohort 2 (n=57)	Cohort 3 (n=51)	p-value
Median pt age (yr)	62	57	61	62	0.053
Median tu size (cm)	4.1	3.3	4	4.5	0.42
LVI present	54 (44.6%)	6 (46.2%)	18 (31.6%)	30 (58.8%)	0.017
CxSInv	9 (7.4%)	0 (0%)	5 (8.8%)	4 (7.8%)	0.786
FIGO stage III	18 (14.9%)	1 (7.7%)	4 (7.0%)	13 (25.5%)	0.019

Conclusions: LGEECas with OMH invasion due to tu-cAM show a similar risk of advanced stage disease to LGEECas with IMH invasion. Although a cohort comparison showed no statistical difference between groups with respect to recurrence, no case in Cohort 1 with f/u data recurred. These findings suggest that LGEECas with OMH invasion due to tu-cAM are more similar to FIGO stage IA than IB disease.

1030 Mesonephric-Like Carcinoma of the Endometrium: a Subset of Endometrial Carcinoma Exhibiting Aggressive Behavior

Elizabeth Euscher[1], Preetha Ramalingam[2], Anais Malpica[1]
[1]The University of Texas MD Anderson Cancer Center, Houston, TX, [2]Houston, TX

Disclosures: Elizabeth Euscher: None; Preetha Ramalingam: None; Anais Malpica: None

Background: Mesonephric-like endometrial carcinoma (MenCA) shares histologic features with endocervical mesonephric carcinoma but lacks a topographical relationship to mesonephric remnants.This study is a single institution experience encompassing the largest series of MenCA reported to date.

Design: We evaluated 17 cases of MenCA (2004 to present) for the following clinicopathologic features: patient (pt) age, tumor (tu) size, % myometrial invasion (MI), cervical stromal invasion (CxSInv), lymphovascular invasion (LVI), lymph node (LN) status, tu stage and pt follow up (f/u). Available H&E and immunohistochemical (IHC) slides were reviewed for the presence/absence of eosinophilic intraluminal secretions, types of architectural patterns, nuclear characteristics, IHC stain results and genomic testing. Cases of primary endocervical mesonephric CA were excluded.

Results: Clinicopathologic features are summarized in Table 1. F/U (range 7-84 mo, median 21) was available for 11 pts. 2 cases are recent, and 4 pts are lost to follow up. 9 pts recurred: lung, 6 pts; peritoneum, 1 pt; pelvis, 1 pt; site unknown,1 pt. 1 pt never achieved remission, and 1 pt (FIGO stage IA) remains without disease. H&E slides (available in 14 cases) showed intraluminal eosinophilic secretions (focal to prominent) in all cases. All tu had a mixture of architectural patterns in varying proportions including: glandular 14/14; solid 11/14; papillary 6/14; slit-like 5/14; spindle cell 4/14; and trabecular 2/14. All cases at least focally had vesicular nuclei with nuclear grooves in 7 cases. IHC facilitated diagnosis in 15 cases: keratin 9/9; ER 3/13; PR 0/9; AR 0/2; CD10 9/10; calretinin 6/11; GATA3 5/5; TTF-1 1/3; PAX-8 4/5; WT-1 0/8. Genomic testing identified KRAS mutation in all 5 tested cases.

Clinicopathologic Features of 17 Mesonephric-Like Endometrial Carcinoma

Case	Age	Presentation	Tu size	>%MI	CxSInv	LVI	+LN	FIGO stage
1	53	Abnl bleeding	unkn	yes	no	yes	yes	III
2	55	Abnl bleeding	unkn	yes	yes	no	no	II
3	60	Abnl bleeding	unkn	unkn	unkn	unkn	unkn	unkn
4	58	Abnl bleeding	4 cm	yes	no	yes	no	IB
5	58	Abnl bleeding	unkn	yes	no	yes	yes	III
6	42	Abnl bleeding	8 cm	yes	yes	yes	yes	IV
7	41	Abnl bleeding	3.5 cm	yes	no	no	yes	III
8	52	Abnl bleeding	unkn	no	no	no	no	IA
9	58	Abnl bleeding	2.5 cm	yes	no	no	no	IB
10	68	Abnl bleeding	5.5 cm	yes	no	yes	no	IB
11	64	Abnl bleeding	9 cm	yes	no	no	no	IB
12	73	Abnl bleeding	11 cm	yes	no	yes	no	IB
13	60	Abnl bleeding	5.5 cm	yes	no	yes	no	IB
14	60	Abnl bleeding	4 cm	yes	no	yes	no	IB
15	64	Abnl bleeding	2.1 cm	yes	no	yes	yes	IV
16	61	Abnl bleeding	4.3 cm	yes	no	yes	yes	III
17	75	Abnl bleeding	6 cm	yes	yes	yes	yes	III

Conclusions: MenCA is uncommon and characterized by the presence of eosinophilic luminal secretions, heterogeneous architectural patterns, vesicular nuclei and an IHC profile showing diminished or lost hormone receptors, and expression of CD10, calretinin and/or GATA3. All tested cases demonstrated a KRAS mutation. Nearly all cases in this series had at least one risk factor for advanced stage with nearly half presenting as FIGO stage III or IV. 90% of pts with f/u recurred or never achieved remission with distant recurrence (lung) most common. The demonstrated aggressive behavior by these tumors underscores the need for proper recognition of this rare subtype of endometrial CA.

1031 Endometrial Tumors With Yolk Sac Tumor-Like Morphologic Patterns or Immunophenotypes: An Expanded Appraisal

Oluwole Fadare[1], Nada Shaker[2], Abrar Alghamdi[3], Raji Ganesan[4], Krisztina Hanley[5], Jonathan Hecht[6], Lynn Hoang[7], Philip Ip[8], Nuha Shaker[1], Andres Roma[2], Vinita Parkash[9], Hussain Abubakr[10]
[1]University of California, San Diego, La Jolla, CA, [2]University of California, San Diego, San Diego, CA, [3]University of Alabama at Birmingham, Birmingham, AL, [4]Birmingham Women's Hospital, Birmingham, United Kingdom, [5]Emory University, Atlanta, GA, [6]Beth Israel Deaconess Medical Center, Boston, MA, [7]University of British Columbia, Vancouver, BC, [8]The University of Hong Kong, Hong Kong, Hong Kong SAR, [9]Yale University School of Medicine, New Haven, CT, [10]King Abdulaziz University, Jeddah, Saudi Arabia

Disclosures: Oluwole Fadare: None; Nada Shaker: None; Abrar Alghamdi: None; Raji Ganesan: None; Krisztina Hanley: None; Jonathan Hecht: None; Lynn Hoang: None; Philip Ip: None; Nuha Shaker: None; Andres Roma: None; Vinita Parkash: None; Hussain Abubakr: None

Background: Uterine yolk sac tumors (YST) have gained increased recognition in recent years. The current study is a multi-faceted examination of "yolk sac differentiation" and other diagnostic aspects of this phenomenon in endometrial tumors

Design: Three analytic group were established: Group-1, the “index” group, comprised of 9 cases from multiple institutions that had been classified as YST; these cases were centrally assessed with a 35-marker immunohistochemical panel to define an expanded profile; Group-2, comprised of 70 morphologically prototypical endometrial carcinomas of various histotypes, was assessed for expression of SALL4, Glypican-3 (GPC3), and alpha-fetoprotein (AFP). Group-3 was established to define the frequency of YST-like morphology in 693 archived cases of endometrial carcinoma (593 endometrioid, 100 non-endometrioid). Any Group-2 case that expressed GPC3, AFP and/or SALL4, and any Group-3 case that showed YST-like morphology was further assessed with additional immunohistochemical markers

Results: 100% of Group-1 cases were positive for SALL4, GPC3, E-cadherin, and DNA MMR proteins. Less uniformly expressed markers included AFP (89%), Villin (89%) and PLAP (78%), 34βE12 (67%), CAM 5.2 (62.5%), EMA (56%), CD117 (50%), and p16 (50%), CDX2 (44%), p53 (44% aberrant), MOC31 (37.5%), CK7 (33%), GATA3 (33%), CK5 (25%), PAX8 (11%), and p63 (12.5%). All Group-1 cases were negative for estrogen, androgen, and progesterone receptors, calretinin, WT1, Inhibin, Napsin-A, OCT4, CD30, chromogranin, synaptophysin, and p40. For Group-2, 29 (41%) of 70 endometrial carcinomas showed expression of at least one of the 3 tested markers, and 28 (96%) of the 29 positive cases was a high-grade histotype. Additional immunohistochemical analyses on the positive cases confirmed the originally assigned histotypes. GPC3, SALL4, and AFP were positive in 30%, 20%, and 2.8% of cases respectively. Co-expression of any 2 markers was seen in <9% of cases, and co-expression of all 3 markers was seen in only 1.4%. For Group-3, we identified potential YST-like morphology in 5 (0.7%) of 693 cases, and 3 (0.4%) of these were ultimately deemed to be true YSTs based on their morphologic/immunophenotypic similarity to the Group-1 cases

Conclusions: These findings highlight the broad immunophenotypic spectrum of YST, the potential pitfalls associated with using immunophenotypes alone to define YST differentiation in endometrial carcinoma, and the utility and limitations of morphologic assessment in identifying YSTs

1032 Utility of Histology-Guided Mass Spectrometry To Define a Predictive Signature For Recurrence In Surgically-Staged, Low Risk Endometrial Cancer: A Pilot Assessment

Oluwole Fadare[1], Katy Smoot[2], Vinita Parkash[3], Erin Seeley[2], Somaye Zare[1]
[1]University of California, San Diego, La Jolla, CA, [2]New River Labs, LLC, Morgantown, WV, [3]Yale University School of Medicine, New Haven, CT

Disclosures: Oluwole Fadare: None; Katy Smoot: *Employee*, New River Labs; Vinita Parkash: None; Erin Seeley: *Employee*, New River Labs; Somaye Zare: None

Background: A small subset of "low risk" endometrial cancers recur. A *priori* prediction of which otherwise low risk cancers are most likely to recur will be clinically useful, since such patients can be more aggressively managed. The goal of this pilot study is determine whether histology guided mass spectrometry can be successfully applied to resected low risk endometrial cancers to distinguish between recurring and non-recurring cases that are otherwise clinicopathologically similar.

Design: From an institutional database, we identified 259 consecutive cases of low risk endometrial carcinoma defined as such by 2016 ESMO-ESGO-ESTRO consensus criteria (stage I, FIGO grade 1 or 2, LVSI-negative, <50% myometrial invasion). Recurrences were identified in 8% (21/259). Among the subset with available material, the patients ranged in age from 39-87 (median 62, mean 64.1), 57% were FIGO grade 1, and the average follow-up period was 49 months. We also established a control group of low risk endometrial carcinomas that did not recur, carefully matched to be similar to the study group in age, grade distribution, absence of variant morphology or adjuvant treatments, and follow-up duration. 30 cases (15 cases from each group) were assessed using histology guided mass spectrometry on a tumoral sample from the hysterectomy specimen on each case. After sample processing, mass spectrometry data were collected from approximately twenty 100 µm tumoral areas per sample as designated in an H&E stained serial section. We assessed for a classification model that significantly stratified the samples into recurring and non-recurring groups, followed by an internal validation

Results: From the combined dataset of recurring and non-recurring cases, we identified 339 spectral peaks, 117 (34.5%) of which showed significant differences between the 2 groups (wilcoxon rank sum test, p <0.00015). An internal cross validation accuracy of 82.7% was achieved when comparing the recurring and non-recurring cases.

Conclusions: Our pilot study indicates that there are some phenotypic differences between recurring and non-recurring low risk endometrial cancers, even when they otherwise appear to be clinicopathologically similar. Based on analyses of the primarily resected tumors in both groups, we established a spectral model that significantly distinguished between recurring and non-recurring low risk endometrial cancers with an 82.7% accuracy rate. This raises the theoretical possibility of predicting potentially-recurrent cases.

1033 Risk-Reducing Surgery in Patients with Lynch Syndrome, A Clinicopathologic Study

Faysal Fedda[1], Elizabeth Euscher[2], Preetha Ramalingam[1], Anais Malpica[2]
[1]Houston, TX, [2]The University of Texas MD Anderson Cancer Center, Houston, TX

Disclosures: Faysal Fedda: None; Elizabeth Euscher: None; Preetha Ramalingam: None; Anais Malpica: None

Background: Recommendations for processing risk-reducing hysterectomy & bilateral salpingo-oophorectomy (RRHBSO) in Lynch syndrome range from routine sections to entirely submitting the endometrium & bilateral adnexa. This study details the clinicopathologic findings of 29 RRHBSO for LS obtained in our institution over a period of 13 years.

Design: Patients (pt) age, personal (P) & family (F) history (hx) of Ca, genetic testing results, surveillance endometrial biopsy (EMB), preoperative (Preop) EMB, symptoms, gross findings, RRHBSO diagnoses, & follow-up (F/U) were recorded.

Results: Pts ages, 34 to 69 yrs; median, 50. 28 pts had RRHBSO, & 1 pt had RRH & bilateral salpingectomy. 18 pts had a Phx of Ca: colon (13/18), breast (2/18), thyroid (2/18); sebaceous (1/18); pancreatic (1/18). 1 pt had colon & breast Ca. All pts had strong FHx of Ca & 9/29 pts presented for testing after dx of Ca in a family member. 28 pts had genetic testing: MLH1 11/28 (39%); PMS2 7/28 (25%); MSH2 7/28 (25%); MSH6 3/28 (10%). 1 pt had PMS2 & CHEK2 while a second had MSH2 & RET mutations. 15 pts had 1-9 surveillance EMBs (mean 2.3) prior to RRHBSO. 11 pts had preop EMB, of those pts 3 were also on surveillance. No pts had uterine neoplasia related symptoms. 6 pts (20%) had endometrial polyps & 8 (27%) had adnexal masses or cysts. The entire endometrium was examined microscopically in 23 cases (79%) & the entire bilateral ovaries (OVs) & fallopian tubes (FTs) in 22 (78%) cases. 5 pts (17%) had atypical hyperplasia in the RRHBSO. All of these pts had preop EMBs: 4 with atypical hyperplasia & 1 with endometrioid CA, FIGO grade 1; 2 of them were on surveillance. 2 FTs had focal epithelial atypia but without immunohistochemical support for serous neoplasia. Two OVs had serous cystadenoma/fibroma. 6 pts had endometriosis (20%) involving the adnexa. F/U available for all pts ranged from 1-140 mo (mean 47). No pts had gynecologic Ca s/p RRHBSO, but 1 had recurrent breast Ca & 1 had colon Ca.

Conclusions: Preop EMB predicts both the presence & absence of preneoplastic/neoplastic endometrial lesions in RRH. Submission of the entire endometrium may be limited to cases with abnormal preop EMB, but no gross lesion in the RRHBSO. No case had malignancy as an incidental microscopic finding. No STIC or microscopic Ca was identified in entirely submitted ovaries & fallopian tubes. If gross lesions are absent, representative sections of the endometrium, OV and FTs is sufficient to provide an accurate histologic assessment of these cases.

1034 A Single Institution Experience with Uterine Transplants: a Histopathologic Approach

Sarah Findeis[1], James Mitchell[2], Metin Punar[1], Giovanna Saracino[1], Karen Pinto[1], Peter Dysert[1], Atin Agarwal[1]
[1]Baylor University Medical Center, Dallas, TX, [2]Baylor Scott & White Health, Dallas, TX

Disclosures: Sarah Findeis: None; James Mitchell: None; Metin Punar: None; Giovanna Saracino: None; Karen Pinto: None; Peter Dysert: None; Atin Agarwal: None

Background: The world of uterine transplant is rapidly developing. The first live birth from a uterine transplant was in 2014. From that a scoring system for assessing uterine transplant rejection for ectocervical biopsies was proposed with following categories of “negative, borderline, Grade 1, Grade 2, and Grade 3”. We present our institutional experience with uterine transplant biopsies.

Design: Based on the seminal article by J. Mölne, et.al, four main categories (squamous mucosa, stroma, arteries, and microvasculature) for the ectocervical biopsies were assessed (Table 1). A total of 3 H&E slides (each slide containing 2 levels) were evaluated for the histologic parameters and the slide/level with maximum histopathologic changes was included for data analysis. The histologic criteria from J. Mölne, et.al were also applied to score each biopsy.

Results: From 5 patients, a total of 105 biopsies were collected from the ectocervix (86), endocervix (2) and transformation zone (17). Ectocervical biopsies were included in evaluation by Spearman’s p correlation analysis to compare each variable. The variables that had the most correlations that were statistically significant (p ?0.0005) were squamous mucosa apoptotic bodies (6 correlated variables), squamous mucosa interface inflammation (5), squamous mucosa spongiosis (4), stroma overall inflammation (3), microvasculature

capillary dilatation (3), microvasculature perivascular inflammation (2), squamous mucosa lymphocytic exocytosis associated with apoptotic bodies (3), squamous mucosa overall inflammation (2), and squamous mucosa lymphocytic exocytosis (1). The ectocervical biopsies were scored for rejection as follows: negative (55), borderline (1), Grade I (1), Grade II (1), and non-conforming (28).

Table 1: Histologic features assessed for each ectocervical biopsy
SQUAMOUS MUCOSA
Overall inflammation intensity (0-4): none (0), focal/minimal (1), mild (2), moderate (3), severe (4)
Interface inflammation: none (0), unifocal (1), bifocal (2), multifocal (3), diffuse (4)
Lymphocytic exocytosis: none (0), focal/minimal (1), scattered/mild (2), numerous/moderate (3), diffuse/severe (4)
Apoptotic bodies: none (0), one focus (1), few, scattered non-confluent (2), confluent (3), severe (4)
Lymphocytic exocytosis with associated apoptotic bodies (Y/N)
Neutrophilic infiltrate (Y/N)
Spongiosis: none (0), focal/minimal (1), mild (2), moderate (3), severe (4)
Basal vacuolization (Y/N)
Dyskeratotic keratinocytes: none (0), focal/rare (1), scattered/mild (2), numerous/moderate (3), diffuse (4)
Surface erosion/ulceration (Y/N)
STROMA
Overall inflammation intensity: none (0), minimal (<100 inflammatory cells/mm^2; 1), mild (100-500 inflammatory cells/mm^2; 2), mod (500-1000 inflammatory cells/mm2; 3), severe (>1000 inflammatory cells/mm2; 4)
Location: None (N/A), sub-epithelial (1), superficial (2), deep (3), diffuse (4)
Other stromal changes [ischemia (ghost cells), edema, fibrosis] (Y/N)
ARTERIES
Endarteritis (Y/N)
Obliterative arteriopathy (Y/N)
Thrombi (Y/N)
MICROVASCULATURE
Perivascular inflammation: none (0), unifocal (1), bifocal (2), multifocal (3), diffuse (4)
Capillary dilatation: none (0), focal/minimal (1), minority (2), majority (3), diffuse/all (4)
Endothelial cell hypertrophy (Y/N)
Intravascular leukocytes (Y/N)
Venous congestion/hemorrhage (Y/N)
C4d [0, <10% (1), 10-50% (2), >50% (3)]

Conclusions: In creating a grading scheme, the correlation between variables and the statistical significance of that correlation should be accounted for. Based on our experience with “normal” cervical biopsies (preliminary studies, data not presented), we found that the proposed scoring system requires some adjustments. Although experience is invaluable in this new field, a statistical approach may clarify the important parameters in creating a revised scoring system. Our future work aims to do this by comparing uterine transplant biopsies with “normal” (same inclusion criteria as for transplant patients) and adding significant information to this new and challenging field.

1035 Whole Genome Mutation Analysis of Mullerian Adenosarcoma: A Tumor With Complex Genetic Alterations

Jean Fischer[1], Yanli Ban[2], Kruti Maniar[3], Xinkun Wang[3], Serdar Bulun[4], Jian-Jun Wei[4]
[1]McGaw Medical Center of Northwestern University, Chicago, IL, [2]Northwestern University, Feinberg School of Medicine, Chicago, IL, [3]Northwestern University Feinberg School of Medicine, Chicago, IL, [4]Northwestern University, Chicago, IL

Disclosures: Jean Fischer: None; Yanli Ban: None; Kruti Maniar: None; Xinkun Wang: None; Serdar Bulun: None; Jian-Jun Wei: None

Background: Mullerian adenosarcoma (AS) is an uncommon biphasic malignant neoplasm found in the uterus, cervix and less frequently in the adnexa. While AS is typically low-grade, variants with sarcomatous overgrowth (SO) or cytologically high-grade sarcoma can occur with associated worse clinical outcomes. The cause of the disease remains unknown, and there is significant morphologic overlap with mimics, leading to diagnostic challenges. Prior studies have been limited by low case numbers or the selective molecular analysis. To better characterize whole genome alterations in AS, we performed whole genome sequencing (WGS) on the largest subset of ASs to date.

Design: 29 AS cases diagnosed between 2002-2017 were included. Clinical data were obtained from the medical records. DNA was isolated from formalin-fixed paraffin-embedded tissue and WGS was performed on 10 cases. Bioinformatic analysis was performed and the findings of the major target gene alterations due to copy number variations (CNV), chromosome (chr) rearrangement and hot gene mutations were further analyzed and validated by immunohistochemistry, PCR-based fusion gene evaluation and NGS gene capture.

Results: Patients' ages ranged from 22-86 (median 44) yrs. Among the 29 cases (20 uterine, 5 cervical, and 4 adnexal), 15 cases (57.7%) contained SO, and 11 cases (37.9%) were cytologically high-grade. 45 CNVs were identified involving 32 genes (Table 1), with higher rates of CNVs present in cases with SO. Among 20 genes of gain or loss detected by CNV, 50.0% of them (*BCL-1, CDK4, HMGA2, KIF14, MDM2, NDUFB6, CDKN2A, NF1, YWHAE*, and *BAP1*) showed significant upregulations in AS in comparison to myometrial controls. Gain of chr 12q12-15 was seen in 8/10 cases and chromothripsis was frequently seen in chr 2, 6, 7, 16 and 17. In particular, chromosomal rearrangements were a characteristic finding with frequent genomic alterations identified in chr 7q. A total of 46 oncogenes or tumor suppressors with frequent mutations in coding regions (10-60%) were selected for target validation which is ongoing.

Table 1. Major gene alterations in Mullerian adenosarcoma

Gene	Gain/ Loss	Case No										Freq
		1	2	3	4	5	6	7	8	9	10	
MDM2	G		X	X	X	X		X				5/10
CDK4	G		X	X	X	X		X				5/10
HMGA2	G		X		X	X		X				4/10
DICER1	G										X	1/10
BAP1	L		X	X		X	X					4/10
TP53	L		X		X	X		X				4/10
MYBL1	G		X					X				2/10
TERT	G	X	X					X				3/10
Akt signaling		X	X		X			X	X			5/10
p53 signaling			X	X	X	X	X	X				6/10

Abbreviations: Freq, Frequency; G, Gain; L, Loss

Conclusions: Mullerian AS is a genetically complex disease. The DNA instability present in AS may be a defining feature as compared to other Mullerian sarcomas. In our cohort of ASs, gain of oncogenes in chr 12q12-15 and frequent chromosomal rearrangements involving chr 7q were identified which warrants further investigation. Further defining the hot gene mutation signature may help in the distinction of AS from other entities.

1036 Immunohistochemical Evaluation of GATA3, CK13 and CK17 as Markers for the Diagnosis of Differentiated Vulvar Intraepithelial Neoplasia

Ashley Flaman[1], Sarah Strickland[1], Aleksandra Paliga[2]
[1]University of Ottawa, Ottawa, ON, [2]The Ottawa Hospital, General Campus Site, Ottawa, ON

Disclosures: Ashley Flaman: None; Sarah Strickland: None; Aleksandra Paliga: None

Background: Differentiated vulvar intraepithelial neoplasia (dVIN) is a precursor to invasive squamous cell carcinoma. Its morphologic features, however, may be subtle and can overlap with reactive conditions, leading to high inter-observer variability and under-diagnosis. Immunohistochemical (IHC) stains, such as p53 and Ki67, have thus far shown limited utility. We aim to evaluate potential IHC diagnostic adjuncts by characterizing the staining pattern of dVIN with GATA3, CK13 and CK17.

Design: 21 cases of dVIN and 17 histologic mimics (6 lichen sclerosus [LS], 4 condyloma, 3 lichen planus, 2 usual-type VIN and 2 lichen simplex chronicus) were reviewed and stained with CK13, CK17 and GATA3 by IHC. The staining pattern for each IHC marker was independently reviewed and scored by 3 reviewers, with discrepancies decided by consensus.

Results: 21 cases of dVIN were identified (4 biopsies, 17 excisions). 20 (95.2%) displayed lesional epithelial immunoreactivity for CK17, most (85.7%) with diffuse staining in the superficial layers but sparing of the basal layer. 2 cases showed diffuse staining including cells in the basal layer. In contrast, in the 6 cases of LS, only 1 (16.7%) showed immunoreactivity, including staining of the basal layer.

18 (85.7%) dVIN cases displayed absent expression of CK13 in the basal layer. The remaining 3 cases showed linear basal staining. In contrast, only 1 of 6 cases of LS (16.7%) showed absence of staining in the basal layer.

17 (81.0%) of dVIN cases displayed decreased expression of GATA3 in the basal layer and weak nuclear staining above it. The remaining 4 (19.0%) showed linear/patchy basal staining with stronger staining above it. In the 6 cases of LS, no clear pattern was evident: 3 showed patchy basal staining and 3 had absent basal staining.

No single IHC marker was specific for dVIN; however, the pattern of all stains in combination could differentiate dVIN from almost all mimickers.

Conclusions: Compared to normal vulvar squamous epithelium, the pattern of staining most common in dVIN was expression of CK17 in the superficial and mid-epithelium and decreased or absent staining of CK13 and GATA3 in the basal layer. Although this study is limited by a low number of cases, the authors believe it is the first to suggest the utility of an IHC pattern-based approach for the diagnosis of dVIN, a notoriously difficult diagnosis, using a combination of CK13, CK17 and GATA3. Further study of these IHC markers is warranted.

1037 LAG-3 and GAL-3: Emerging Avenues for Immunotherapy in Mismatch Repair-Deficient Endometrial Carcinoma

Lisa Friedman[1], Kari Ring[1], Anne Mills[1]
[1]University of Virginia, Charlottesville, VA

Disclosures: Lisa Friedman: None; Anne Mills: None

Background: Mismatch repair-deficient (MMRd) endometrial carcinomas (ECs) are associated with higher neoantigen loads and more robust immune responses when compared to their mismatch repair intact (MMRi) counterparts. This unique tumor microenvironment results in increased PD-L1 expression and confers susceptibility to immunotherapy targeting the PD-1/PD-L1 checkpoint axis. However, this pathway is one of many that can contribute to tumoral immune evasion. Lymphocyte activation gene 3 (LAG-3) is another immunosuppressive checkpoint expressed on T-cells that increases tumor tolerance. One of its ligands, the glycoprotein Galectin 3 (GAL-3), can be expressed on tumor cells and promotes neoplastic progression both through the LAG-3 interaction and other mechanisms. Drugs targeting LAG-3 and GAL-3 are currently under investigation in clinical trials, but their expression in ECs has not been well studied.

Design: LAG-3 and GAL-3 immunohistochemistry (IHC) were performed on whole sections from 59 ECs [24 Lynch Syndrome (LS)-associated, 20 MLH1 promoter hypermethylated, and15 MMR-intact,]. LAG-3 positive immune cells were enumerated over 10 high-power fields (hpf) and averaged. Tumoral GAL-3 (GAL-3) staining extent was semi-quantitatively classified as negative (<1%), 1-5%, 6-10%, 11-25%, 26-50%, and >50%.

Results: LAG-3+ lymphocytes were elevated in MMRd vs MMRi ECs, with highest counts observed in LS-associated cases [93 cells/hpf in LS-associated, 81 cells/hpf in MLH1-hypermethylated, and 46 cells/hpf in MMRi]. The majority [76%] of ECs demonstrated ≥1% tumoral positivity for GAL3 with higher expression rates in MMRd vs. MMRi tumors [86% vs 47%, p = 0.004]. LS-associated ECs were more likely than MMRi ECs to have >5% GAL-3 staining [63% vs 27%, p = 0.048], but this was not true of MLH1-hypermethylated tumors [50% vs

27%, p = 0.296]. LAG-3+ immune cells and tumoral GAL-3 expression were positively correlated in LS-associated ECs [0.422, p = 0.040] but not in MLH1-hypermethylated or MMRi tumors [-0.363, p = 0.22; 0.190; p = 0.48] (**Figure 1**).

Figure 1 - 1037

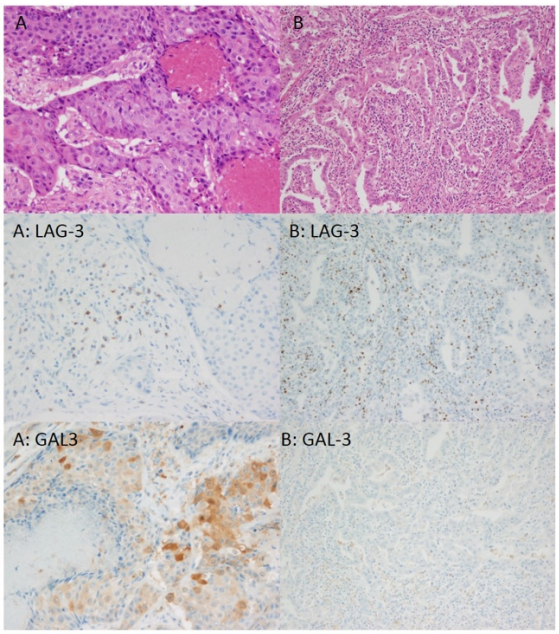

Figure 1: Overall, LAG-3 and GAL-3 expression were positively correlated in LS-associated EC [0.442, p = 0.040]. However, across individual tumors this correlation was variable, as shown in the MSH6-deficient tumors A and B. Tumor A demonstrates scattered LAG-3 positive lymphocytes in association with tumoral GAL-3 expression, while tumor B demonstrates a robust LAG-3-positive infiltrate without tumoral GAL-3 staining.

Conclusions: LAG-3+ tumor-associated lymphocytes and tumoral GAL3 expression are common in MMRd cancers, particularly LS-associated EC. This supports a role for immunotherapies targeting LAG-3/GAL-3 in a subset of EC, potentially in concert with other checkpoint inhibitors. The higher rates of >5% GAL3 expression observed in LS-associated vs. MLH1 hypermethylated tumors suggests that MMR mutations may be more immunogenic than epigenetic modification.

1038 First-Trimester Abortion and Molar Pregnancies. A Diagnostic Workflow for Triage of Hydatiform Mole: Sequential Application of p57, ki-67 and Ch17 SISH

Cinzia Giacometti[1], Luciana Maria Teresa Poletto[1], Mauro Cassaro[1]
[1]ULSS6 Euganea, Camposampiero, Italy

Disclosures: Cinzia Giacometti: None; Luciana Maria Teresa Poletto: None; Mauro Cassaro: None

Background: Diagnosis of first trimester abortion lacks of specific, univocal and widely accepted morphologic parameters in order to identify a possible cause of abortion. Many specimens are collected after many days of intrauterine retention and suffer of widely regressive changes and/or cromosomal alterations and villi harbour morphologic features suggesting partial hydatiform mole (PHM) or early complete hydatiform mole (eCHM). Distinction of hydatidiform moles from nonmolar specimens and subclassification of hydatidiform moles as complete hydatidiform mole (CHM), PHM), or eCHM are important for both clinical practice and investigational studies. The unique genetic features of CHMs (androgenetic diploidy), PHMs (diandric triploidy), and nonmolar specimens (biparental diploidy) allow for molecular techniques, such as immunohistochemical analysis of p57 expression (a paternally imprinted maternally expressed gene). Recently, a scoring method for ploidy analysis using silver in situ hybridisation (SISH) with a chromosome 17 centromere probe has been applied and validated to determine ploidy in first trimester abortion with morphological features of possible HM.

Design: The aim of the study was to discriminate between non molar specimen, PHM and eCHM using a novel diagnostic approach. Case with morphology consistent with HM (either eCHM and PHM) were tested for immunoistochemical expression of p57 and MIB1. p57 and MIB1 expression was evaluated on trophoblastic cells. SISH evaluation was conducted on at least 50 trophoblastic and stromal cells.

Results: Between January 2015 and September 2018, 558 consecutive specimen of first trimester abortion were evaluated. Histological diagnoses are summarized in Table 1. Cases with morphologic features suggesting molar pregnancy were tested for SISH. All cases of non-molar abortion (possible chromosomal anomalies) were diploid when tested for ch17 SISH. Among 23 cases classified as PHM on the

basis of morphology and immunohistochemistry, 4 cases were diploid and thus diagnosed as eCHM. Nineteen cases were confirmed as PHM (triploid status).

Histological Diagnosis	N. of cases (total=558)	Histological Features	Immunohistochemistry
Elective abortion	62	Normal first trimester chorial villi	None
Intrauterine Retention	105	Regressive changes of chorial villi	None
Inadequate for diagnosis	101	Absence of: villi/ embryo-fetal tissues/ implantation-site decidua	None
Feto-Maternal Interface Pathology	10	Absence of spiral arteries remodeling	None
CHM	18	Large atypical villi with "cisternae", atypical trophoblastic hyperplasia, trophoblastic inclusions	p57 (negative) ki-67 >90% (trophoblastic cells)
Possible chromosomal pathology	239	"Dysmorphic" villi, atypical trophoblastic configuration, trophoblastic inclusions	None
Differential diagnosis: Possible chromosomal pathology/PHM/eCHM	23	"Dysmorphic" villi, atypical trophoblastic configuration/hyperplasia trophoblastic inclusions, "cisternae", abnormal villous vessels	p57 (+; discontinous) ki-67 20-60% (trophoblastic cells)

Table 1. Histology and immunohistochemistry results

Conclusions: The application of this diagnostic workflow allowed the correct re-classification of 4 cases of eCHM (9% of molar pregnancies), erroneously diagnosed as PHM. The use of p57, MIB1 and SISH for Ch17 is easily applicable in routine diagnostic procedure and reliable in diagnostic workout of first trimester abortion specimens with morphologic features of molar pregnancies.

1039 Immunohistochemical Expression of Human Equilibrative Nucleoside Transporter-1 (hENT-1) in Gestational Diabetes Mellitus (GDM): a Preliminary Report

Cinzia Giacometti[1], Monica Guidi[2], Luciana Maria Teresa Poletto[1], Lucetta Vidotto[3], Sara Ghiretti[1], Mauro Cassaro[1]
[1]ULSS6 Euganea, Camposampiero, Italy, [2]ULSS6 Euganea, San Martino di Lupari, Italy, [3]Department of Pathology - ULSS6 Euganea, Camposampiero, Italy

Disclosures: Cinzia Giacometti: None; Monica Guidi: None; Luciana Maria Teresa Poletto: None; Lucetta Vidotto: None; Sara Ghiretti: None; Mauro Cassaro: None

Background: Gestational diabetes mellitus (GDM) is a metabolic disease that can affect placental villous maturation and villous vascularity. The main effects of GDM on placental growth are delay of villous maturation (DVM), decrease formation of vasculo-syncytial membranes and chorangiosis. Human equilibrative nucleoside transporte-1 (hENT-1) is an adenosine transporter expressed in human umbilical vein endothelial cells (HUVEC) and human placenta microvascular endothelium (hPMEC). Its role is crucial in maintaining physiological fetal adenosine levels in pregnancies and its reduction has been widely described in GDM pregnancies. We investigated immunohistochemical expression in hENT-1 delivered placentas of GDM patients subjected to dietary treatment.

Design: Twenty-one delivered placentas from patients with basal glycemia <90 mg/dl (9 hours from last feeding) and > 140 mg/dl 2 hours after an oral glucose tolerance test (OGTT) were diagnosed with GDM and subjected to dietary treatment restriction were analyzed for immunohistochemical expression of hENT-1. All placentas were formalin-fixed; sampling and diagnoses were performed according to Amsterdam protocol. Umbilical cord and placental parenchyma samples were incubated with hENT-1 antibody and its expression was quantitatively evaluated in HUVEC and hPMEC, using the proportion of positive cells and multiplying the percentage of cells demonstrating each intensity (scored from 0, absent, to 3, strong) and adding the results. Delivered placentas with histological diagnosis other than DVM served as control cases for hENT-1 expression.

Results: Patient's characteristics and pathologic results are summarized in Table 1. hENT-1 expression was inversely correlated with maternal basal glycemia (p=0.03). Sixteen cases (72%) were consistently negative and 5 cases (5/22; 22%) showed chorangiosis; 6 cases with milder form of DVM showed mild expression of hENT-1 (p=0.001). All control cases showed diffuse, moderate to intense expression (p<0.001). One control case was negative and showed chorangiosis. No correlation was found with maternal, fetal and placental weight and with OGTT at 60 and 120 minutes.

N. of cases = 22	
Patients' caracteristics (mean±SD)	
Maternal age (yrs)	34±5
Maternal weight (kg)	67±13
Basal glycemia (mg/dl)	87±2,5
OGTT 60' (mg/dl)	157±25
OGTT 120' (mg/dl)	147±28
Fetal weight (gr)	3065±435
Placentas' characteristics	
Placenta weight (gr)	459±58
Placenta diameter (cm)	17±1
Umbilical Cord Index (UCI)	0,35±0,14
Diagnosis	DVM (15/22; 68%); DVM+MVM (7/22; 34%)
Chorangiosis	5/22 (22%)
hENT-1 expression (cases vs control)	10±21 vs 149±76 (p<0.001)

Conclusions: This is the first report of hENT-1 expression in human placenta of patients with GDM. The inverse correlation with maternal basal glycemia may help to correctly classify GDM patients, even when clinically classified as normal. The absence of hENT-1 in all cases with chorangios may indicate a potential role in microvascular adaptative mechanism.

1040 Uterine Tumor Resembling Ovarian Sex Cord Tumor: A Molecular Study of Eight Cases

Emily Goebel[1], Fei Dong[1], Christopher Fletcher[1], Christopher Crum[1], Marisa Nucci[2], David Kolin[1]
[1]Brigham and Women's Hospital, Boston, MA, [2]Brigham and Women's Hospital, Harvard Medical School, Boston, MA

Disclosures: Emily Goebel: None; Fei Dong: None; Christopher Fletcher: None; Christopher Crum: None; Marisa Nucci: None; David Kolin: None

Background: Uterine tumors resembling ovarian sex cord tumors (UTROSCT) are rare uterine tumors, which usually have an indolent course. Despite their morphologic resemblance to ovarian sex cord-stromal tumors, previous studies have not found mutations in genes such as *FOXL2* or *DICER1* that are known to occur in the ovarian tumors. In addition, although originally postulated as potentially representing stromal tumors with pure sex cord differentiation, molecular abnormalities characteristic of stromal neoplasia have not been identified. This study sought to better characterize the landscape of molecular alterations

Design: Eight cases previously diagnosed as UTROSCT were reviewed and the diagnosis was confirmed by two gynecological pathologists. These UTROSCTs underwent massively parallel sequencing to detect single nucleotide variants (SNV), copy number variations (CNV), and structural variants using a targeted hybrid-capture based assay that assesses alterations in exons of 447 genes and 191 regions across 60 genes for rearrangement detection.

Results: There were no recurrent molecular alterations common to all tumors in this series. SNVs in *PIK3CA* and *ARID1B* were identified in one case, which also had a *JAZF1-SUZ12* translocation. 1 of 8 cases (12.5%) had a known pathogenic missense mutation in *MUTYH*. 2 of 8 cases (25%) contained *BRCA2* mutations (frameshift and missense) with allele fractions suggesting possible germline variants. One of the *BRCA2* mutations has a known pathogenic significance and the other is of uncertain significance. No tumor had single nucleotide variations in *FOXL2, DICER1, STK11,* or *AKT1*, which are all genes that can be mutated in ovarian sex cord-stromal tumors. One tumor had focal gain in *FOXL2*, however this was of uncertain biological significance. Copy number variants were infrequent, but 2 of 8 cases (25%) had loss of one copy of chromosome 11.

Conclusions: The typical single nucleotide variations seen in ovarian sex cord-stromal tumors are not present in UTROSCTs, and recurrent genomic abnormalities were not found. Of note, one case showed a *JAZF1-SUZ12* translocation; this case was an 11.5 cm, well circumscribed mass, that did not show typical areas of stromal differentiation suggesting UTROSCT rarely may represent stromal neoplasms with pure sex cord differentiation. In summary, UTROSCT is remarkable for its relatively low mutational burden, possibly suggesting a single molecular alteration that is not identified by this panel.

1041 Retrospective Detection of Isolated Tumor Cells in Endometrial Carcinoma by Immunohistochemistry

Emily Goebel[1], Marisa Nucci[2]
[1]Brigham and Women's Hospital, Boston, MA, [2]Brigham and Women's Hospital, Harvard Medical School, Boston, MA

Disclosures: Emily Goebel: None; Marisa Nucci: None

Background: Sentinel lymph node (SLN) biopsy for endometrial carcinoma can negate the need for lymphadenectomy. Several studies have reported on optimizing ultrastaging protocols, however the clinical significance of isolated tumor cells (ITCs) detected by ultrastaging is unknown. This study aims to retrospectively detect ITCs in patients with endometrial carcinoma and report clinicopathological features of these patients.

Design: All patients with endometrial carcinoma and SLN sampling from 2012 to 2014 were reviewed to determine lymph node (LN) status. SLNs of a subset of these patients with reported negative SLNs were further examined for detection of ITCs. The SLNs were previously sectioned at 2mm intervals, entirely submitted, and had 1 to 3 H&E levels reviewed at time of issuance of the pathology report. For this study, additional sections of SLNs were stained with cytokeratin AE1/3 at 1, 10, 20 and 50 um levels to examine for ITCs.

Results: Overall, 244 patients with endometrial carcinoma had SLN sampling +/- concurrent LN dissection between 2012 and 2014. 233 of 244 cases (95%) had negative SLNs. Of these, 49 patients (21%) had a concurrent uni- or bilateral LN dissection. 3 of the 49 patients (6%) with concurrent LN dissection had metastatic disease in non-sentinel LNs, but negative SLNs.

A subset of 25 patients and a total of 70 SLNs were examined by immunohistochemistry for ITC detection. 13 of 25 (52%) patients had concurrent uni- or bilateral LN dissection. ITCs were detected in 2 of 70 lymph nodes (2.9%) for two different patients. Both patients had endometrioid histology (grade 1 and 3); one had outer half myometrial invasion and lymphovascular invasion. The other had tumor present in paranodal and left obturator space soft tissue. Both patients received adjuvant radiation and chemotherapy.

Conclusions: Examining SLNs by immunohistochemistry detected only a small number of cases with ITCs that were not identified on routine H&E staining. Although this is a small sample, in the patients where ITCs were detected, other parameters determined treatment, including tumor grade, depth of myometrial invasion, lymphovascular invasion and disease at other sites and thus identification of low volume nodal disease would not have altered management in these cases. Larger studies are necessary to further elucidate the significance of ITCs in isolation.

1042 P16 Positive Histologically Bland Squamous Metaplasia of the Cervix: What does It Signify?

Abha Goyal[1], Lora Ellenson[1], Edyta Pirog[1]
[1]New York-Presbyterian/Weill Cornell Medical Center, New York, NY

Disclosures: Abha Goyal: None; Lora Ellenson: None; Edyta Pirog: None

Background: With increasing use of p16 immunohistochemistry (IHC) in characterization of HPV-associated premalignant lesions of cervix, we occasionally encounter p16 positivity (i.e. strong and diffuse positivity) in squamous metaplastic epithelium that lacks morphologic characteristics of “atypical squamous metaplasia” or of squamous intraepithelial lesion (SIL). Our study aims to investigate if transcriptionally active HPV can be identified in p16 positive bland squamous metaplasia of cervix and if there is any relationship between these foci and squamo-columnar junction (SCJ) cells (the postulated target of HPV infection).

Design: p16 immunostain positive cases of cervical specimens from high-risk HPV positive women (by APTIMA assay) were retrieved (April 2016-April 2018). Additionally, cervical cases reported as “atypical squamous metaplasia” that were p16 positive (January 2011- April 2018) were obtained. Of these, cases that contained at least a focus of p16 positive histologically bland squamous metaplasia, were selected upon consensus review. HPV E6/E7 mRNA in situ hybridization (RISH) using HR RNA18 probe that detects E6/E7 for 18 high-risk HPV types, was performed. If material was still present, IHC for CK7 (SCJ biomarker), Ki67 and HPV16 E2, was performed. Follow-up information was obtained from electronic medical record.

Results: 22 cases of p16 positive histologically bland squamous metaplasia of cervix were identified. Four cases were excluded due to insufficient tissue. Of the final 18 cases, HPV RISH was positive in all. The positivity was graded as weak (6 cases), moderate (8 cases) or strong (4 cases). HPV RISH was also positive in SCJ cells, identified adjacent to bland metaplasia in one case. CK7 (on 16 cases) was positive in 15, negative in one. Ki67 (on 15 cases) was positive in 10, negative in 5. HPV16 E2 (on 15 cases) was negative in all. Of the 18 study cases, concomitant high-grade squamous intraepithelial lesion (HSIL) and low-grade squamous intraepithelial lesion were identified in 11 and 3 cases respectively. Histologic/cytologic follow-up was available in 14 patients (duration:1-19 months). Six patients showed HSIL on histologic follow-up.

Conclusions: Our study demonstrates that p16 positivity in cervix is associated with the presence of transcriptionally active high-risk HPV even when there are no clear morphologic features of dysplasia. Our results suggest that these lesions are early SILs, most of which arise from SCJ and should be closely followed.

1043 Endometrial Serous Carcinoma Following Risk-reducing Prophylactic Salpingo-oophorectomy in BRCA Patients

Zakaria Grada[1], Jonathan Hecht[1], Douglas Lin[2]
[1]Beth Israel Deaconess Medical Center, Boston, MA, [2]Beth Israel Deaconess Medical Center, Needham, MA

Disclosures: Zakaria Grada: None; Jonathan Hecht: None; Douglas Lin: None

Background: An association between BRCA germline gene mutations and endometrial serous carcinoma (EMSC) has been previously proposed; however, BRCA patients typically undergo risk-reducing salpingo-oophorectomy (RRSO) without concurrent hysterectomy. The goal of this study was to determine the incidence and clinico-pathological characteristics of EMSC in a cohort of BRCA patients that had previously undergone RRSO with subsequent long-term follow-up.

Design: Seventy-six patients with BRCA germline mutations that underwent RRSO between 2002 and 2014 with a minimum 4-year follow-up after RRSO were identified from a large tertiary hospital. Clinico-pathological data of RRSO patients, BRCA mutation status, pelvic washings, incidental tubo-ovarian serous carcinomas at time of RRSO and subsequent development of endometrial or peritoneal serous carcinoma were analyzed.

Results: The mean age of cohort at the time of RRSO was 52 (range: 35–77y) and the mean clinical follow-up was 115 months (59–179 months). Forty women had BRCA1 germline mutation (52.6%, 40/76), 35 exhibited BRCA2 mutations (46.1%, 35/76), and one patient had BRCA mutation not otherwise specified (1.3%, 1/76). Two patients (2.6%, 2/76) had incidental microscopic foci of high grade tubo-ovarian serous carcinoma at the time RRSO. Long term follow-up after RRSO revealed that three patients (3.9%, 3/76) developed endometrial carcinoma within 48 to 96 months after prophylactic RRSO. Of these, 2 cases (2.6%, 2/76) were serous-type endometrial carcinoma in two patients with BRCA1 germline mutations. Patient age at time of EMSC diagnosis was 47 and 57 years old. One EMSC was low stage, pT1aN0, while the second case was high stage, pT3bN1. Both patients were alive without recurrence at least 6 years post hysterectomy. Immunohistochemistry revealed that both EMSC cases exhibited mutant p53 pattern of expression and loss of BRCA1. The third endometrial carcinoma case in the cohort was a FIGO grade 2 endometrioid endometrial carcinoma in a patient with BRCA2 germline mutation (1.3%,1/76). In contrast, 2 additional patients (2.6%, 2/76) developed peritoneal high grade serous carcinoma within 66 months following prophylactic RRSO.

Conclusions: Our study corroborates a potential association of BRCA germline mutations, in particular BRCA1, with a small (~2.5%) but not null risk of endometrial serous carcinoma. The role of endometrial cancer surveillance and/or prophylactic hysterectomy in this patient population is yet to be determined.

1044 Mesenchymal Dysplasia of Placenta – Retrospective Study of 8707 Human Placentas

Sarka Hadravska[1], Magdalena Dubova[2], Ondrej Daum[2], Bohuslava Saskova[3], Martina Putzova[2], Petr Mukensnabl[2], Michal Michal[1]
[1]Biopticka Laborator SRO, Plzen, Czech Republic, [2]Biopticka laborator s.r.o., Plzen, Czech Republic, [3]Biopticka Laborator Plzen, Plzen, Czech Republic

Disclosures: Sarka Hadravska: None; Magdalena Dubova: None; Ondrej Daum: None; Bohuslava Saskova: None; Martina Putzova: None; Petr Mukensnabl: None; Michal Michal: None

Background: Mesenchymal dysplasia of placenta (MDP) is a rare (published frequency range: 0.002-0.2%) and still mysterious placental anomaly with ,,grape-like vesicles" resembling partial hydatidiform mole by USG and macroscopic examination, apparently often associated with Beckwith–Wiedemann syndrome (BWS) and female sex of the fetus. The etiology is not yet fully understood.

Design: During the period January 1995 – July 2018 we examined 8707 placentas, 7 of them having been found to represent cases of MDP. Cytogenetic and DNA ploidy studies, and immunohistochemical staining for $p57^{KIP2}$ was performed in all 7 cases with histologic signs of MDP (i.e. edematous stem villi with cisterns and thick-walled vessels, normal terminal villi, and lack of trophoblastic proliferation, inclusions and scalloping of villi).

Results: All mothers were healthy, details on pregnancies and fetal and placental findings are shown in Table 1. Briefly, in 4 cases (A-D) the prenatal USG or genetic findings led to termination of pregnancy, case E was a missed abortion, in cases F (male mo-bi twins) and G fetuses were delivered spontaneously and are healthy. Immunohistochemical staining for $p57^{KIP2}$ was positive in villous stromal and cytotrophoblastic cells in all villi including cystic stem villi in all cases.

	Mother	Prenatal USG week of gestation	Maternal hCG	Maternal AFP	Fetus	Placental karyotype
A	24 yrs, G3, P0	Fetal congenital anomalies, placental cysts (18th week)	4.69 MoM (99.687 IU/L)	Normal	47,XY+13	47XY+13
B	32 yrs	0 (17st week)	NA	NA	47,XX+21	NA
C	31 yrs	0 (18st week)	NA	NA	Trisomy 18 (sex unknown)	NA
D	34 yrs, G2, P1	Fetal congenital anomalies, placental cysts (21st week)	Normal	Normal	47,XY+13	NA
E	33 yrs, G3, P2	Dead fetus, small placental cysts (23rd week)	Normal	Normal	46,XX	Normal karyotype
F	39 yrs, G3, P2	Mild IUGR, mild polyhydramnion in 1 fetus (37st week)	NA	Normal	Two healthy fetuses, 46,XY	Normal karyotype
G	29 yrs, G3, P1	0 (40st week)	NA	NA	Healthy fetus, 46,XX	Normal karyotype

Conclusions: We present 7 cases of MDP (frequency 0.08%), 1 of them occurring in a mo-bi twin placenta (case F). None of the cases was associated with BWS, M:F ratio of fetuses was 4:3. Neither DNA analysis nor $p57^{KIP2}$ examination revealed any molar karyotype in any of the placentas. Our series shows association of MDP with normal fetal karyotype and karyotype 47XY(X)+13, 18, 21.

1045 Novel Immunohistochemical Panel Utilizes DNA Methylation Markers 5HMC and H327Kme3 to Characterize Uterine Smooth Muscle Tumors

Chelsea Halprin[1], Gaurav Khullar[2], Serhan Alkan[3], Jean Lopategui[4], Bonnie Balzer[5], Fabiola Medeiros[5]
[1]Los Angeles, CA, [2]Cedars Sinai Medical Center, Los Angeles, CA, [3]Cedars-Sinai Medical Center, Beverly Hills, CA, [4]Cedars-Sinai Medical Center, West Hollywood, CA, [5]Cedars-Sinai Medical Center, Los Angeles, CA

Disclosures: Chelsea Halprin: None; Gaurav Khullar: None; Serhan Alkan: None; Jean Lopategui: None; Bonnie Balzer: None; Fabiola Medeiros: None

Background: The term smooth muscle tumor of uncertain malignant potential (STUMP) provides an alternative category for neoplasms that do not meet diagnostic criteria for leiomyosarcoma (LMS) but whose histologic features suggest increased risk for an aggressive clinical course. Histologic evaluation of smooth muscle tumors is sometimes challenging, especially when the type of necrosis cannot be determined with certainty or the mitotic index is moderately increased. In this study, we explore two immunohistochemical markers 5HMC and H3K27me3 as a potential aid in the differential diagnosis of LMS, STUMP and leiomyoma with bizarre nuclei (LEIO). Both 5-hydroxymethylcytosine (5HMC) and H3K27me3 are important components of the DNA methylation pathway. Their presence leads to heterochromatin formation and gene silencing, whereas their absence is associated with unregulated gene expression and tumorigenesis.

Design: The study comprised a total of 66 cases including 23 LMS, 22 STUMP, and 21 LEIO. Immunohistochemistry was performed on formalin-fixed, paraffin embedded sections with antibodies directed against 5HMC and H3K27me3. The tumors were classified as having retained expression of these markers when showing moderate to strong nuclear staining in >50% of lesional cells, and decreased expression when demonstrating moderate to strong nuclear staining in <50% of lesional cells, weak staining in any percentage of cells, or absent nuclear staining. The review was blind to the histopathologic diagnoses.

Results: 36 cases demonstrated concordant 5HMC and H3K27me3 staining patterns with 22/36 cases showing retained expression for both markers (4 LMS, 9 STUMP and 9 LEIO) and 14/36 cases revealing decreased expression for both markers (8 LMS, 5 STUMP and 1 LEIO). There was discrepant staining in 19 cases where 5HMC demonstrated retained expression and H3K27me3 showed decreased expression (8 LMS, 4 STUMP and 7 LEIO) and 11 cases where 5HMC was decreased but H3K27me3 was retained (3 LMS, 4 STUMP and 4 LEIO). Decreased expression of both makers was seen in 34.8% of LMS, 22.7% of STUMP and 4.8 % of LEIO. Retained expression of both makers was seen in 17.4% of LMS, 40.9% of STUMP and 33.3% of LEIO.

Conclusions: Although there is a trend for decreased expression of these markers inverse to the potential for aggressive biologic behavior of these neoplasms, the findings appear to have relatively low sensitivity and specificity and are therefore unlikely to be helpful in the differential diagnosis of uterine smooth muscle tumor

1046 Improved Prognostic Stratification of the Chemotherapy Response Score with Ki-67 Labeling Index: A Single Institution Study of 177 Tubo-Ovarian Carcinomas

Michelle Heayn[1], Li Zhu[2], Stephanie David[1], Esther Elishaev[3], Rohit Bhargava[4]
[1]UPMC Magee-Womens Hospital, Pittsburgh, PA, [2]University of Pittsburgh, Pittsburgh, PA, [3]Pittsburgh, PA, [4]Magee-Womens Hospital of UPMC, Pittsburgh, PA

Disclosures: Michelle Heayn: None; Li Zhu: None; Stephanie David: None; Esther Elishaev: None; Rohit Bhargava: None

Background: The Chemotherapy Response Score (CRS) has been validated as a reproducible method for determining the response of tubo-ovarian carcinoma to neoadjuvant chemotherapy (NACT). This system defines CRS-1 as minimal or no therapy response, CRS-2 as moderate therapy response, and CRS-3 as marked therapy response including both pathologic complete response (no residual tumor) and minimal residual disease (less than 2 mm). Using these criteria, we have analyzed the prognostic value of the CRS in a large cohort of tubo-ovarian carcinomas at a tertiary care center. In addition, we evaluated Ki-67 proliferative index on post-NACT samples for additional prognostic information.

Design: A database search was performed to identify tubo-ovarian carcinoma patients treated with NACT and interval debulking surgery. The post-NACT slides were reviewed to determine the CRS. For each case with residual disease a block from the omentum, or adnexa/peritoneum if no omental disease was present, was stained for Ki-67. The average and highest Ki-67 labeling index, CRS, disease-free survival (DFS), and overall survival (OS) were determined for each case.

Results: A total of 177 patients were identified with a median age at diagnosis of 67.5 years, median DFS of 15.8 months, and median OS of 36.1 months. Younger age at diagnosis is significantly associated with longer DFS and OS. The majority of the specimens (131, 74%) showed moderate treatment effect, while 27 (15.2%) showed minimal or no treatment effect (CRS-1), and 19 (10.7%) showed a marked treatment effect (CRS-3). Eight of the CRS-3 cases showed a complete pathologic response. Patients with CRS-1 and CRS-2 had statistically significantly shorter DFS and OS compared to CRS-3 (Figure 1). Further, in the subset of cases with CRS-1 or CRS-2, the average or highest Ki-67 labeling index was predictive of DFS and OS at multiple cutoff points with 10% intervals. The best separation for both DFS and OS was observed with a cutoff for highest Ki-67 labeling of 50% (Figure 2).

Figure 1 - 1046

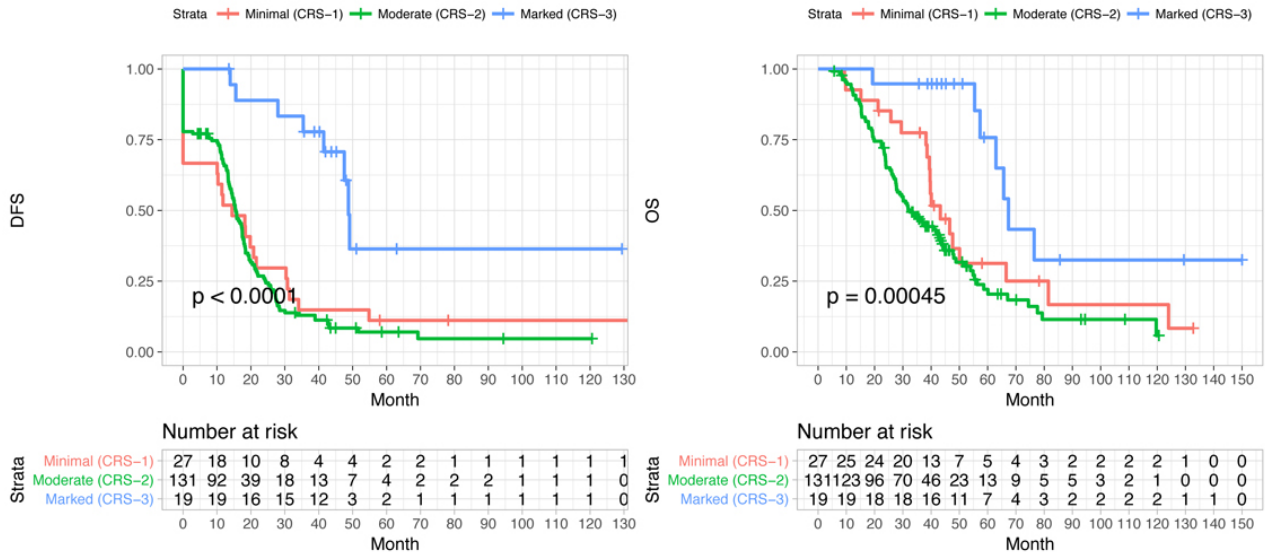

Figure 2 - 1046

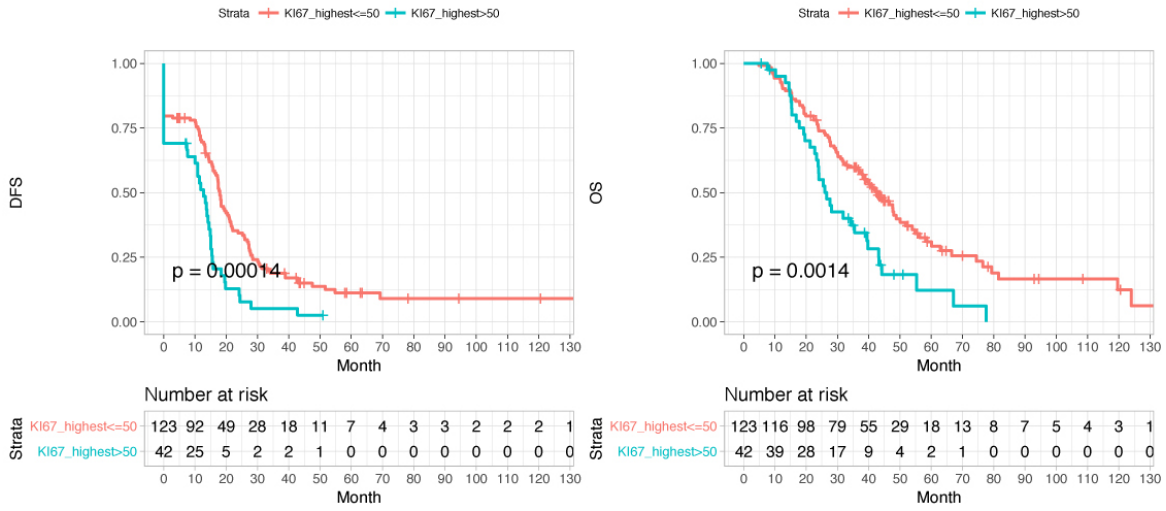

Conclusions: Our data support prior studies which demonstrate significantly longer DFS and OS in patients with marked or complete pathologic response (CRS-3) than those with minimal or moderate response (CRS-1, CRS-2). The Ki-67 labeling index may provide additional prognostic information in the subset of patients with CRS-1 and CRS-2.

1047 Clinical Outcome of Endometrial Mucinous Lesions in Correlation with their KRAS Mutation status

Jane Date Hon[1], Serena Wong[2], Natalia Buza[3], Pei Hui[1]
[1]Yale University School of Medicine, New Haven, CT, [2]Yale New Haven Hospital, New Haven, CT, [3]Yale University, New Haven, CT

Disclosures: Jane Date Hon: None; Serena Wong: None; Natalia Buza: None; Pei Hui: None

Background: Endometrial mucinous lesions with complex architecture are considered precursor lesions to endometrioid adenocarcinoma and are frequently associated with mutations of KRAS, an oncogene in the RAS-MAPK pathway often detected in mucinous malignancies of other organs. In this study, we investigate the clinical outcome of KRAS-mutant mucinous lesions of the endometrium.

Design: Consecutive endometrial biopsies or curettings with KRAS mutation evaluation due to the presence of complex mucinous lesions (with or without associated atypical hyperplasia or endometrioid adenocarcinoma) were identified at a single tertiary medical center from 2012 to 2018. Complex mucinous lesions included epithelial papillation, stratification, presence of microglandular or cribriform configurations. The cases were separated into two study cohorts based on their KRAS mutation status and the follow up specimens were comparatively reviewed.

Results: Among 129 cases, KRAS mutation was detected in 65 cases (50%). Clinical follow-up was available in 80 cases ranging from 1 month to 96 months (average 5 months), among which KRAS mutation was detected in 44 (55%) cases. Of the 80 cases with follow-up, the initial histology was complex mucinous change in 38 cases, 19 of which harbored KRAS mutation, and 13 (68%) cases had persistent complex mucinous change or progressed to atypical hyperplasia or carcinoma. In contrast, only 9 (47%) cases without KRAS mutation persisted or progressed. Atypical hyperplasia with complex mucinous change had similar outcome between those with KRAS mutation and those without the mutation (Table 1). Carcinomas with mucinous differentiation also showed similar outcome regardless of their KRAS mutation status (Table 1).

Type of Lesion	Follow-up (TAH/EMC)	Ki-Ras Mutant (N=44)	Ki-Ras Wild-Type (N=36)
Complex Mucinous Change (N=38)	Resolved	6 = 32%	10 = 53%
	Persistent	3 = 16%	0 = 0%
	Atypical Hyperplasia	5 = 26%	4 = 21%
	Endometrioid Carcinoma	5 = 26%	5 = 26%
Atypical Hyperplasia with Complex Mucinous Change (N=30)	Resolved	7 = 37%	3 = 27%
	Atypical Hyperplasia	9 = 47%	6 = 55%
	Endometrioid Carcinoma	3 = 16%	2 = 18%
Endometrial Carcinoma with Mucinous Differentiation (N=12)	No residual	1 = 17%	0 = 0%
	Persistent	5 = 83%	6 = 100%

Conclusions: KRAS mutation positive endometrial complex mucinous lesions have a higher risk of disease persistence or progression, whereas lesions with wild type KRAS resolve in over 50% of the cases. However, KRAS mutation status in complex mucinous changes with atypical hyperplasia or endometrial carcinoma does not confer significant outcome difference. KRAS mutation analysis may be most useful in prognostication of complex mucinous change without associated atypical hyperplasia or carcinoma.

1048 Fumarate Hydratase-Associated Leiomyomas: Morphologic Spectrum and New Insights

Tieying Hou[1], Anais Malpica[1], Elizabeth Euscher[1], Preetha Ramalingam[2]
[1]The University of Texas MD Anderson Cancer Center, Houston, TX, [2]Houston, TX

Disclosures: Tieying Hou: None; Anais Malpica: None; Elizabeth Euscher: None; Preetha Ramalingam: None

Background: Uterine leiomyoma (LM) associated with hereditary leiomyomatosis and renal cell carcinoma syndrome i.e. Reed syndrome (RS), a rare autosomal dominant disease caused by germline mutations in the fumarate hydratase (*FH*) gene, exhibits unique histopathological features including bizarre/multinucleated cells, eosinophilic inclusion-like nucleoli, intracytoplasmic/intranuclear inclusions, hemangiopericytoma-like vascular pattern, and stromal edema. The aim of our study was to examine the clinicopathologic features of LM with microscopic features associated with FH-deficiency.

Design: 21 cases of uterine LM with histological features suggestive of fumarate hydratase deficiency (FH-LM) were retrieved (2004-2018). The search was performed for patients (pts) with a diagnosis of smooth muscle tumor of uncertain malignant potential (STUMP) and slides reviewed to determine if features of FH-LM were present prior to description of this entity. Recent cases had a diagnosis of LM with features associated with FH deficiency. The histologic and clinical features, immunohistochemical stains and results of genetic testing when available were evaluated. Of the 26 STUMPs with available H&E slides, 3 had histologic features of FH-LM.

Results: Of 21 patients (pts) 10 were Caucasian, 3 Asian, 2 African American, 2 Hispanic and 4 unknown. Average number of slides reviewed was 4 (range 1-16). Tumor size ranged from 2.5 to 24 cm (mean: 8.9cm). Histologic features are summarized in Table 1. 4 cases of FH-LM-like tumors were negative for FH immunostain, 3 of 21 pts (mean age 31yrs, range 27-36 yrs) had known clinical features and/or germline mutation (GM) associated with RS. Of the 18 pts with FH-LM-like features (mean age 43.3yrs, range 29-83yrs), 2 had negative genetic testing for FH GM, 4 had low risk for RS due to either age, negative family history and absence of cutaneous/renal lesions; the clinical/genetic testing status of other pts is unknown. All 3 pts with RS are alive with no evidence of recurrent SMT (follow up range 1-64 mos).

Table 1: Histopathologic Features of RS-LM versus FH-LM-Like Tumors

	BN/MNC	CRN	INI	ICI	HPVA	Edema	Smudgy Nuclei	Verocay-body-like pattern
RS	3/3 (100%)	3/3 (100%)	3/3 (100%)	3/3 (100%)	3/3 (100%)	3/3 (100%)	0/3 (0%)	0/3 (0%)
FH-LM-like tumor	18/18 (100%)	13/18 (72%)	3/18 (17%)	18/18 (100%)	15/18 (83%)	8/18 (44%)	3/18 (17%)	2/18 (11%)

BN/MNC: Bizarre nuclei/multinucleated cells; CRN: Cherry red nucleoli, INI: Intranuclear cytoplasmic inclusions, ICI: Intracytoplasmic eosinophilic inclusions, HPVA: Hemangiopericytoma-like vessels

Conclusions: Most of the histologic features of RS-LM are also present in FH-LM-like tumors with no clinical or genetic evidence of the syndrome. Edema and intranuclear inclusions were seen in all RS-LM but not in most FH-LM-like tumors. FH immunostain is not specific for RS-LM. Awareness of the histologic features of FH-LM will prevent over diagnosis of STUMP and alert the clinician to exclude RS, particularly in women younger than 35 years of age with symptomatic leiomyomas.

1049 ICCR Criteria For The Diagnosis of Multifocal pT1a1 Squamous Cell Carcinoma of the Cervix: A Retrospective Analysis

Jingjing Hu[1], Mariah Leivo[1], Dennis Adams[2], Somaye Zare[3], Oluwole Fadare[3]
[1]University of California, San Diego, San Diego, CA, [2]Stanford University School of Medicine, Mountain View, CA, [3]University of California, San Diego, La Jolla, CA

Disclosures: Jingjing Hu: None; Mariah Leivo: None; Dennis Adams: None; Somaye Zare: None; Oluwole Fadare: None

Background: The frequency of multifocality in stage Ia1 cervical squamous carcinomas (SCC) has reportedly ranged from 12% and 25%, and these patients have been reported to have a good prognosis. The International Collaboration on Cancer Reporting (ICCR) recently amalgamated published data and proposed diagnostic criteria for multifocal pT1a1 cervical cancers: cancer foci 1) separated by blocks of uninvolved cervical tissue; 2) located on separated cervical lips with discontinuous tumor; 3) situated far apart from each other in the same section. In this study, we assess our experience with mutifocal stage Ia1 cervical SCC that were retrospectively classified as such using ICCR criteria

Design: 52 consecutive cases of AJCC stage pT1 cervical SCCs diagnosed in a conization (n=20) or LEEP (n=32) specimen were reviewed. ICCR criteria were used to re-classify cases and to define multifocality in the stage Ia1 subset. Multifocal and unifocal cases were compared regarding patient outcomes

Results: After reclassification by ICCR criteria, there were 21, 13, and 18 cases in stages 1a1, 1a2, and Ib respectively. 8 (38%) of the 21 stage 1a1 cases were classified as multifocal (5 had hysterectomy; after a mean follow-up duration of 5.8 years, 86% showed no recurrences, 1 patient developed distant recurrence 2 years after a hysterectomy; this patient also had lymphovascular invasion in the original LEEP); the remaining 13 were classified as unifocal (6 had hysterectomy; none developed recurrent disease over a mean follow-up duration of 5 years). Multifocal and unfocal cases were comparable regarding patient age (49 vs 47), mean depth of stromal invasion (1.9 mm vs 1.2 mm), and rates of positive margins on cone/LEEP. None of the stage 1a1 patients had adjuvant chemo-radiation. For patients that underwent a hysterectomy post-cone/LEEP, the rate of finding residual carcinoma in the multifocal group (60%) was higher than in the unifocal group (30%)

Conclusions: With strict adherence to ICCR criteria, we found a higher frequency (38%) of multifocal disease than some previously published studies, which may be related to these criteria and/or geographic/population differences. Favorable patient outcomes were demonstrable for both unifocal and multifocal cases. However, we did identify a multifocal stage 1a1 case that recurred, and multifocal cases appeared to have a higher rate of residual disease in the subset that underwent a hysterectomy, highlighting the necessity for close follow-up in multifocal cases

1050 IFITM1 as an Endometrial Stromal Marker: Diagnostic Use in Determining Myoinvasion in Endometrial Carcinoma and Distinction of Stromal Lesions from Smooth Muscle Tumors

Sarah Hugar[1], Eric Statz[1], Mirka Jones[2], Esther Elishaev[3], Rohit Bhargava[4]
[1]University of Pittsburgh Medical Center, Pittsburgh, PA, [2]University of Pittsburgh, Pittsburgh, PA, [3]Pittsburgh, PA, [4]Magee-Womens Hospital of UPMC, Pittsburgh, PA

Disclosures: Sarah Hugar: None; Eric Statz: None; Mirka Jones: None; Esther Elishaev: None; Rohit Bhargava: None

Background: Interferon-induced transmembrane protein 1 (IFITM1) is a novel endometrial stromal marker which has recently been described as being superior to CD10 in the evaluation of myometrial invasion by uterine endometrioid adenocarcinoma (Parra-Herran et al 2014, Busca et al 2016) and in differentiating endometrial stromal sarcomas from smooth muscle neoplasms of the uterus (Busca et al 2018).

Design: We investigated the immunohistochemical staining pattern of IFITM1 and CD10 in 14 cases of endometrioid adenocarcinoma of the uterus with myoinvasion, 9 of which had concurrent involvement by adenomyosis. We also investigated the staining pattern of IFITM1 and CD10 in 21 cases of leiomyoma, 10 cases of atypical leiomyoma, 3 smooth muscle tumors of uncertain malignant potential (STUMP), and 36 cases of leiomyosarcoma. Staining was scored for intensity and distribution according to the schema previously defined by Busca et al (0 = absent, 1 = weak/<50%, 2 = moderate/50-75%, 3 = strong/>75%) (Busca et al 2016, Busca et al 2018). A total score was obtained by adding intensity and distribution scores and classified as positive (score 3-6) or negative (score 0-2).

Results: 13 of 14 cases of invasive endometrioid adenocarcinoma of the uterus showed loss of IFITM1 staining in the stroma around the glands of interest, while 0 of the 14 cases showed loss of CD10 staining. 7 of 9 foci of adenomyosis showed preserved IFITM1 staining in the stroma around the glands of interest, while 9 of 9 showed CD10 staining. Unlike CD10, IFITM1 staining was significantly different between areas of adenomyosis and adenocarcinoma (p = 0.001). Additionally, 0 of 34 cases of leiomyoma, atypical leiomyoma, or STUMP showed categorically positive staining with IFITM1 or CD10. In contrast, 9 of 36 (25%) cases of leiomyosarcoma showed positive staining with IFITM1, whereas 11 of 36 (30%) cases of leiomyosarcoma showed positive staining with CD10 (the difference was not statistically significant, p=0.79).

Figure 1 - 1050

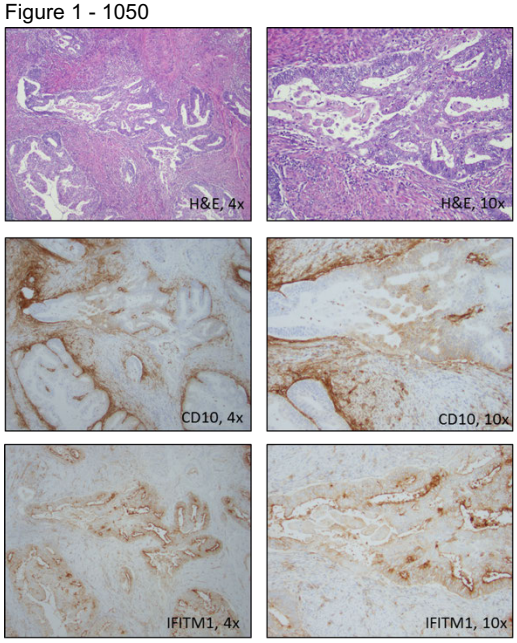

Conclusions: IFITM1 is superior to CD10 in differentiating adenomyosis (preserved staining around glands) from areas of invasive endometrioid adenocarcinoma of the uterus, where peri-glandular staining is expected to be lost. In our experience, IFITM1 and CD10 staining may be seen in a minority of cases of leiomyosarcoma, while it is not observed in leiomyoma, atypical leiomyoma, or STUMP. Both IFITM and CD10 antibodies are equally suitable in a panel to distinguish smooth muscle tumors from stromal tumors.

1051 Evaluation of criteria for distinguishing uterine smooth muscle tumors of uncertain malignant potential (STUMP) from mimics and improved prediction of patient outcome: A multi-institutional study of 51 cases

Philip Ip[1], Zehra Ordulu[2], Diana Lim[3], Robert Soslow[4], Robert Young[5], Liwei Jia[4], Sarah Chiang[4], Esther Oliva[6]
[1]The University of Hong Kong, Hong Kong, Hong Kong SAR, [2]Massachusetts General Hospital, Dorchester, MA, [3]National University Hospital, Singapore, Singapore, [4]Memorial Sloan Kettering Cancer Center, New York, NY, [5]Harvard Medical School, Boston, MA, [6]Massachusetts General Hospital, Boston, MA

Disclosures: Philip Ip: None; Zehra Ordulu: None; Diana Lim: None; Robert Soslow: *Speaker*, Ebix/Oakstone; Robert Young: None; Liwei Jia: None; Sarah Chiang: None; Esther Oliva: None

Background: The diagnostic criteria for uterine smooth muscle tumor of uncertain malignant potential (STUMP) have varied. In addition to the Bell criteria, there have been other proposed parameters for typical spindle cell tumors.

Design: Uterine STUMPs/low-grade leiomyosarcomas seen in consultation (n=72) and from our respective tertiary hospitals (n=28) were reviewed in 2 multi-head microscopy sessions when ≥4 of us were present at any time. After consensus review, 49 cases were excluded (18 diffusely epithelioid and 4 diffusely myxoid tumors, 2 inflammatory myofibroblastic tumors, 3 high-grade leiomyosarcomas, 13 benign variants and 9 with other unique morphologies). The remaining 51 cases (37 were consults) were evaluated using the Bell criteria (atypia, mitotic count and tumor cell necrosis) and classified into atypical leiomyomas with low-risk of recurrence (ALLRR), atypical leiomyomas with limited experience (ALLE) and smooth muscle tumors of low-malignant potential (SMTLMP). These were further assessed for presence of long sweeping fascicles (defined as broom-like, long and occupying >75% of the field diameter of a x10 objective, hypercellular of at least moderate degree, nuclei with a clonal, uniform appearance and with a palisading/herringbone arrangement), focal myxoid or epithelioid areas, infiltrative margins, vascular space intrusion/invasion (VSI) and atypical mitoses.

Results: The median age of patients was 46 years. The median size of tumors was 7.5 cm. Follow-up was obtained in 33/51 patients (64.7%). After a median disease-free period of 84 months, 15 patients (45.5%) had a recurrence. Histologically, there were 8 ALLRR, 6 ALLE, and 1 SMTLMP. Among these, 5 had an infiltrative border, 3 had VSI and 1 had focal epithelioid differentiation. All 15 tumors had extensive long sweeping fascicles. In tumors without recurrence, 8 were ALLRR, 5 were ALLE, 2 were SMTLMP. Two others had focal myxoid areas, and 1 had focal atypia and indeterminate necrosis. Among tumors without a recurrence, 6 had an infiltrative border, 2 had VSI and 1 with atypical mitoses. None of these 18 tumors had long sweeping fascicles. As controls, 51 other benign leiomyomas were reviewed but none contained fascicles which met our criteria of long sweeping fascicles.

Conclusions: The only parameter in our study which was associated with a subsequent recurrence was long sweeping fascicles. Whether the other parameters in combination can predict outcome in cases of problematic spindle cell smooth muscle tumors remains to be evaluated.

1052 "Amyloidogenic High-Risk HPV" in Localized Amyloidosis Associated with Classic-Type High-Grade Vulvar Squamous Intraepithelial Neoplasia!

K Islam[1], Gahie Nam[2], Kamaljeet Singh[3], Katrine Hansen[4], C. James Sung[1], M. Ruhul Quddus[1]
[1]Women & Infants Hospital/Alpert Medical School of Brown University, Providence, RI, [2]Rhode Island Hospital/Brown University, Providence, RI, [3]Women and Infants Hospital, Providence, RI, [4]Women and Infants Hospital of Rhode Island, Providence, RI

Disclosures: K Islam: None; Gahie Nam: None; Kamaljeet Singh: None; Katrine Hansen: None; C. James Sung: None; M. Ruhul Quddus: None

Background: Classic-type vulvar squamous intraepithelial neoplasia (VIN) is reported to be uniformly associated with high-risk HPV type 16 (hrHPV). Localized amyloidosis has been recently reported in association with classic VINs (Quddus 2014). The components of the amyloid were found to be Cytokeratin 5 (CK5) and Cytokeratin 14 (CK14) by LC-MS/MS studies. The hrHPV subtype(s) associated with these cases have not yet been identified or reported. The current study is designed to identify hrHPV subtype(s) in classic-type high grade VINs associated with localized amyloidosis.

Design: Forty five samples of localized vulvar amyloidosis associated with classic high grade VINs were retrieved from the archival files. The H&E and Congo-Red slides were reviewed, the diagnoses confirmed, and residual paraffin embedded tissue blocks were selected. DNA was extracted using the QIAamp DNA FFPE Tissue Kit (QIAGEN Inc, Valencia, CA 91355, Cat No. 56404). The hrHPV genotyping was performed by using propriatory GenomeMeTM's GeneNavTM HPV One qPCR Kit (GenomeMe, Richmond, BC, Canada) which specifically detects HPV 16 &18 and non-specifically detects 12 other rare subtypes (HPV 31, HPV 33, HPV 35, HPV 39, HPV 45, HPV 51, HPV 52, HPV 56, HPV 58, HPV 59, HPV 66, and HPV 68). Subsequently all non-16/18 + samples were further genotyped by a second Kit, GenomeMeTM's GeneNavTM HPV Genotyping qPCR Kit. All tests were performed on the Bio-RAD CFX Touch qPCR instrument.

Results: The distribution of hrHPV subtypes is shown in the pie chart (Figure 1). Figure 2 shows two cases of high grade VINs with amyloidosis (H&E and Congo Red).

Figure 1 - 1052

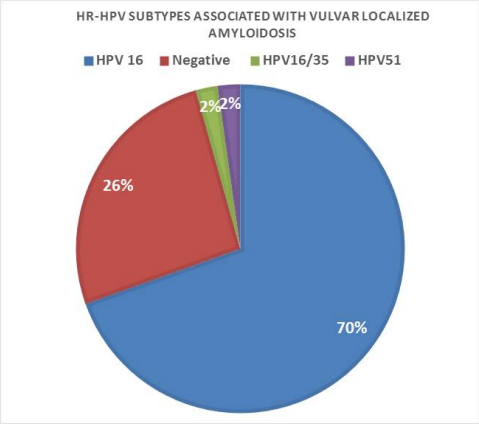

Figure 2 - 1052

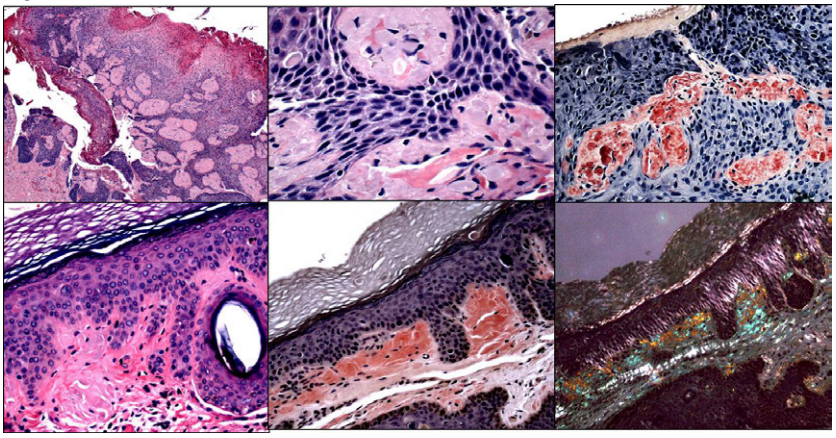

Conclusions: Although the constitutents of amyloid in localizaed vulvar amyloidosis is now known the exact pathogenesis of amyloid deposition in classic type hrHPV-related VIN is still unknown. Lack of demonstrable HrHPV in a significant proportion of such cases (25%) raises many interesting questions. It is not unreasonable to speculate that amyloid deposition may represent a response of the body to

fight against the HPV infection and possibly represent regressive changes in VIN. It is also not impossile that there are yet unknown HPV subtypes that are associated with amyloid deposition in classic-type high grade VIN.

Reference:

Quddus MR, Sung CJ, Simon RA, Lawrence WD.Localized amyloidosis of the vulva with and without vulvar intraepithelial neoplasia. Report of a series.Hum Pathol 2014;45:2037-2042.

1053 Acute Funisitis Correlates with the Risk for Early-onset Sepsis in Term Newborns Assessed Using the Kaiser Sepsis Calculator

Hongxiu Ji[1], Lennart Tan[2], Margie Bridges[3], Michele McRae[3], Kristin Graham[3], Shilpi Chabra[4]
[1]Incyte Diagnostics, Spokane, WA, [2]Spokane, WA, [3]Overlake Hospital Medical Center, Bellevue, WA, [4]University of Washington, Seattle, WA

Disclosures: Hongxiu Ji: None; Shilpi Chabra: None

Background: The risk of neonatal early-onset sepsis (EOS) is traditionally assessed on maternal signs of clinical chorioamnionitis per guidelines established by CDC. Recently, an online EOS risk calculator was developed by Kaiser Permanente using maternal and neonatal clinical parameters, which has gained attraction among obstetricians and neonatologists. Initial data suggests that the Kaiser Sepsis Calculator appears superior to the CDC guidelines in triaging neonates for EOS. We are interested in whether an increased Kaiser sepsis risk score correlates with histologic acute chorioamnionitis or acute funisitis.

Design: Included in this retrospective review were term neonates (gestational age of 37-42) admitted to Neonatal Intensive Unit (NICU) immediately after delivery from January 1, 2015 and December 31, 2016 for maternal clinical chorioamniotis. The clinical charts from the mother-baby pairs were reviewed. An EOS risk score was obtained using the online Kaiser Sepsis calculator. Placental pathology reports and/or histologic sections were available in 119 of 135 (88.1%) cases, which were reviewed. The presence or absence of acute chorioamnionitis and acute funisitis were recorded. The severity of the acute inflammation was categorized based on the recently published Amsterdam diagnostic criteria. A SPSS software (IBM, New Jersey) was used for statistical analysis.

Results: Blood cultures were negative in all 119 neonates; yet all of them received intravenous antibiotics and NICU observation for 48 hours. There were no instances of readmission for sepsis after discharge. The Kaiser Sepsis Calculator could identify 97 of 119 (81.5%) neonates without increased risk for sepsis, which would markedly reduce the need for blood culture and NICU admissions. Acute chorioamnionitis was present in 100 of 119 cases (84%), in which 44 cases (44%) show severe acute chorioamniotis. Acute fuinisitis was recognized in 87 of 119 (73.1%) cases, all of which had concurrent acute chrioamnionitis. Severe umbilical cord inflammation was seen in 38 of the 87 cases (44%). We found that the Kaiser Sepsis risk score correlates with the presence and severity of acute funisitis ($p=0.037$ and $p=0.044$, respectively) but not with the presence or the severity of acute chorioamnionitis ($p=0.672$ and $p=0.105$, respectively).

Conclusions: Acute funisitis, as an objective measure for fetal inflammatory response to acute insults and occasional ascending infection, correlates with the EOS risk score obtained from the recently developed Kaiser Sepsis Calculator. Our study supports the notion that the Kaiser Sepsis Calculator may help to effectively reduce unwarranted blood culture, antibiotics treatment and NICU admission in term neonates.

1054 A comparison of Daxx (Death domain associated protein 6) in different endometrial carcinoma histotypes

Cao Jin[1], Sean Hacking[2], Mansoor Nasim[3]
[1]Donald and Barbara Zucker School of Medicine at Hofstra/Northwell, Lake Success, NY, [2]Northwell Health, Queens, NY, [3]Northwell, Lake Success, NY

Disclosures: Cao Jin: None; Sean Hacking: None; Mansoor Nasim: None

Background: Daxx (death domain-associated) is an H3.3-specific histone chaperone. By interaction with ATRX (α-thalassemia/mental retardation syndrome X-linked) , the protein complexes are required for H3.3 incorporation at the telomeres. Inactivation of either Daxx or ATRX can be associated with alternative lengthening of telomeres (ALT), which mechanism can sustain limitless replicability of cancer cells. Recently, Daxx point mutations have been found to in a high percentage of tumors including angiosarcoma, glioblastoma, pancreatic neuroendocrine tumor or uterine leiomyosarcoma etc. In accordance, the Daxx mutations correlated with loss of protein expression by IHC analysis. Uterine carcinoma represents a histologically diverse group of tumors carrying different clinicopathological features. Therefore, in this study, we sought to determine the (1) if loss of Daxx is present in uterine carcinoma (2) if the Daxx expression pattern the same across all the uterine carcinoma subtypes

Design: We studied a series of 65 uterine carcinomas (30 endometrioid type (12 Grade 1, 12 Grade 2 and 6 Grade 3), 8 serous type, 14 clear cell type and 13 undifferentiated/dedifferentiated type (UEC/DDEC)). Immunohistochemical stains for Daxx was assessed on tissue sections. In all cases the percentage of nuclear staining positivity of Daxx were graded as 0-50%, 50-75% and more than 75%.

Results: Results are summarized in Table 1.

Nuclear expression of Daxx showed variable patterns among different histotypes. Among all high grade carcinomas (G3, serous, clear cell and UEC/DDEC), there were 61% (25/41) of the cases showed significant retained Daxx nuclear staining (>75%) compared to the low grade carcinomas (G1 and G2, 1/24) (61% vs 4.2% *p*= 0.0001). In addition, in the 11 DDEC cases, all the differentiated components showed loss of Daxx nuclear staining compared to the undifferentiated components whereas Daxx mainly retained nuclear staining.

Tumor type	**Percentage of Daxx nuclear positivity**		
(n=65)	**0-50%**	**50-75%**	**>75%**
UEC/DDEC (n=13)	0	2	11 (on UC component)
Clear cell carcinoma (n=14)	5	4	5
Uterine serous carcinoma (n=8)	2	0	6
Uterine endometrioid carcinoma (n=30)			
G1 (n=12)	10	1	1
G2 (n=12)	11	1	0
G3 (n=6)	0	3	3

Conclusions: We conclude that loss of Daxx is associated with low grade endometrial carcinomas, however such association is not present in the high grade ones. This may suggest that Daxx plays an important role in the progression. Such findings may have significant implications for target therapies in high grade endometrial carcinomas.

1055 The ProMisE Algorithm Segregates High Grade Endometrial Endometrioid Carcinoma into Prognostically Significant Groups

Amy Joehlin-Price[1], Jessica Van Ziffle[2], Karuna Garg[2]
[1]Cleveland Clinic, Cleveland, OH, [2]University of California, San Francisco, San Francisco, CA

Disclosures: Amy Joehlin-Price: None; Jessica Van Ziffle: None; Karuna Garg: None

Background: Multiple studies have shown that FIGO grade 3 endometrial endometrioid carcinoma (EEC) is a heterogeneous group of tumors with variable morphology, IHC staining pattern and clinical outcome. This may be related to the variety of underlying molecular alterations, as FIGO grade 3 EEC is represented across all 4 molecular groups in the TCGA. Yet grade 3 EEC is often treated clinically as one entity. Recently, the ProMisE clinical classifier has been proposed as a practical alternative to intensive molecular analysis. We wanted to apply this algorithm in a large set of high grade EEC from a single institution and correlate the results with clinical outcome.

Design: IRB approval was obtained and the pathology database was searched to identify all patients FIGO grade 3 EEC who underwent hysterectomy at our institution. Slides were reviewed to confirm the diagnosis. A small next generation sequencing panel was performed to identify mutations in the exonuclease domain of *POLE*. Immunohistochemistry (IHC) including mismatch repair (MMR) proteins and p53 was performed on a mixture of triplicate core TMAs and whole sections. The ProMisE algorithm was used to classify the EEC into 4 groups: MMR deficient followed by *POLE*-mutant followed by p53 aberrant. We also applied an alternative strategy of segregating the tumors, first by POLE mutation then followed by MMR and p53 to evaluate for any differences in results.

Results: Ninety-seven cases underwent *POLE* mutation testing and IHC for p53 and the MMR proteins (see table). The overall survival was significantly different in the four groups (see figure). When separating *POLE*-mutant tumors first, a similar overall survival curve was produced.

	POLE-mutated (n=12, 12%)	MMR deficient (n=42, 43%)	p53 aberrant (n=18, 19%)	NSMP (n=25, 26%)
Median age at diagnosis, years (range)	55.5 (52-77)	62.5 (53-96)	66 (38-88)	62 (44-82)
FIGO stage I-II	10 (83%)	29 (69%)	9 (50%)	12 (48%)
FIGO stage III-IV	2 (17%)	13 (31%)	9 (50%)	13 (52%)
Adjuvant therapy	5 (42%)	16 (38%)	11 (61%)	10 (40%)
No evidence of disease	12 (100%)	28 (67%)	6 (33%)	12 (48%)
Dead of disease	0 (0%)	4 (10%)	8 (44%)	5 (20%)
Alive with disease	0 (0%)	1 (2%)	2 (11%)	4 (16%)
Dead of other or unknown causes	0 (0%)	9 (21%)	2 (11%)	4 (16%)

Figure 1 - 1055

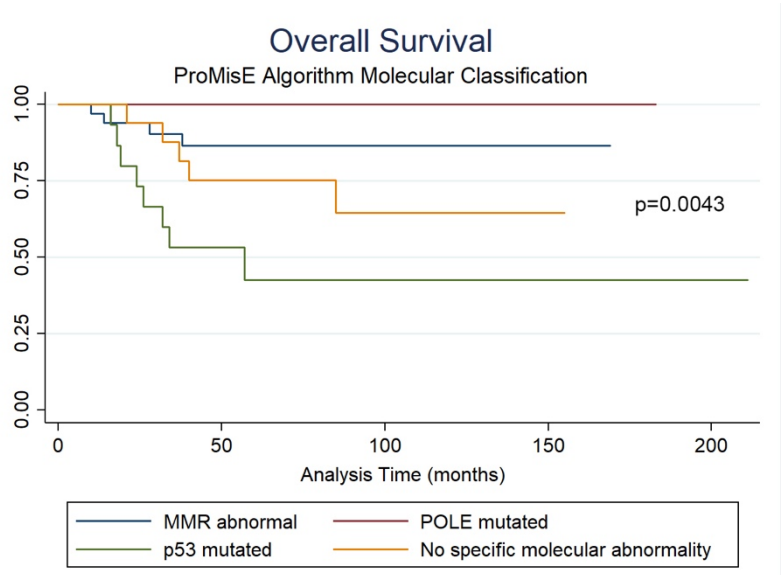

Conclusions: Our study validates the ProMisE algorithm which stratified high grade EEC by clinical outcome with the *POLE*-mutant group showing excellent prognosis and the p53 aberrant group showing the worst clinical outcomes. The overall survival curves were similar for both the ProMisE clinical classifier and a schema by which *POLE*-mutated tumors were removed from the cohort ahead of mismatch repair abnormal cases.

1056 Clinicopathologic Features of a Cohort of POLE-Mutated FIGO Grade 3 Uterine Endometrioid Adenocarcinomas

Amy Joehlin-Price[1], Jessica Van Ziffle[2], Karuna Garg[2]
[1]Cleveland Clinic, Cleveland, OH, [2]University of California, San Francisco, San Francisco, CA

Disclosures: Amy Joehlin-Price: None; Jessica Van Ziffle: None; Karuna Garg: None

Background: Endometrial cancers with a *POLE* mutation have an excellent prognosis, despite many being FIGO grade 3 endometrial endometrioid carcinoma (EEC). Recognizing these tumors may have prognostic and therapeutic implications. Some have suggested morphologic features that could enable their recognition. We aimed to further evaluate the morphologic, immunohistochemical (IHC) and clinical features of grade 3 EEC with an established *POLE* mutation.

Design: The pathology database was searched to identify grade 3 EEC; slides were reviewed. Clinical data was obtained via EMR and an institutional cancer registry. A small next generation sequencing panel identified mutations in the exonuclease domain of *POLE*. IHC for MMR proteins, p53 and PTEN was performed on TMAs.

Results: Sixteen FIGO grade 3 EEC with a *POLE* mutation were identified (16%). POLE mutations included p.P286R (n=9), p.M444K (n=2), p.V411L, p.P286H, p.S459F, p.A456P, and p.A426V (n=1 each).

Clinical features: Age ranged from 52 to 77 (median 56) in *POLE*-mutated cases. Most presented at FIGO stage I (81%) while 3 presented at high stage (III-IV). Lymphovascular invasion was noted in 6. Three received radiation (2 beam, 1 implant) and 2 received chemotherapy.

Six were recommended adjuvant treatment but refused. All 16 showed no evidence of disease, with follow up ranging from 7 to 183 months. One died of an unrelated cause 183 months after diagnosis.

Morphology: Two cases were diffusely pleomorphic, but 11 additional cases demonstrated foci of markedly pleomorphic (serous-like) cells in a background of uniform tumor cells. Peritumoral lymphocytes (PTLs) were seen in 15 cases and there were significant tumor infiltrating lymphocytes (TILs) in 13. The morphologic features were non-specific; non-*POLE*-mutated tumors had overlapping findings (see table).

IHC: Four cases of *POLE*-mutant tumors showed concurrent loss of MMR proteins: one with absent MLH1/PMS2, two with absent PMS2, and one with loss of MSH2/MSH6. Two cases showed aberrant p53 expression, one of which also showed PMS2 loss. Five cases showed PTEN loss.

	POLE-mutant (n=16)	Non-*POLE*-mutant, MMR abnormal (n=38)	Non-*POLE*-mutant, p53 aberrant (n=18)	NSMP (n=25)
Peritumoral lymphocytes (PTLs)	15 (94%)	26 (68%)	12 (66%)	8 (32%)
Tumor infiltrating lymphocytes (>40 lymphocytes per 10 HPF) (TILs)	13 (81%)	28 (74%)	9 (50%)	11 (44%)
Foci of marked nuclear pleomorphism ("serous-like")	13 (81%)	14 (37%)	12 (66%)	9 (36%)

Conclusions: Our evaluation of *POLE*-mutant tumors confirms previous reports describing grade 3 EEC with "serous-like" cytologic atypia and abundant PTLs and TILS. However, these features were not restricted to *POLE*-mutant EEC. All *POLE*-mutated cases demonstrated excellent clinical outcome (including those with concurrent MMR deficiency and/or aberrant p53 staining), despite many patients forgoing adjuvant treatment.

1057 Mismatch Repair Status of Uterine Leiomyosarcomas: A Study of 36 Cases and Correlation with PD-L1 Immunohistochemistry

Mirka Jones[1], Terrell Jones[2], Swikrity Upadhyay Baskota[2], Eric Statz[2]
[1]University of Pittsburgh, Pittsburgh, PA, [2]University of Pittsburgh Medical Center, Pittsburgh, PA

Disclosures: Mirka Jones: None; Terrell Jones: None; Swikrity Upadhyay Baskota: None; Eric Statz: None

Background: Leiomyosarcomas (LMS) are malignant uterine tumors with poor prognosis and a high risk of recurrences and metastases. They are also the most common type of uterine sarcoma associated with Lynch Syndrome. The treatment of uterine LMS remains difficult and the search for effective therapy continues. The status of mismatch repair (MMR) genes in LMS has not yet been well investigated, however, an association between mismatch repair defects and PD-L1 expression has been described in other malignant neoplasms including endometrial and ovarian carcinomas. Since it is known that mismatch repair loss or impairment significantly increases the risk of mutations in tumor cells, immunotherapy may represent a possible new treatment pathway for these highly aggressive tumors.

Design: Immunohistochemical staining for the MMR proteins MLH1, MSH2, MSH6, and PMS2, as well as PD-L1 was performed on representative sections of 36 LMS. The MMR proteins expression was classified as preserved, lost or significantly impaired (weak staining of 10% or less of tumor cells). Complete loss was diagnosed in the presence of positive staining of inflammatory cells, endothelial cells or endometrial cells as an internal control. Results for PD-L1 were scored in tumor cells and in tumor infiltrating immune cells, with equal or greater than 5% staining considered positive. The status of MMR protein expression was correlated with PD-L1 results.

Results: Five (13.9%) of 36 LMS showed abnormal MMR immunoexpression (Table 1). PMS2 expression was lost in 2 and significantly impaired in two. Of two LMS with PMS2 loss, one showed loss and the other significant impairment of MLH1. MSH6 expression was significantly impaired in one. Two out of 5 LMS with lost or impaired MMR expresssion showed positive immunohistochemical staining for PD-L1 in 40% and 20% of tumor cells, respectively. The remaining 3 LMS were PD-L1 negative. The clinical follow-up included pelvic recurrences in two women and lung metastases in two. One woman presented with thyroid carcinoma a year after diagnosis of LMS, one had mature cystic teratoma of the ovary. History of malignancy in siblings, parents and aunts was reported in 4 women and included colon, lung, breast and sinus carcinomas.

Table 1. Correlation of deficient MMR status and PDL1 in LMS

Case	MLH1	MSH2	MSH6	PMS2	PD-L1 (%)
1	L	P	P	L	0
2	P	P	SI	P	2
3	P	P	P	SI	40
4	P	P	P	SI	20
5	SI	P	P	L	0

Legend: P: Preserved; L: Lost; SI: Significantly Impaired.

Conclusions: Since the loss of MMR proteins does occur in patients with leiomyosarcomas, they may benefit from MMR screening. Knowing the PD-L1 immunoprofile may be especially important in MMR deficient tumors as these may be more sensitive to immunotherapy.

1058 Clinicopathologic Features of Acute and Chronic Inflammatory Lesions in Preterm Placentas

Rohini Kannuswamy[1], Abigail Hardin[2], Rex Bentley[2], Jennifer Gilner[3], Kyle Strickland[2]
[1]Duke University, Cary, NC, [2]Duke University Medical Center, Durham, NC, [3]Duke University, Durham, NC

Disclosures: Rohini Kannuswamy: None; Abigail Hardin: None; Rex Bentley: None; Jennifer Gilner: None; Kyle Strickland: *Consultant*, Foundation Medicine, Inc.; *Consultant*, Almac Pharmaceuticals

Background: Inflammatory lesions of the placenta are associated with preterm delivery and are characterized by neutrophilic or lymphoplasmacytic infiltration resulting from infectious or immunologic conditions. Chronic placental inflammatory lesions include chronic chorioamnionitis (CC), chronic deciduitis (CD), and chronic villitis (CV), which may appear only focally at the time of histologic evaluation. The aims of the current study were: 1) to compare the clinicopathologic features of acute and chronic inflammatory lesions of preterm placentas and 2) to determine if immunohistochemistry (IHC) for CD3 can improve detection of CV.

Design: Placentas were collected at the time of delivery and evaluated by standard protocols, with at least one additional block of placental parenchyma obtained per an IRB-approved protocol. Clinical data were abstracted from the medical record, including gestational age (GA), mode of delivery, and birth weight. H&E slides were evaluated for acute chorioamnionitis (AC), CC, CV, CD, placental infarction, and decidual vasculopathy (DV). Patients were stratified according to the presence of AC by histology. CD3 IHC was performed on blocks obtained via the research protocol.

Results: The cohort included 99 preterm placentas with a median GA of 30 weeks (range 23 to 33), from infants with a median birth weight of 1310 g (range 420 to 2550). AC was present in 27%, CC in 20%, CV in 4%, and CD in 7%. AC was associated with a lower gestational age at birth ($p<0.01$), lower average birth weight ($p<0.01$), and vaginal delivery ($p=0.03$). Hemorrhage was present in 3%, and placental infarction was identified in 32%, which was not coincident with AC (0%, $p<0.01$). CC appeared mutually exclusive of AC ($p=0.01$) and was associated with both increased decidual lymphocytes ($p<0.01$) and DV ($p=0.01$). Of the 4 cases of CV identified, 2 were identified histologically and 2 were identified only after evaluation of CD3 IHC. Time from placental delivery to accessioning was not associated with any specific histologic findings ($p>0.05$).

Conclusions: This study highlights important clinically-relevant differences between acute and chronic inflammatory lesions of the placenta. AC was more common at lower GA and small birth weights, whereas chronic lesions were more commonly associated with DV and placental infarction. This study also highlights a potential role for CD3 IHC for the improved detection of chronic villitis, which doubled the detection rate in this limited study.

1059 Expression of Immune Checkpoint Regulator CTLA-4 in Uterine Cervical Cancers

Ari Kassardjian[1], Neda Moatamed[2]
[1]University of California, Los Angeles, West Hollywood, CA, [2]David Geffen School of Medicine at UCLA, Los Angeles, CA

Disclosures: Ari Kassardjian: None; Neda Moatamed: None

Background: The introduction of immune checkpoint inhibitors in cancer therapy has had a significant impact in oncology. One of the immune checkpoint mediators is cytotoxic T-lymphocyte associated protein 4 (CTLA-4) which is of interest in this study because multiple inhibitory antibodies are currently in active clinical testing to enhance the therapeutic antitumor responses. Inhibition of the CTLA-4 pathway has already led to the FDA approval of Ipilimumab (anti-CTLA-4), a targeted therapy for melanoma. We investigated the expression of CTLA-4 in benign and malignant uterine cervical tissues to determine whether the uterine cervical cancers are potential targets for the immunotherapy.

Design: We assessed CTLA-4 expression on a tissue microarray (TMA) comprising of 100 normal, non-neoplastic, and neoplastic cervical tissues. Mouse anti-human CTLA-4 monoclonal antibody (clone F8) was obtained from Santa Cruz Biotechnology (Dallas, TX) and used for immunohistochemical stain of the TMA. When detected as strong granular cytoplasmic reaction in the epithelial cells, CTLA-4 expression was scored as positive regardless of the number of positive cells.

Results: Table 1 summarizes the frequency of CTLA-4 positivity in cervical tissue. Overall, CTLA-4 was positive in 30% (30/100) of the cervical malignancies. Subcategorically, 20% (2/10) of invasive endocervical adenocarcinomas (Figure 1), 63% (5/8) of adenosquamous carcinomas, and 31% (23/74) of squamous cell carcinomas (SCCs, Figure 2) were positive for CTLA-4 with a tendency toward lower grades SCCs. CTLA-4 was negative in normal tissues, benign cervical lesions, and non-invasive endocervical adenocarcinomas.

Table 1. CTLA-4 Expression in Normal, Benign, and Neoplastic Lesions of Uterine Cervix on a Tissue Microarray Including Median Age (MA)

Diagnosis (Total Cores: 100)	MA	n	CTLA-4+ (n)	CTLA-4+ (%)
Normal	64	2	0	0
Cervicitis	48	3	0	0
Endocervical Adenocarcinoma in situ	40	3	0	0
Endocervical Adenocarcinoma	39.5	10	2	**20**
Adenosquamous Carcinoma	40	8	5	**63**
Squamous Cell Carcinoma, All Grades	44	74	23	**31**
Grade I	46	7	3	43
Grade II	44	52	16	31
Grade III	39	15	4	27

Figure 1 - 1059

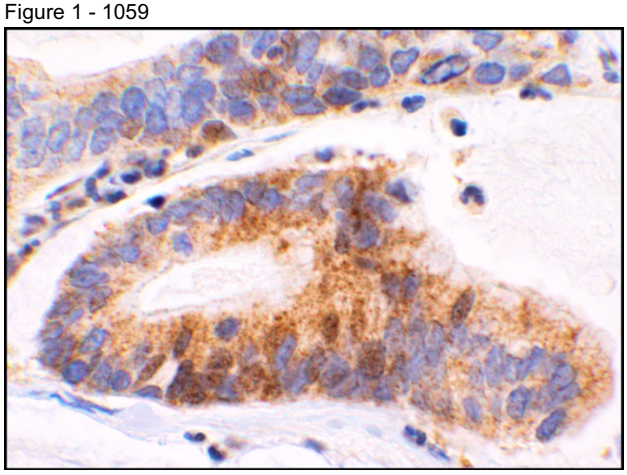

Figure 2 - 1059

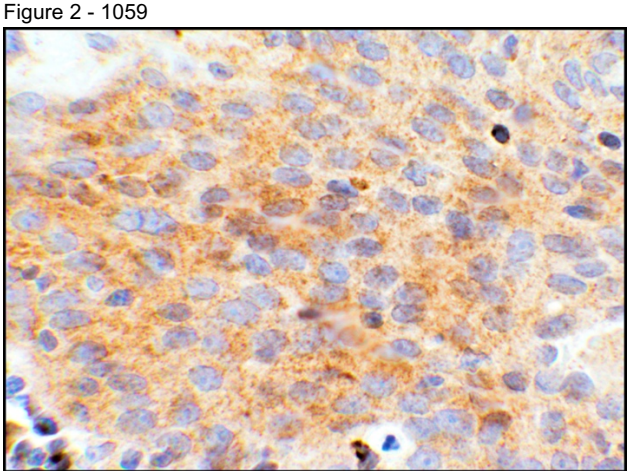

Conclusions: This study has found a significant expression of CTLA-4 in cervical cancer cells with potentials for future targeted immunotherapy. Further studies are required to investigate the predictive and/or therapeutic roles of CTLA-4 expression in uterine cervical cancers.

1060 Exposure to Platelets accelerates Mitosis in SKOV3 Cells

Tanya Kelly[1], Cara Martin[2], Bashir Mohamed[3], Sharon O'Toole[2], Cathy Spillane[1], John O'Leary[1]
[1]Trinity College Dublin, Dublin, Ireland, [2]Trinity St. James's Cancer Institute, Dublin, Ireland, [3]Trinity College, Dublin, Ireland

Disclosures: Tanya Kelly: None; Cara Martin: None; Bashir Mohamed: None; Sharon O'Toole: None; Cathy Spillane: None; John O'Leary: None

Background: Ovarian cancer is the 7th leading cause of cancer in women worldwide. There are almost 250,000 new cases diagnosed annually, and 140,000 deaths each year. Platelet-cancer cell interactions are integral to wound-healing, and to haematogeneous metastasis in ovarian cancer. Here, we investigate the effects of platelets on wound healing in the context of wound-edge migration velocity as it relates to the cell-cycle.

Design: SKOV3 cells were used as an *in vitro* model of metastatic ovarian cancer. In a wound-healing assay, cells were treated with platelets for 24h, or not treated. A wound was induced at the 24h mark, at which point untreated cells received fresh cell culture medium (FM), one set of cells treated with platelets received FM, and a second set of cells treated with platelets received platelet releasate (obtained by centrifugation of the supernatants from those wells). Cells were observed for 24h for wound closure, and photographed at 0h, 6h, 20h, and 24h. Wound closure was assessed using ImageJ, and rates were calculated using velocity = Δposition/time. Acceleration was calculated using $a = \Delta v/\Delta t$. Flow cytometry to ascertain cell-cycle phase at each time point is currently in progress.

Results: Platelets and their releasate significantly expedite wound healing in SKOV3 cells *in vitro* during the first six hours. This is demonstrated by a sharp increase in wound edge velocity during the time period 0-6h. All treatment types decelerate from 6h-20h to approximately the same velocity. There is another acceleration from 20h-24h, which is greatest in the cells treated with platelets and then platelet releasate after wound induction.

Wound Recovery Rate (mm^2/h)			
ElapsedTime (h)	**UNT**	**PLT/FM**	**PLT/REL**
0-6	1.467386	6.158206	8.435137
6-20	1.033598	1.385582	1.259038
20-24	8.242079	5.894685	3.839442
Average Velocities of Wound Edge Migration (µm/h)			
ElapsedTime (h)	**UNT**	**PLT/FM**	**PLT/REL**
0-6	4.277778	30.11111	65
6-20	2.97619	10.85714	7.214286
20-24	13.58333	14.66667	22
Average Accelerations of Wound Edge Migration ($\mu m/h^2$)			
ElapsedTime (h)	**UNT**	**PLT/FM**	**PLT/REL**
0-6	0.712962963	5.018519	10.83333
6-20	-0.092970522	-1.37528	-4.12755
20-24	2.651785714	0.952381	3.696429

Figure 1 - 1060

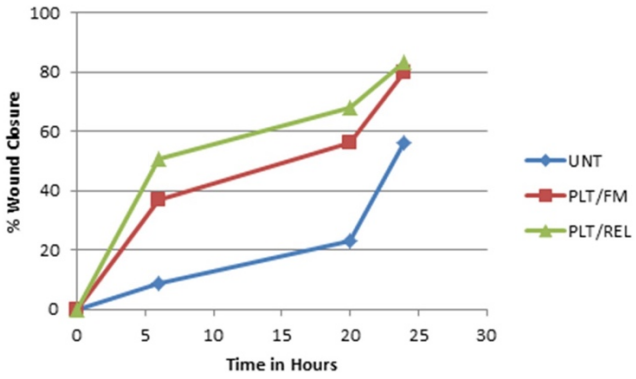

Figure 2 - 1060

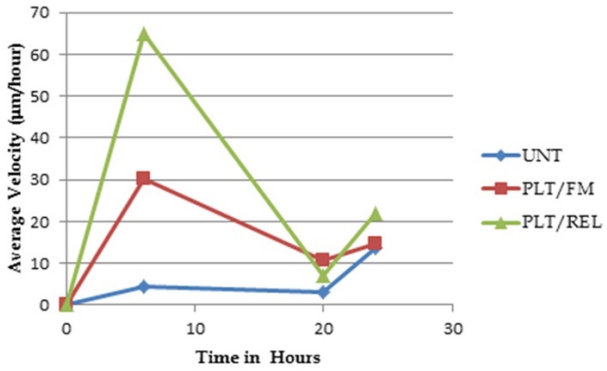

Conclusions: These results show that platelets are essential to cell motility and wound healing. As these are key factors in the metastatic process, it is important to understand the mechanisms involved in platelet-cancer cell interactions. Previous work by our team has demonstrated that platelets are essential to metastasis across multiple types of cancer. This experiment suggests that it is not solely the initial encounter between the platelets and the cancer cells, but the continued exposure to the platelet releasate that is influential in the metastatic process. This is currently being validated by flow cytometry.

1061 Combination of MCM2 and P16 Immunohistochemistry Can Reliably Distinguish Uterine Leiomyosarcomas

Kianoosh Keyhanian[1], Zohreh Eslami[2], Janice Lage[3], Elizaveta Chernetsova[4], Harmanjatinder Sekhon[5], Shahidul Islam[6]
[1]University of Ottawa/The Ottawa Hospital, Ottawa, ON, [2]Scarborough and Rouge Hospital, Toronto, ON, [3]Seneca, SC, [4]Ottawa, ON, [5]Ottawa Hospital, Ottawa, ON, [6]The Ottawa Hospital, Ottawa, ON

Disclosures: Kianoosh Keyhanian: None; Zohreh Eslami: None; Janice Lage: None; Elizaveta Chernetsova: None; Harmanjatinder Sekhon: None; Shahidul Islam: None

Background: Smooth muscle tumors (SMT) are the most common uterine neoplasms. Although often easily distinguishable based on histology, diagnostic challenges are relatively common in tumors with borderline features. Our objective was to evaluate the diagnostic utility of two new proliferation markers, cyclin D1 and minichromosome maintenance complex component 2 (MCM2), in comparison with P16, P53 and Ki67 in differentiating the spectrum of smooth muscle tumors.

Design: A total of 45 cases were included. An institutional database search from 2009 to 2017 identified 10 cases of uterine leiomyoma with bizarre nuclei (LBN), 12 smooth muscle tumors of uncertain malignant potential (STUMP) and 13 leiomyosarcomas (LMS). In addition, ten resected leiomyomas (LM) were included as controls. Immunohistochemistry for cyclin D1, MCM2, P16, Ki67 and P53 was performed on the befitting representative block from each case.

Results: Cyclin D1 nuclear positivity in LMs, LBNs and STUMPs ranged from 0-65% of neoplastic cells with mostly weak to moderate staining intensity. On the other hand, cyclin D1 expression was <5% in all LMSs (Fig 1). Ki67 staining followed the expected results with all LM and LBN cases showing <10%, STUMP cases showing 1-15% and LMS cases showing 10-60% staining. As well, most benign cases demonstrated less than 10% positivity with P53 (20/22) and 38% of LMSs showed more than 50% staining (5/13).

The ratio of MCM2 positivity exhibited a similar wide range (less than 1% to 80%) in LMs, LBNs and STUMPs but interestingly, 92% (12/13) of LMSs were diffusely and strongly positive for MCM2 (>80% cell positivity) (Fig 2). Overall, for diagnosis of LMS, the sensitivity for diffuse intense MCM2 nuclear staining was relatively higher (92%) compared to diffuse staining for p16 (77%); however, specificity of MCM2 and p16 was comparable (94% and 97% respectively) (table).

	Sensitivity	Specificity
a. Diffuse MCM2 (>80% cell positivity)	92%	94%
b. Cyclin D1 (<5% cell positivity)	100%	52%
Combined a and b	92%	94%
c. Diffuse P16 (>80% cell positivity)	77%	97%
Combined a and c	77%	100%
Combined a or c	92%	91%

Figure 1 - 1061

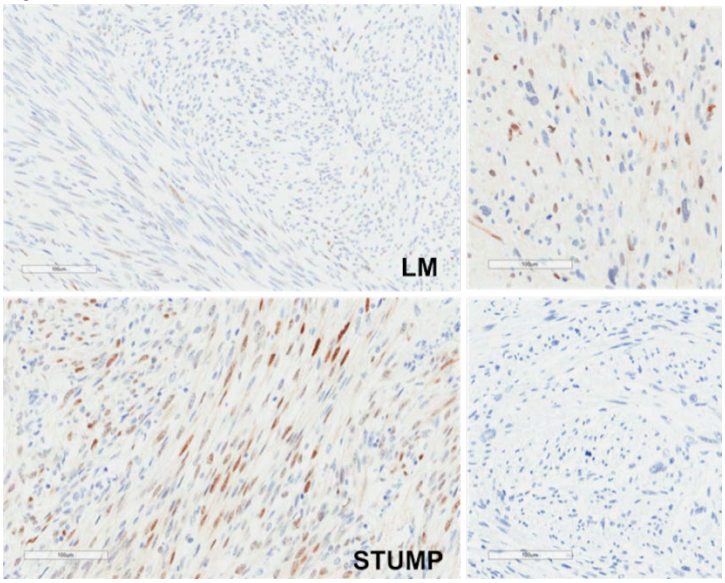

Figure 2 - 1061

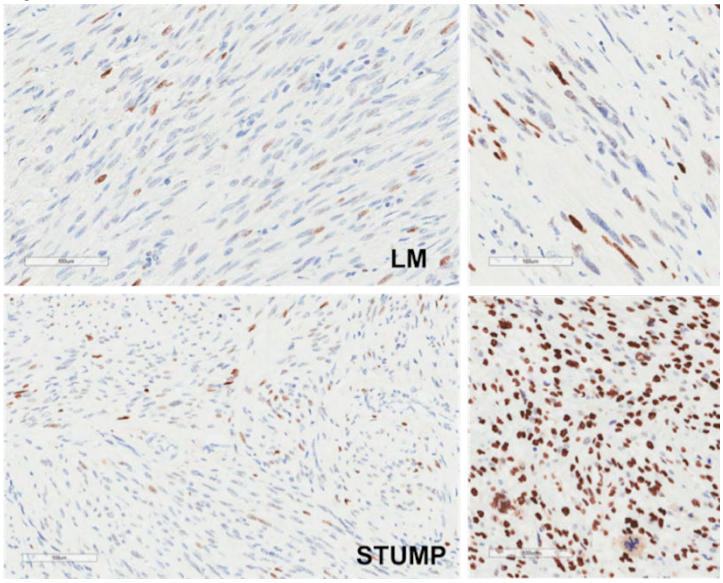

Conclusions: Herewith, we describe the immunohistochemical profile of two new proliferation markers, cyclin D1 and MCM2 in uterine SMTs. A combination of strong and diffuse MCM2 and P16 positivity can reliably distinguish LMSs from more benign histological mimics. Compared to P16, the exclusively nuclear nature of MCM2 staining allows for a more consistent and accurate interpretation. Further evaluation with a larger cohort is needed for validation of our preliminary findings.

1062 Pancreatic Adenocarcinomas Metastasized to the Ovary; A Report of 20 Cases with a Previously Undescribed Histopathologic Features

Kyu-Rae Kim[1], Joo Young Kim[2], Hosub Park[2], Jeong-hwa Kwon[3]
[1]Asan Medical Center, Seoul, Korea, Republic of South Korea, [2]Seoul, Korea, Republic of South Korea, [3]Asan Medical Center, Seoul, Korea, Republic of South Korea

Disclosures: Kyu-Rae Kim: None; Joo Young Kim: None; Hosub Park: None

Background: As in other metastatic carcinomas, pancreatic carcinomas metastasized to the ovary (PCMO) may closely mimic primary ovarian mucinous neoplasm. A better understanding of the histopathologic features is required for the correct diagnosis, however, only a few descriptions can be retrieved from the literature.

Design: Herein, we described detailed histopathologic features of 31 ovaries from 20 patients with PCMO.

Results: Macroscopic features of PMCO were diverse; unilocular or oligolocular cysts mimicking mucinous cystadenoma (four ovaries), large and dilated multiloculated cysts indistinguishable from mucinous borderline tumor or well differentiated adenocarcinoma (11 ovaries),

semisolid mass with numerous small honeycomb-like cysts grossly resembling cystadenofibroma (three ovaries), multiple solid mural nodules within uniloculated or multiloculated cysts (seven ovaries), and solid multilobulated nodules (one ovary). They showed diverse microscopic features including dilated multiloculated cyst lined by multilayered differentiated cells almost indistinguishable from mucinous borderline tumors (thirteen cases) or by significantly atypical cells (twenty-one cases) resembling mucinous cystadenocarcinoma, distended round shaped glands in a fibroblastic stroma resembling mucinous adenofibroma (two cases), "garland" pattern with intraluminal dirty necrosis resembling metastatic colorectal carcinoma (one case). However, they frequently showed "cyto-architectural mismatch", in which significant cytologic atypia and high Ki67 proliferating index were identified even in a single layered epithelium in contrast to the primary mucinous cystadenoma or adenofibroma. Cytologic atypia was significantly higher than that of mucinous borderline tumor. Quite different from the intraovarian growth, outside of the ovary and the ovarian surface showed extensive desmoplastic invasive growth in all cases, suggesting that intraovarian environment may have some influence to induce cytological differentiation and reduce desmoplastic stromal response. To differentiate metastatic from primary mucinous tumors of varying degrees, immunonegativity for PAX8, loss of Dpc4, diffuse positivity for MUC5AC were most helpful.

Figure 1 - 1062

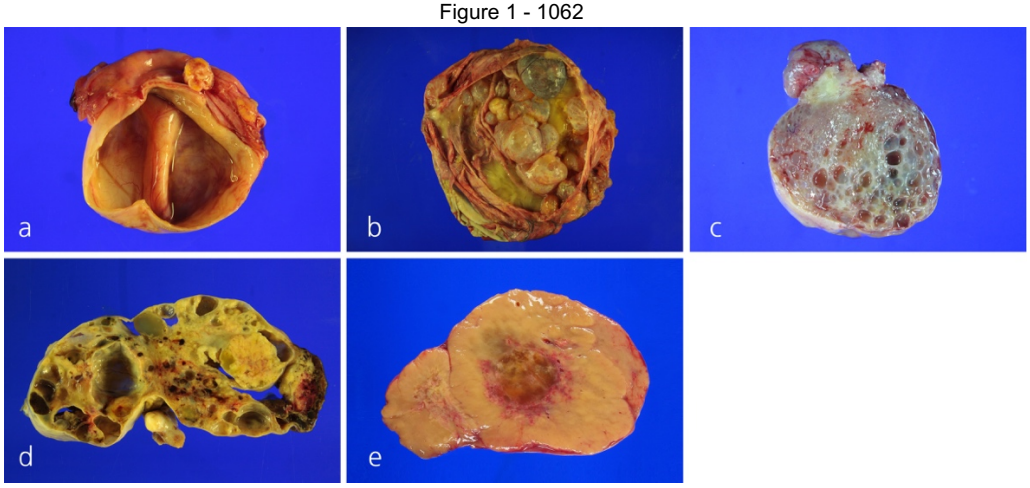

Figure 2 - 1062

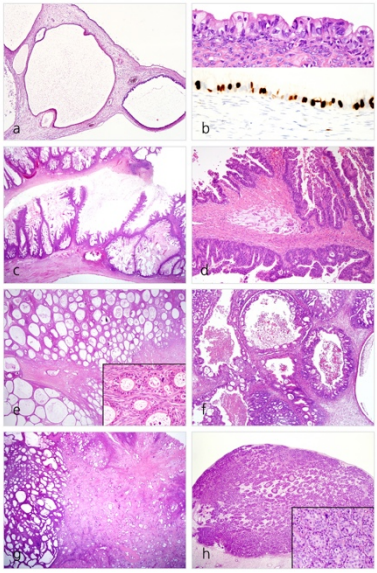

Conclusions: Clinical history, notion of the diverse gross and microscopic features, scrutinized histopathologic features for "cyto-architectural mismatch", and an application of the panels of biomarkers can be helpful in the differential diagnosis of PCMO.

1063 Histological Outcome of Single and Multiple High-risk Human Papillomavirus Infections in Japan

Ayami Kiriyama[1], Tomomi Koide[2], Ryota Ando[1], Ai Ito[1], Masahiko Fujino[1], Masafumi Ito[1]
[1]Japanese Red Cross Nagoya First Hospital, Nagoya, Japan, [2]Japanese Red Cross Nagoya First Hospital, Nagoya-shi, Japan

Disclosures: Ayami Kiriyama: None; Tomomi Koide: None; Ryota Ando: None; Ai Ito: None; Masahiko Fujino: None; Masafumi Ito: None

Background: It is well known that cervical cancer and cervical intraepithelial neoplasm (CIN) are caused by persistent high-risk (HR) human papillomavirus (HPV) infection. Coinfection with multiple HPV types has been detected; however, the relationship of multiple-type infection and CIN progression is unclear. The aim of this study was to evaluate the difference of histological outcomes between multiple and single HR-HPV infection cases in Japan.

Design: Retrospectively, we reviewed pathological records in the Japanese Red Cross Nagoya 1st Hospital from 2010 to 2017. HR-HPV DNA genotyping revealed 11 genotypes of HPV (16, 18, 31, 33, 35 39, 45, 51, 52, 56, and 58); 1866 cases were examined by RT-PCR, and simultaneously, by cervical biopsy and cytology analysis. Biopsied samples were diagnosed by 3 pathologists according to the WHO criteria. Histological outcomes were classified as: CIN stable, regression, and progression. Progressed CIN lesions in multiple-type HPV infection cases were micro-dissected.

Results: Out of 1128 HPV-positive cases, 764 (67.7%) showed single, while 364 (32.3%) showed multiple infection; 169 single and 107 multiple HR-HPV cases were analyzed by cytology, colposcopy, and HR-HPV tests, and deemed eligible for this study. In single HR-HPV infection cases, the final HPV status was single in 135 and negative in 34 cases. There were 54 (32.37%) progressed, 35 (20.7%) regressed, and 80 (47.3%) stable cases. In multiple HR-HPV infection cases, the final HPV status was multiple in 57, single in 41, and negative in 9 cases. There were 39 (36.4%) progressed, 14 (13.0%) regressed, and 54 stable cases. HPV typing test showed that out of 47 cases of multiple HPV infection with HPV 16, 17 (36.1%) were progressed. Progression rate of persistent HPV 16 infection was high: 15/30

(50%). Progressed CIN 3 lesions from 23 multiple-type HPV infection cases were micro-dissected. After HPV genotype testing, single HR-HPV types were detected in these lesions: 15 (65.2%) cases with type 16.

Conclusions: There was no statistically significant difference of CIN progression rate in multiple and single HR-HPV infection cases. In multiple infection cases, progression rate of persistent HPV 16 infection was high; HPV 16 was detected in micro-dissected progressed lesions of multiple infection cases. CIN progression in multiple infection may be due to the clonal evolution of a single type of HR-HPV, especially HPV 16. Thus, persistent multiple HR-HPV infection with HPV 16 should be monitored carefully.

1064 SMARCA4-Deficient Uterine Sarcoma and Undifferentiated Endometrial Carcinoma are Distinct Clinicopathologic Entities

David Kolin[1], Charles Quick[2], Fei Dong[1], Christopher Fletcher[1], Christopher Crum[1], Marisa Nucci[3], Brooke Howitt[4]
[1]Brigham and Women's Hospital, Boston, MA, [2]University of Arkansas for Medical Sciences, Little Rock, AR, [3]Brigham and Women's Hospital, Harvard Medical School, Boston, MA, [4]Stanford University School of Medicine, Stanford, CA

Disclosures: David Kolin: None; Charles Quick: None; Fei Dong: None; Christopher Fletcher: None; Christopher Crum: None; Marisa Nucci: None; Brooke Howitt: None

Background: Undifferentiated/dedifferentiated endometrial carcinomas (UDEC) are rare and aggressive uterine malignancies. One recently described entity, SMARCA4-deficient undifferentiated uterine sarcoma (SDUS), has a morphologic appearance similar to undifferentiated carcinoma but clinicopathologic features akin to that of ovarian small cell carcinoma, hypercalcemic type (SCCOHT). This study sought to determine clinical, morphologic, immunohistochemical, and molecular features that differentiate UDEC and SDUS.

Design: Undifferentiated (n=12) and dedifferentiated (n=15) endometrial carcinoma and SDUS (n=9) were collected from 3 institutions. Immunohistochemistry (IHC) for SMARCA4, INI-1, and claudin-4 was performed. Microsatellite stability was assessed by mismatch repair (MMR) IHC or molecular profiling. A subset of tumors underwent targeted next generation sequencing (NGS) assays. Additional cases of UDEC with clinicopathologic data were abstracted from 2 published series. All cases of undifferentiated and dedifferentiated carcinomas (UDEC) were pooled for analysis (n=82).

Results: Patients with SDUS were significantly younger than those with UDEC (35 y; range 25-58 vs. 61 y; range 23-93). Both SDUS and UDEC frequently presented with high stage disease (100% vs 70%, p=0.1). SDUS was always MMR intact (6/6), compared to 42/72 cases of UDEC (58%) (p=0.040). Loss of SMARCA4 or INI-1 occurred in all cases of SDUS (8/8), but in only 11/50 cases of UDEC (22%) ($p < 0.001$). *TP53* abnormalities (detected either by NGS or IHC) were more common in UDEC than SDUS (51% vs 0%, p=0.014). Claudin-4 expression was more common in UDEC than SDUS (57% vs 0%, p = 0.02). UDEC often contained mutations typically associated with endometrioid carcinoma (*PTEN, PIK3CA, CTNNB1*). These endometrioid-associated mutations were not found in SDUS, which were characterized by *SMARCA4* mutations and relatively few others. Disease-specific survival (DSS) was worse with SDUS than UDEC (log-rank p=0.018).

Conclusions: UDEC and SDUS are both aggressive endometrial tumors which share a similar morphology. SDUS appears to have a worse DSS. Given the molecular and morphologic similarities to SCCOHT, there may be both treatment and germline implications for identifying cases of SDUS. Patient age and IHC including MMR, SMARCA4, INI-1, p53, and claudin-4 may help to resolve the differential diagnosis, but targeted NGS remains the most reliable method to differentiate these entities.

1065 Epigenetic Characterisation of Uterine Stromal Sarcomas

Felix Kommoss[1], Friedrich Kommoss[2], Dietmar Schmidt[3], Hans-Anton Lehr[4], Daniel Schrimpf[5], Kenneth Chang[6], Laura Romero-Pérez[7], Thomas Grünewald[7], Manfred Gessler[8], Stefan Pfister[9], Hans-Peter Sinn[10], Gunhild Mechtersheimer[11], Peter Schirmacher[11], Andreas von Deimling[12], Christian Koelsche[13]
[1]University of Heidelberg, Heidelberg, Germany, [2]Institute of Pathology, Friedrichshafen, Germany, Friedrichshafen, Germany, [3]Institute of Pathology and Cytology, Viersen, Germany, [4]Pathologisches Institut Friedrichshafen Gemeinscha, Friedrichshafen, Germany, [5]Institute of Pathology, Heidelberg, Germany, [6]KKH, Singapore, Singapore, [7]LMU Munich, Munich, Germany, [8]Wuerzburg University, Wuerzburg, Germany, [9]Hopp Children's Cancer Center at the NCT Heidelberg (KiTZ), Heidelberg, Germany, [10]University Hospital Heidelberg, Heidelberg, Germany, [11]Institute of Pathology, Heidelberg University Hospital, Heidelberg, Germany, [12]Heidelberg University Hospital, Heidelberg, Germany, [13]Ruprecht-Karls-University Heidelberg, Heidelberg, Germany

Disclosures: Felix Kommoss: None; Friedrich Kommoss: None; Dietmar Schmidt: None; Hans-Anton Lehr: None; Kenneth Chang: None; Laura Romero-Pérez: None; Thomas Grünewald: None; Manfred Gessler: None; Gunhild Mechtersheimer: None; Peter Schirmacher: None

Background: Endometrial stromal sarcoma (ESS) is a mesenchymal tumor derived from endometrial stromal cells. As classified by the WHO (2014), histomorphology, immunohistochemistry and specific chromosomal rearrangements define low-grade (LGESS) and high-grade (HGESS) tumors. Undifferentiated uterine sarcoma (UUS) is a high-grade tumor lacking typical stromal histomorphology, and so far,

only little is known about its genetic background. We aimed to define subtype specific DNA-methylation signatures of uterine sarcomas in a retrospective cohort of tumors, previously diagnosed as LGESSs, HGESSs, and UUSs.

Design: DNA-methylation analysis (850K) and RNA sequencing from formalin-fixed paraffin-embedded material was performed on a retrospective multicenter cohort of tumors primarily diagnosed as LGESS, HGESS and UUS. Data were analyzed by unsupervised clustering and t-distributed stochastic neighbor embedding analysis and compared with a reference methylation data set of well-characterized prototypical sarcomas encompassing over 16 subtypes, among them potential histopathological mimics of ESS and USS.

Results: In a cohort of 17 LGESS and 4 HGESS DNA-methylation clustering revealed two homogenous methylation groups clearly separating LGESS and HGESS. LGESS carried the specific JAZF1-SUZ12 gene fusion in 10 cases and clustered in close proximity with uterine leiomyomas, irrespective of their individual gene fusion status. In contrast, HGESS carried specific gene rearrangements, namely YWHAE-NUTM2 and ZC3H7B-BCOR in two cases each. Surprisingly, HGESS were epigenetically similar to clear-cell sarcoma of the kidney, central nervous system high-grade neuroepithelial tumors, and certain types of Ewing-like sarcomas, independent of their individual chromosomal translocation.

Conclusions: Array-based DNA-methylation analysis of uterine sarcomas is a powerful tool to classify LGESS and HGESS. Ongoing methylation-based analysis of a cohort of UUS shows potential to clarify whether these tumors represent another homogenous epigenetic group of uterine sarcoma. An optimized classifier for ESS could be helpful to more reliably diagnose morphologically ambiguous cases of LGESS, HGESS, and UUS, thus possibly contributing to more specific treatment algorithms and approaches in uterine sarcoma research.

1066 T-Lymphocyte Subtypes in Endometrial Carcinoma: Distribution and Significance

Eleni (Helen) Kourea[1], Vasileios Mousafeiris[1], Charalampos Kordoulis[1], Vasiliki Tzelepi[2], Apostolos Kaponis[3], Maria Melachroinou[4]
[1]University of Patras, School of Medicine, Patras, Greece, [2]University of Patras, Patras, Greece, [3]Patras University School of Medicine, Patra, Greece, [4]University of Patras, Patras, Greece

Disclosures: Eleni (Helen) Kourea: None; Vasileios Mousafeiris: None; Charalampos Kordoulis: None; Vasiliki Tzelepi: None; Apostolos Kaponis: None; Maria Melachroinou: None

Background: The immune infiltration patterns and their significance in endometrial carcinoma (EC) have not been adequately studied. This study aims to map the distribution of CD8 and FOXP3 tumor infiltrating lymphocyte (TIL) subtypes in EC and correlate the findings with clinicopathologic and outcome parameters, in order to meaningfully guide the TIL evaluation methodology.

Design: Immunohistochemical analysis of CD8 and FOXP3 TILs and mismatch repair (MMR) proteins was performed on 92 EC cases with available clinicopathologic data and follow-up. Intraepithelial (e) and intratumoral stromal (s) TIL counts were recorded in 4 HPF, avoiding hot-spots and depleted areas. Average counts of CD8 and FOXP3 eTILs and sTILs and the corresponding CD8/FOXP3 ratios were correlated with clinicopathologic parameters (Mann-Whitney U test) and disease-free and overall survival (logrank test) using SPSS 18. The 25% quartile was used as a cut-off for survival analysis.

Results: CD8 and sTILs outnumbered FOXP3 and eTILs, respectively (eCD8 TILs: median 6.5, range 0-230, sCD8 TILs: 22, 0.25-302, eFOXP3 TILs: 0.25, 0-19, s FOXP3 TILs: 2.75, 0-71). Higher numbers of CD8 eTILs were associated with grade 3 (p=0.011), cervical (p=0.009) and pelvic (p=0.049) invasion, MMR-deficient (MMR-D) status (p=0.001) and patient demise (p=0.005). Higher FOXP3 sTILs were associated with cervical (p=0.01) and pelvic (p=0.016) invasion. Higher eCD8/eFOXP3 ratio was associated with type 2 EC (p=0.039), grade 3 (p=0.016), MMR-D status (p=0.009) and patient demise (p=0.004). Higher sCD8/sFOXP3 ratio was associated with absence of pelvic extension (p=0.042) and better overall survival (p=0.004).

Conclusions: The association of CD8 eTILs with higher grade and stage and of FOXP3 sTILs with higher stage in EC implies a possible blunting of CD8 TIL function by stromal FOXP3 TILs. Furthermore, the association of elevated CD8 eTILs with MMR-D status rationalizes the use of immune checkpoint inhibitors in EC. Although higher CD8/FOXP3 ratio in the epithelial compartment was associated with adverse parameters and outcome, higher CD8/FOXP3 ratio in the intratumoral stromal compartment was associated with better survival. This might reflect the effect of the significantly more numerous stromal TIL population. sCD8/FOXP3 ratio, encompassing for the function of both cell types, appears to represent a more accurate prognostic indicator, than single cell type evaluation.

1067 Importance of CTNNB1 Mutation in Intermediate Risk, Stage I Endometrial Cancer Patients Considered for Adjuvant Radiation Therapy

Katherine Kurnit[1], Bryan Fellman[1], Russell Broaddus[1]
[1]The University of Texas MD Anderson Cancer Center, Houston, TX

Disclosures: Katherine Kurnit: None; Bryan Fellman: None; Russell Broaddus: None

Background: We have previously shown that somatic *CTNNB1* mutations are associated with worse recurrence-free survival in low grade (grades 1,2), early stage (stages I,II) endometrial endometrioid adenocarcinoma patients. We next wanted to determine if *CTNNB1* mutation status could potentially impact patient management decisions. Current NCCN Guidelines for endometrial cancer are vague regarding the use of adjuvant radiation in patients with stage I disease. We hypothesized that the use of current adjuvant therapy strategies would improve survival outcomes in *CTNNB1* mutant early stage endometrial cancer patients.

Design: Patients with stage I endometrioid endometrial cancer who received care at our institution were included in this study. Demographic and clinical information were obtained by review of the electronic medical record. *CTNNB1* mutation status was determined using either next-generation sequencing panels or focused Sanger sequencing of exon 3 of the *CTNNB1* gene. Comparative statistics were used to compare baseline characteristics, and Kaplan-Meier product limit estimator was used to determine recurrence-free survival (RFS).

Results: 253 stage I endometrial cancer patients were identified. Of these, 45 (18%) had *CTNNB1* mutations. In patients with low risk endometrial cancer (no lymphatic/vascular invasion, no or superficial myometrial invasion less than 50% myometrial thickness, endometrioid grades 1 or 2) who did not receive adjuvant therapy, *CTNNB1* mutation status was not associated with significantly worse RFS (8.1 vs. 11.3 years, p=0.64). However, in patients with deep myometrial invasion and/or lymphatic/vascular space invasion with any endometrioid grade (n=71), the presence of a *CTNNB1* mutation was associated with shorter RFS (2.4 vs 8.5 years, p = 0.01). Furthermore, those patients with somatic *CTNNB1*mutations who did not receive adjuvant radiation therapy demonstrated the worst RFS (Table 1).

Table 1. Recurrence-free survival (RFS) stratified by the presence or absence of somatic *CTNNB1* mutation and stratified by the presence or absence of adjuvant therapy.

***CTNNB1* mutation**	**Adjuvant therapy**	**N**	**Events**	**Median RFS in years (CI)**	**p-value**
No	No	19	6	7.2 (1.0 – NE)	0.011
No	Yes	41	13	8.5 (2.2 –NE)	
Yes	No	6	5	1.6 (0.2 – NE)	
Yes	Yes	5	2	4.0 (2.4 - NE)	

Conclusions: In stage I endometrioid endometrial cancer patients with intermediate risk factors, treatment of patients whose tumors harbor *CTNNB1* mutations resulted in improved recurrence-free survival. Molecular characteristics including *CTNNB1* mutation status should be incorporated into adjuvant therapy treatment algorithms. Prospective trials such as PORTEC4a in Europe will potentially help elucidate which adjuvant therapies are most beneficial.

1068 Age- and Weight-Dependent Influences on Endometrial Cancer Phenotype and Genotype

Katherine Kurnit[1], Laura Washburn[2], Russell Broaddus[1]
[1]The University of Texas MD Anderson Cancer Center, Houston, TX, [2]The University of Texas MD Anderson Cancer Center, Fort Worth, TX

Disclosures: Katherine Kurnit: None; Laura Washburn: None; Russell Broaddus: None

Background: *MLH1* gene methylation with subsequent MLH1 protein loss is one of the most common molecular changes in endometrial cancer. This epigenetic alteration is the most common cause for sporadic mismatch repair-deficient endometrial cancer, a distinctive subtype associated with endometrioid histology, increased tumor-infiltrating lymphocytes, and better response to checkpoint inhibitors. It is well established that environmental influences, such as nutritional state, can induce epigenetic changes in gene expression, both in the germline and in a tumor. We therefore hypothesized that environmental factors were associated with *MLH1*-methylated endometrial cancers.

Design: Patients with sporadic mismatch repair intact and mismatch repair deficient *MLH1*-methylated endometrial carcnomas were identified following the usual clinical evaluation for Lynch Syndrome. Patients with suspected Lynch Syndrome based on this screening were excluded. Clinical and pathology characteristics were identified by review of pathology reports and medical record and were compared across groups using comparative statistics.

Results: 463 endometrial cancer patients were included. 349 (75%) had carcinomas that were mismatch repair intact, and 114 (25%) had carcinomas that had MLH1 loss due to *MLH1*-methylation. Patient and tumor characteristics are summarized in Figure 1. Patients with *MLH1*-metylated tumors were significantly older than those with mismatch repair intact tumors. *MLH1*-methylated tumors were more often grade 3 and more often had lymphatic/vascular space invasion (LVSI). Further analyses of the environmental factors age and body mass index (BMI) were performed after stratifying endometrioid carcinomas into low (grades 1-2) and high grade (grade 3). Patients with low grade, *MLH1*-methylated tumors were significantly older at diagnosis. Alternatively, patients with high grade, *MLH1*-methylated tumors had significantly higher body mass indeces.

Figure 1 - 1068

		Mismatch Repair Intact (n=349)	Mismatch Repair Deficient due to *MLH1* methylation (n=114)	p-value
ALL HISTOLOGIES				
Age, (mean, years)		57.7	64.9	**< 0.001**
Race, n (%)				0.50
	White	241 (71%)	85 (75%)	
	Hispanic	35 (10%)	7 (6%)	
	Black	30 (9%)	12 (11%)	
	Asian	17 (5%)	5 (4%)	
	Other	17 (5%)	5 (4%)	
BMI (mean, kg/m2)		35.7	35.6	0.86
Histology, n (%)				0.64
	Endometrioid	306 (88%)	101 (89%)	
	Mixed	27 (8%)	10 (9%)	
	Non-endometrioid	16 (5%)	3 (3%)	
Endometrioid grade, n (%)				**<0.001**
	1	78 (25%)	10 (10%)	
	2	214 (70%)	77 (76%)	
	3	16 (5%)	14 (14%)	
LVSI present, n (%)		91 (27%)	45(42%)	**0.003**
Deep myometrial invasion, n (%)		81 (24%)	34 (32%)	0.11
ENDOMETRIOID HISTOLOGY ONLY, STRATIFIED BY GRADE				
Age (mean, years)				
	Low grade (1, 2)	56.6	65.3	**< 0.001**
	High grade (3)	57.9	59.7	0.66
BMI (mean, kg/m^2)				
	Low grade (1, 2)	36.7	36.0	0.58
	High grade (3)	28.1	36.1	**0.02**

Conclusions: The relationship of endometrioid grade with environmental factors is complex. While causality cannot be certain, these data suggest that the environmental impact of obesity promotes *MLH1* methylation, which is associated with increased prevalence of grade 3 disease and LVSI, two pathological characteristics associated with adverse outcomes. A provocative hypothesis moving forward is that weight loss could induce a "molecular switch" to alter the histologic and molecular characteristics of an endometrial tumor.

1069 Corded and Hyalinized Endometrioid Adenocarcinoma of the Endometrium Shows Nuclear Beta-Catenin With Loss of E-Cadherin and Pancytokeratin

Nicholas Ladwig[1], Joseph Rabban[2], Charles Zaloudek[3], Karuna Garg[4]
[1]San Francisco, CA, [2]UCSF Pathology, San Francisco, CA, [3]UCSF Medical Center at Mission Bay, San Francisco, CA, [4]University of California, San Francisco, San Francisco, CA

Disclosures: Nicholas Ladwig: None; Joseph Rabban: *Employee*, Merck & Co., Inc.; Charles Zaloudek: None; Karuna Garg: None

Background: Endometrial endometrioid carcinoma (EEC) may show a variety of uncommon morphologic patterns, causing diagnostic challenges. One such variant, the so-called "corded and hyalinized endometrioid carcinoma" (CHEC) is characterized morphologically by cords of epithelioid cells admixed with spindle/fusiform cells embedded within a hyalinized stroma. This appearance can be a morphologic mimic of a variety of tumors in the gynecologic tract, including endometrial stromal neoplasm (ESN), uterine tumor resembling ovarian sex cord tumor (UTROSCT), adenosarcoma, and carcinosarcoma. There is limited information on the immunohistochemical (IHC) staining pattern of CHEC. The aim of our study was to perform a detailed clinicopathologic and IHC evaluation of uterine EEC with CHEC.

Design: Hysterectomy specimens containing EEC with CHEC morphology were reviewed using multiple immunohistochemical (IHC) markers, evaluated in both the glandular and CHEC components. Clinical information was obtained from the EMR.

Results: Six cases of CHEC with prototypic low-grade morphologic features were identified (cases 1-6). Two additional EEC showed CHEC-like morphology but the CHEC displayed high-grade cytologic features (cases 7 and 8).

1. CHEC shows aberrant nuclear expression of beta-catenin.
    a. Increased nuclear expression also seen in glandular areas immediately adjacent to CHEC.
    b. Glandular components distant from CHEC shows only rare nuclear expression.
2. CHEC shows loss of E-cadherin (retained in glandular component).

3. Pankeratin is often absent or only focal in CHEC.
4. EMA is patchy or focal in CHEC.
5. CHEC may show patchy staining for FOXL2.
6. Five cases showed loss of PTEN and one displayed loss of MLH1 and PMS2 staining.
7. While most cases were FIGO grade 1-2, there were 2 cases with high grade cytology both of which showed loss of PTEN, aberrant p53 expression and loss of Rb.
8. Although we have limited clinical follow-up data, two patients died of disease and one is alive with disease (molecular analysis is pending).

See Table for clinicopathologic and IHC details.

Case		1	2	3	4	5	6	7	8
Age		48	50	69	35	19	54	64	36
FIGO Stage		IIIA	IA	IA	II	IB	II	IA	IIIC2
Clinical Status (yr)		DOD (4)	NED (3)	NED (6)	NED (<1)	AWD (13)	DOD (4)	NED (<1)	NED (<1)
FIGO Grade		2	2	3	2	1	2	2	3
Extent of CHEC		<10%	<10%	20%	<10%	25%	10%	20%	>90%
Squamous Morules		+	-	-	+	-	+	+	+
Beta-catenin	Gland	P	P	F	F	P	P	NA	N
	CHEC	D	D	P	D	D	D	D	N
E-Cadherin	Gland	D	D	D	D	P	D	NA	D
	CHEC	N	N	N	N	N	N	F	P
PanCK	Gland	D	D	D	P	D	D	NA	D
	CHEC	F	N	F	N	N	F	P	P
EMA	Gland	D	D	D	D	D	D	NA	D
	CHEC	P	P	P	F	F	D	F	P
FOXL2	Gland	F	N	F	N	N	N	NA	N
	CHEC	F	P	F	P	N	N	N	N
PTEN	Gland	L	R	R	L	R	L	NA	L
	CHEC	L	R	R	L	R	L	L	L
ARID1A	Gland	R	R	L	R	R	R	NA	R
	CHEC	R	R	L	R	R	L	L	R
RB	Gland	R	R	R	R	R	R	NA	L
	CHEC	R	R	R	R	R	R	L	L
p53	Gland	WT	WT	WT	WT	WT	WT	NA	A
	CHEC	WT	WT	WT	WT	WT	WT	A	A
P16	Gland	N	N	N	N	N	N	NA	D
	CHEC	D	N	N	N	N	N	D	D
ER	Gland	P	P	P	D	D	D	NA	P
	CHEC	P	P	P	F	F	N	N	N
WT1	Gland	N	C	P	N	C	N	NA	N
	CHEC	C	C	C	C	C	C	C	N
PAX8	Gland	P	D	F	P	D	D	NA	P
	CHEC	F	P	N	P	P	N	N	N
MLH1		R	R	L	R	R	R	R	R
PMS2		R	R	L	R	R	R	R	R
MSH2		R	R	R	R	R	R	R	R
MSH6		R	R	R	R	R	R	R	R

Key:
DOD = dead of disease
NED = no evidence of disease
L = lost
R = retained
WT = wild-type
A = aberrant
N = Negative
D = diffuse
P = patchy
F = focal
C = cytoplasmic
NA = not available

1. CHEC frequently shows nuclear beta-catenin expression and loss of E-cadherin staining.
2. CHEC can show relative lack of expression for epithelial markers which can lead to diagnostic difficulty.
3. CHEC may show FOXL2 expression which can raise the possibility of ESN or UTROSCT.

1070 Ovarian Germ Cell Tumors in Women >35 Years of Age are Genetically Distinct From Ovarian Germ Cell Tumors in Adolescents

Nicholas Ladwig[1], Joseph Rabban[2], Bradley Stohr[3], Sarah Umetsu[3], Karuna Garg[3], Charles Zaloudek[4]
[1]San Francisco, CA, [2]UCSF Pathology, San Francisco, CA, [3]University of California, San Francisco, San Francisco, CA, [4]UCSF Medical Center at Mission Bay, San Francisco, CA

Disclosures: Nicholas Ladwig: None; Joseph Rabban: *Employee*, Merck & Co., Inc.; Bradley Stohr: None; Sarah Umetsu: None; Karuna Garg: None; Charles Zaloudek: None

Background: Germ cell tumors (GCT) of the gynecologic tract are typically seen in children/adolescents and are rare in women over 40 years of age. Those found in young patients (“usual type” GCT) contain large structural chromosomal abnormalities including isochromosome 12p, with a low overall mutation burden. These tumors typically respond to traditional GCT chemotherapy.

GCT are rarely seen in women over 40 years of age, and in this age group are often admixed with carcinoma, and have been called "somatic" GCT. Although morphologically and immunohistochemically identical to usual type GCT, somatic GCT typically present at a more advanced stage, are resistant to GCT chemotherapy, and have a higher rate of clinical progression.

Although recent molecular studies characterizing ovarian GCTs have been published, the vast majority of tumors studied were usual type GCTs in young women. The aim of this study is to investigate the molecular profile of GCTs in women >35 years of age.

Design: We identified 9 cases of GCT in women >35 (see Table 1), six of which were admixed with carcinoma. DNA was purified from FFPE tumor tissue and next-generation sequencing targeting 479 cancer genes was performed on all GCT and any admixed carcinoma.

Results: See Table for clinical data.

1. Mutations in several pathways were identified:
    a. PI3K/AKT/MTOR (7 of 9 cases) - *PIK3CA, PTEN, MTOR*
    b. Chromatin Remodeling (5 of 9 cases) - *ARID1A, SMARCA4*
    c. MAPK (6 of 9 cases) - *KRAS, RASA1, MAP2K2, MAP2K1*
    d. Cell Cycle Regulation (3 of 9 cases) - *TP53, CDK2NA, MYCN*
2. Among the 6 GCT mixed with carcinoma:
    a. 3 showed several shared mutations between the GCT and carcinoma as well as mutations unique to each component
    b. 2 showed identical mutations between the GCT and carcinoma
    c. 1 showed mutations only in the carcinoma with none in the GCT
3. Among the 3 pure GCTs:
    a. 2 showed multiple mutations
    b. 1 showed copy number changes only with no demonstrable mutations

	Germ Cell Tumor Only				Germ Cell Tumor + Carcinoma					
Case	1	2	3		4	5	6	7	8	9
Age	56	49	49		58	47	57	45	36	63
Site	O	O	O		O	E	O	O	O	O
FIGO Stage	IIIC	IIIB	N/A		IC	IIIB	I	III	III	I
Carcinoma	None	None	None		EC CCC	EC	HGSC CCC NEC	EC CCC	EC	MBT
Germ Cell Tumor	YST	YST	YST IT		YST	YST	YST	YST	YST	YST
Key:	O = ovary									
	E = endometrium									
	YST = yolk sac tumor									
	IT = immature teratoma									
	EC = endometrioid adenocarcinoma									
	CCC = clear cell carcinoma									
	HGSC = high-grade serous carcinoma									
	NEC = neuroendocrine carcinoma									
	MBT = mucinous borderline tumor									

1. Although morphologically identical, GCT in women >35 years of age harbor a greater mutational burden than GCT seen in adolescents, suggesting tumors in these populations are genetically distinct.
2. The increased mutational burden may correlate with resistance to traditional GCT chemotherapy.
3. Cases with carcinoma admixed with GCT show common mutations between the two components, consistent with both tumor types arising from a common clone with subsequent molecular divergence.

1071 Circumferential Horizontal Extent in Microscopic Invasive Cervical Cancer, Is It Relevant?

Barrett Lawson[1], Anais Malpica[1], Stephen Gruschkus[1], Roland Bassett[1], Elizabeth Euscher[1]
[1]The University of Texas MD Anderson Cancer Center, Houston, TX

Disclosures: Barrett Lawson: None; Anais Malpica: None; Stephen Gruschkus: None; Roland Bassett: None; Elizabeth Euscher: None

Background: FIGO and the AJCC TNM systems require the measurement of the depth of invasion (DOI) and horizontal extent (HE) for invasive (Inv) cervical (Cx) cancer (Ca) diagnosed only by microscopic examination (i.e., not clinically visible). The HE is measured as the length of the focus of InvCxCa measured on the glass slide (longitudinal HE, LHE). Recent CAP guidelines require the measurement of a third dimension, circumferential HE (CHE) which consists of the addition of consecutive tissue sections with InvCa x 2.5-3mm. The use of this third dimension has the potential to upstage a case from FIGO stage IA to IB. We studied a cohort of Inv CxCa with no visible disease to determine if adding CHE is clinically relevant.

Design: 53 cases of microscopic squamous, adeno - and adenosquamous InCxCa (2000-2013) were evaluated for patient (pt) age, tumor (tu) grade, lymphovascular invasion (LVI), DOI, LHE, number of sequential tissue sections with InvCa, treatment, recurrence, death and follow up (f/u). CHE was calculated by adding number of sequential sections with tu and multiplied by 2, 3 and 4mm, simulating potential tissue section thickness.

Results: Pts' ages ranged from 18-77 yrs (median 36). Histology, tu grade, LVI, FIGO stage and outcome are summarized in Table1. 11 (20.8%) pts had observation, 15 (28.3%) had simple hysterectomy, 17 (13.2%) had radical hysterectomy, and 3 (5.7%) pts had radiation only. Using DOI and LHE, 30 cases were FIGO stage 1A1 (56.6%); 9 (17.0%) 1A2; and 14 (26.4%) 1B1. Adding CHE with 2, 3 or 4 mm multiplier, we identified 4 cohorts: #1, cases that would not be upstaged by CHE;#2, cases that possibly could be upstaged by CHE;# 3, cases that definitely would be upstaged to 1B1 by CHE;# 4, cases already staged to 1B1 by DOI or LHE. Comparing cohorts 1-4 showed

no significant differences with regard to recurrence (p=0.567) or death (p=0.68). Combining the possible and definite upstaging cohorts (2 and 3) yielded similar results (p=0.362 and p=0.528 respectively).

Table 1	Summary of Overall Patient and Cohort Characteristics				
	Overall (N=53)	Cohort 1 (N=14)	Cohort 2 (N=17)	Cohort 3 (N=8)	Cohort 4 (N=14)
FIGO Stage					
1A1	30	13	11	6	0
1A2	9	1	6	2	0
1B1	14	0	0	0	14
Histology					
Squamous	30	12	9	3	6
Adenocarcinoma	20	2	7	4	7
Adenosquamous	3	0	1	1	1
Tumor Grade					
Well diff.	12	6	4	1	1
Moderate diff.	22	4	8	3	7
Poorly diff.	10	0	2	3	5
Unknown	9	4	3	1	1
Lymphovascular invasion					
No	28	10	7	4	7
Suspected	12	1	9	0	2
Yes	13	3	1	4	5
Recurrence/(Death)					
No	48	12	16	7	14
Yes	4(1)	2(1)	1	1	0

Conclusions: CHE is problematic due to the inability to standardize the tissue section thickness and is at best an estimate. Therefore, its use should be discouraged as it has the potential to upstage microscopically InvCxCa and has no significant impact on pt outcome.

1072 A 3 Tier Chemotherapy Response Score For Ovarian/Fallopian Tube/Peritoneal High Grade Serous Carcinoma, Is It Clinically Relevant?

Barrett Lawson[1], Elizabeth Euscher[1], Roland Bassett[1], Jinsong Liu[1], Preetha Ramalingam[2], Yanping Zhong[1], Nicole Fleming[1], Anais Malpica[1]
[1]The University of Texas MD Anderson Cancer Center, Houston, TX, [2]Houston, TX

Disclosures: Barrett Lawson: None; Elizabeth Euscher: None; Roland Bassett: None; Jinsong Liu: None; Preetha Ramalingam: None; Yanping Zhong: None; Nicole Fleming: None; Anais Malpica: None

Background: The CAP requires a chemotherapy response score (CRS) for ovarian/fallopian tube/peritoneal (O/Ft/P) high grade serous carcinomas (HGSCs) status post (s/p) neoadjuvant chemotherapy (NACT) as this parameter has shown to be a predictive factor for progression free survival (PFS). This is not universally accepted. Up front laparoscopic examination with “Scope and Score” (SS), an index of resectability and bulkiness of disease, is used to triage patients (pts) with advanced FIGO stage O/Ft/P HGSCs and no imaging evidence of unresectability. This study ascertains the clinical value of CRS and compares CRS and SS to determine which one is a better predictor of outcome.

Design: 131 O/FT/P HGSCs, FIGO stages 3 or 4, s/p NACT (4/2013-2/2018) were identified. We recorded: pts’ ages, FIGO stage, BRCA status, SS index, date of first chemotherapy cycle (CC), number of pre and post-operative CCs, and follow up (f/u).CRS was assigned for the omentum (Om) and adnexal (Ad) tissue after reviewing the criteria by Böhm, et al., and online training. Slides were scored by 2 pathologists jointly.

Results: Pts’ ages, 36 to 80 yrs; mean, 61.2. FIGO stage: 3, 69(52.2%) and 4, 62 (47.8%). Om and Ad CRSs are shown in Table 1. Om and Ad CRSs were equal in 51 cases (45.2%), Om CRS was higher in 48(42.4%), and Ad CRS was higher in 14(12.4%). Preoperative CCs ranged from 3 to 9; median, 3. Postoperative CCs ranged from 2 to 13; median, 3. 41 pts had SS, ranging from 2 to 14, median 9. 17/99 tested pts had BRCA mutations. 128 pts had sufficient f/u: 101(78.3%) died or had disease progression (median PFS, 1.2 yrs). 46 (34.8%) pts died of disease; median time of survival, 3.5 yrs. The 2 and 3 tiered (tr) Om and Ad CRS, and the SS showed no significance for predicting overall survival (OS). The 3 tr Om and Ad CRS and 2 tr Ad CRS showed no significance for predicting PFS. The 2 tr Om CRS was significant in predicting PFS (HR 0.61, 0.48-0.99 95%CI, p=0.05), while SS was also significant in predicting PFS (HR 1.16, 1.03-1.31 95%CI, p=0.015), with higher scores associated with worse prognosis. Age was the only variable that was associated with predicting PFS (HR 1.13, p=0.016) and OS (HR 1.31,p=0.0008).

Variable	CRS	Total Number
Omental Score	1	21
	2	61
	3	31
Adnexal Score	1	47
	2	49
	3	17

Conclusions: This study shows the lack of predictive value of the 3 tr Om CRS and confirms that Ad CRS has no prognostic significance. We found that the 2 tr Om CRS is a better predictor of PFS following NACT, while the SS is significant in predicting PFS prior to NACT. Neither CRS or SS have an impact on overall survival.

1073 Novel Discovery of GITR Expression in Human Ovarian Cancer Cells

Christine Lee[1], Neda Moatamed[2], Itsushi Shintaku[1]
[1]University of California, Los Angeles, Los Angeles, CA, [2]David Geffen School of Medicine at UCLA, Los Angeles, CA

Disclosures: Christine Lee: None; Neda Moatamed: None; Itsushi Shintaku: None

Background: Glucocorticoid-**i**nduced **t**umor-necrosis-factor **r**eceptor-related protein (GITR) is expressed on cell membranes of regulatory T lymphocytes (Tregs). Tregs act as suppressors in immune response and inhibit anti-tumor cytotoxic T cell (CTL) activity. Experimentally it has been shown that GITR gene ablation in murine cells results in modulation of T lymphocyte activation and proliferation more than the wildtype. Currently, GITR is used as an immunotherapeutic target that has shown promising results in murine models. In this treatment, anti-GITR antibody is utilized as the ligand binding to GITR to inactivate the Tregs resulting in enhancement of the effector $CD8^+$ T cells activity. Subsequently, the tumor is either eliminated or there would be a decrease in cancer cell proliferation. In all murine tumors, cancer micro-environment Tregs are the targets for immunotherapy. Though GITR expression and activity have been studied in murine models, the role of GITR is relatively unknown in human systems.

Design: A tissue microarray (TMA), containing 224 human ovarian tissues, was used for immunohistochemical stain utilizing a goat anti-human GITR antibody. The TMA had normal, benign, and neoplastic tissue cores. Expression of GITR, regardless of the number of positive tumor cells and intensity of the reactions, was considered positive. The cores were divided into the diagnostic categories and the number as well as the percentage of GITR positive cores were determined for each diagnosis (Table 1).

Results: The expression of GITR was either cytoplasmic or combined cell membrane and cytoplasmic, where cytoplasmic reactions were granular. An example of the combined reaction is shown in Figure 1. Overall, 19.3% of the primary non-metastatic ovarian neoplastic cores had some degree of GITR expression. The breakdown of the reactions is shown in Table 1.

Table 1. GITR Expression (Exp) in Normal and Neoplastic Tissue Cells of Ovary with Patients' Median Age (MA)

Diagnoses, Total (n) = 224	**MA**	**n**	**Exp (n)**	**Exp (%)**
Normal	48.5	10	0	0
Benign	42	49	0	0
Serous, Borderline	33	11	2	**18.2**
Serious, Carcinoma	54	47	8	**17.0**
Mucinous, Borderline	39.5	2	0	0.0
Mucinous, Carcinoma	45.5	18	4	**22.2**
Clear Cell Carcinoma	44.5	8	2	**25.0**
Endometrioid Carcinoma	51	41	5	**12.2**
Germ Cell Tumors	23	20	10	**50.0**
Sex Cord Tumors	44	15	0	0.0
Sarcomas	39	4	2	**50.0**
Other Tumors	54	5	0	0.0
Metastatic Lesions	43.5	14	0	0.0

Figure 1 - 1073

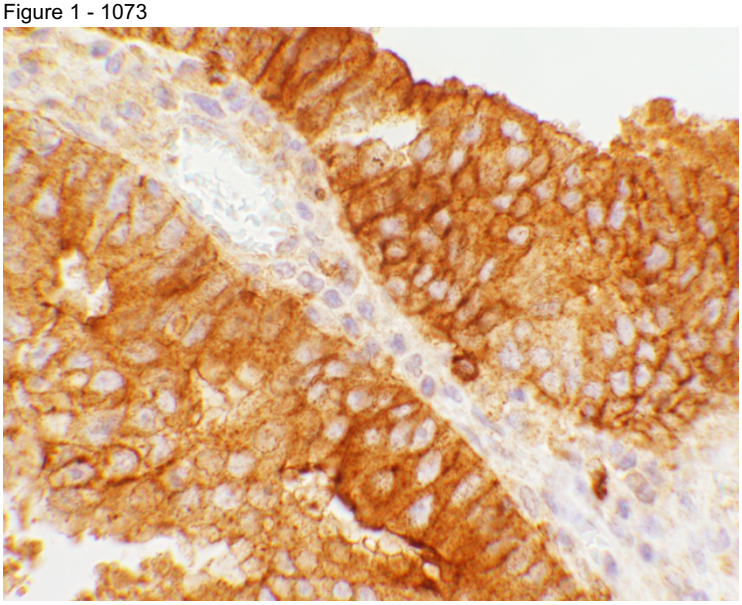

Conclusions: We report expression of GITR for the first time in human ovarian cancer cells. Previous reports demonstrate GITR expression only on tumor infiltrating lymphocytes. We propose that cancer cells with GITR expression act as a proxy for Tregs in the tumor micro-environment and suppress CD8+ anti-tumor lymphocytes. We believe tumors with GITR expression may be potential strong candidates for GITR-targeted immunotherapy. Future studies can investigate the association of GITR expression with the number and function of effector T cells and clinical outcomes.

1074 Women with Anal Cancer Precursors: Clinicopathological Characteristics and Concomitant Genital Tract Neoplasia

Volha Lenskaya[1], Yuxin Liu[2]
[1]Icahn School of Medicine at Mount Sinai, New York, NY, [2]Mount Sinai Health System, New York, NY

Disclosures: Volha Lenskaya: None; Yuxin Liu: None

Background: Two thirds of high-risk human papillomavirus (hrHPV)-related anal cancers occur in women. Half of the cases present at advanced stages, underscoring a significant deficiency in anal cancer screening for women. We thus aimed to identify the clinicopathological characteristics of women with anal precancerous lesions (i.e. Anal Intraepithelial Neoplasia, AIN 2/3, synonymous high-grade squamous intraepithelial lesions) and to determine whether their AIN 2/3 is associated with Cervical, Vulvar and Vaginal Intraepithelial Neoplasia (CIN/VIN/VAIN).

Design: We performed a retrospective study of women who had undergone high-resolution anoscopic examination and biopsy between 2010 and 2018. Patients with diagnosis of AIN 2/3 were included. Medical records were reviewed and all colposcopic examination results were recorded.

Results: 100 women with AIN 2/3 (median age 54 years, range 27-74) were identified. Among the subjects, 97 were HIV-positive. Anal hrHPV prevalence was 100%, including HPV16/18 (73%). Cervical hrHPV prevalence was 67%, including HPV16/18 (40%). For women with anal and cervical coinfection, hrHPV types were concordant in half of the cases. 42 women had concurrent or history of genital high-grade lesions, including CIN 2/3 (n=40); Cervical Adenocarcinoma-In-Situ (n=2); VIN 3 (n=7), and VAIN 3 (n=2). Six had high-grade lesions at 2 genital sites. When comparing women who had AIN 2/3 alone and those who had high-grade lesions at both anal and genital sites, there was no statistical difference in clinicopathological characteristics such as age, race/ethnicity, HIV status, smoking history, and HPV genotypes (P>0.4). Among women with both AIN 2/3 and CIN 2/3, 11 (27%) developed anal lesions more than 10 years following the successful treatment of cervical lesions by LEEP or hysterectomy.

Characteristic	AIN 2/3 alone (n=58)	High-grade lesions at both anal and genital sites (n=42)
Age median (range)	55 (29-79)	52 (24-64)
HIV status		
Positive	57 (98)	40 (95)
Negative	1 (2)	2 (5)
Race/ethnicity*		
African American	21 (36)	25 (60)
White	7 (12)	2 (5)
Hispanic	23 (40)	9 (21)
Other	7 (12)	6 (14)
Smoking history		
Current	27 (47)	16 (38)
Former	19 (33)	13 (31)
Never	12 (21)	13 (31)
Other STD		
Yes	25 (43)	19 (45)
No	33 (57)	23 (55)
HPV genotype		
16/18	40 (74)	29 (74)
Non-16/18	14 (26)	10 (26)
Unknown	4	3

***p=0.07, all other p-values >0.4**

Conclusions: HIV-positive women and those with genital high-grade lesions are at great risk of developing anal cancer precursors. AIN 2/3 can present as an isolated lesion or after long intervals beyond the treatment of cervical lesions. Consequently, we recommend integrating anal cancer screening with the standard gynecological examination for all high-risk women.

1075 Clinicopathologic and immunohistochemical features of HPV associated and independent squamous cell carcinoma of the vulva: a retrospective study

Sofia Lerias[1], Susana Esteves[2], Cristina Azedo[1], Ana Ferreira[3], Mario Cunha[4], Daniela Cochicho[2], Luís Martins[2], Ana Félix[5]
[1]Instituto Portugues de Oncologia Francisco Gentil, Lisboa, Portugal, [2]Instituto Portugues de Oncologia de Lisboa, Francisco Gentil, Lisboa, Portugal, [3]Institute Portugues de Oncologia de Lisboa, Francisco Gentil, Almada, Portugal, [4]Portuguese Institute of Oncology, Lisbon, Portugal, [5]Instituto Portugues de Oncologia de Lisboa/CEDOC, Lisboa, Portugal

Disclosures: Sofia Lerias: None; Susana Esteves: None; Cristina Azedo: None; Ana Ferreira: None; Mario Cunha: None; Daniela Cochicho: None; Luís Martins: None; Ana Félix: None

Background: The presence or absence of HPV separates vulvar squamous cell carcinoma (VSCC) into two distinct clinicopathological and molecular entities. This study aims to correlate p16, p53, EGFR immunostaining in VSCC with HPV status, tumour stage and overall survival (OS).

Design: We report 93 cases of VSCC with clinical, histological and prognosis data diagnosed over a period of 14 years (2002 to 2016). HPV DNA detection was done using SPF-10 PCR/ DEIA/LIPA v2 system. Immunohistochemistry for p16, p53, and EGFR was performed on tissue microarrays. Only >70% of tumor cells staining with p16 and >50% of tumour nuclei staining with p53 were considered positive. EGFR scoring was based on intensity of membrane staining (scoring system Berchuck). Kaplan-Meier estimator and multivariable Cox regression analysis controlling for FIGO stage and age were used.

Results: HPV status was determined in all, 64 HPV-negative, 29 HPV-positive, of which 11 HPV16-positive. Lymph node metastasis was present in 40% of the cases and the mean lymph node metastasis size was 10.3 mm (range 0.4-39mm). FIGO stage was I in 47%, II in 10% and III in 43% of the cases. 37% of the patients died of disease. HPV associated tumours were more likely to have koilocytotic change ($p<0.01$). No differences were found between HPV-positive and -negative tumours regarding other histological features and OS (hazard ratio (HR) =1.08, 95% CI=1.21-4,17, 0.56-2.06 p=0.82). Patients who underwent surgery had superior OS (HR=0.51, 95% CI=0.26-0.99 p=0.04) and lymph node metastasis size ?5mm was associated with a statistically significant inferior OS (HR=1.88, 95% CI=1.22-2.92 p=0.004). VSCC demonstrated p53 positive staining in 31% of the tumours and EGFR heavy staining in 15% of the tumours. We found p16 expression was inversely associated with p53 and EGFR immunophenotype.

	p16 negative(<70%)	%	p16 positive (>70%)	%	p-value
p53 immunophenotype					
p53 negative (<50%)	52	65%	12	92%	p=0.06
p53 positive (>50%)	28	35%	1	8%	
EGFR immunophenotype					
EGFR negative (0 to 2+)	66	83%	13	100%	p=0.20
EGFR positive (3+)	14	18%	0	0%	

Conclusions: Patients who underwent surgery had a superior OS compared to other treatments and in patients with lymph nodes metastasis ?5mm the OS was inferior. Expression of p16 was associated with HPV+ VSCC and correlated with a superior OS (HR=0.30, CI 0.073-1.263, p=0.01). Expression of p53 and EGFR was not associated with HPV status, p16 expression, FIGO stage and Overall Survival.

1076 PD-L1 in Primary Vulvar Cancer, Recurrences and Lymph Node Metastasis

Sofia Lerias[1], Fernanda Silva[2], Ana Félix[3]
[1]Instituto Portugues de Oncologia Francisco Gentil, Lisboa, Portugal, [2]NOVA Medical School, Queijas, Portugal, [3]Instituto Portugues de Oncologia de Lisboa/CEDOC, Lisboa, Portugal

Disclosures: Sofia Lerias: None; Fernanda Silva: None; Ana Félix: None

Background: In cervical carcinomas, as in other neoplasms, new agents targeting the positive tumor surface expression of programmed death-1/programmed death-ligand-1 (PD-L1) have been approved. Our aim was to evaluate the presence of PD-L1 immunoexpression in primary tumors, recurrences and lymph-node metastasis of vulvar squamous cell carcinoma (VSCC), a carcinoma with poor outcome, and determine its prognostic value.

Design: We selected 93 cases of VSCC with known HPV status (HPV DNA detection used SPF-10 PCR/ DEIA/LIPA v2 system), clinical, histological and prognosis data diagnosed over a period of 14 years (2002 to 2016). Twenty-nine tumors were found to have HPV (31%). Heavy peritumoral lymphocytic infiltrate was present in 5 cases. FIGO stage was I in 47%, II in 10% and III in 43%. Recurrences occurred in 43 patients (pts). In 14 and 3 pts, two and three recurrences occurred, respectively. Lymph node metastasis were identified in 37 patients (40%). Immunohistochemistry for PD-L1 (clone 22C3, M3653 from DAKO) was performed on tissue microarrays, containing 87 primary tumors (87 pts), 41 different recurrences (28 pts), and 20 lymph node metastasis (20 pts). PD-L1 expression in tumour cells was scored quantitatively (accordingly with OAK and POPLAR studies). Statistical analysis was performed using Kaplan-Meier estimator and multivariable Cox regression analysis controlling for FIGO stage and age.

Results: In primary tumors, PD-L1 expression (?1%) was observed in 21 cases (24%), although only 8 cases (9%) had moderate to high expression (?5%). PD-L1 expression was correlated with tumor heavy lymphocytic infiltrate (p=0.02). In recurrences, PD-L1 was present in 6/41 (14%), only one case negative in primary tumor become positive in recurrence. Of all 21 PD-L1+ , 5 recurred and 2 lost their positive expression. PD-L1 was positive in 2/20 metastasis (10%); none was positive when the primary was negative and 4 metastasis lost PD-L1 expression. No association was found between PD-L1 expression and other clinical-pathological parameters such as HPV status, recurrence, FIGO stage and OS.

Conclusions: Strong PD-L1 expression in vulvar carcinoma is uncommon. Although, PD-L1 immunoexpression in the majority of the cases is very similar in primary, recurrences and lymph node metastasis, if PD-L1 scoring is used to select patients for target therapy it has to be re-tested in all recurrences and lymph node metastasis. PD-L1 expression is not a prognostic factor in squamous cell carcinomas of the vulva.

1077 Comparison of Human Papillomavirus Detection in Genital Seborrheic Keratosis-Like Lesions Using HPV In-Situ Hybridization and SPF10 PCR

Daniel Levitan[1], Nina Schatz-Siemers[2], Cathleen Matrai[1], Abha Goyal[1], Lora Ellenson[1], Edyta Pirog[1]
[1]New York-Presbyterian/Weill Cornell Medical Center, New York, NY, [2]New York, NY

Disclosures: Daniel Levitan: None; Nina Schatz-Siemers: None; Cathleen Matrai: None; Abha Goyal: None; Lora Ellenson: None; Edyta Pirog: None

Background: Association of Human Papillomavirus (HPV) with seborrheic keratosis-like lesions of the genital skin is still controversial. Tardio et al (2012) reported that 70% of the lesions were positive for HPV, while Reutter et al (2014) reported that HPV detection in vulvar seborrheic keratosis was very rare in women over the age 50. In order to further clarify the role of HPV in the pathogenesis of genital seborrheic keratosis-like lesions we sought to test these lesions using both HPV in-situ hybridization and the highly sensitive polymerase chain reaction (PCR) based assay SPF10.

Design: Twenty-six consecutive cases of genital seborrheic keratosis-like lesions were collected between 2002 and 2017. Ten cases of conventional condylomata acuminata with PCR-proven HPV6/11 were collected to serve as positive controls. Five cases of genital fibroepithelial polyps were collected to serve as negative controls. HPV PCR was performed using SPF10 PCR-LiPA assay. HPV in-situ hybridization was performed using the RNAscope® HPV assay with probes for HPV6 and 11 according to manufacturer instructions (Advanced Cell Diagnostics, Inc).

Results: HPV testing by SPF10 PCR-LiPA detected HPV DNA in 100% of genital seborrheic keratosis-like lesions and 100% of conventional condylomata, but in 0% of fibroepithelial polyps. HPV genotypes detected in seborrheic keratosis-like lesions included: HPV 6 in 88.5% of cases and HPV 11, 18, 51, 39, 90, 91 in single cases, each. Two cases showed infection with multiple HPV types. The results of genotyping were not statistically different between genital seborrheic keratosis-like lesions and typical condylomata ($p > 0.05$). In-situ hybridization for HPV RNA was positive in 14/26 genital seborrheic keratosis-like lesions, 9/10 conventional condylomata, and 0/5 fibroepithelial polyps. Patients with genital seborrheic keratosis-like lesions ranged in age from 25 to 79 years old with an average age of 45.9. This was not significantly different from patients with conventional condylomata (age range: 23 to 83 years old, average age: 45.2).

Conclusions: Sensitive HPV PCR testing confirmed HPV etiology in all genital seborrheic keratosis-like lesions, regardless of patient age. On the other hand, in-situ hybridization failed to find a viral etiology in 46% of cases. The viral and clinical characteristics of patients with genital seborrheic keratosis-like lesions and conventional condylomata are very similar, suggesting that genital seborrheic keratosis-like lesions are a form of condyloma.

1078 Divergent Clonal Origins of Multiple Serous Tubal Intraepithelial Carcinomas (STICs) Demonstrated by TP53 Mutations Using Amplicon Sequencing

Shiou-Fu Lin[1], Tiffany Chu[2], Brant Wang[3], Alexander Baras[4], Russell Vang[5], Ie-Ming Shih[6], Tian-Li Wang[7]
[1]Taipei Medical University-Shuang Ho Hospital, New Taipei City, Taiwan, [2]Johns Hopkins University, Baltimore, MD, [3]Falls Church, VA, [4]Baltimore, MD, [5]Johns Hopkins Hospital, Ellicott City, MD, [6]Johns Hopkins Hospital, Baltimore, MD, [7]Johns Hopkins Medical Institutions, Baltimore, MD

Disclosures: Shiou-Fu Lin: None; Tiffany Chu: None; Brant Wang: None; Alexander Baras: None; Russell Vang: None; Ie-Ming Shih: None; Tian-Li Wang: None

Background: STIC is the putative precursor lesion of ovarian high-grade serous carcinoma (HGSOC). STIC bears a similar molecular and histological profile to HGSOC. However, due to the rarity and minute size of discrete STICs, their molecular features are not well understood. Some studies demonstrated a linear evolution from STIC to HGSOC while others proposed diverse evolutionary trajectories. Multiple STICs have been observed with or without HGSOC, but the multifocal pathogenesis and their molecular heterogeneity have not yet been well clarified. We applied next-generation amplicon sequencing to analyze common molecular alterations of STICs.

Design: We retrieved ovarian and fallopian tube specimens from 16 patients, for a total of 2 HGSOCs and 28 STICs (21 with Ki-67 $\geq$10% (Ki-high) and 7 with Ki-67 < 10% (Ki-low)). 8 patients had 2 or more STICs; a 9th patient had HGSOC and 1 STIC. Tumor epithelial cells were enriched via laser capture microdissection. Amplicon libraries were prepared using the Accel-Amplicon 56G Oncology panel covering TP53 and 55 other genes and sequenced on the Illumina HiSeq 2000.

Results: We were able to detect TP53 mutations in 12/16 patients comprising 21/30 lesions in our cohort (15/21 Ki-high, 5/7 Ki-low, 1 cancer). The mean TP53 allele frequency was 0.37 (0.10-0.79) with a cutoff value of 0.10. Of the four patients without somatic TP53 mutations, one had a germline TP53 mutation and another had a germline MUTYH mutation, accounting for six lesions (4Ki-high, 1 Ki-low, 1 cancer). Of the eight patients with multiple lesions, three had non-clonal TP53 mutations present in their lesions. The heterogeneous TP53 mutation pattern identified in some patients is consistent with our previous report.[1]

Conclusions: Non-identical TP53 mutations in multiple STICs from the same patient were found in a subset of these cases. This indicates the possibility of multiple origins of ovarian cancer precursors in the fallopian tube, with only one or two progressing to carcinoma later in life. In contrast, the same TP53 mutations in those multiple STICs may represent the intra-tubal spread from the original clones; therefore they all shared the same TP53 mutations.

Kuhn E, Kurman RJ, Vang R, et al. TP53 mutations in serous tubal intraepithelial carcinoma and concurrent pelvic high-grade serous carcinoma—evidence supporting the clonal relationship of the two lesions. The Journal of Pathology. 2012;226(3):421-426. doi:10.1002/path.3023.

1079 Budget Impact Analysis of Reflex BRCA Tumor Testing Compared to Counselling-Directed BRCA Testing for High Grade Serous Müllerian Cancer

Nicole Look Hong[1], Sharon Nofech-Mozes[1], Ekaterina Olkhov-Mitsel[2], Karen Ott[2], Yutaka Amemiya[3], Arun Seth[1], Lilian Gien[4], Andrea Eisen[5], Nadia Ismiil[1], Bojana Djordjevic[6]
[1]Sunnybrook Health Sciences Centre - University of Toronto, Toronto, ON, [2]Sunnybrook Health Sciences Centre, Toronto, ON, [3]Sunnybrook Research Institute, Toronto, ON, [4]Sunnybrook Odette Cancer Center, Toronto, ON, [5]Sunnybrook Health Sciences Centre - Medical Oncology, Odette Cancer Centre, Toronto, ON, [6]University of Toronto, Scarborough, ON

Disclosures: Nicole Look Hong: None; Sharon Nofech-Mozes: None; Ekaterina Olkhov-Mitsel: None; Karen Ott: None; Yutaka Amemiya: None; Arun Seth: None; Lilian Gien: None; Andrea Eisen: None; Nadia Ismiil: None; Bojana Djordjevic: *Speaker*, Astra Zeneca

Background: Ascertainment of *BRCA1/2* mutational status in high grade serous cancer (HGSC) of the upper Müllerian tract has critical implications for family counselling and targeted treatment of patients with platinum-sensitive recurrent disease. In some healthcare systems, however, referral rates for genetic counselling are low due to a number of logistical challenges. In addition, 13% of *BRCA1/2* germline mutation negative patients have HGSC with somatic *BRCA1/2*mutations. Therefore, reflex *BRCA* testing strategies in pathology laboratories are being explored. The objective of this study was to evaluate the comparative cost impact of reflex tumor testing for *BRCA1/2* mutations compared to standard counselling-directed testing.

Design: A decision analytic cost model comparing the current counselling-directed referral to medical genetics vs. reflex tumor testing in pathology laboratories was constructed. The model was populated with data from the following sources: a) institutional medical genetics database evaluating HGSC patients for *BRCA1/2* germline mutations b) rates of germline and somatic *BRCA1/2* mutations in a published large cohort of HGSC patients c) cost estimates for *BRCA1/2* mutation testing with next generation sequencing of blood and formalin fixed paraffin embedded tumor specimens (germline test being approximately 95% of tumor test cost), and cost of genetic counselling. The outcome was defined as ascertainment of somatic and/or germline *BRCA1/2* mutation status. Sensitivity analysis was conducted with the variable "% of patients recruited for genetic counselling" as a plausible value ranging from 10% to 95%. Costs are reported in non-adjusted 2018 Canadian dollars.

Results: The table illustrates the variable of "% of patients recruited for genetic counselling" in low, intermediate and high scenarios. At any rate of patient recruitment for genetic counselling, reflex tumor testing would identify more patients with *BRCA1/2* germline and/or somatic mutations. With a recruitment rate of >74%, reflex tumor testing also becomes less costly on a mean per patient basis.

% of patients recruited for genetic counselling	COUNSELLING-DIRECTED: % of possible patients with germline and/or somatic *BRCA1/2*mutations identified by system	TUMOR REFLEX: % of possible patients with germline and/or somatic *BRCA1/2* mutations identified by system	Mean Cost Differential TUMOR REFLEX vs. COUNSELLING DIRECTED ($CAD) per patient
13 (Low)	11	94	667
43 (Intermediate)	37	94	335
89 (High)	77	97	-161

Conclusions: Reflex *BRCA1/2* mutation testing of HGSC tumors in the pathology laboratory is a more cost-effective strategy for centers with capacity to recruit a high proportion of eligible patients for genetic counselling. Even in centers with high recruitment rates for genetic counselling, up-front tumor testing identifies a significantly higher percentage of possible patients with germline and/or somatic *BRCA1/2* mutations.

1080 Microsatellite Instability Status and Tumor Mutational Burden Analysis by Whole Exome Sequencing in Endometrial Cancer

Xilu Ma[1], Hyeon Jin Park[2], Gloria Cheang[3], Kenneth Eng[4], Evan Fernandez[5], Lora Ellenson[1], Wei Song[6]
[1]New York-Presbyterian/Weill Cornell Medical Center, New York, NY, [2]Weill Cornell Medicine, Hartsdale, NY, [3]Weill Cornell Medical College, New York, NY, [4]Englander Institute for Precision Medicine, Brooklyn, NY, [5]Weill Cornell Medicine, New York, NY, [6]Weill Cornell Medical College, Short Hills, NJ

Disclosures: Xilu Ma: None; Hyeon Jin Park: None; Gloria Cheang: None; Kenneth Eng: None; Evan Fernandez: None; Lora Ellenson: None; Wei Song: None

Background: Microsatellite instability (MSI) status predicts response to immune checkpoint inhibitors, leading to the FDA approval of pembrolizumab for any type of advanced pediatric or adult cancer based strictly on its genetic profiles, including MSI-H or dMMR. Current evaluation of MSI status relies on either MMR protein IHC or polymerase chain reaction-based methods, however, the utility of large panel next-generation sequencing (NGS), including whole exome sequencing, in analyzing MSI status has not been well characterized.

Additionally, tumor mutational burden (TMB) has recently been shown to be a promising, independent biomarker in predicting immune checkpoint inhibitor response particularly in non-small cell lung and colorectal cancers. At the present, these studies have not focused on endometrial cancer. Here, we sought to analyze MSI status by whole exome sequencing in endometrial cancers and explore its relationship with TMB.

Design: 45 endometrial cancer cases were matched according to mismatch repair protein expression by IHC (24 dMMR and 21 pMMR cases), as well as FIGO Grade and Stage. Paired tumor and normal tissues were sequenced through our in-house whole exome sequencing pipeline, EXaCT-1. MSIsensor, a C++ program, automatically detects somatic microsatellite changes by examining around 5000 foci in the whole human exome.

Results: By using an MSIsensor score >=2 to define MSI high, 2 of 2 dMMR cases were MSI-H and 2 of 2 pMMR cases were MSS – 4.71 and 2.43 for the two dMMR cases and 0.09 and 0 for the two pMMR cases, respectively. Moreover, the two MSI-H cases showed significantly higher TMB than those of MSS – 22.1 and 15.1 mutations/Mb vs. 2.4 and 2.0 mutations/Mb, respectively. The remaining 41 EC cases are being currently sequenced and analyzed.

Conclusions: Preliminary results indicate that NGS technique, including whole exome sequencing, can be used to reliably assess MSI status in endometrial cancer. Combining assessment of both MSI and TMB through NGS test in endometrial cancers may help further characterize tumors in patients that can benefit from treatment with immune checkpoint inhibitors.

1081 MLH1 Methylated Endometrial Carcinoma: Histopathologic findings of a cohort of cases

Mona Maghsoodi[1], Poonam Khullar[2]
[1]NYU, Mineola, NY, [2]NYU Winthrop Hospital, Mineola, NY

Disclosures: Mona Maghsoodi: None; Poonam Khullar: None

Background: Lynch syndrome is an inherited, autosomal dominant disorder with germline mutations in mismatch repair genes (MMR) - MLH-1, PMS2, MSH2 and MSH6 and can be seen in up to 6% of all endometrial carcinomas (EC). Women with Lynch syndrome have an increased lifetime risk for syndromic cancers, including endometrial cancer (60%), colon cancer (up to 50%), ovary, upper urothelial tract, upper GI tract, etc. A diagnosis of a sentinel cancer associated with Lynch syndrome initiates surveillance of the patient and family members. Currently, testing is performed on tumor tissue, using immunohistochemistry (88 to 95% concordance with MSI analysis). Immunohistochemical loss of MSH2, MSH6 or PMS2 is considered adequate for reflex genetic counseling and germline testing. However, immunohistochemical loss of MLH-1 may be due to epigenetic methylation of the MLH1 promoter gene in up to 75% of cases; the remainder are presumed to be associated with Lynch syndrome and require germline MLH-1 testing. Epigenetic silencing of MLH-1 alone or MLH1/PMS2 has been associated most commonly with sporadic EC. We reviewed histopathologic findings of all MLH1 methylated EC resected at our institution between 01/2016 and 8/2018.

Design: We reviewed our files for all endometrial cancers submitted for MLH1 methylation analysis between 1/2016 and 8/2018 and identified 50 cases. Of these, 46 cases were methylated - 44 cases were negative for MLH1/PMS2 and 2 cases for MLH1/PMS2/MSH6 by immunohistochemistry. We then reviewed the pathology reports of these cases for: age of patient, tumor volume, histologic type, FIGO grade, depth of invasion, lymphatic invasion (LVI), involvement of LUS/cervix, nodal status, TNM stage.

Results: Age of pts: 50's (26%); 60's to 79 (71%). **Tumor type**: Endometrioid (93%); Others (7%).

Tumor Volume (cu mm): <1000 = 13%; 1000 to 15000 = 58.7%; 15000 to 50000 = 28.2%.

Depth of invasion: 0 = 21.7%; <50% = 47.8%; >50% = 30.4%.

Depth >50% with tumor vol: <10000 = 28%; > 10000 = 53%.

LVI = 17.4%; **LVI with tumor vol**. <10000 = 10%; >10000 = 31%.

LUS involved = 15.2%; **Cx involved** = 6.5%; **Nodes**: Neg = 95%;

TNM: pT1aN0/NX = 63%; pT1bN0/NX =28%; pT1bN1, pT2N0, pT2NX, pT3aN1 = 2% each.

Conclusions: MLH1 methylated cancers are predominantly endometrioid FIGO1, but one was FIGO III, two cases also had serous and dedifferentiated components. Bulky tumors showed a higher incidence of >50% myometrial invasion and lymphatic invasion. MLH1 methylated tumors may behave aggressively.

1082 Mismatch Repair Deficient Endometrial Cancer with Biallelic Somatic Mutations: Shedding Light on Lynch-like Syndrome in Endometrial Cancer Patients

Sundis Mahmood[1], Jessica Dillon[2], Laura Tafe[3]
[1]Dartmouth Hitchcock Medical Center, Lebanon, NH, [2]Johns Hopkins Hospital, Baltimore, MD, [3]Dartmouth-Hitchcock Medical Center, Lebanon, NH

Disclosures: Sundis Mahmood: None; Jessica Dillon: None; Laura Tafe: None

Background: Lynch-like syndrome (LLS) is a proposed term for colorectal (CRC) or endometrial cancer (EC) patients with mismatch repair deficiency (MMRd) or microsatellite instability within the tumor that are negative for germline mutations in Lynch-associated genes. In CRC cohorts, up to 70% of LLS have biallelic somatic muations in MMR genes and many patients also have germline mutations in other cancer susceptibility genes (PMID: 29723603, 28693799). In this study, we describe our experience with EC patients with biallelic somatic mutations in MMR genes.

Design: Universal screening for Lynch syndrome (LS) on all EC hysterectomy specimens began in May 2015 in our institution, using a panel of four immunohistochemistry (IHC) markers (MLH1, MSH2, MSH6 and PMS2). In cases of MLH1/PMS2 loss, reflex *MLH1* promoter methylation was performed. Patients with loss of MSH2/MSH6 or isolated loss of MSH2, MSH6, or PMS2 and those with negative *MLH1* promoter methylation were referred for genetic counseling for consideration of additional germline and somatic testing. Prior to 2017, germline testing only was typically offered to these patients. Starting in 2017, paired germline and somatic testing (Ambry TumorNext-Lynch +/- OvaNext) was offered.

Results: Between May 2015 and May 2018, 473 EC patients were screened for LS by IHC. Seven (1.5%) patients were identified that had negative germline testing for LS associated variants. Four also had paired somatic testing and biallelic somatic mutations in MMR genes, corresponding to the loss of IHC expression, were identified in all (100%) (Table). Interestingly, two patients had a family history of colon and endometrial cancers with a personal history of multiple colon polyps and breast cancer, respectively. The patient with breast cancer also had a germline *MRE11A* variant of undetermined significance detected by sequencing. A third patient had a subsequent screening colonoscopy and a polyp with invasive adenocarcinoma was identified.

Table. Clinical data and biallelic mutations detected in seven LLS patients. (NP – not performed; N/A – not applicable)

	Age	stage	Histology	grade	IHC for MMR proteins	Mutation 1	Mutation 2
1	57	pT1a	ENDOMETRIOID	III	Loss of MSH6	NP	NP
2	62	pT1a	ENDOMETRIOID	I	Loss of MSH6	NP	NP
3	73	pT1b	SEROUS	N/A	Loss of MSH6	NP	NP
4	56	pT3b	ENDOMETRIOID	III	Loss of MSH2/MSH6	MSH2 c.939delT	MSH2 c.943-2A>G
5	55	pT1a	ENDOMETRIOID	III	Loss of MSH2/MSH6	MSH6 c.3261dupC	MSH2 c.1077-1G>T
6	71	pT1b	ENDOMETRIOID	I	Loss of MSH2/MSH6	MSH2 c.1277-1G>A	MSH2 p.K661*
7	79	pT1b	SEROUS	N/A	Loss of MSH6	MSH6 c.88_100del13	MSH6 c.710delG

Conclusions: EC patients with LLS were rare (1.5%) in our screening population; all patients were 55 years of age or older. A proportion of these patients have a family or personal history suggestive of a germline alteration other than LS that possibly remains uncharacterized. EC patients with biallelic somatic mutations are a heterogenous group and clinical surveillance recommendations for these patients likely require customization. MMR deficiency with paired germline and somatic testing can identify this cohort of patients.

1083 MMR IHC and MSI PCR Co-testing of Endometrial Cancer for Lynch Syndrome: An Institutional Experience

Padmini Manrai[1], Douglas Rottmann[2], Xinyu Wu[1], Natalia Buza[3], Pei Hui[4]
[1]New Haven, CT, [2]Yale University School of Medicine, Hamden, CT, [3]Yale University, New Haven, CT, [4]Yale University School of Medicine, New Haven, CT

Disclosures: Padmini Manrai: None; Douglas Rottmann: None; Xinyu Wu: None; Natalia Buza: None; Pei Hui: None

Background: Inactivating mutations of four DNA mismatch repair (MMR) genes (*MLH1, PMS2, MSH2 and MSH6*) are the fundamental genetic basis of Lynch syndrome, leading to profound genetic instability and increased risk for endometrial and colon cancer development. Immunohistochemistry (IHC) and PCR-based microsatellite instability analysis of endometrial cancer have become an integral screening to identify Lynch syndrome proband. We summarize our institutional experience of Lynch syndrome screening using reflex combined MMR IHC and MSI PCR strategy.

Design: All newly diagnosed endometrial cancer specimens that underwent reflexed MMR IHC and MSI PCR were included during a 2.5-year study period with tumor tissue sources including hysterectomy, endometrial biopsy/curettage, metastatic tumors involving the ovary, lung, bladder, abdominal wall or omentum. MSI PCR results were reevaluated based on the refined criteria incorporating minimal nucleotide shift as MSI-high.

Results: A total of 408 cases were identified. The histological types of endometrial cancers included endometrioid adenocarcinoma (316 of 410, 77%), serous carcinoma (44 of 410, 10.7%) and malignant mixed Mullerian tumor (27 of 410, 6.5%, see Figure 1). DNA MMR deficiency was were detected in 81 of 408 cases by IHC (19.8%), whereas MSI analysis detected microsatellite instability in 83 of 408 cases (20.3%). The test concordance between MMR IHC and MSI analysis was 94%. Overall 25 cases (6%) had discordant MMR IHC and molecular MSI results (Figure 2). Seven cases were found to have a minimal MSI shift upon rereview leading to categorical change of the MSI status in these seven cases (see Figure 2).

Figure 1 - 1083

Figure 1: Distribution of histological subtypes of endometrial cancer in the study cohort.

Histologic Subtype	No.
Endometrioid Type (with mucinous differentiation)	315 (1) (77%)
Clear cell carcinoma	8 (1.9%)
Mucinous carcinoma	2 (<1%)
Serous carcinoma	44 (10.7%)
Endometrial adenocarcinoma mixed type	
• Clear cell/endometrioid	1 (<1%)
• Serous/endometrioid	8 (1.9%)
• Serous/mucinous	1 (<1%)
• Malignant Mixed Mullerian Tumors	27 (6.5%)
• Dedifferentiated	1 (<1%)

Figure 2 - 1083

Figure 2: Minimal shift observed in endometrial adenocarcinoma cases.

Initial Diagnosis	Diagnosis upon rereview	MMR IHC – PCR-MSI
MSI Low (n=5)	MSI High (5)	Concordant (4) Discordant (1)
MS Stable (n=2)	MSI High (1) MSI Low (1)	Concordant (2)

Conclusions: There is high concordance in testing endometrial cancers between MMR IHC and MSI PCR testing. MSI PCR interpretation requires careful evaluation for the presence of minimal microsatellite shift as evidence of instability. False negative result occurs with both screening tests, indicating that reflex co-testing of all newly diagnosed endometrial cancers by MMR IHC and MSI PCR has an optimized chance in capturing Lynch syndrome related endometrial cancers.

1084 The Controversy That Is Chronic Endometritis: A survey of pathologists

Samantha Margulies[1], Valerie Flores[1], Jonathan Hecht[2], Oluwole Fadare[3], Lubna Pal[1], Vinita Parkash[1]
[1]Yale University School of Medicine, New Haven, CT, [2]Beth Israel Deaconess Medical Center, Boston, MA, [3]University of California, San Diego, La Jolla, CA

Disclosures: Samantha Margulies: None; Valerie Flores: None; Jonathan Hecht: None; Oluwole Fadare: None; Lubna Pal: None; Vinita Parkash: None

Background: While acute endometritis is a reasonably well-defined entity of ascending infection and attendant active inflammation, chronic endometritis (CE) is a somewhat less defined disease entity. As part of a broad effort to define and refine the diagnostic criteria and management of the disease, we conducted parallel surveys of both gynecologists and pathologists on their current understanding and practices on CE. The findings of the pathologist survey are discussed herein.

Design: Members of national and international professional pathology societies (primarily the International Society of Gynecological Pathologists, British Association of Gynecological Pathology and the American Society of Clinical Pathology) were surveyed utilizing anonymous electronic surveys designed to examine diagnostic criteria, etiological understanding and treatment implications of a pathologic diagnosis of CE. A parallel survey queried gynecological societies (ACOG, others) and are reported separately.

Results: At the time of submission of this abstract, 336 pathologists responded. Findings demonstrate substantial variability on histological diagnostic criteria (25% requiring 1 plasma cell for diagnosis; 35-35% not diagnosing if gestational or secretory endometrium; 37% not diagnosing in the presence of co-existent pathology e.g. polyps, fibroids, hyperplasia), and use of ancillary immunohistochemistry (60% never; always or sometimes-40%). Fewer specialist gynecological pathologists diagnosed CE based on the presence of a single plasma cell, but this was not statistically significant (21% vs 25%, p=0.6). Specialists diagnosed CE in the setting of secretory endometrium more commonly (56% vs 47% p = 0.2). Although there was reasonable consensus that CE was a “specific entity” among pathologists (76%), there was marked variability on the probable primary etiology (49% infectious vs others). A similar variability of understanding on etiological contributors (68% infectious), presenting symptoms, criteria for diagnosis (histology only 55%, vs others including hysteroscopy) and management existed among gynecologists (N=71; surveys still open).

Conclusions: Our survey shows that even among pathologists, there is substantial variability in the diagnostic criteria for chronic endometritis, therefore, affecting who is diagnosed with CE and furthermore has the potential for treatment. In addition, it appears that even pathologists that specialize in gynecological pathology have difficulty with diagnosing.

1085 Interobserver Reproducibility in the Differential Diagnosis of Cellular and Spindle Ovarian Sex-Cord Stromal Tumors in Comparison with FOXL2 Mutational Analysis

Fabiola Medeiros[1], Joema Felipe Lima[2], Shabnam Zarei[3], Gary Keeney[4], Amy Clayton[5], Michael Henry[4], Andrew Folpe[4], David Schembri-Wismayer[4], Rafael Jimenez[4], Carol Reynolds[4], Sarah Kerr[4], Andre Oliveira[4], Debra Bell[4]
[1]Cedars-Sinai Medical Center, Los Angeles, CA, [2]Toronto, ON, [3]Cleveland Clinic, Cleveland, OH, [4]Mayo Clinic, Rochester, MN, [5]Mayo Clinic, Byron, MN

Disclosures: Fabiola Medeiros: None; Shabnam Zarei: None; Gary Keeney: None; Amy Clayton: None; Andrew Folpe: None; Rafael Jimenez: None; Sarah Kerr: None ; ebra Bell: None

Background: The differential diagnosis of cellular and spindled ovarian sex cord-stromal tumors (C/SSCST), particularly some adult-type granulosa cell tumors (GCT), cellular fibromas (CF) and thecomas (TH), is difficult due to their close histologic resemblance and limited availability of discriminatory ancillary tests. *FOXL2*402C→G (C134W) has been reported to be a sensitive and specific marker for GCT. However, data is limited regarding the detection rate of this mutation in diffuse-type GCT (GCTd) and GCT with prominent fibrothecomatous component (GCTft). We evaluated the level of diagnostic agreement for C/SSCST when comparing gynecologic pathologists to general surgical pathologists tracing a parallel with the diagnostic utility of *FOXL2* mutational analysis in this setting.

Design: 108 ovarian tumors, including 62 C/SSCST (17 GCTd, 15 GCTft, 21 CF and 9 TH), 23 conventional GCT (GCTc) and 20 negative controls were studied. All C/SSCST were blindly and independently reviewed by 8 surgical pathologists (4 general and 4 gynecologic) and were evaluated by reticulin, inhibin and calretinin stains. DNA was extracted from FFPE tissue followed by PCR and sequencing of *FOXL2*. Reproducibility rates for the diagnosis of C/SSCST were calculated using kappa statistics. The most common call amongst eight pathologists was used as the gold standard.

Results: The agreement rate for the general and gynecologic pathologists, each group in isolation, in diagnosing GCT (GCTd + GCTft), TH and CF was 0.52 and 0.54, respectively. There was higher agreement for GTCd than GCTft in both groups. *FOXL2*mutations were detected in 20 of 23 GCTc (86.9%), 10 of 17 GCTd, (58.8%), 5 of 15 GCTft (33.3%), 2 of 9 TH (18.2%), 1 of 21 CF (4.7%), and none of the negative controls. At least 2 of 4 gynecologic pathologists diagnosed the tumor as GCT in 16 (of 18) cases when a *FOXL2*mutation was present (88.9%). In this same category, at least two of four general pathologists diagnosed the tumor as GCT in 14 (of 18) cases (77.8%).

Conclusions: This study confirms the difficulty in distinguishing between diffuse granulosa cell tumors, granulosa cell tumors with a prominent thecomatous component and their largely benign counterparts, cellular fibroma and thecoma, both by morphology as analyzed by general and subspecialist gynecologic pathologists and by *FOXL2*mutational analysis. These findings indicate that further studies are needed on the biologic significance of *FOXL2*mutations in these tumors correlated with their biologic behavior.

1086 PD-L1, PD-1 Expression and DNA Mismatch Repair Genes in Cervical Squamous Cell Carcinoma, and Their Prognostic Significance

Rachelle Mendoza[1], Ying Yin Zhou[1], Elmer Gabutan[1], Tamineh Haidary[1], Wen-Ching Lee[1], Raag Agrawal[2], Yi-Chun Lee[1], Raavi Gupta[1]
[1]SUNY Downstate Medical Center, Brooklyn, NY, [2]SUNY Downstate, Brooklyn, NY

Disclosures: Rachelle Mendoza: None; Wen-Ching Lee: None; Raag Agrawal: None; Yi-Chun Lee: None; Raavi Gupta: None

Background: PD-L1 expression is a way for tumor cells to evade immune response, and high expression is linked to good response to immunotherapy. Previous studies observed low PD-L1 expression in cervical cancer and association between PD-L1 expression with deficient mismatch repair (MMR) genes. We aim to determine PD-L1 expression in our patient population and its clinical significance.

Design: A total of 198 patients with SCC were identified and 60 had evaluable tumor specimens and clinical data. Immunohistochemistry on MMR genes, PD-L1 (SP263, Ventana Roche) and PD-1 expression was performed. PD-L1 expression was classified as negative (<1%), low (1 to 50%) and high (>50%). PD-1 expression of tumor infiltrating immune cells (TIC) was classified as low if less than the median number of PD-1 positive TIC per mm². MMR status was determined as intact or deficient. Correlation between PD-L1, PD-1 expression, MMR status and clinical parameters was analyzed using $\chi 2$ or Fisher's exact test. Cumulative 5-year survival was analyzed using Kaplan-Meier curves and log rank test.

Results: Of the 60 patients, 90% were black, 55% between ages of 30-55 and 40% older than 55. 33 patients had poorly, 20 moderately, and 7 well-differentiated tumors. At 5-year follow up, 12 had recurrence, 14 patients died of disease and 6 lost to follow up. 93.3% of

tumors had positive staining for PD-L1 with 56.7% showing high expression. Patients aged 30-55 showed a higher rate of PD-L1 and PD-1 expression on TIC. Majority had intact MMR (91.7%).

Correlation analysis showed that there are significant correlations between age and PD-L1 expression on tumor cells (p=0.047) and PD-1 expression on TIC (p=0.013). Early stage tumors had significantly higher PD-1 expression on TIC (*p*=0.009). No correlation between MMR status and PD-L1/PD-1 expression is observed.

Mean disease free survival (DFS) was 43.7, 36.5, and 6.3 months for high, low and negative PD-L1 expression, respectively (*p*=0.002). In patients with stage I-II disease, mean DFS was 52.2, 42.6 and 7.6 months for high, low and negative PD-L1 expression, respectively (*p*=0.001). In patients with stage III-IV disease, mean DFS was 26.1, 10.7 and 3.6 months for high, low, and negative PD-L1 expression, respectively (p=0.37). Similar direct relationship is observed with overall survival.

Patient Characteristics	Chi-Square Tests / *Fisher's Exact test								
	PD-L1			PD-1			MMR Status		
	Value	df	p-value	Value	df	p-value	Value	df	p-value
Age Group	3.949	1	0.047	6.228	1	0.013	0.555	1	0.862
Race	5.752	8	0.675	5.529	4	0.237	0.606	4	0.962
Clinical Stage	5.891	6	0.436	10.553	3	0.014	2.576	3	0.462
Histologic Grade	1.777	4	0.777	2.266	2	0.322	1.547	2	0.461
PD-L1 Expression	-	-	-	0.053	2	0.974	1.441	2	0.487
PD-1 Expression	0.053	2	0.974	-	-	-	0.055	1	0.814 0.596*
MMR Status	1.441	2	0.487	0.055	1	0.814 0.596*	-	-	-

Figure 1 - 1086

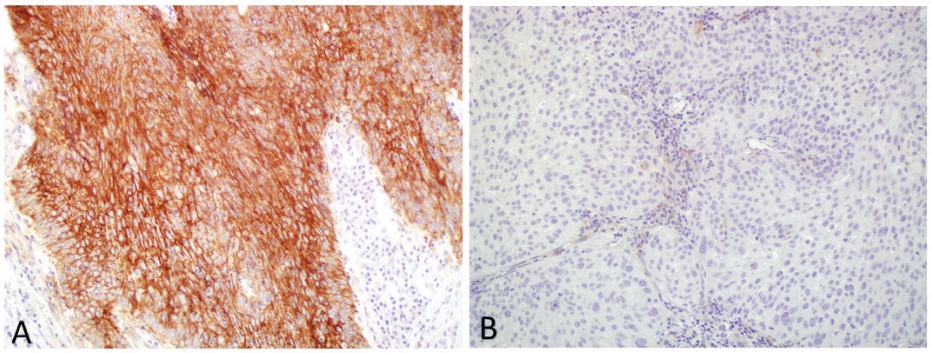

A. PD-L1 positive tumor cells (high expression). B. PD-L1 negative tumor cells.

Figure 2 - 1086

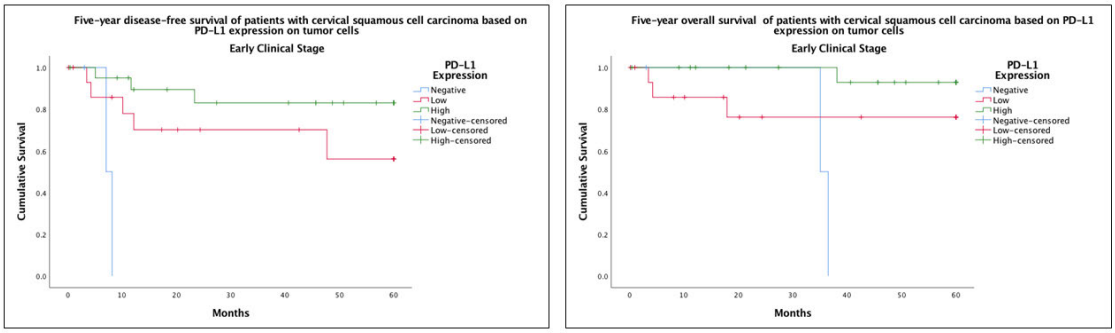

Conclusions: Contrary to previous studies, our results showed remarkably high rate of PD-L1 expression in cervical SCC, which is associated with longer DFS and OS, especially in early stage tumors.

1087 Clinicopathologic and Molecular Characteristics of Copy-Number Low Endometrial Adenocarcinomas

Rhonda Mittenzwei[1], Vivienne Meljen[1], Allison Puechl[1], Rex Bentley[1], Julia Elvin[2], Andrew Berchuck[3], Rebecca Previs[4], Kyle Strickland[1]
[1]Duke University Medical Center, Durham, NC, [2]Foundation Medicine, Cambridge, MA, [3]Duke University Medical Center, Chapel Hill, NC, [4]Durham, NC

Disclosures: Rhonda Mittenzwei: None; Vivienne Meljen: None; Allison Puechl: None; Rex Bentley: None; Julia Elvin: *Employee*, Foundation Medicine., Inc; Andrew Berchuck: None; Rebecca Previs: None; Kyle Strickland: *Consultant*, Foundation Medicine, Inc.; *Consultant*, Almac Pharmaceuticals

Background: Four subtypes of endometrial adenocarcinoma (EMCA) were described by The Cancer Genome Atlas (TCGA) project, with the largest subset demonstrating a microsatellite stable, copy-number low (CNL) molecular phenotype and lacking alterations in *POLE* and *TP53*. The majority of CNL cancers never relapse; however, *CTNNB1*-mutated (*CTNNB1*m) EMCAs are associated with increased rates of recurrence and are enriched in CNL EMCAs. The aim of this study was to evaluate whether morphologic patterns, genetic alterations, and/or ?-catenin immunohistochemistry (IHC) in CNL EMCAs can identify patients with increased risk of recurrence.

Design: We identified 19 CNL EMCAs with next-generation or whole genome sequencing and available material for ?-catenin IHC from our institution. Clinical data were abstracted from the electronic medical record, and H&E slides were reviewed to assess morphologic features, which were correlated with mutation status of select genes.

Results: *CTNNB1* mutations were present in 12 cases (63%). Mucinous differentiation was identified in 3 CNL EMCAs (16%) and was present only in KRAS-mutated, *CTNNB1*-wildtype (*CTNNB1*wt) tumors ($p<0.01$). Squamous differentiation was present in 52% of CNL tumors and was more often observed in *CTNNB1*m tumors ($p=0.02$). Nuclear localization of ?-catenin was highly predictive of mutation status and was present in the 10 *CTNNB1*m tumors and zero *CTNNB1*wt tumors ($p < 0.01$, sensitivity 0.83, specificity 1.00, positive predictive value 1.00, negative predictive value 0.78). 25% of *CTNNB1*m tumors harbored a concurrent mutation in *ESR1* (3/12), which were present only in *CTNNB1*m tumors and in none with wildtype *CTNNB1* ($p=0.02$). *ESR1* mutations were associated with shorter RFS among all CNL tumors ($p < 0.01$) and *CTNNB1*m EMCAs ($p = 0.03$). Evaluation of *ESR1* alterations in the larger EMCA TCGA dataset confirmed co-occurrence of *CTNNB1* and *ESR1* mutations ($p < 0.01$), as well as shorter RFS in patients with *ESR1*-mutated CNL tumors ($p < 0.01$).

Conclusions: CNL EMCAs exhibited diverse morphologic and molecular features. *KRAS* mutations were associated with mucinous differentiation and appeared mutually exclusive of *CTNNB1* alterations. *CTNNB1* mutations were associated with squamous differentiation and nuclear localization of ?-catenin. CNL EMCAs with concurrent mutations in *CTNNB1* and *ESR1* were associated with worse clinical outcomes and recurrence risk and may represent a subset of patients who can benefit from adjuvant therapeutic or surveillance strategies.

1088 Evaluation of Copy Number Alterations of MYC Family of Genes, RB1 gene and AURKA in Endometrial Carcinomas

Amir Momeni Boroujeni[1], Maria Arcila[2], Marc Ladanyi[2], Robert Soslow[2], Jason Chang[2]
[1]Memorial Sloan Kettering Cancer Center, Brooklyn, NY, [2]Memorial Sloan Kettering Cancer Center, New York, NY

Disclosures: Amir Momeni Boroujeni: None; Maria Arcila: None; Marc Ladanyi: None; Robert Soslow: *Speaker*, Ebix/Oakstone; Jason Chang: None

Background: The products of *MYC* family genes including *MYC*, *MYCN* and *MYCL* are transcription factors regulating the expression of many other genes; these genes are involved in cell proliferation and are regularly altered in different cancers. Studies have shown the interplay of MYC family gene alterations along with *RB1* and *AURKA* in different cancers; MYC amplification (AMP) along with *RB1* loss and *AURKA* amplification have been shown to be drivers of neuroendocrine transformation in cancers of different sites, especially prostate. In this study, we examine the frequency of copy number alterations (CNA) of these genes in endometrial cancers (EC).

Design: Genomic profiles of 981 EC patients analyzed by a hybridization-capture next-generation sequencing assay were screened for *MYC*, *AURKA* amplification and *RB1* loss. The pathology reports and the survival data for these cases were also examined.

Results: CNA of *MYC*, *AURKA*, and *RB1* were seen in 81 (8%) of endometrial cancers, with *MYC* AMP being most common at 5% followed by *RB1* Loss, *MYCN* AMP, *AURKA* AMP and *MYCL* AMP at 1.6%, 0.9%, 0.8% and 0.2% respectively. These alterations were not uncommon in uterine carcinosarcomas (UCS) (28/135, 21%) and uterine serous carcinomas (USC) (19/176, 11%), but rare in uterine endometrioid adenocarcinomas (14/465, 3%). Patients with EC harboring these alterations had a significantly worse overall survival outcome ($p=0.00004$). Even in the tumors with traditionally worse survivals, the presence of these alterations was associated with significantly poorer survival outcomes ($p=0.0317$). Within a 5-year follow-up, 49% of patients with these alterations died of disease, and 81% had persistence or progression of disease. Tumors harboring these alterations were also highly prone to metastasize (83%). Out of 42 patients with clinical stages less than IVB at the time of resection, 37 patients (88%) were upstaged within the follow-up period, with 32

patients having a final stage of IVB (76%). Evaluation of data from TCGA database was consistent with our findings. Furthermore, the mRNA expression data for these genes showed a strong correlation with survival for *MYC* and *AURKA* expression (p=0.01 and 0.006).

Figure 1 - 1088

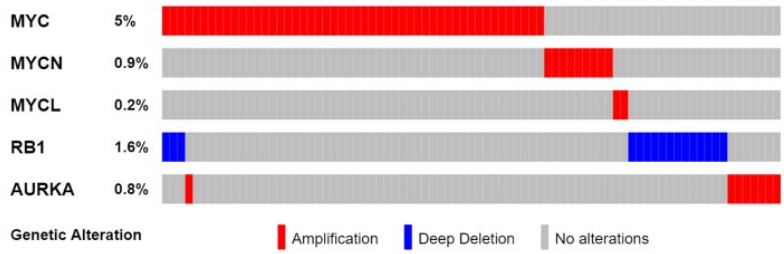

Figure 2 - 1088

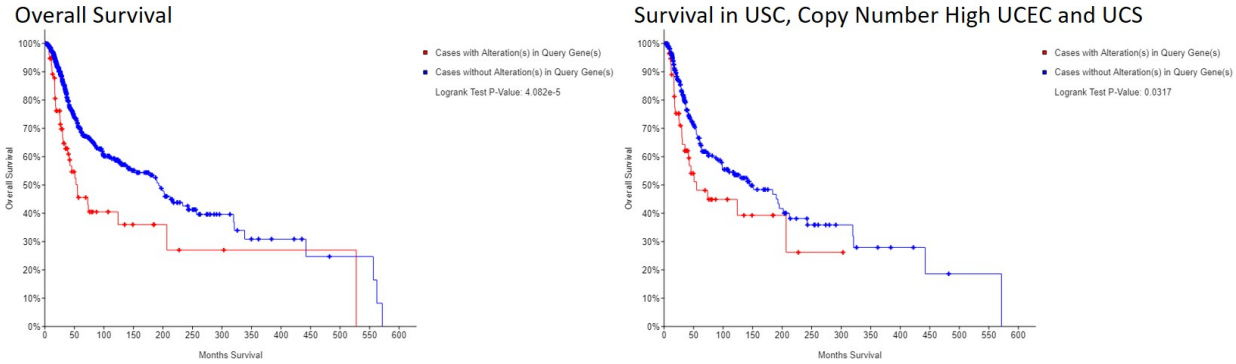

Conclusions: CNA of *MYC* family, *AURKA* and *RB1* are highly deleterious events in endometrial cancers. Even tumors with low initial clinical stage that harbor these alterations had poor survival outcomes. Therefore, screening for these alterations can potentially identify patients who will likely require more aggressive management course.

1089 The Immune Checkpoint TIM-3 is Highly Expressed in a Subset of Endometrial Carcinomas, Particularly in the Context of MLH1-Hypermethylation

Margaret Moore[1], Kari Ring[1], Anne Mills[1]
[1]*University of Virginia, Charlottesville, VA*

Disclosures: Margaret Moore: None; Kari Ring: None; Anne Mills: None

Background: Mismatch repair-deficient (MMRd) endometrial carcinomas (ECs) are associated with increased neoantigen loads and more vigorous immune responses when compared to mismatch repair intact (MMRi) ECs. This activated immune microenvironment manifests in increased tumoral PD-L1 expression and vulnerability to agents targeting the PD-1/PD-L1 axis, particularly in tumors with Lynch syndrome (LS)-associated mutations. TIM-3 is a checkpoint molecule with similar immune inhibitory function to PD-1/PD-L1, with expression documented on both innate and tumor-associated immune cells and on cancer cells. Increased expression of TIM-3 has been documented in a variety of tumor types, and several drugs targeting TIM-3 are being investigated in clinical trials. However, little is known about TIM-3 expression in ECs.

Design: TIM-3 immunohistochemistry (IHC) was performed on whole sections from 59 ECs [24 MMRd LS-associated, 20 MMRd MLH1 promoter hypermethylated, and 15 MMRi]. Tumoral TIM-3 staining was semi-quantitatively classified as negative (<1%), 1-5%, 6-10%, 11-25%, 26-50%, and >50%. Immune cells with positive TIM-3 staining were enumerated and semi-quantitatively classified as absent, focal (1-20/HPF), moderate (20-40/HPF), or robust (>40/HPF).

Results: The majority [60% of MMRi and 77% of MMRd] of ECs showed at least 1% tumoral positivity for TIM-3. The MLH1-hypermethylated subset was more likely to demonstrate >5% tumoral staining [65%], when compared to both MMR-intact ECs [13%, p<0.005] and LS- associated ECs [29%, p<0.05]. All tumors showed at least focal immune-cell staining with TIM-3. However, there was a higher rate of moderate and robust TIM-3 immune expression in the MMRd subset [68%], when compared to MMRi ECs [13%,p<0.001].

There was no significant difference between the degree of immune staining between the LS-associated and MLH1-hypermethylated subsets.

Figure 1 - 1089

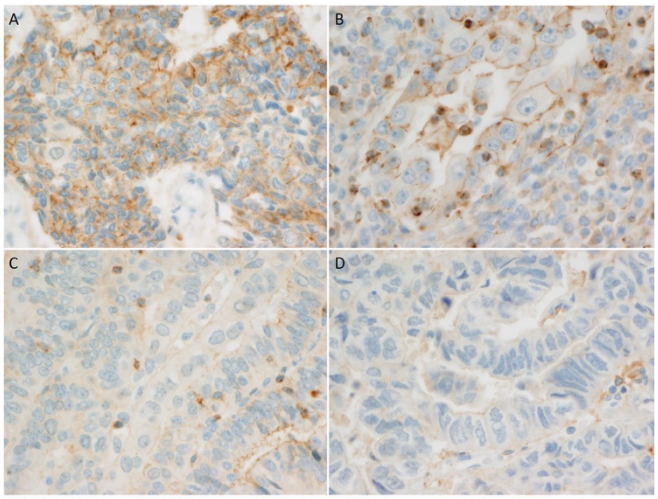

FIGURE 1. Patterns of TIM3 Expression in EC: Tumoral TIM-3 expression defined by circumferential membranous staining was seen in a subset of EC, as pictured in cases **A** and **B**. Case **B** also shows robust associated immune cell staining. Cases **C** and **D** show moderate and focal immune cell staining, respectively, without associated tumoral expression.

Figure 2 - 1089

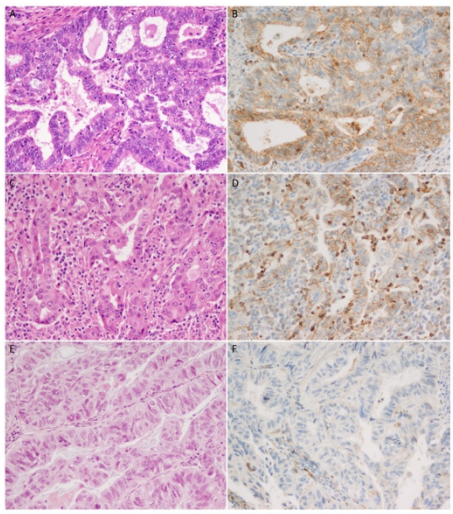

FIGURE 2. TIM-3 Expression across MMR Subsets: Tumoral and immune-cell expression of TIM-3 varied across MMR subsets of EC. Some cases, including the MLH-1 hypermethylated MMRd EC pictured in **A-B** and the MMRd LS-associated EC pictured in **C-D** showed strong, membranous tumoral staining as well as moderate to robust tumor-associated immune cell staining. Others, including the MMRi EC pictured in **E-F**, showed no TIM-3 expression on tumor cells and only focal immune cell staining.

Conclusions: Tumoral expression of the immune checkpoint TIM-3 is common in both MMRi and MMRd cancers, with the highest levels of expression identified in MLH1-hypermethylated ECs. Immune cell expression of TIM-3 is present in both MMRi and MMRd cancers, but with significantly more robust immune cell expression in MMRd cancers. These data support a potential role for checkpoint inhibitors targeting TIM-3 in a subset of ECs, particularly those demonstrating MLH1 hypermethylation.

1090 Impact of Endometrial Intraepithelial Neoplasia (WHO2014) Terminology Adoption: 4-year Experience at a Single Institution with Follow-Up

Gahie Nam[1], Kamaljeet Singh[2], Katrine Hansen[3], C. James Sung[4], M. Ruhul Quddus[4]
[1]Rhode Island Hospital/Brown University, Providence, RI, [2]Women and Infants Hospital, Providence, RI, [3]Women and Infants Hospital of Rhode Island, Providence, RI, [4]Women & Infants Hospital/Alpert Medical School of Brown University, Providence, RI

Disclosures: Gahie Nam: None; Kamaljeet Singh: None; Katrine Hansen: None; C. James Sung: None; M. Ruhul Quddus: None

Background: Endometrial hyperplasia is a precursor lesion of endometrioid type endometrial carcinoma. The presence of atypia in these lesions further elevates the cancer risk up to 45-fold. The previous WHO (1994) classification adopted four categories depending on the architecture and the cytological atypia. Due to lack of reproducibility and standardized clinical implications of this classification, a two- tiered nomenclature was endorsed by WHO (2014). In this study, we describe our experience of clinico-pathological follow-up using WHO 2014 in contrast to WHO 94 at a tertiary care gynecologic oncology hospital.

Design: Endometrial biopsies (EMB) with complex atypical hyperplasia (CAH) between 2008- 2010 and endometrial intraepithelial neoplasia (EIN) between 2016- 2018 were selected. Clinico-pathological data and histological findings (polyps vs. non polyps) of subsequent specimens were collected. Statistical comparison was performed using Pearson test.

Results: 116 EMB with CAH (group 1) and 109 EMB with EIN (group 2) were identified. The median age at time of diagnosis was 54 years. The median follow-up time was 0.5- 89 months (mean: 7.2 months). 92 % (n=207) of the patients had follow-up resections or additional endometrial sampling. The rates of follow-up hysterectomies were 77.4% for CAH and 65.6% for EIN (p=0.157). Follow-up resections showed higher rate of cancer in CAH (32.5%) than in EIN (22.2%), p=0.024. Of hysterectomies with cancer from CAH biopsies, 85% (n=24) were FIGO grade 1 and 78.6% (n=22) were pT1a. Of hysterectomies with cancer from EIN biopsies, 79% (n=11) were FIGO grade 1 and 100% (n=14) were pT1a. The rate of persistent EIN/CAH on hysterectomies for EIN was 50.7% and 29% for CAH. Hyperplasia without atypia on resections was higher in CAH (19.8%) versus 4.8% in EIN. Additional findings are in Results Table. These follow up resection diagnoses were statistically significant (p=0.0062).

	Confined to Polyp	Median follow-up (months)	Follow-up		Hyperplasia on F/up		Carcinoma on F/up	
			Bx	Hyst	Bx	Hyst	Bx	Hyst
CAH (n=116) Group 1	26/116 (22.4%)	0.5- 89 (mean: 10, median: 4)	25 /111 (22.5%)	86/111 (77.4%)	8/25 (32%)	17/86 (19.8%)	0/25 (0%)	28/86 (32.5%)
EIN (n=109) Group 2	27/109 (24.7%)	0.5-48 (mean: 4, median: 3)	33/96 (34.3%)	63/96 (65.6%)	3/33 (9.1%)	3/63 (4.8%)	2/33 (6.1%)	14/63 (22.2%)

Conclusions: Despite some studies showing EIN classification to be a better predictor of progression to cancer, our study revealed increased rate of endometrial cancer on hysterectomies in CAH biopsies compared to EIN biopsies. These findings may be due to the perception among the pathologists that any lesion that is morphologically not similar to the background endometrium represents EIN causing an over diagnosis of EIN. The definition of EIN needs further refinement to avoid over diagnosis.

1091 Prognostic and Immunological Significance of ARID1A Status in Endometriosis-Associated Ovarian Cancers

Tayyebeh Nazeran[1], Madeline Mason[2], Sandra Lee[3], Bronwyn Gibson-Wright[4], Katy Milne[4], Ellen Goode[5], Susan Ramus[6], David Huntsman[7], Brad Nelson[8], Aline Talhouk[9], Martin Kobel[10], Michael Anglesio[1]
[1]University of British Columbia, Vancouver, BC, [2]Vancouver, BC, [3]Calgary, AB, [4]Trev and Joyce Deeley Research Centre, Victoria, BC, [5]Mayo Clinic, Rochester, MN, [6]University of New South Wales, Sydney, NSW, Australia, [7]British Columbia Cancer Research Institute, Vancouver, BC, [8]BC Cancer, Victoria, BC, [9]University of British Columbia and British Columbia Cancer Agency, Vancouver, BC, [10]University of Calgary, Calgary, AB

Disclosures: Tayyebeh Nazeran: None; Madeline Mason: None; Sandra Lee: None; Bronwyn Gibson-Wright: None; Katy Milne: None; Ellen Goode: None; Susan Ramus: None; David Huntsman: None; Brad Nelson: None; Aline Talhouk: None; Martin Kobel: None; Michael Anglesio: None

Background: ARID1A plays an important role as a tumor suppressor in many cancer types. Almost 50% of clear cell ovarian carcinomas (CCOC) and 30% of endometrioid ovarian carcinomas (ENOC) have a loss of function mutation in *ARID1A*. ARID1A inactivation is prognostic in a number of malignancies; however, there are contradictory reports regarding its clinical value in ovarian carcinomas. Using large cohorts of CCOC and ENOC cases, we investigated associations between ARID1A mutations and prognosis, CD8+ tumor-infiltrating lymphocytes (CD8 TIL), and DNA mismatch repair deficiency (dMMR).

Design: Tissue microarrays with 1,024 ENOC and 595 COCC from local resources, the Ovarian Tumor Tissue Analysis (OTTA) consortium, and The Canadian Ovarian Experimental Unified Resource (COEUR), were analyzed for ARID1A loss, using a validated immunohistochemistry (IHC) surrogate for loss-of-function mutation. Subsets of samples were analyzed for loss of MLH1, PMS2, MSH2, or MSH6, and correlated with data on CD8 TIL. Additional quantitative analysis of CD3 TIL, B/plasma cells (CD20/CD79), and macrophage/immune checkpoint pathways (CD68/PD1/PDL1) is in progress.

Results: ARID1A expression was negative in 41% of CCOC and 24% of ENOC . ARID1A negativity showed no correlation with outcome or stage in CCOC (p=0.65) or ENOC (p=0.77). There were trends toward decreased progression free survival (PFS) in low-stage ARID1A mutant CCOC, and increased PFS in high-stage ARID1A mutant ENOC, but these did not reach statistical significance. CD8 TIL were present at some level in 53.5% of CCOC and 74% of ENOC with loss of ARID1A expression, however the number of CD8 TIL did not correlate with ARID1A status (p=0.4086 and p=0.9482). Finally, loss of MMR proteins in ENOC showed a strong association with ARID1A loss (p=0.0006).

Conclusions: In contrast to prior smaller studies, we found no evidence that ARID1A status is prognostically significant in either CCOC or ENOC. Similar to reports in endometrial and gastric cancers we observed association between ARID1A loss and dMMR amongst ENOC. Given these aforementioned cancers have implicated dMMR as causative of ARID1A mutations, analysis of ENOC for specific ARID1A mutation type and potential sub-clonal patterns is justified. Finally, lack of association between CD8 TIL and ARID1A mutation status suggests ARID1A status may not influence CD8 TIL mediated anti-tumor immunity, although further work with additional immune markers is warranted.

1092 PAX2 is a useful biomarker in distinguishing endometrial neoplastic lesions from benign mimics

Shuang Niu[1], Ruijiao Zhao[2], Yiying Wang[3], Hao Chen[4], Ping Zhou[5], Rongzhen Luo[6], Elena Lucas[7], Glorimar Rivera Colon[8], Wenxin Zheng[9]
[1]Frisco, TX, [2]Henan Provincial Peoples' Hospital, Zhengzhou, China, [3]Henan Provincial People's Hospital, Zhengzhou, China, [4]Coppell, TX, [5]Qianfoshan Hospital Affiliated with Shandong University, Jinan, China, [6]Sun Yat-sen University Cancer Center, Guangzhou, China, [7]University of Texas Southwestern, Dallas, TX, [8]Dallas, TX, [9]University of Texas Southwestern Medical Center, Dallas, TX

Disclosures: Shuang Niu: None; Ruijiao Zhao: None; Yiying Wang: None; Hao Chen: None; Ping Zhou: None; Rongzhen Luo: None; Elena Lucas: None; Glorimar Rivera: None; Wenxin Zheng: None

Background: Transcription factor Paired box gene2 (PAX2) plays a critical role in embryogenesis of multiple organs. It has mainly been used in European countries as a biomarker differentiating endometrial neoplastic lesions from benign morphologic mimics. PTEN, in contrast, is a well-recognized biomarker applied in this setting worldwide. However, PTEN commonly shows strong background staining, which limits its application in routine practice. Here we evaluated the utility of PAX2 compared to PTEN in differentiating endometrial neoplastic lesions from their benign mimics.

Design: Immunohistochemical (IHC) staining using antibodies against PAX2 and PTEN was performed on 118 endometrial specimens, including normal endometrium (n = 16), benign hyperplasia (n = 20), atypical hyperplasia (AH) / endometrial intraepithelial neoplasia (EIN) (n = 52), and well differentiated endometrioid carcinoma (n = 30). Only complete loss of staining in lesional areas was considered as "loss", while partial loss or presence of cytoplasmic staining was considered "intact". The diagnosis was based on WHO criteria. Results of staining were analyzed by Fisher exact test.

Results: Intact PAX2 and PTEN stains were present in both non-hyperplastic endometrium and in endometrial hyperplasia without atypia as expected. In cases with AH/EIN, loss of PAX2 stain was seen in 44/52 (84.6%), while loss of PTEN was seen in 29/52 (55.8%). In endometrioid carcinomas, PAX2 loss was identified in 21/30 (70%), while PTEN loss was found in 16/30 (53.3%). There were 6 AH/EIN and 5 cancer cases with uninterpretable PTEN, while all PAX2 stains were clear-cut. The incidence of PAX2 loss was significantly higher in AH/EIN (p<0.00001) and endometrioid carcinoma (p<0.00001) when compared to the hyperplasia without atypia group and/or non-neoplastic group. Similarly, the incidence of complete PTEN loss was significantly higher in AH/EIN (p<0.00001) and endometrioid carcinoma (p<0.00001) when compared to the hyperplasia without atypia group and/or non-neoplastic group. There was no significant difference between AIH/EIN and endometrioid carcinoma for both PAX2 and PTEN.

Conclusions: PAX2 is a useful diagnostic biomarker in distinguishing neoplastic lesions (AH/EIN and endometroid carcinoma) from non-neoplastic endometrium. Compared to PTEN, results of PAX2 are easier to interpret. Together with PTEN, PAX2 is useful when differential diagnosis of AH/EIN is encountered.

1093 CK7 status in CIN2 biopsies predicts the presence or absence of high-grade lesions in subsequent LEEP

Shuang Niu[1], Qingping Jiang[2], Ping Zhou[3], Rongzhen Luo[4], Hao Chen[5], Elena Lucas[6], Wenxin Zheng[7]
[1]Frisco, TX, [2]Third Affiliated Hospital, Guangzhou Medical University, Guangzhou, China, [3]Qianfoshan Hospital Affiliated with Shandong University, Jinan, China, [4]Sun Yat-sen University Cancer Center, Guangzhou, China, [5]Coppell, TX,[6]University of Texas Southwestern, Dallas, TX, [7]University of Texas Southwestern Medical Center, Dallas, TX

Disclosures: Shuang Niu: None; Qingping Jiang: None; Ping Zhou: None; Rongzhen Luo: None; Hao Chen: None; Elena Lucas: None; Wenxin Zheng: None

Background: It is well known that diagnoses of cervical intraepithelial neoplasia 2 (CIN2) has a low reproducibility. It is also well recognized that there is a significant proportion of negative finding (no comparable lesions) in subsequent LEEP excision specimens following a CIN2 diagnosis on cervical biopsies. The biomarker p16 has been commonly used in this setting in clinical practice. However, lesions with CIN2 and confirmed by p16 stain also has a low predictive value for HISL (CIN2+) in subsequent LEEP excisions. This dilemma leads to seeking better prognostic markers. CK7 identifies a special group of squamocolumnar junction cells, which are stem cell in nature. We sought to investigate the predictive value of CK7 status for those CIN2 lesions on biopsy to correlate to the subsequent LEEP findings.

Design: A total of 33 cases with CIN2 diagnosed on biopsies and their corresponding LEEP resection specimens were studied. Among the 33 cases, 18 cases showed CIN2+ in subsequent LEEP excisions, while 15 cases with either benign or lesions less than CIN2. The diagnosis of CIN2 for all cases were confirmed by p16 and Ki-67 stains based on LAST guideline. All cervical biopsies with the diagnosis of CIN2 were stained with CK7. Pathologic diagnosis and staining results were reviewed by 3 pathologists. Positive CK7 stain was defined as more than 3 layers strong positive (membranous) squamous epithelia cells in targeted area. Focal, weak, or less than 3 layers cellular positivity was considered as negative.

Results: Significantly more cases showed positive CK7 staining among biopsies with CIN2+ LEEP findings than biopsies with CIN2- LEEP findings (14/18, 77% vs. 6/15, 40%). Overall, CK7 positivity alone in biopsies has a sensitivity of 77.8%, specificity of 60%, positive predictive value of 70%, and negative predictive value of 70.2% for a subsequent LEEP excision showing lesions of CIN2+.

Conclusions: By applying stringent interpretation criteria, CK7 reactivity in CIN2 biopsy showed good predictive values for subsequent finding of HSILs in excisional specimens. Application of CK7 biomarker stain could potentially be used to guide clinical management.

1094 Clinicopathologic Features Of Gynecologic Malignant Neoplasms With Trousseau's Syndrome

Kazuya Onuma[1], Takanori Fukuda[1], Kenji Hishikawa[1], Yutaka Kohata[1], Shinichi Teshima[1], Hiromi Inoue[1]
[1]Shonan Kamakura General Hospital, Kamakura, Japan

Disclosures: Kazuya Onuma: None

Background: Trousseau's syndrome (TS) is originally described as unexplained thrombotic events preceding the diagnosis of an underlying visceral malignancy. TS is known to be typically associated with mucin producing tumor including pancreatic, gastric, or pulmonary carcinoma. Although studies demonstrated the strong association of venous thromboembolism (VTE) with gynecologic malignancies, particularly ovarian carcinoma, clinicopathologic features of gynecologic malignant neoplasms presented with TS have not been well studied.

Design: The database was searched for gynecologic malignant neoplasms diagnosed and treated at our institution from January of 2012 to December of 2017. The second search was to identify cases with the document of TS, infarction, or embolism. Cases with asymptomatic peripheral DVT were excluded. Medical records were retrieved to extract demographic and clinical data listed as follows: Age, BMI, clinical manifestation, D-Dimer (DD), CA125, platelet count (Plt), stage, outcome. Pathologic reports and slides were also reviewed to collect size and histologic type of tumors and background histology. For the cases meeting the diagnosis of classic TS, the data were documented and tabulated.

Results: A total of 177 endometrial carcinomas and 130 ovarian/tubal/primary peritoneal carcinomas were registered during the period. Seven cases presented with classic TS, consisting of 5 cases of ovarian carcinomas (4 clear cell carcinoma and 1 mucinous carcinoma), 1 case of primary peritoneal high grade serous carcinoma, and 1 case of endometrial carcinoma (G2 endometrioid). No cervical or vulvar carcinomas presented with TS. The patient age ranged from 47 to 67 (median 64). The thromboembolic events were pulmonary embolism (PE) in 5, and cerebral infarction (CI) in 2. The clinicopathologic features are summarized in Table1.

	Age	BMI	Tumor histology	Size(cm)	Laterality	Stage	Symptoms	TS	DD	CA125	Plt	Outcome
	65	25.3	EMC G2 endometrioid	n/a	n/a	iiiC	dyspnea	PE	45.2	82.7	16.6	DD
	64	22.4	Ova clear cell and endometrioid	14	Left	IIIC	dyspnea	PE	23.3	372	20.1	DD
	47	19.4	Ova mucinous	16	Left	IIIA	dyspnea	PE	28.2	532	25.2	A
	58	18.2	PPCa high grade serous	n/a	n/a	IIIC	hemiparesis	CI	11.6	986	15.9	A
	63	21	Ova clear cell	12.5	Left	IIIC	Gerstman	CI	39.0	698	11.3	A
	51	29.5	Ova clear cell	11	Right	IC	dyspnea	PE	20.1	17675	30.5	A
	67	16.6	Ova clear cell	10	Right	IC	dyspnea	PE	16.9	142	44.4	A

EMC: endometrial carcinoma, Ova: ovarian, PPCa: primary peritoneal carcinoma, DOD: Died of disease, A:Alive

Conclusions: Among gynecologic malignant neoplasms, TS mostly occurred in association with ovarian carcinoma (the incidence was 4.6%) and clear cell carcinoma is the major histologic type (TS incidence was 13%), supporting its greatest risk of coagulation disorder. Endometrial carcinomas rarely presented with TS. While DD was the only discriminatory clinical parameter, there were no specific pathologic/morphologic features associated with TS occurrence. TS itself did not affect the prognosis with prompt management. Further study is needed to characterize malignant neoplasms with TS, particularly ovarian clear cell carcinoma to elucidate the mechanism.

1095 HPV-negative Tumors of the Uterine Cervix

Jaume Ordi[1], Inmaculada Nicolás[2], Adela Saco[1], Natalia Rakislova[2], Pere Fusté[2], Cristina Martí Delgado[2], Adriano Rodriguez-Trujillo[2], Marta del Pino[2]
[1]Barcelona, Spain, [2]Hospital Clinic, Barcelona, Spain

Disclosures: Jaume Ordi: None; Inmaculada Nicolás: None; Adela Saco: None; Natalia Rakislova: None; Pere Fusté: None; Cristina Martí Delgado: None; Adriano Rodriguez-Trujillo: None; Marta del Pino: None

Background: Human papillomaviruses (HPV) are the causative agents of virtually all cervical carcinomas (CC). Nevertheless, a small proportion of CC are negative for HPV, although the significance of this finding remains unclear. We aimed to provide insight into the differential clinico-pathological characteristics of this unusual subset of HPV-negative CC.

Design: We performed HPV DNA detection using a highly sensitive PCR test (SPF10) and p16 immunostaining in 214 CC specimens from women treated at the Gynecological Oncology Unit of the Hospital Clinic (Barcelona, Spain) from 2012 to 2015. The clinical and pathological characteristics, including disease-free survival (DFS) and overall survival (OS), of HPV-negative and -positive CC were compared.

Results: Twenty-one out of 214 tumors (9.8%) were negative for HPV DNA. HPV-negative tumors were more frequently of the non-squamous type (9/21, 42.9% vs.37/193, 19.2%; p<0.01) and showed negative p16 staining (9/21; 42.9% vs. 7/193; 3.6%; p<0.01). HPV-negative tumors were more frequently diagnosed at advanced FIGO staging (19/21, 90.5% vs. 110/193, 57.0%; p<0.01) and more frequently had lymph node metastases (14/21, 66.7% vs. 69/193, 35.8%; p<0.01). Patients with HPV-negative CC had a significantly worse DFS (59.8 months, 95% confidence interval [CI] 32.0-87.6 vs. 132.2 months, 95%CI118.6-145.8; p<0.01) and OS (77.0 months, 95% CI 47.2-106.8 vs. 153.8 months, 95% CI 142.0-165.6; p=0.01) than women with HPV-positive tumors. However, on multivariate analysis only advanced FIGO stage and lymph node metastases remained associated with a poor DFS and OS.

The analysis of the squamous cell carcinomas (SCC) separately, showed that patients with HPV-negative SCC (n=12) were more frequently diagnosed at advanced FIGO staging than HPV-positive SCC (n=156). Patients with HPV-negative SCC had a significantly worse DFS (47.6 months [95%CI: 10.5-84.7] vs. 130.7 months [95%CI: 115.5-145.9]; p<0.01) and OS (70.0 months [95% CI 27.3-112.7] vs. 150.0 months [95% CI 136.6-163.5]; p=0.04) compared to women with HPV-positive SCC. Although HPV was associated with relapse and mortality risk on univariate analysis in the subset of SCC, only lymph node metastases and advanced FIGO staging remained associated with a worse prognosis on multivariate analysis.

Conclusions: A low percentage of CC arise via an HPV-independent pathway. HPV-negative CC frequently present at advanced FIGO staging and more frequently have lymph node metastases.

1096 Molecular Profile of Cervical Neuroendocrine Carcinomas

Zehra Ordulu[1], Koen Van de Vijver[2], Gian Franco Zannoni[3], Ana Félix[4], Adele Wong[5], Robert Young[6], Mari Mino-Kenudson[7], Valentina Nardi[7], Esther Oliva[7]
[1]Massachusetts General Hospital, Dorchester, MA, [2]University Hospital Ghent, Ghent, Belgium, [3]Catholic University of Sacred Heart, Rome, Italy, [4]Instituto Portugues de Oncologia de Lisboa/CEDOC, Lisboa, Portugal, [5]KK Women's and Children's Hospital, Singapore, Singapore, [6]Harvard Medical School, Boston, MA, [7]Massachusetts General Hospital, Boston, MA

Disclosures: Zehra Ordulu: None; Koen Van de Vijver: None; Gian Franco Zannoni: None; Ana Félix: None; Adele Wong: None; Robert Young: None; Mari Mino-Kenudson: None; Valentina Nardi: None; Esther Oliva: None

Background: Neuroendocrine carcinoma of the cervix is a rare entity with poor prognosis and limited treatment options. Among the histologic variants, small cell neuroendocrine carcinoma (SCNEC) is the only one with molecular analyses described in the literature.

Design: Cervical non-SCNEC (9) and SCNEC (3) were analyzed with targeted next generation sequencing of 99 genes to identify nucleotide variations and 95 for copy number variations. The mutations were assessed using publicly available databases and our in-house database.

Results: More than half of the non-SCNEC (5/9) had somatic alterations. Mutations in p53 (1), RB1 (2), KRAS (2), PIK3CA (1), POLE (1), TSC2 (1), BRCA1 (1) as well as C-MYC amplification (1), PIK3R1 and MAP3K1 deletions (2) were detected. The two tumors with KRAS mutations showed similar multifocal pleomorphic cells. The specific POLE mutation (c.876G>T) detected in one tumor was not reported in any cancer types in public databases. Unlike the characteristic hypermutated phenotype of the POLE-mutated endometrial carcinomas, this was the only mutation noted in this tumor. Interestingly, a review of our in-house database revealed the same POLE mutation in a thymic neuroendocrine carcinoma with similar non-SCNEC morphology and malignant behavior (bone metastases), which also did not have a hypermutated phenotype. The SCNEC with somatic alterations (3/3) had mutations in PIK3CA (2), p53 (1), PTEN (2), with 1 case showing N-MYC (1). Amplification of N-MYC has not been previously described (or studied) in cervical SCNEC, but was detected in pulmonary SCNEC and is considered as a poor prognostic factor in neuroblastoma.

Case Number	Histology	Genes Altered
Case 1	Non-SCNEC	POLE
Case 2	Non-SCNEC	KRAS
		PIK3CA
		C-MYC (CNV, amplification)
Case 3	Non-SCNEC	KRAS
		RB1
		PIK3R1 (CNV, deletion)
		MAP3K1 (CNV, deletion)
Case 4	Non-SCNEC	TSC2
		BRCA1
		PTEN (CNV, deletion)
		PIK3R1 (CNV, deletion)
		MAP3K1 (CNV, deletion)
Case 5	Non-SCNEC	TP53
		RB1
Case 6	Non-SCNEC	No definitive somatic alteration
Case 7	Non-SCNEC	No definitive somatic alteration
Case 8	Non-SCNEC	No definitive somatic alteration
Case 9	Non-SCNEC	No definitive somatic alteration
Case 10	SCNEC	PIK3CA
		RB1
		PTEN
Case 11	SCNEC	PIK3CA
		N-MYC (CNV, amplification)
Case 12	SCNEC	TP53

Conclusions: Cervical NECs show a variety of alterations implicated in NETs of other locations involving AKT/mTOR pathway (PIK3CA, PIK3R1, MAP3K1, TSC2, PTEN), MYC (C-MYC, N-MYC), p53 and RB1; as well as those reported in cervical adenocarcinomas (KRAS). In addition, we identified a novel POLE mutation detected in two non-SCNEC (cervical and thymic), which does not result in a hypermutated phenotype. These molecular characteristics might inform potential therapeutic targets.

1097 Automated identification of precancerous neoplastic foci (EIN) in endometrial biopsies – a computational tool with diagnostic insight

David Papke[1], Sebastian Lohmann[2], Michael Downing[3], Peter Hufnagl[2], George Mutter[4]
[1]Brigham and Women's Hospital, Boston, MA, [2]Charité University Medicine Berlin, Berlin, Germany, [3]Acton, MA, [4]Brigham and Women's Hospital, Harvard Medical School, Boston, MA

Disclosures: David Papke: None; Sebastian Lohmann: None; Michael Downing: None; Peter Hufnagl: None; George Mutter: None

Background: Endometrial intraepithelial neoplasia (EIN) is a premalignant proliferation of cytologically altered glands that aggregate in clusters, often diagnostic focally within a few background tissue fragments. We hypothesize that image analysis can distinguish individual glands as normal (background, or NL) vs. neoplastic (EIN), and their distribution within the tissue can be used to highlight locations diagnostic for EIN.

Design: Tissue from 108 patients (34 EIN, 74 normal by H&E) was immunostained for pan-keratin, and all slides were scanned digitally. Image analysis (Visiopharm Integrator System, Horsholm, Denmark) of keratin stained glands was used to segment epithelium and its component structures. Individual glands in the validation set were scored as background or neoplastic based on positive or negative PAX2 stain status (a transcription factor lost in neoplastic EIN glands), respectively, and their location was mapped to companion image analysis results from the keratin stain. For each gland, morphometric segmentation data was extracted. Nuclear positions were used as vertices to generate a Delaunay triangulation triangle graph (DTTG) for each gland. 713 segmentation and 1248 graph summary statistical variables were used to develop random forest algorithms to classify each gland as neoplastic (component of EIN) or background (NL).

Results: 91 patients in the training set contributed 877 neoplastic-EIN and 5,742 background-NL glands, and 17 in the validation set contributed 1124 neoplastic-EIN and 1429 background-NL glands. DTTG statistics alone had a classification accuracy of up to 77.9% in the independent validation set (36.1% EIN error rate, 6.2% NL error rate). Classification accuracy improved with stricter gland inclusion criteria, such as minimum number of nuclei necessary to include a gland. Although the EIN error rate for single glands was high, the high specificity and presence of many EIN glands per case enabled identification of lesional foci in validation set cases (Fig 1).

Figure 1 - 1097

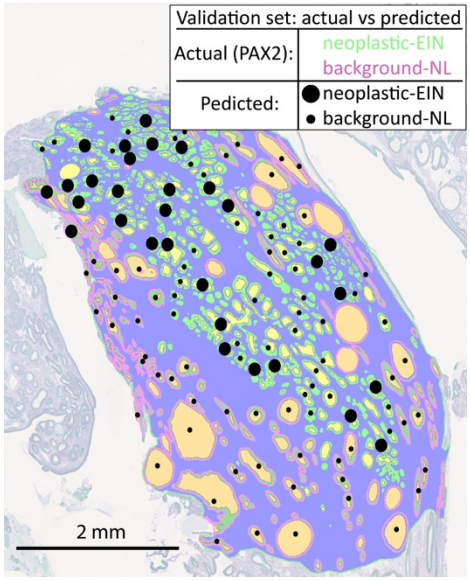

Conclusions: Our single-gland classification algorithm identifies EIN lesion epicenters in whole tissue fragments as dense clouds of individual glands classified as neoplastic-EIN. This result confirms that histologic features at the single gland level, when mapped back to larger scale tissue architecture, are useful for localization and diagnosis of EIN.

1098 Tumoral PDL1 And P53 Expression In Vulvar Carcinoma

Vishakha Pardeshi[1], Neeraja Yerrapotu[2], Ibrahim Tsolakian[3], Ira Winer[4], Sudeshna Bandyopadhyay[5], Rouba Ali-Fehmi[5]
[1]Westland, MI, [2]Wayne State University/Detroit Medical Center, Detroit, MI, [3]Wayne State University/Detroit Medical Center, Livonia, MI, [4]Wayne State University/Karmanos Cancer Center, Detroit, MI, [5]Wayne State University, Detroit, MI

Disclosures: Vishakha Pardeshi: None; Neeraja Yerrapotu: None; Ibrahim Tsolakian: None; Sudeshna Bandyopadhyay: None; Rouba Ali-Fehmi: None

Background: Vulvar carcinoma is commonly seen in elderly women. The incidence of vulvar carcinoma is on the rise due to aging population. Vulvar carcinomas not related to HPV progress through the p53 pathway. These carcinomas are hypothesized to show expression of PDL1 and play a major role in suppressing the immune system. p53 plays an important role in PDL1 regulation in patients with lung carcinoma. In our study we determined the expression of PDL1, and p53 in a subset of in situ and invasive vulvar squamous cell carcinoma. Expression of PDL1 in in-situ/VIN3 and invasive vulvar squamous cell carcinomas may be helpful in improving patient outcome through immunotherapeutic approaches.

Design: Retrospective review of VIN3 and invasive squamous cell carcinoma (n=61) was conducted in a subset of patients from 2000 to 2018. Blocks and slides for these patients were collected. Slides were reviewed for features of invasive squamous cell carcinoma and VIN3. Immunohistochemical stains were performed on these blocks for p53 and PDL1. PDL1 expression in tumor cells was evaluated per established criteria, and the expression of p53 and PDL1 CC was compared using the Z test.

Results: 43 cases (70.49%) of VIN3 and 46 cases (75.41%) of invasive squamous cell carcinoma were identified. PDL1 CC positivity was identified as membranous honey comb staining pattern of the tumor cells with more than 5% of the tumor cells staining, regardless of their intensity. p53 positivity was identified as more than 70% tumor cells with nuclear staining. 10 (23.25%) of VIN3 cases revealed p53 expression and 20 (46.51%) expressed PDL1 within tumor cells. Out of 46 (75.41%) cases with invasive squamous cell carcinoma, 10(21.73 %) were p53 positive and 23 (50%) were PDL1 positive in tumor cells. Expression of PDL1 showed positive trend between the in situ and invasive squamous cell carcinoma. There was no statistically significant difference in the expression of p53 and PDL1 between VIN3 and invasive squamous cell carcinoma (Z= 0.173; p=0.87) and (Z= -0.33; p= 0.74) respectively.

Table 1:

Stains	VIN3=43 (70.49%)	SCC=46 (75.41%)
P53 (+)	10 (23.25 %)	10 (21.73%)
PDL1 CC (+)	20 (46.51 %)	23 (50%)

Conclusions: Expression of PDL1 and p53 positivity showed no significant difference between in situ and invasive squamous cell carcinoma. Further studies with a bigger sample size might help us detect a significant difference which might raise the potential possibility in its application for immunotherapy in both in situ and invasive squamous cell carcinoma.

1099 Comprehensive Genomic Profiling of HPV-related and Gastric-type Endocervical Adenocarcinoma

Carlos Parra-Herran[1], Anjelica Hodgson[2], Neal Lindeman[3], Brooke Howitt[4], Marisa Nucci[5]
[1]Sunnybrook Health Sciences Centre - University of Toronto, Toronto, ON, [2]University of Toronto, Toronto, ON, [3]Brigham and Women's Hospital Pathology, Boston, MA, [4]Stanford University School of Medicine, Stanford, CA, [5]Brigham and Women's Hospital, Harvard Medical School, Boston, MA

Disclosures: Carlos Parra-Herran: None; Anjelica Hodgson: None; Neal Lindeman: None; Brooke Howitt: None; Marisa Nucci: None

Background: Our understanding of the molecular landscape of endocervical adenocarcinoma (EA) is still evolving. A number of recurrent mutations have been identified in EA (e.g. *PIK3CA*, *KRAS*) some of which carry prognostic significance. Most studies have used targeted panels and have not discriminated between EA types with distinct biologic differences, namely HPV-related (HPV-EA) and gastric-type adenocarcinoma (G-EA), the most common type of HPV-unrelated EA. Our aim was to comprehensively describe the genomic profile of EA in relation to type (HPV-EA vs G-EA) and clinical behavior.

Design: Institutional EAs (2002-2018) with material available and confirmation of the diagnosis by three gynecologic pathologists were included. DNA extraction followed by targeted next generation sequencing (NGS) was performed on paraffin-embedded tissue. NGS surveyed exonic regions of 447 genes to identify single nucleotide variations and copy number variations. Findings were correlated with clinicopathologic variables including EA type and patient outcome.

Results: The final cohort consisted of 57 EAs. Most frequent mutations involved *KRAS* (18%), *TP53* (18%), *PIK3CA* (16%), *GNAS* (12%), *ERBB2* (11%) and *STK11* (9%). Potentially actionable and/or prognostic mutations and amplifications (*MYC*, *ERBB2*) were identified in 17 (30%) patients. Recurrence and/or tumor-related deaths were observed in 15/50 (30%) patients with follow-up available (mean 38 months, range 1-133). EAs in patients with adverse events had a higher mutational burden than indolent EAs (3.1 vs 1.7 mutations/case, p=0.007, unpaired t-test). Likewise, EAs with adverse outcome had higher frequency of *KRAS*, *GNAS*, *CDKNA* and *STK11* pathogenic mutations (p<0.05 in all, Fisher's exact test). Regarding EA type, 46 (81%) cases were HPV-EA and 11 (19%) G-EA. Compared to HPV-EA, patients with G-EA were older (p=0.002) and more likely to present at advanced stage (p<0.001). Mutational burden differed between G-EA and HPV-EA approaching significance (3 vs 2, p=0.06). *CDKN2A* and *STK11* mutations were significantly more frequent in G-EA (p=0.02 and 0.04, respectively).

Conclusions: In this comprehensive analysis of EA, we document a correlation between the mutational profile of EA and clinical behavior (recurrences / death) as well as EA type. Thus, NGS can serve as a prognostic and histotype classification tool in EA. It can also identify mutations with known predictive and prognostic value, which can particularly benefit patients with recurrent and refractory disease.

1100 High Expression Of Neuromedin U In High Grade Serous Ovarian Cancer Confers A Progression Free Survival Advantage

Eilis Perez[1], Bashir Mohamed[2], Danny Di Capua[3], Noreen Gleeson[3], Claire Thompson[3], Feras Abu Saadeh[3], Cara Martin[4], Lucy Norris[5], Ciaran O'Riain[2], Mark Bates[5], Lorraine O'Driscoll[5], John O'Leary[5], Sharon O'Toole[4]
[1]Trinity College Dublin, Tyrrelstown, Ireland, [2]Dublin, Ireland, [3]St James's Hospital, Dublin, Ireland, [4]Trinity St. James's Cancer Institute, Dublin, Ireland, [5]Trinity College Dublin, Dublin, Ireland

Disclosures: Eilis Perez: None; Bashir Mohamed: None; Danny Di Capua: None; Noreen Gleeson: None; Claire Thompson: None; Fera; Abu Saadeh: None; Cara Martin: None; Lucy Norris: None; Ciaran O'Riain: None; Mark Bates: None; Lorraine O'Driscoll: None; John O'Leary: None; Sharon O'Toole: None

Background: Ovarian cancer is a major cause of cancer death in women worldwide with less than 40% of women surviving beyond 5 years post diagnosis. This is due mainly to late diagnosis and the development of recurrent chemoresistant disease. High grade serous is the most common and most lethal subtype of ovarian cancer. While chemotherapy response rates are initially good in ovarian cancer, patients often develop recurrent, chemoresistant disease. There is a need for novel biomarkers for improved diagnostics and patient stratification in ovarian cancer. Neuromedin U (NmU) is a neuropeptide found to have distinct roles in various cancers depending on context and cancer type. In breast cancer NmU is associated with more aggressive disease, HER2-targeted therapy resistance and poorer prognosis. NmU protein expression is transiently increased in the ovary during ovulation and increased NmU mRNA expression has been observed previously in ovarian cancer. The aim of this study was to assess the role of NmU in high grade serous ovarian cancer.

Design: Cases were identified from the Discovary bioresource in the Department of Obstetrics and Gynaecology in Trinity College Dublin. All patients gave informed consent and ethical approval was received. Two tissue microarrays were constructed; five 0.6mm cores were selected from representative tumour regions from (n=102) high grade serous stage 3-4 FFPE tissue blocks. Immunohistochemistry was performed using a NmU antibody (1:50 NmU; HPA025926, Atlas Antibodies, Stockholm, Sweden). NmU protein expression was then evaluated and scored as a product of intensity (scored 0-3) and percentage of cells stained (0-10%=1, 10-40%=2, 40-70%=3, 70-100%=4)

Statistical analysis was performed using SPSS Software (IBM). Kaplan Meier survival curves were used with calculated log-ranks for univariate analysis. Data was censored for cases where an event had not occurred by the time of analysis. The criterion for statistical significance applied was $p < 0.05$.

Results: NmU was over-expressed in ovarian high grade serous carcinoma tissue compared to benign controls. Increased NmU expression correlated with a significant progression free survival advantage (p=0.004) and increased disease-free interval (p=0.022) in the evaluable patient cohort (n=88).

Conclusions: These findings suggest that NmU may have a role in the pathogenesis of high grade serous carcinoma and may represent a novel prognostic and potentially diagnostic biomarker for this disease worthy of further in

1101 Common Challenges in Histologic Evaluation of FIGO Grade 1 and 2, Low Stage Endometrioid Adenocarcinoma: an Interobserver Study on Myoinvasion, LVI and Histologic Grading

Adam Perricone[1], Uma Krishnamurti[1], Marina Mosunjac[2], Krisztina Hanley[1]
[1]Emory University, Atlanta, GA, [2]Atlanta, GA

Disclosures: Adam Perricone: None; Uma Krishnamurti: None; Marina Mosunjac: None; Krisztina Hanley: None

Background: Histologic parameters that influence adjuvant treatment decisions in low grade/stage (FIGO grade 1-2, pT1) endometrioid adenocarcinoma (EA) include depth of myoinvasion and lymph-vascular invasion (LVI). Tumor distance to serosa (DTS) is found to be a stronger predictor of prognosis. Recent studies examined the interobserver reliability (IR) of various means of assessing depth of invasion (DOI). Challenges due to different patterns of invasion (PI) in EA have not been extensively studied.

Design: Electronic search for low grade/stage EA was performed. 51 cases were identified and the following parameters analyzed by 3 independent observers: PI, FIGO grade, LVI, %DOI, absolute DOI, and DTS. Primary and secondary PI were classified as either infiltrative, broad, adenomyosis-like, or MELF (microcystic, elongated and fragmented) with an optional comment if DOI was difficult to measure. Interobserver consistency of absolute DOI and DTS was assessed via intraclass correlation coefficient (ICC); IR was measured via calculation of Light's kappa (?).

Results: No significant differences in absolute DOI or DTS were seen between observers. Interobserver consistency of DTS was greater than that of absolute DOI (ICC=0.95 vs 0.71). IR was strong for %DOI and fair for LVI (?=0.78 and 0.6, respectively), but was poor for FIGO grade (?=0.17). Eight cases had MELF as primary or secondary PI; of these, 7 showed LVI discordance. Irregular endometrial-myometrial junction and adenomyosis-like PI were the most common challenges when measuring DOI. Discrepancies in histologic parameters which may impact adjuvant treatment were seen in 13/51 (25.5%) cases. Of these 6/51 (11.7%) were upgraded to FIGO 3, 3/51 (5.9%) change in stage (T1a to T1b) and 4/51 (7.85%) positive for LVI (originally negative).

Conclusions: DTS is a reliable method of assessing tumor depth, and its use can eliminate the need to delineate the endometrial-myometrial junction and overcome sampling challenges of large exophytic tumors. Differentiating MELF from LVI is a known challenge. Small foci of MELF may be overlooked and DOI or DTS underestimated. Poor IR for FIGO grading can be explained by subjectivity of determining solid growth and cytologic atypia. Interestingly, broad PI cases were particularly enriched for discordance. In summary, different PI may each present specific challenges to the pathologist, and awareness of these challenges is important for the accurate histological evaluation and appropriate clinical management of EA.

1102 Verrucous Carcinomas of the Vulva: Targeted Next Generation Sequencing (NGS) and p53 Immunohistochemistry (IHC) Reveals p53 Aberrations in 50% of Cases

Jennifer Pors[1], Basile Tessier-Cloutier[2], Julie Ho[3], Emily Thompson[4], Richard Wong[5], Giorgia Trevisan[6], C. Blake Gilks[7], Lynn Hoang[2]

[1]Vancouver, BC, [2]University of British Columbia, Vancouver, BC, [3]Vancouver Coastal Health, Vancouver, BC, [4]Vancouver General Hospital/University of British Columbia, Vancouver, BC, [5]Pamela Youde Nethersole Eastern Hospital, Hong Kong, Hong Kong SAR, [6]Barts Health NHS Trust, London, United Kingdom, [7]Vancouver General Hospital, Vancouver, BC

Disclosures: Jennifer Pors: None; Basile Tessier-Cloutier: None; Julie Ho: None; Emily Thompson: None; Richard Wong: None; Giorgia Trevisan: None; C. Blake Gilks: None; Lynn Hoang: None

Background: Squamous cell carcinomas (SCC) which arise independent of human papillomavirus (HPV) infection have been shown to be more clinically aggressive than HPV-driven SCC in the vulva. Verrucous carcinomas, however, are a subset of HPV-independent SCC of the vulva, but exhibit clinically indolent behavior. We hypothesized that verrucous carcinomas, unlike the vast majority of HPV-independent SCC, do not harbor *TP53* mutations, which might explain their clinically favorable prognosis. We also performed targeted NGS to better understand the genetic drivers of vulvar verrucous carcinomas.

Design: We performed p53 and p16 immunohistochemistry on all cases. p53 was scored as wild-type (patchy basal and parabasal staining), overexpressed (strong basal and parabasal staining in >70% of cells) and null-type (complete absence of basal and parabasal staining with normal staining in adjacent skin for control). Targeted NGS (including 120 hotspots and 17 exons in 33 known cancer genes) was performed on 3 cases.

Results: From 1991-2013, we identified 8 cases of vulvar verrucous carcinoma where tissue was available for testing. Patients ranged from 46-88 years of age (mean 76 years) and were mostly low-stage (FIGO stage IA=1, IB= 4; II=3). One patient (case 1) had multifocal verrucous carcinomas. Three cases had adjacent deVIL (differentiated exophytic vulvar intrapepithelial lesion).

All cases were p16 negative. Abnormal p53 IHC staining was observed in 4 of 8 cases (Table 1). Of the 3 tumors where NGS was performed, 1/3 had a *TP53* mutation (which correlated with the p53 IHC pattern), 1/3 had a *HRAS* mutation and 2/3 had a *PIK3CA* mutation. Of the 4 patients with abnormal p53 expression, 1 recurred and 3 did not. Of the 4 patients with normal p53 expression, 2 recurred and 2 did not. Recurrences were local and ranged from 9 months to 3 years. Abnormal *TP53*/p53 did not correlate with the risk of local recurrence (p=0.49). No patients had metastatic disease (lymph nodes or distant).

TABLE 1. Summary of Clinicopathologic Features of 8 Verrucous Carcinomas

Case	Age	Stage	Recurrence	p53 IHC	Mutational Status		
					TP53	HRAS	PIK3CA
1	79	IA	Yes	Wild-type	No mutation detected		
2	76	IB	No	Wild-type		c.37G>C	c.1624G>A
3	81	IB	Yes	Overexpressed	c.733G>A		c.1624G>A
4	80	II	No	Wild-type	Not Done		
5	82	IB	No	Overexpressed	Not Done		
6	76	IB	No	Overexpressed	Not Done		
7	46	II	No	Overexpressed	Not Done		
8	88	II	Yes	Wild-type	Not Done		

Conclusions: Unlike previous reports, we found p53/*TP53* aberrations in half of verrucous carcinomas of the vulva. p53/*TP53* aberrations however, did not correlate with the risk of local recurrence. Our findings suggest that abnormal p53/*TP53* can be seen in clinically indolent verrucous carcinomas and does not necessarily portend a worse prognosis. Our small study also revealed that verrucous carcinomas harbor mutations in *HRAS* and *PIK3CA*.

1103 Primary Mucosal Melanoma of the Uterine Cervix: Clinicopathologic and Molecular Analysis

Dinesh Pradhan[1], Anais Malpica[1], Victor Prieto[1], Jonathan Curry[2], Carlos Torres-Cabala[1], Doina Ivan[2], Phyu Aung[1], Jeffrey Gershenwald[1], Michael Davies[1], Michael Tetzlaff[1], Priyadharsini Nagarajan[2]
[1]The University of Texas MD Anderson Cancer Center, Houston, TX, [2]Houston, TX

Disclosures: Dinesh Pradhan: None; Anais Malpica: None; Victor Prieto: None; Jonathan Curry: None; Carlos Torres-Cabala: None; Doina Ivan: None; Phyu Aung: None; Michael Tetzlaff: None; Priyadharsini Nagarajan: None

Background: Primary uterine cervical mucosal melanoma (PUCM) is exceptionally rare and is characterized by poor prognosis; only a few cases have been reported in the literature. PUCM is conventionally staged using the FIGO system and it is currently unknown if pathologic and molecular parameters that are predictive of outcome in cutaneous and other mucosal melanomas also apply to PUCM.

Design: In this retrospective study (on one of the largest cohorts of PUCM), we identified 10 PUCM patients (pts) from our archives over a period of 20 years and recorded clinical, pathologic and molecular features.

Results: The median age of the pts was 51 years (range: 37-82) and seven (70%) were Caucasian. Most of the lesions involved both anterior and posterior cervical walls diffusely (80%) as well as both endo- and ectocervical surfaces (70%), while 2 were confined to the endocervix. The melanomas were of nodular or mucosal-lentiginous histologic types and ulcerated, with median tumor thickness of 4.0 mm (range: 1.5-18.0). Lymphovascular invasion and satellitosis were present in 40% and 10% of cases, respectively.

Next generation sequencing (NGS) using a 50-gene panel was performed on 5 (50%) pts. This revealed isolated mutations involving *TP53* in 2 pts (c.529C>T p.P177S and c.645T>A p.S215R), *NRAS* (c.181C>A p.Q61K) in 1 pt and *KRAS*(c.35G>T p.G12V) in 1 pt. Somatic mutations were not identified in the tumor from 1 pt. One of the pts also had an *ERBB2* c.2329G>T p.V777L alteration, which may correspond to a germline variant. Of note, hotspot mutations involving *BRAF*, *KIT*, *NF1* and *SF3B1* genes were not identified.

At presentation, two (20%) patients had disease localized to cervix, while 3 (30%) had regional and 5 (50%) had distant metastasis. Median time to metastasis was 61 days from the date of diagnosis (range: 0-633). Nine (90%) pts developed metastasis: 1 (10%) regional only, 1 (10%) distant only and 7 (70%) both. Distant metastases involved the lung (n=1; M1b), viscera (n=5; M1c) and brain (n=2; M1d), according to AJCC 8th edition staging system for cutaneous melanoma. Eight (80%) pts died due to progression of their melanoma (median survival: 31 months), one (10%) was lost to follow-up, while 1 (10%) was alive at the last follow-up (27 months).

Conclusions: In this retrospective analysis, we found that PUCM predominantly affects middle-aged Caucasian women, most of whom developed metastasis and died due to progression of melanoma. Hot spot mutations common to cutaneous melanomas are not seen in PUCM.

1104 EZH2 Expression in High-Grade Ovarian Serous Carcinoma and Resistance to Therapy

Brett Reid[1], Ozlen Saglam[1], Jennifer Permuth[1], Thomas Sellers[1]
[1]Moffitt Cancer Center, Tampa, FL

Disclosures: Brett Reid: None; Ozlen Saglam: None; Jennifer Permuth: None; Thomas Sellers: None

Background: Enhancer of Zeste homologue 2 (EZH2), a polycomb-group protein that serves as the primary H3K27 methyltransferase, is over-expressed in numerous cancers including ovarian cancer where it has been found to be upregulated in cisplatin-resistant ovarian cancer cells compared with cisplatin-sensitive cells in in vitro and in vivo studies. Here, we used immunohistochemistry to study the association between EZH2 expression and response to platinum-based therapy in human high-grade serous ovarian carcinoma (HGSOC) samples.

Design: Levels of EZH2 expression were evaluated in a tissue microarray (TMA) that included HGSOC samples from 96 women and non-neoplastic ovarian and fallopian tube (FT) samples from 16 controls. EZH2 expression was scored by ”H-score” (0-300) that was calculated by multiplying the percentage of positively stained cells with nuclear staining intensity (1+, 2+, 3+). Readings from multiple cores were averaged. Treatment response was considered complete when patients demonstrated a disappearance of all measurable disease or, in the absence of measurable lesions, a normalization of CA-125 level for 4 weeks. Patients with partial response, stable disease, or progression were considered incomplete responders. For cancer cases, the association of tumor EZH2 expression with clinical characteristics and response to chemotherapy was evaluated using logistic regression.

Results: EZH2 was overexpressed in neoplastic ovarian tissue compared to paired normal FT tissue in 31 cases ($P=7.3x10^{-11}$) and compared to normal FT ($P=5.4x10^{-9}$) from 14 controls. Benign epithelial cysts also displayed upregulation of EZH2 compared to normal FT (P=0.006). Among tumors, EZH2 expression was not associated with stage (P=0.94) while higher expression was observed for cases with suboptimal debulking status (P=0.03). Expression of EZH2 was not associated with response to chemotherapy (OR=1.01, 95% CI=1.0-1.02, P=0.14). However, four cases with very high expression of EZH2 (>200, above 90th percentile) displayed very high expression in all cores (mean SD=1.9) and three of these were incomplete responders (OR=10.8, 95% CI=1.06-109.5, P=0.04).

Conclusions: EZH2 expression in primary, chemo naïve tumors does not appear to be predictive of chemotherapy response for most cases. Whether rare cases with very high, homogeneous expression of EZH2 are at increased risk for incomplete response is worth further exploration, especially as they may benefit from EZH2 inhibitors that are now in clinical trials.

1105 MELF Pattern Invasion in Endometrial Carcinoma: Clinicopathologic Analysis of 307 Cases and Epithelial-Mesenchymal Transition Markers

Armando Reques[1], Eva Coll[2], Carmen Alborch[1], Carlos López Gil[3], Nikaoly Ciriaco[1], Adriana Zucchiatti Ll.[1], Javier de la Torre[1], Santiago Ramon Y Cajal[4], Eva Colás[2], Ángel García[1]
[1]Vall d'Hebron University Hospital, Barcelona, Spain, [2]VHIR, Barcelona, Spain, [3]Vall d'Hebron Institut de Recerca, Barcelona, Spain, [4]Vall d'Hebron University Hospital, Barcelona, Catalonia, Spain

Disclosures: Armando Reques: None; Eva Coll: None; Carmen Alborch: None; Carlos López Gil: None; Nikaoly Ciriaco: None; Adriana Zucchiatti Ll.: None; Javier de la Torre: None; Santiago Ramon Y Cajal: None; Eva Colás: None; Ángel García: None

Background: Endometrial Carcinoma (EC) is one of the most frequent neoplasm in the female genital tract. According to the American Cancer Society, more than 58000 EC cases will be diagnosed in 2018 only in the USA.

In 2003, Murray et al described a pattern of invasion characterized by Microcystic, Elongated and Fragmented (MELF) neoplastic glands, surrounding by a desmoplastic stroma. These morphologic features have been associated with few markers of the Epithelial-Mesenchymal Transition (EMT), a well-known process of invasion in epithelial neoplasms that imply loss of adhesion and polarity, and an increase on invasiveness of neoplastic cells. In this study, we aim to profoundly study the association of MELF with the EMT process.

Design: We have studied 307 consecutive patients with EC. Histologic slides were reviewed for the presence of pattern of invasion, myometrial invasion, Lymphovascular Space Invasion (LVSI) and lymph node metastasis. Fisher exact test was performing to compare proportions of cases with these features between MELF and non-MELF cases.

Immunohistochemistry for EMT markers including E-cadherin, SNAIL1 and ZEB1 was performed in a balanced cohort of 67 MELF and non-MELF cases. The slides were reviewed by two pathologists using an H-score. T-student test was performed.

Results: We found that MELF cases were associated to positive lymph node metastasis (41% MELF vs 6% non-MELF; $p<0.01$) and also to the presence of LVSI (46% MELF vs 16% non-MELF; $p<0.01$). Myometrial invasion >50% was also significantly more present in MELF cases (89% MELF vs 36% non-MELF cases; $p<0.01$). By last, extrauterine invasion was present in 28% of non-MELF cases, but in 50% of MELF cases ($p=0.025$). Regarding the immunohistochemistry analysis, we found a significant loss of E-cadherin in MELF areas in comparison to the surrounding invasive front ($p<0.01$). There were not differences between the invasive front of MELF and non-MELF cases. Also, we did not find differences in ZEB1 and SNAIL expression.

	N (%)	MELF pattern [n (%)]		p
		Absent (n=281)	Present (n=26)	
Grade of differentiation				0.1683
1 (Well differentiated)	69 (23)	64 (23)	5 (19)	
2 (Moderately differentiated)	175 (57)	156 (55)	19 (73)	
3 (Poorly differentiated)	63 (20)	61 (22)	2 (8)	
Myometrial invasion				<0.01
No invasion	23 (8)	23 (8)	0 (0)	
<50% depth	160 (52)	157 (56)	3 (11)	
≥50% depth	124 (40)	101 (36)	23 (89)	
Extrauterine invasion				0.025
Absent	215 (70)	202 (72)	13 (50)	
Present	92 (30)	79 (28)	13 (50)	
Lymphovascular space invasion				<0.01
Absent	249 (81)	235 (84)	14 (54)	
Present	58 (19)	46 (16)	12 (46)	
Lymph node metastasis**				<0.01
Absent	198 (90)	185 (94)	13 (59)	
Present	21 (10)	12 (6)	9 (41)	
FIGO stage				<0.01
Ia	141 (46)	140 (50)	1 (4)	
Ib	67 (22)	58 (21)	9 (34)	
II	68 (22)	61 (22)	7 (27)	
IIIa	8 (2)	7 (2)	1 (4)	
IIIb	0 (0)	0 (0)	0 (0)	
IIIc	18 (6)	10 (3)	8 (31)	
IV	5 (2)	5 (2)	0 (0)	

Conclusions: We found that presence of MELF pattern invasion is associated with LVSI, lymph node metastasis, extrauterine invasion and a deeper myometrial invasion. We have demonstrated that loss of E-cadherin is one of the mechanisms implicated in invasiveness of MELF glands; however we have not found differences with ZEB1 and SNAIL expression. More studies should be done to study EMT in this type of invasion. In next steps, we will focus on additional markers of the EMT transition, such as SLUG, ALCAM or N-cadherin.

1106 Uterine Inflammatory Myofibroblastic Tumor: an Under-Recognized Entity that Can Be Misdiagnosed as Leiomyosarcoma

Armando Reques[1], Adriana Zucchiatti Ll.[1], Nikaoly Ciriaco[1], Ángel García[1], Cleofe Romagosa[2]
[1]Vall d'Hebron University Hospital, Barcelona, Spain, [2]Vall d'Hebron Hospital, Barcelona, Spain

Disclosures: Armando Reques: None; Adriana Zucchiatti Ll.: None; Nikaoly Ciriaco: None; Ángel García: None; Cleofe Romagosa: *Speaker*, Novartis

Background: Inflammatory myofibroblastic tumor (IMT) is a mesenchymal neoplasm that was first described in lung but it can occur in uterus. It has low malignant potential, with low risk for metastasis but a high recurrence rate. It is characterized by rearrangements in ALK, ROS1, RET and NTRK3, being ALK the most frequently gene involved. This is reflected in an abnormal expression of ALK protein. Because of its morphology, it can be misdiagnosed as leiomyosarcoma or another malignant uterine mesenchymal neoplasm.

Design: We have studied 29 patients with uterine leiomyosarcomas or bizarre leiomyoma diagnosed in Vall d'Hebron University Hospital between 2003 and 2018. Histologic and immunohistochemistry slides were reviewed for morphologic features, mitotic index and inflammatory infiltrate. We performed immunohistochemistry for ALK and then, in the positive cases, we studied ALK gene rearrangement by fluorescence in situ hybridization (FISH).

Results: In our series, we had 5 of 29 cases with ALK expression, all of them with granular and cytoplasmatic staining: 4 of them with focal staining and one with intense and diffuse staining. Only in this last case we could demonstrate ALK gene rearrangement by FISH. This case attracted our attention for its morphologic appearance. It was a 70 years old woman with uterine mass who underwent hysterectomy

without complementary treatment. The mass was formed by epithelioid cells with some rhabdoid features, with focal areas of spindle cells. The nuclei were irregular and vesiculated, with prominent nucleoli. Moderate lymphocitary infiltrate in perivascular aggregates was present. No mitosis were observed. Immunohistochemically, these cells were positive for smooth muscle actin, desmin, and estrogen receptors but were negative for myo-D1, myogenin, p53, CD30 and CD10. One year later, the patient presented hepatic and peritoneal recurrence. They were removed and started chemotherapy with doxorubicin. Currently, after 9 months, she is disease free.

Conclusions: In our series, we have detected a case of epithelioid IMT. The systematic analysis of ALK by immunohistochemistry in malignant spindle or epithelioid uterine tumors with morphologic changes suggesting myoid differentiation can help detect this subgroup of IMT. Since ALK is a potential therapeutic target, the correct diagnosis of this entity may represent an important change in the treatment and prognosis of these patients.

1107 A DNA Methylation Panel for the Triage of HPV Positive Women in a Primary Screening Population

Stephen Reynolds[1], Christine White[2], Padmaja Naik[3], Roisin O' Brien[3], Rita Ladapo[4], Loretto Pilkington[3], Helen Keegan[3], Caroline Powles[5], Jacqui Barry O'Crowley[3], Prerna Tewari[6], Sharon O'Toole[7], Charles Normand[2], Grainne Flannelly[8], Cara Martin[7], John O'Leary[2]

[1]CERVIVA, Dublin, Ireland, [2]Trinity College Dublin, Dublin, Ireland, [3]Coombe Women & Infants University Hospital, Dublin, Ireland, [4]DIT, Dublin, Ireland, [5]CervicalCheck: The National Cervical Screening Programme, Dublin, Ireland, [6]Trinity College, Dublin, Ireland, [7]Trinity St. James's Cancer Institute, Dublin, Ireland, [8]National Maternity Hospital, Sandymount, Ireland

Disclosures: Stephen Reynolds: None; Christine White: None; Padmaja Naik: None; Roisin O' Brien: None; Rita Ladapo: None; Loretto Pilkington: None; Helen Keegan: None; Caroline Powles: None; Jacqui Barry O'Crowley: None; Prerna Tewari: None; Sharon O'Toole: None; Charles Normand: None; Grainne Flannelly: None; Cara Martin: None; John O'Leary: None

Background: The aim is to evaluate specific methylation markers for the triage of a HPV positive result in a HPV primary screening population. Host methylation factors have been shown to be hypermethylated in cervical cancer/pre-cancer and have the potential to triage women at high risk of cervical cancer. This study aims to investigate methylation of CADM1-M18,MAL-M1 and hsa-mir124-2 in HPV positive women. This study forms part of a larger CERVIVA HPV Primary Screening Study.

Design: In partnership with CervicalCheck, The National Cervical Screening Programme in Ireland, CERVIVA are undertaking a longitudinal HPV primary screening pilot study evaluating triage strategies for managing HPV-positive primary screening tests.13,496 women attending for routine screening have been enrolled. HPV testing is performed using the Cobas HPV DNA test. HPV positive samples are tested for a panel of methylation specific biomarkers[CADM1-M18,MAL-M1, hsa-mir124-2] via qMSP and a Total Methylation Score(TMS) is calculated. Here we present a validation panel of 184 cervical cytology samples with confirmed histology for defining clinically relevant cut-off points. Defined cut-offs are being determined through ROC analysis for the detection of CIN3+. Testing on the study population is underway.

Results: The validation panel comprises of HPV positive and histology confirmed CIN1,CIN2,CIN3(n=50, 34, 50) and HPV negative/cytology no abnormality detected(NAD)(n=50). The panel shows statistically significant differences in methylation scores for all markers between NAD and CIN1 in respect to CIN3(CADM1,MALM1, hsa-mir124-2, TMS($p=0.015,0.016,<0.001,<0.001$)($p=0.018,0.018,0.001,<0.001$ respectively). ROC analysis shows an AUC of 0.910 when CIN3 is compared to NAD.

To date 624 HPV positive cervical smears from the study have been tested for methylation. Against all cytological outcomes, the TMS of HSIL is statistically significant($p=0.001$). The Odds Ratio of having a positive TMS increases as cytological grade increases. Based on preliminary cut-offs, overall 36.6%(n=175/477) demonstrate elevated methylation scores. Elevated Total Methylation was also identified in 30%(67/277), 29%(81/279) and 60%(57/95) of cytology normal, LSIL/ASCUS and HSIL cytology respectively.

Conclusions: The TMS generated by the combination of the methylation markers shows promise in differentiating high grade lesions from normal/low-grade lesions. Longitudinal follow up will be used to determine the clinical value of hyper-methylation in HPV positive women.

1108 Pattern-Based Classification System of Invasive Endocervical Adenocarcinoma: Histologic Features and Clinical Impact

Glorimar Rivera Colon[1], Shuang Niu[2], Hao Chen[3], Elena Lucas[4], Diego Castrillon[4], Jayanthi Lea[5], Wenxin Zheng[6]
[1]Dallas, TX, [2]Frisco, TX, [3]Coppell, TX, [4]University of Texas Southwestern, Dallas, TX, [5]UT Southwestern Medical Center, Dallas, TX, [6]University of Texas Southwestern Medical Center, Dallas, TX

Disclosures; Glorimar Rivera: None; Shuang Niu: None; Hao Chen: None; Elena Lucas: None; Diego Castrillon: None; Wenxin Zheng: None

Background: Diagnosis of cervical adenocarcinoma can be challenging and its clinical behavior is difficult to predict. Differences in the invasive growth pattern has shown relevance in lymph node metastases and clinical outcome. In this study, we detailed and compared histological features in usual type of cervical adenocarcinoma using the three-tiered Pattern Based Classification System (PBCS).

Design: 51 cases of usual type cervical adenocarcinoma (38 resections, 13 biopsies) were reviewed by 4 gynecologic pathologists to evaluate invasive patterns and histological features (Table 1). Clinicopathologic features of each patient were recorded. Statistical analysis was performed to compare these features among different patterns.

Results: Significantly increased stromal desmoplasia was associated with Pattern C (100%) and B (100%) compared to A (0%)($p<0.00001$). Destructive invasion was seen significantly more often in pattern C (96.3%) compared to B (66.7%) ($p= 0.0246$). In addition, destructive invasion was only focally seen in pattern B, whereas it was diffuse in pattern C. No destructive invasion was seen in pattern A. Mucin depletion was more frequent in patterns B (50%) and C (67%) compared to A (22.2%) ($p=0.016$). Importantly, intraluminal debris often present in pattern C (67%) ($p<0.00001$) were only occasionally seen in pattern B (16.7%) ($p=0.0055$, compared with pattern C) and absent in pattern A. No lymphovascular invasion (LVI) was seen in pattern A. Nevertheless, pattern C was related to increased LVI (55.0%, $p=0.0057$) when compared with pattern B (18.2%). High nuclear grade was more frequent in pattern C (26.1%) compared to patterns A and B (0%) ($p=0.0333$). Chronic inflammation showed no significant difference. Deeper stromal invasion was seen in pattern C

(1.27+/- 1.21 *mm*) compared to patterns B (0.433+/-0.409 *mm*) and A (0.673+/- 0.766 *mm*) ($p=0.014263$). Most importantly, pattern C was more commonly associated with a higher clinical stage than patterns A and B ($p=0.0403$).

Table 1. Comparison of Histologic Features and Clinical Outcomes Between Patterns of Invasion

Pattern	Nuclear grade (grade3)	Desmoplasia	Destructive invasion	Intraluminal debri	Mucin depletion	LVI +/-	Depth of invasion	Clinical Stage (stage 2 and above)
A	0/9 (0%)	0/9 (0%)	0/9 (0%)	0/9(0%)	2/9 (22.2%)	0/8 (0%)	0.673	0/8 (0%)
B	0/12 (0%)	12/0 (100%)	8/4 (66.7%)	2/10 (16.7%)	6/6 (50.0%)	2/9 (18.2%)	0.433	0/10 (0%)
C	6/23 (26.1%)	29/0 (100%)	26/1 (96.3%)	20/10 (67.0%)	20/10 (67.0%)	11/9 (55.0%)	1.27	8/27 (30.0%)
P value	*0.0333 (C vs A+B);*	*0.0001(C vs A+B); < 0.00001 (A vs B+C)*	*0.0246 (C vs B); < 0.00001 (C vs A+B); < 0.00001 (A vs B+C); 0.0046 (A vs B)*	*0.0055 (C vs B); < 0.00001 (C vs A+B); 0.0065 (A vs B+C);*	*0.0283 (C vs A+B); 0.016 (A vs B+C);*	*0.0057 (C vs A+B);*	*0.023131* *(C vs B);* *0.014263* *(C vs A+B);*	*0.0403 (C vs A+B)*

Conclusions: There are significant differences in desmoplasia, destructive invasion, and LVI between histologic patterns of endocervical adenocarcinoma. Intraluminal debris, nuclear grade and mucin depletion appear to be the best indicators for tumor patterns, especially in biopsy specimens where the evaluation of other features is often limited by the specimen size and fragmentation. Additionally, this study demonstrates that pattern C is associated with a higher clinical stage.

1109 ERBB2 Amplification Detected by Next Generation Sequencing Is Concordant with HER2 Immunohistochemical Expression in Uterine Serous Carcinoma

Carrie Robinson[1], Beth Harrison[1], Fei Dong[1], Caitlin Perry[2], Marisa Nucci[3], David Kolin[1]
[1]Brigham and Women's Hospital, Boston, MA, [2]Partners Health System, Somerville, MA, [3]Brigham and Women's Hospital, Harvard Medical School, Boston, MA

Disclosures: Carrie Robinson: None; Beth Harrison: None; Fei Dong: None; Caitlin Perry: None; Marisa Nucci: None; David Kolin: None

Background: Uterine serous carcinoma (USC) is an aggressive form of endometrial cancer which accounts for only 10% of endometrial carcinomas, but up to 40% of deaths. Overexpression of HER2 (*ERBB2*) occurs in a subset of these cases, and in some studies *ERBB2* amplification is associated with a poorer prognosis. A recent phase 2 trial demonstrated improved progression-free survival when patients with HER2-overexpressed USC were treated with trastuzumab, a monoclonal antibody that targets HER2. HER2 expression and *ERBB2* amplification in USC is currently measured using immunohistochemistry (IHC) and/or in situ hybridization (ISH), respectively. Next generation sequencing (NGS) is increasingly performed on endometrial carcinomas. However, its ability to detect *ERBB2* amplification has not been studied.

Design: Cases of USC which had been tested by a targeted hybrid-capture NGS assay were retrospectively identified. The NGS panel included the coding regions of at least 275 genes, including *ERBB2*. *ERBB2* copy number (CN) was calculated from the log2 ratio of tumor-to-normal coverage, using the estimated tumor percentage. A threshold *ERBB2* CN of 6 was established as an amplified result. IHC for HER2 (SP3 clone) was performed on all cases and scored independently by two pathologists using the updated 2018 ASCO/CAP guidelines for testing in breast cancer. Discrepancies were resolved via consensus.

Results: 28 cases of USC were identified (Table 1). Two cases had 3+ IHC and both revealed gene amplification by NGS, as did one case with equivocal IHC (2+). Two additional cases with 2+ IHC showed "equivocal" NGS results (CN between 4 and 6). Eleven cases with 2+ IHC were not amplified by NGS. No cases with 0 or 1+ IHC showed amplification by NGS, and no case had polysomy of chromosome 17.

Table 1. Her2 immunohistochemistry and *ERRB2* amplification in USC

	ERRB2 amplification by NGS		
Her2 IHC	Not amplified (CN < 4)	Equivocal (4 ≤ CN < 6)	Amplified (CN ≥ 6)
0	3	0	0
1+	9	0	0
2+	11	2	1
3+	0	0	2

Conclusions: *ERBB2* amplification as measured by NGS shows excellent concordance with Her2 expression by IHC, and suggests NGS may be able to resolve some cases which are equivocal by IHC. NGS shows promise as a method to determine *ERRB2* amplification in USC. Further work is needed to correlate these findings with amplification as detected by ISH, and to determine the most appropriate method to identify patients who may benefit from targeted therapy.

1110 Comparative Analysis of Morphologic and Immunophenotypic Features In Paired Recurrent and Primary Endometrial Carcinomas

Juan Rong[1], Somaye Zare[2], Oluwole Fadare[2]
[1]UCSD Medical Center, San Diego, CA, [2]University of California, San Diego, La Jolla, CA

Disclosures: Juan Rong: None; Somaye Zare: None; Oluwole Fadare: None

Background: Early stage, low risk endometrioid carcinomas of the endometrium only rarely recur. The purpose of this study is to determine if the morphologic and immunophenotypic profiles of these carcinomas are consistently and reliably maintained in their recurrences, based on a detailed comparative appraisal of a small cohort of paired primary and recurrent cancers.

Design: The study set included 10 paired primary and recurrent endometrial carcinomas. These were 10 cases of FIGO stage IA, grades 1 and 2 (i.e low risk) endometrial endometrioid carcinomas that ultimately recurred. Sites of recurrence includes the vaginal apex (n=7), peritoneum, abdominal wall and pelvis (n=3), and pelvic lymph node (n=1). The primary tumor in the hysterectomy specimens, as well as their matched recurrences, were both comparatively appraised for a variety of morphologic and immunophenotypic features, the latter with a 10 marker panel that included the estrogen receptor (ER), progesterone receptor (PR), androgen receptor (AR), MLH1, MSH2, p16, p53, beta-catenin, PTEN, and Ki67

Results: 80% of paired primary and recurrent carcinomas showed essentially similar morphologic profiles, with identical mitotic indices, FIGO grades, and levels of nuclear atypia. The remaining 20% showed an increased grade in the recurrence, manifested as either

increased atypia in one case or increased solid components in another. The former also displayed an increased mean mitotic index. Squamous and clear cells were more easily discernible in the recurence in another case. Paired primary and recurrent cases showed 100% concordance in the extent and patterns of expression for MSH2, MLH1, beta-catenin, p16 and p53. For ER, AR and PR, 20% of cases were positive in the primary and negative in the recurrences. Additonally, one case was negative for AR in the primary and became positive in the recurrence. The Ki67 proliferative index was significantly higher in the recurrence in 30% of cases.

Conclusions: Our findings confirm that most low risk endometrial carcinomas retain their basic morphologic and immunophenotypic profiles in their recurrences. However, in a subset, recurences are of a higher grade with increased solid components or nuclear atypia, which may be accompanied by loss of hormone receptor expression and a higher proliferative index

1111 Correlation of Next Generation Sequencing with HER2 Status by Immunohistochemistry and FISH in Type II Endometrial Carcinomas

Douglas Rottmann[1], Padmini Manrai[2], Xinyu Wu[2], Pei Hui[3], Alessandro Santin[3], Natalia Buza[4]
[1]Yale University School of Medicine, Hamden, CT, [2]New Haven, CT, [3]Yale University School of Medicine, New Haven, CT, [4]Yale University, New Haven, CT

Disclosures: Douglas Rottmann: None; Padmini Manrai: None; Xinyu Wu: None; Pei Hui: None; Alessandro Santin: None; Natalia Buza: None

Background: HER2 overexpression/amplification has been reported in a third of serous endometrial carcinomas and a randomized phase II clinical trial recently showed increased progression-free survival in patients who received targeted trastuzumab therapy in addition to carboplatin-paclitaxel. The current standard methods for assessment of HER2 status include immunohistochemistry (IHC) and FISH. However, genomic profiling of tumors by next generation sequencing (NGS) has become increasingly common in patients with advanced or recurrent malignancies, and provide comprehensive data for potential targeted therapies. A recent study showed high overall concordance of HER2 status by NGS and IHC/FISH in breast and gastroesophageal cancer. We aimed to examine the concordance between the three methods in endometrial type II carcinomas.

Design: All cases of endometrial serous, clear cell, and mixed carcinomas and carcinosarcomas with available HER2 status and NGS data were retrieved from our departmental archives. HER2 IHC was scored per the current ASCO/CAP guidelines for breast cancer. All but one case with 2+ IHC had FISH performed. The IHC, FISH, and NGS reports were then reviewed and compared.

Results: A total of 60 cases were included in the study. Of these, 34 were scored as HER2 IHC 0 or 1+, none of which showed amplification by FISH or NGS. One negative case (IHC 0; 1/45, 2%) had a mutation in *ERBB2* and another (IHC 1+) had a VUS. HER2 IHC score was 2+ in 20 cases, 8 of which were HER2 amplified by FISH; 2 of those showed HER2 amplification by NGS. One case had equivocal HER2 amplification by NGS, but FISH was not performed. Six cases had 3+ score by IHC, 4 of which were also HER2 amplified by NGS (FISH was not performed). Overall, of the 14 IHC and/or FISH positive cases, only 6 had *ERBB2* amplification by NGS (6/14, 43%).

IHC (score)	Number of cases (n)	FISH (positive/negative)	*ERBB2* Molecular Findings
0/1+	34	1 negative, 33 not done	1 mutation, 1 VUS
2+	20	8 positive, 11 negative, 1 not done	2 amplifications (both FISH positive), 1 equivocal amplification (FISH not done)
3+	6	1 negative, 5 not done	4 amplifications

Table 1. IHC, FISH, and molecular findings.

Conclusions: We found 100% concordance between a negative (0, 1+, or 2+ IHC with negative FISH) HER2 score and NGS results. However, the concordance with NGS was only 43% among the HER2 positive (by IHC and/or FISH) cases, and the overall concordance for all 60 cases was 67%. The previously reported significant intratumoral heterogeneity of HER2 expression and amplification in endometrial serous carcinomas and carcinosarcomas may explain the low concordance in our study, and the marked difference from the reported high concordance rates in breast and gastroesophageal cancer.

1112 The Efficacy Of Nanocomplexes Complexed With Specific Biomarker Targets In Ovarian Cancer Treatment, An Ex-Vivo Explant Case Study

Melad Saed[1], Sharon O'Toole[2], Lucy Norris[3], Steven Gray[4], Feras Abu Saadeh[4], John O'Leary[3], Bashir Mohamed
[1]Trinity College, Dublin, Ireland, [2]Trinity St. James's Cancer Institute, Dublin, Ireland, [3]Trinity College Dublin, Dublin, Ireland, [4]St James's Hospital, Dublin, Ireland

Disclosures: Melad Saed: None; Sharon O'Toole: None; Lucy Norris: None; Steven Gray: None; Feras Abu Saadeh: None; John O'Leary: None; Bashir Mohamed: None

Background: Ovarian cancer patients have a good response rate to first line chemotherapy treatment. However, most patients relapse and develop multidrug resistance (MDR) during the course of their treatment. MDR is a major clinical obstacle that critically limits the success rate of chemotherapy in ovarian cancer treatment and is the main cause of treatment failure. In recent years, research has focussed on alternative therapies to enhance the treatment of chemoresistant ovarian cancer. In this regard, nanotechnology has been recognized as a fundamental tool in cancer research, with the potential to increase drug efficacy, in particular when complexed with specific biomarkers. The aim of this study was to assess the efficacy of nanodiamonds complexed with ovarian cancer drugs and specific biomarker targets for ovarian cancer such as HE4 and CA125.

Design: Ovarian tumour explants were cultured following surgical resection. Briefly, the biopsies were cut into 2 – 3 mm^3, and cultured in 96 well plates using supplementary RPMI media for 7 days. Expression of the HE4 and CA125 were assessed on ovarian tumour explants. The cytotoxic effect of the nanocomplexes comprising nanodiamond coupled with paclitaxel, carboplatin and doxorubicin and conjugated with HE4 and CA125 antibody was evaluated by measuring LDH release into the supernatant after 48h of treatment using the LDH Cytotoxicity Detection Kit. Protein was extracted after the ovarian tumour explants were treated with the nanocomplexes and drugs to assess the mechanism of cytotoxicity. Caspase-3 expression was measured by western blot to assess apoptosis.

Results: LDH activity was elevated in ovarian tumour explants following exposure to drugs alone and the nanocomplex treatments but not in untreated control ovarian tumour explants. The nanocomplexes coupled with carboplatin and doxorubicin induced significant caspase-3 upregulation in the ovarian tumour explants, while the drugs alone did not.

Conclusions: The novel nanocomplexes developed in this study were successfully taken up by ovarian tumour explant cells and specifically delivered the desired drugs into targeted ovarian tumour explants which more closely resemble the *in vivo* situation. This is the first time that NDs complexed with ovarian cancer drugs and coupled with HE4 and CA125 antibodies have shown efficacy in an explant system. The mechanism of apoptosis observed seems to be via the caspase-3 pathway. The use of nanocarriers has the potential to transform ovarian cancer therapeutics.

1113 Molecular Profile of Corded and Hyalinized Endometrioid Carcinoma

Nida Safdar[1], Christina Isacson[2], Robert Young[3], C. Blake Gilks[4], Esther Oliva[5]
[1]Bedford, MA, [2]CellNetix Pathology, Seattle, WA, [3]Harvard Medical School, Boston, MA, [4]Vancouver General Hospital, Vancouver, BC, [5]Massachusetts General Hospital, Boston, MA

Disclosures: Nida Safdar: None; Christina Isacson: None; Robert Young: None; C. Blake Gilks: None; Esther Oliva: None

Background: Corded and hyalinized endometrioid carcinoma (CHEC) of the uterus and ovary, characterized by cords of epithelial cells, spindle cells, and hyalinized stroma, is a rare variant of endometrioid carcinoma (EC) that may morphologically be confused with malignant müllerian mixed tumors (MMMTs). They were originally thought to represent a form of low-grade MMMTs, however, their clinical and histologic features - in addition to differences in p53 and beta-catenin expression - have aided in their distinction from the latter. Recent advances in the molecular classification of endometrial carcinomas has led to the characterization of four prognostically significant molecular classes including the ultramutated POLE, microsatellite instable, p53 mutated, and no specific molecular profile/p53 wildtype subgroups. The aim of the study was to evaluate the molecular profile of CHEC using The Cancer Genome Atlas based molecular classifiers.

Design: Eight patients with CHEC diagnosed on hysterectomy (n=6), endometrial biopsy (n=1), or oophorectomy (n=1) were identified and clinical and histologic features reviewed. Immunohistochemistry for mismatch repair proteins (PMS2, MSH6) and p53 were performed on seven tumors. POLE exonuclease domain mutations (EDM) were evaluated by Sanger sequencing in all cases.

Results: The median age at diagnosis was 46.5 (range 34-73) years. Tumors were grade 1 (n=4), grade 2 (n=3), and grade 2-3 (n=1). A prominent corded and hyalinized component was present in six comprising 25-90% of the tumor, and a spindled component was present in four comprising 15-30% of the tumor. Squamous differentiation was identified in 75% (6/8) of tumors. Staging information was available for six patients (stage IA, n=4 and stage II, n=2). All tumors were p53 wildtype with preserved expression of PMS2 and MSH6 and no POLE EDM mutations were identified.

Conclusions: CHEC appears to present at a younger age and exhibit squamous differentiation at an increased frequency compared to typical EC. Unlike MMMTs which frequently harbor TP53 mutations, CHECs exhibit p53 wild-type expression including the grade 2-3 tumor in this study. Furthermore, they are not associated with MLH-1 hypermethylation as seen in many EC from young patients with known risk factors. Based on this series, these tumors appear to fall into the no specific molecular profile subgroup of EC and within that group those comprising grade I or II tumors.

1114 PD-L1 and CD8 Expression in Poorly Differentiated Cervical Squamous Cell Carcinoma

Ozlen Saglam[1], Jun-Min Zhou[1], Xuefeng Wang[1], José Conejo-Garcia[2]
[1]Moffitt Cancer Center, Tampa, FL, [2]H. Lee Moffitt Cancer Center & Research Institute, Tampa, FL

Disclosures: Ozlen Saglam: None; Jun-Min Zhou: None; Xuefeng Wang: None; José Conejo-Garcia: None

Background: Programmed cell death-1 and programmed cell death ligand-1 (PD-1/PD-L1) blockage is used in the treatment of high-risk patients with Cervical Squamous Cell Carcinoma (CSCC). PD-L1 and CD8 expression was studied by immunohistochemistry in CSCC samples and expression levels were correlated with clinicopathologic parameters.

Design: Levels of PD-L1 expression were evaluated in a tissue microarray (TMA) composed of 45 CSCC and 48 benign control tissue. In the following step, full-tissue sections from poorly differentiated (pd) tumor samples (n=22) were stained with CD8 and PD-L1 antibodies. PD-L1 expression levels were evaluated as categorical (negative: <1%, expressed: 1-49% and highly-expressed ≥ 50%) and continuous (percentage of positively stained cells) data. $CD8^+$ Tumor Infiltrating Lymphocyte (TIL) density within the neoplastic epithelium and tumor stroma was graded separately in 15-20 high-power fields and divided into 3 groups:1+ (less than 5 TIL), 2+ (6-19) and 3+ (20 or more TIL).

Results: In TMA samples PD-L1 expression was higher in neoplastic tissue compared to the benign epithelium. Pd-tumor samples expressed PD-L1 in higher levels compared to grade II tumors (p=0.04). In pd-CSCC samples, tumors from younger patients (median age: 36) had higher PD-L1 expression levels (p=0.02). Lymphovascular invasion was more commonly associated with low PD-L1 expressing tumors. PD-L1 expression and $CD8^+$ TIL density were positively correlated with each other. High CD8 density (3+) in both neoplastic epithelium and tumor stroma is associated with better overall survival rates (figure 1).

Figure 1 - 1114

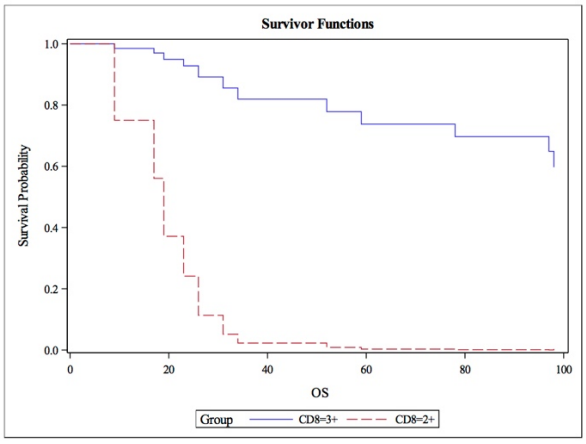

Figure 1: Stage-adjusted Overall Survival and CD8 Expression

Conclusions: Clinicopathologic features including patient age, tumor grade, and host immune response can be important for selection of patient subgroup with CSCC who would benefit most from immunotherapy. More detailed studies are warranted in a larger cohort.

1115 Are Multinucleated and Giant Tumor Cells in High Grade Serous Carcinoma of the Ovary Blastomere-like Cancer Stem Cells?

Alireza Salem[1], Karen Pinto[1], Meghan Koch[1], Elvio Silva[2]
[1]Baylor University Medical Center, Dallas, TX, [2]The University of Texas MD Anderson Cancer Center, Houston, TX

Disclosures: Alireza Salem: None; Karen Pinto: None; Meghan Koch: None; Elvio Silva: None

Background: The presence of multinucleated and giant tumor cells in high grade serous carcinoma of the ovary have been recognized for long time. Different explanations have been given to these cells ranging from degenerative changes to being a very important step in the development of high grade serous carcinoma. In this study we investigate possible explanations for the multinucleated and giant tumor cells in high grade serous carcinoma.

Design: We reviewed 33 cases of high grade serous carcinoma of the ovary. 12 cases were stage I, 7 were stage II, and 14 were stage III. On each case we counted the number of the multinucleated and giant tumor cells in 20 consecutive 10 X fields. In 11 cases where the multinucleated and giant tumor cells were easily found we stained the slides with Ki-67, p53, and OCT ¾.

Results: Patients with multinucleated and giant tumor cells were older than patients without the multinucleated and giant tumor cells. The median age was 62 vs 59 years for stage I, 73 vs 57 years for stage II, and 71 vs 53 years for stage III. Multinucleated and giant tumor cells were more frequent in stage I lesions (75%) than in stages II or III (57% in both). In 87% of stage III cases the number of multinucleated and giant tumor cells in the metastases was lower than in the primary ovarian tumor. Mitotic figures were present in the regular sized cells but were absent in the multinucleated and giant tumor cells. All cases were negative for OCT3/4. In 7 cases, more than 10% of the regular mononuclear cells were positive for Ki-67. In these 7 cases there was a similar percentage of positive cells in the regular mononuclear cells and in the multinucleated and giant tumor cells. p53 had a perfect correlation in regular sized mononuclear cancer cells, and in multinucleated and giant tumor cells. Null in 4 cases and diffusely positive in 7 cases.

Conclusions: 1. Multinucleated and giant tumor cells are found in most high grade serous carcinoma of the ovary. 2. Their number decreases in metastatic lesions. 3. They are all negative for OCT3/4. 4. Ki-67 and p53 have similar reactions in the regular sized cancer cells and in the multinucleated and giant tumor cells.

These results show that the multinucleated and giant tumor cells are neither degenerative cells, nor traditional cancer stem cells, but most probably they represent an intermediate, blastomere-like cancer cells, step between stem cells and mature tumor cells formed by endoreplication.

1116 Heterogenous Immunohistochemical Staining Pattern of Mismatch Repair Proteins in Endometrial Cancer: Is It Time to Re-evaluate the Guidelines?

Ashley Scheiderer[1], Kristopher Kimball[1], Larry Kilgore[1], Daniel Snyder[2], Amila Orucevic[1]
[1]University of Tennessee Medical Center, Knoxville, TN, [2]University of Kentucky, Knoxville, TN

Disclosures: Ashley Scheiderer: None; Kristopher Kimball: None; Larry Kilgore: None; Daniel Snyder: None; Amila Orucevic: None

Background: The current reporting guidelines for mismatch repair protein (MMRP) immunohistochemistry (IHC) for Lynch syndrome (LS) screening consider the presence of any positive nuclear staining as intact MMRP expression. This would include tumors that display combined or heterogenous areas of retention and loss of staining. Our study aims to evaluate the clinical significance of reporting heterogenous staining patterns of MMRP IHC in endometrial cancer.

Design: We retrospectively reviewed 455 consecutive MMRP IHC results of endometrial cancer in hysterectomy specimens from 2012-2017. Cases with heterogenous MMRP staining were identified, and percent loss of staining was recorded. These results were compared with the patient's personal and family history of LS-associated cancer, MLH1 hypermethylation status, and LS genetic testing.

Results: Heterogenous staining of MMRP was seen in 48 cases (10.5%), 14 of which showed loss in >40% of the tumor. Thirty cases displayed isolated heterogenous staining, and 18 cases had heterogenous staining in combination with complete loss of other MMRP (Table). The 30 cases of isolated heterogenous MMRP staining were reported by pathologists as follows: heterogenous (n = 5), complete MMRP loss (n = 4), and intact MMRP (n = 21). Cases reported as heterogenous or complete MMRP loss had appropriate clinical follow-up. Two of 2 cases with isolated heterogenous MSH6 loss tested positive for Lynch syndrome. Both patients had no personal or family history of LS-related cancer. One of 3 cases with isolated heterogenous MLH1/PMS2 loss was negative for MLH1 promoter hypermethylation, but the patient could not afford genetic testing. In 18 of 21 patients with heterogenous MMRP staining reported as intact MMRP expression LS genetic testing was deemed not clinically indicated, although 9 of these patients had a family history of LS-associated cancer. The 18 cases of heterogenous MMRP staining in combination with complete loss of other MMRP were appropriately followed because of reported complete loss of MMRP.

Correlation of Reporting Heterogenous MMRP IHC Staining in Endometrial Cancer Patients with Clinical Follow-up

Reported MMRP Status in Cases with Heterogenous Staining	MMRP Observed with Heterogenous Staining		Family History of LS-Associated Cancer		Genetic Testing Results for LS-Associated Germline Mutations				
					Tested		Not Tested		
	MMRP Affected	Number of Cases	Positive	Negative	Positive	Negative	Denied by Patient[#]	MLH1 HM	Reported Intact
Intact expression (n = 21)	MLH1/PMS2	8	5	3	0	0	1	0	7
	MSH2/MSH6	0	0	0	0	0	0	0	0
	MSH6	0	0	0	0	0	0	0	0
	MSH6/PMS2	7	2	5	0	2	0	0	5
	PMS2	6	2	4	0	0	0	0	6
Complete Loss of MLH1/PMS2 (n = 19)	MLH1/PMS2	4*	4	0	0	2	0	2	0
	MSH2/MSH6	2	0	2	0	1	0	1	0
	MSH6	13	6	7	1[+]	2	3	7	0
	MSH6/PMS2	0	0	0	0	0	0	0	0
	PMS2	0	0	0	0	0	0	0	0
Complete Loss of MSH2/MSH6 (n = 3)	MLH1/PMS2	2	0	2	0	1	1	0	0
	MSH2/MSH6	0	0	0	0	0	0	0	0
	MSH6	0	0	0	0	0	0	0	0
	MSH6/PMS2	0	0	0	0	0	0	0	0
	PMS2	1	0	1	0	0	1	0	0
Heterogenous Loss of MSH6 (n = 2)	MLH1/PMS2	0	0	0	0	0	0	0	0
	MSH2/MSH6	0	0	0	0	0	0	0	0
	MSH6	**2**	0	2	**2**[++]	0	0	0	0
	MSH6/PMS2	0	0	0	0	0	0	0	0
	PMS2	0	0	0	0	0	0	0	0
Heterogenous Loss of MLH1/PMS2 (n = 3)	MLH1/PMS2	**3**	0	3	0	1	**1**	1	0
	MSH2/MSH6	0	0	0	0	0	0	0	0
	MSH6	0	0	0	0	0	0	0	0
	MSH6/PMS2	0	0	0	0	0	0	0	0
	PMS2	0	0	0	0	0	0	0	0
Total (n = 48)			*19*	*29*	*3*	*9*	*7*	*11*	*18*

[#]This category includes loss to follow-up, declined by patient, and refusal due to insurance or cost.

*Reported as complete loss of MLH1/PMS2 in fact showed only heterogenous MLH1/PMS2 staining.

[+]Tested positive for MLH1 germline mutation.

[++]Tested positive for MSH6 germline mutation.

Abbreviations: MMRP, mismatch repair protein; LS, Lynch syndrome; MLH1 HM, MLH1 hypermethylation.

Conclusions: Our study reveals that Lynch syndrome germline mutations and negative MLH1 promoter hypermethylation (highly indicative of a LS germline mutation) can be detected in endometrial cancer patients whose tumors display sole heterogenous MMRP staining. Our results stress the importance of reporting heterogenous staining patterns to ensure appropriate clinical follow-up and suggest that current guidelines regarding MMRP expression reporting should be re-evaluated.

1117 Molecular Analysis of Uterine Myxoid Sarcomas Shows Absence of BCOR Alterations in Myxoid Leiomyosarcomas and Improves the Diagnosis of Morphologically Ambiguous Lesions

Cindy Schmelkin[1], Adrian Marino-Enriquez[1], Marisa Nucci[2], Carlos Parra-Herran[3]
[1]Brigham and Women's Hospital, Boston, MA, [2]Brigham and Women's Hospital, Harvard Medical School, Boston, MA, [3]Sunnybrook Health Sciences Centre - University of Toronto, Toronto, ON

Disclosures: Cindy Schmelkin: None; Adrian Marino-Enriquez: None; Marisa Nucci: None; Carlos Parra-Herran: None

Background: Uterine myxoid sarcomas comprise a variety of different diagnostic entities including the recently described HG-ESS with myxoid morphology that harbors characteristic *BCOR* gene fusions and internal tandem duplications (ITDs). However, the presence of these alterations in other uterine myxoid neoplasms, particularly myxoid leiomyosarcoma (mLMS) is not well characterized. Thus, we investigated the frequency of BCOR immunohistochemical (IHC) staining and *BCOR* fusions / ITDs across a cohort of uterine sarcomas with myxoid morphology.

Design: A cohort of 25 myxoid uterine sarcomas was identified. Following strict criteria, 13 were classified as of smooth muscle type (mSMT, 12 mLMS and 1 myxoid STUMP), 2 were compatible with BCOR-ESS and 1 with YWHEA-NUTM2 ESS; the remaining 9 could not be further classified based on H&E and IHC staining available (BCOR, CD10, desmin, caldesmon, SMA, cyclin D1, and ER) and were

labelled myxoid sarcoma NOS (mS-NOS). *BCOR* fusions were interrogated on paraffin-embedded tissue using a RNA hybridization technique (Nanostring nCounter) which surveys 174 unique sarcoma fusions. RT-PCR and Sanger sequencing were performed to detect *BCOR* ITDs (exon 15). Clinical follow up data was noted when available.

Results: All HG-ESS on morphology had expected fusions confirmed by molecular testing (two *ZC3H7B-BCOR* and one *YWHEA-NUTM2*). In addition, one mS-NOS was found to harbor *ZC3H7B-BCOR* fusion. None of the tumors classified as mSMTs harbored *BCOR* fusions. One mLMS harbored *SEC31A-ALK* (ALK IHC negative), and one mS-NOS a *EWSR1-FLI1* fusion. None of the tumors in the cohort harbored *BCOR* ITDs. By IHC (Table 1), BCOR was positive in 3/3 confirmed BCOR-ESS (1+ in one), as well as in 2/13 mSMT (both 1+) and 5/8 mS-NOS (3+ in 2). CD10 was positive in 3/3 BCOR-ESS (3+ in all), 5/9 mSMT (3+ in 3) and 3/7 mS-NOS. 12/25 (48%) cases had follow-up available; recurrence and/or tumor-related death was documented in 4/6 mLMS, 0/1 mSTUMP, 3/4 mS-NOS and 1/1 HG-ESS.

Table 1. Immunohistochemical Results for Uterine Myxoid Sarcomas

Case No.	Diagnosis	BCOR	CD10	Desmin	Caldesmon	SMA	Cyclin D1	ER (%)	Molecular
1	mLMS	0	1+	1+	0	1+	ND	0%	Neg
2	mLMS	0	0	2+	0	1+	ND	10%	Neg
3	mLMS	0	3+	3+	3+	2+	ND	70%	Neg
4	mLMS	0	0	0	0	1+	ND	0%	Neg
5	mLMS	0	0	1+	0	3+	ND	0%	Neg
6	mLMS	1+	3+	2+	0	3+	ND	0%	SEC31A-ALK
7	mLMS	0	ND	3+	0	2+	ND	ND	Neg
8	mLMS	0	ND	3+	3+	ND	ND	70%	Neg
9	mLMS	0	0	3+	0	3+	ND	50%	Neg
10	mLMS	0	ND	3+	3+	ND	1+	ND	Neg
11	mLMS	0	1+	1+	0	0	2+	0%	Neg
12	mLMS	0	ND	ND	ND	ND	ND	ND	Neg
13	mSTUMP	1+	3+	3+	1+	ND	ND	ND	Neg
14	mS-NOS	1+	0	0	0	0	2+	0%	Neg
15	mS-NOS	3+	0	0	0	0	2+	+	Neg
16	mS-NOS	0	ND	3+	1+	3+	0	80%	Neg
17	mS-NOS	3+	0	1+	0	1+	1+	+	Neg
18	mS-NOS	0	1+	1+	1+	0	1+	70%	Neg
19	mS-NOS	1+	1+	0	0	1+	ND	+	EWSR1-FLI1
20	mS-NOS	1+	0	0	ND	ND	0	80%	Neg
21	mS-NOS	0	3+	0	0	1+	1+	ND	Neg
22	mS-NOS	1+	3+	2+	1+	2+	ND	ND	ZC3H7B-BCOR
23	HG-ESS	3+	2+	0	ND	0	ND	ND	ZC3H7B-BCOR
24	HG-ESS	3+	3+	0	0	0	2+	0%	ZC3H7B-BCOR
25	HG-ESS	3+	0	0	0	0	3+	0%	YWHEA-NUTM2

Conclusions: We show that mSMTs, when diagnosed using stringent criteria, lack *BCOR* alterations. Likewise, classic HG-ESS morphology tends to correlate with *ZC3H7B-BCOR* or *YWHAE-NUTM2* fusions. However, a significant subset of myxoid uterine sarcomas lacks definitive differentiation (SMT or ESS), and molecular testing can aid in their categorization. In this context, BCOR IHC lacks specificity, similar to CD10 and smooth muscle markers. Thus, IHC should be interpreted in light of the morphology and molecular profile, if available.

1118 Clinicopathologic analysis of MMR-deficient endometrial carcinosarcomas

Sheila Segura[1], Yaser Hussein[2], Robert Soslow[1], Deborah DeLair[3]
[1]Memorial Sloan Kettering Cancer Center, New York, NY, [2]Atlantic consolidated laboratory, Morris Plains, NJ, [3]NYU Langone Medical Center, New York, NY

Disclosures: Sheila Segura: None; Yaser Hussein: None; Robert Soslow: *Speaker*, Ebix/Oakstone; Deborah DeLair: None

Background: Uterine carcinosarcomas (UCSs) are aggressive, biphasic neoplasms composed of high-grade malignant epithelial and mesenchymal elements with the vast majority (~90%) showing *TP53* abnormalities. A subset, however, shows mismatch repair deficiency (MMR-D) and little is known about their clinical, morphologic, and molecular characteristics. We sought to describe these features.

Design: Clinical and pathologic data of 15 MMR-D UCSs were recorded including age, stage, clinical follow-up, MMR and p53 immunohistochemistry (IHC) results, *MLH1* promoter methylation studies, germline genetic testing, and targeted massively parallel sequencing.

Results: The median age of diagnosis was 60 years (range 44-75). Heterologous elements were present in 40% (6/15) of cases, (4 rhabdomyosarcoma, 2 chondrosarcoma). MMR IHC loss is as follows: MLH1 and PMS2 60% (9/15), MSH2 and MSH6 20% (3/15), MSH6 only 13% (2/15), and PMS2 only 7% (1/15). Six of these showed *MLH1* promoter methylation while 2 patients had a deleterious germline mutations (*MLH1*, *MSH2*). Cases with p53 IHC showed a wild-type pattern in 63% (5/8), an aberrant pattern in 25% (2/8) while 1 was equivocal. Of cases with targeted sequencing, 86% (6/7) showed a hypermutated phenotype. The high-grade carcinoma component consisted of endometrioid, undifferentiated, and clear cell in 53%, 40%, and 7% of cases respectively. None of the cases showed a serous carcinoma component and one case displayed an adenosarcomatous architecture. In addition, 47% (7/15) also showed a low-grade endometrioid component. FIGO stage at presentation was as follows: I (n=8), II (n=2), III (n=4) and IV (n=1). The median follow-up was 38 months (range 1 month–12.6 years). At the time of follow-up, 20% (3/15) of patients died of disease, 67% (10/15) showed no evidence of disease (NED) while 13% (2/15) are alive with disease.

Conclusions: Patients with MMR-D UCS appear to be younger than the reported median age (65 years) for traditional UCS and most do not show p53 abnormalities. Low-grade endometrioid and undifferentiated carcinoma components were seen in approximately half of all cases. Although UCSs have a high tendency to early extrauterine spread, most patients (67%) in our cohort presented at early stage (I-II) and at the time of follow up were NED. MMR-D UCSs appear to show distinct clinical, morphologic, and molecular features than those seen in traditional UCSs.

1119 Defining Morphologic Features of Clinically Significant Lymphovascular Invasion in Endometrioid Adenocarcinoma of the Endometrium

Nuha Shaker[1], Nada Shaker[2], Hussain Abubakr[3], Andres Roma[2], Oluwole Fadare[1]
[1]University of California, San Diego, La Jolla, CA, [2]University of California, San Diego, San Diego, CA, [3]King Abdulaziz University, Jeddah, Saudi Arabia

Disclosures: Nuha Shaker: None; Nada Shaker: None; Hussain Abubakr: None; Andres Roma: None; Oluwole Fadare: None

Background: Lymphovascular invasion (LVI) is a prognostic factor that is routinely incorporated into risk-stratification schemes for endometrial carcinomas, and which therefore directly affects patient management. However, there is some interobserver variability in the diagnosis of lymphovascular invasion. In this study, we evaluated several morphologic attributes and potential morphologic iterations of LVI, to determine which features are most significantly associated with recurrences in endometrioid carcinomas of the endometrium.

Design: We reviewed 553 cases of endometrioid carcinoma of the endometrium, and detailed a variety of morphologic characteristics in foci of LVI (features listed in table 1). These findings were then correlated with outcomes in the subset of patients with significant follow-up (n=353, median follow-up of 823 days). The primary outcome measure was recurrence after primary surgical staging, which was observed in 38 (10.8%) of the 353 patients with follow-up. There were 57 patients with LVI and follow-up, divided into recurring (9) and non-recurring cases (48), which were then compared regarding each variable

Results: Overall, LVI was identified in 112/553 (20%) of cases (15 FIGO grade 1, 39 grade 2, 58 grade 3). For the entire cohort of patients with follow-up, LVI was significantly associated with recurrences (p=0.01), but not in the stage I subset and not when adjusted for grade. Among the 57 patients with LVI and follow-up, the frequencies of the assessed variables are outlined in table 1. Among all variables, only two (tumor involving a vein, and tumor cells attached to endothelial cells of a vessel) were significantly associated with recurrences (p=0.008 and p=0.03 respectively), with all other variables showing no statistically significant differences between recurring and non-recurring cases.

Table 1: Frequencies of various LVI-associated morphologic features, and associations with recurrence

Variable	Percentage of all cases with variable	Percentage of recurring cases with variable	p-value (recurring versus non-recurring cases)
More than one focus of LVI	54.3%	66.6%	0.14
LVI involving artery	3.5%	0%	1.0
LVI involving vein	12.2%	44.4%	**0.008**
LVI involving lymphatic vessel	98.2%	88.8%	0.15
Tumor conforms to shape of vascular space	82.4%	88.8%	1.0
Fibrin with tumor in vascular space	15.7%	33.3%	0.14
Blood with tumor in vascular space	26.3%	33.3%	0.68
Tumor attached to endothelial cells of vessel	54.3%	88.8%	**0.03**
LVI in outer 50% of myometrial wall	61.4%	88.8%	0.13
LVI Involving lymphatic vessel and vein	10.5%	33.3%	0.098
LVI Involving lymphatic vessel and artery	3.5%	0%	1
Both fibrin & blood associated with tumor in vascular space	10.5%	22.2%	0.29

Conclusions: In this pilot analysis, we found LVI to be significantly associated with recurrences in endometrial cancers, but not when adjusted for stage and grade. Certain properties of LVI show more significant associations with recurrence than others, including tumor involving a vein, and tumor cells being attached to endothelial cells of a vessel. A variety of other traditional morphologic parameters of LVI (such as tumor conforming to shape of vessel, blood or fibrin associated with tumor, etc) were not significantly associated with recurrence. These findings may have utility in defining the most clinically significant and reproducible iterations of LVI

1120 ALDH1 Expression Predicts Progression of Premalignant Lesions to Cancer in Type I Endometrial Carcinomas

Hania Shakeri[1], John Elshimali[2], Vei Mah[3], Madhuri Wadehra[1]
[1]David Geffen School of Medicine at UCLA, Los Angeles, CA, [2]Nantomics, Northridge, CA, [3]David Geffen School of Medicine at UCLA, La Jolla, CA

Disclosures: Hania Shakeri: None; John Elshimali: None; Vei Mah: None; Madhuri Wadehra: None

Background: Endometrial carcinoma is the fourth most common cancer in women in the United States and 80 % occurs in postmenopausal women. Of the two types, type 1 endometrial cancer is associated with unopposed estrogen stimulation and are often preceded by endometrial hyperplasia. Aldehyde dehydrogenase 1 (ALDH1) has been identified as a putative cancer stem cell (CSC) marker in several cancer types, and our group has recently shown that it is expressed in endometrial cancer (EC). However, the clinicopathological and prognostic value of this protein in disease remains controversial. The aim of this study is to investigate the clinical impact of ALDH1 expression in endometrial hyperplasia and to determine its ability to predict progression to cancer.

Design: We performed a systematic review and meta-analysis of primary tissue assessing the clinical and prognostic significance of ALDH1 expression in endometrial cancer. A TMA was constructed to contain a wide representation of histopathologies of the endometrium from 207 individuals over time ("metachronous") who either developed or did not develop EC. ALDH1 expression was determined by standard immunohistochemistry using clone 44/ALDH (BD Biosciences) with expression scored by a pathologist blinded as the percentage of cells with staining intensities of 0 to 3 (0 = below the level of detection, 1 = weak, 2 = moderate, 3 = strong).

Results: Utilizing the data from 1837 tissue cores, the expression of ALDH1 was evaluated, and it predominantly displayed a cytoplasmic distribution. Within the functionalis, ALDH1 was largely absent from normal proliferative and secretory endometrium, although interestingly, it was commonly expressed within the basalis. Characterizing the expression within premalignant lesions and the tumor parenchyma, the

percentage of patients with any ALDH1 expression showed a step-wise increase between endometrial hyperplasia, atypia, and endometrial cancer (Kruskal-Wallis p=6.75e-14). Moreover, ALDH1 was an independent prognostic indicator of patients with atypical hyperplasia who progress to cancer (p=0.02). It also could predict patients with simple or complex hyperplasia who would develop the disease (p=0.01).

Figure 1 - 1120

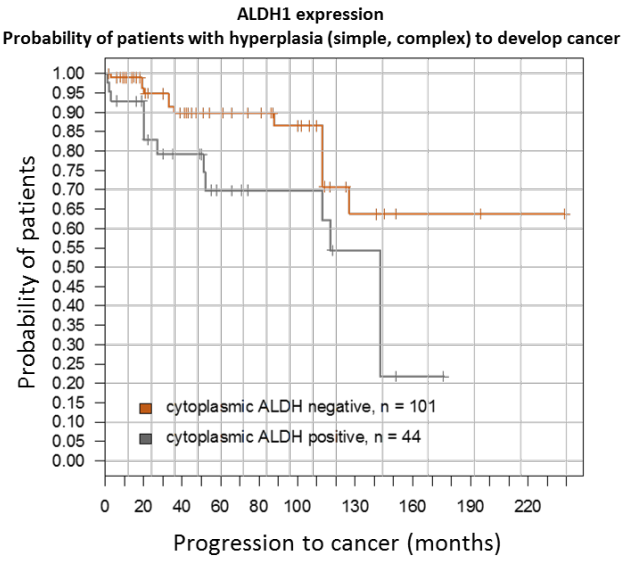

Figure 2 - 1120

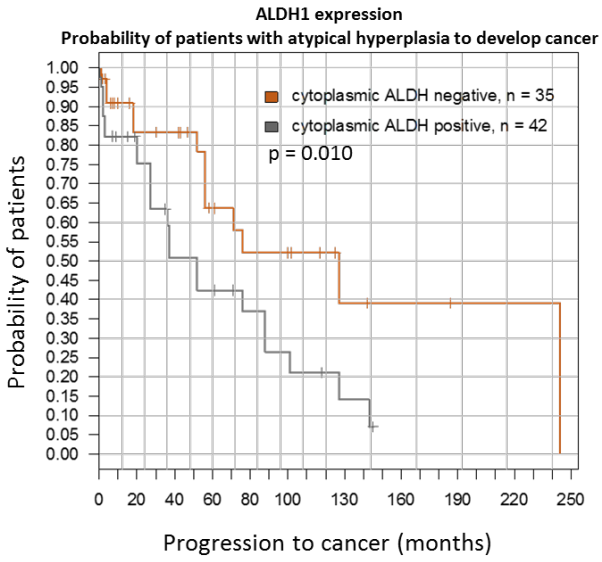

Conclusions: ALDH1 predicts progression to cancer from hyperplasia and atypical hyperplasia. This meta-analysis shows ALDH1 expression in endometrial carcinoma is connected with disease progression and possible disease-free survival and thus marks a worse prognosis.

1121 PD-L1 Expression in Uterine Smooth Muscle Tumors: Implications for Immunotherapy

Elisheva Shanes[1], Anne Mills[1]
[1]University of Virginia, Charlottesville, VA

Disclosures: Elisheva Shanes: None; Anne Mills: None

Background: Immunotherapies targeting the PD-1/PD-L1 checkpoint axis have shown promise in a variety of gynecologic carcinomas and are of growing interest for the treatment of mesenchymal neoplasms. Given the poor prognosis of uterine leiomyosarcoma (LMS) and the paucity of available therapeutic options, the potential impact of immunotherapy in this patient population may be significant. However, the range of PD-L1 expression patterns in uterine LMS, as well as in lower grade uterine smooth muscle tumors (USMT), has not been well investigated.

Design: 50 USMT comprised of 23 LMS, 8 smooth muscle tumors of uncertain malignant potential (STUMP), 8 atypical leiomyomas (AL), and 11 benign leiomyomas (BL) were immunostained for PD-L1, CD8, and FoxP3. Tumoral PD-L1 expression was semi-quantitatively scored by extent (negative, 1-5%, 6-10%, >10%) and PD-L1-positive tumor-associated immune (TAI) infiltrates were scored as absent, focal, moderate, or brisk. The presence of a Combined Positive Score >1 was documented [(#PD-L1+ tumor cells, lymphocytes, and macrophages)/(total #tumor cells) x 100]. CD8-positive and FoxP3-positive lymphocytes were manually enumerated and averaged across 5 to 10 high-power fields. Follow-up status and therapeutic history was recorded where available.

Results: Tumor PD-L1 expression was seen in 70% of LMS and 25% of AL; no cases of STUMP or BL demonstrated tumoral PD-L1. PD-L1 positivity was seen in TAI in 78% of LMS, 25% of STUMP, no cases of AL, and 9% of BL. Of the 23 cases of LMS, 15 (65%) had a CPS >1, while of the 27 other SMTs, only 1 (4%), a BL, had a CPS >1. Additional results can be seen in Table 1.

Of the 23 patients with LMS, 6 (26%) were confirmed dead of disease (DOD), with an additional 4 discharged to hospice and presumed DOD (total DOD 10 (43%)). 2 (9%) LMS patients were alive with progressive disease. 5 (22%) LMS patients were alive with no evidence of disease, and 6 (26%) LMS patients were lost to follow up. The average age of patients with LMS was 54, while the average age of patients with STUMP was 34 (p=0.0003).

Tumor Type	Tumor PD-L1+	TAI PD-L1+	CPS >1	CD8+/ HPF (range)	FoxP3+/HPF (range)
LMS	**Total:** 16 (70%) **>1%:** 10 (43%) **>5%:** 2 (9%) **>10%:** 4 (17%)	**Total:** 18 (78%) **Mild:** 8 (35%) **Mod:**5(22%) **Brisk:** 5(22%)	15 (65%)	87 (0-300)	9 (0-45)
STUMP	**Total:** 0 **>1%:** 0 **>5%:** 0 **>10%:** 0	**Total:** 2 (25%) **Mild:** 2 (25%) **Mod:** 0 **Brisk:** 0	0 (0%)	11 (1-41)	1 (0-8)
AL	**Total:** 2 (25%) **>1%:** 2 (25%) **>5%:** 0 **>10%:** 0	**Total:** 0 **Mild:** 0 **Mod:** 0 **Brisk:** 0	0 (0%)	12 (2-30)	2 (0-9)
BL	**Total:** 0 **>1%:** 0 **>5%:** 0 **>10%:** 0	**Total:** 1 (9%) **Mild:** 0 **Mod:** 0 **Brisk:** 1 (9%)	1 (9%)	26 (2-165)	0 (0-2)

Figure 1 - 1121

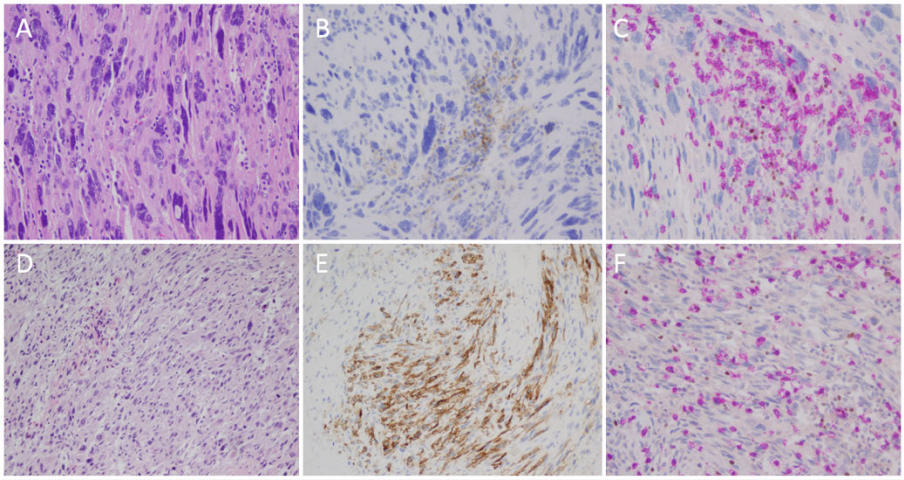

Figure 1. A-C: LMS with PD-L1-positive TAI but no tumoral PD-L1 expression [A: H&E; B: PD-L1; C: FOX3p (brown) and CD8 (pink) dual stain]. D-F: LMS with PD-L1 expression in TAI and scattered tumor cells [D: H&E; E: PD-L1; F: FOX3p (brown) and CD8 (pink) dual stain].

Conclusions: A significant percentage of LMS exhibit expression of tumoral and TAI PD-L1 when compared to STUMP, AL, and BL ($p < 0.00001$). Of therapeutic note, 65% of LMS demonstrated a CPS >1, compared to only 1 non-LMS SMT ($p < 0.00001$). These data suggest the possibility that treatment with PD-L1-targed immunotherapy may be appropriate in a selected population of patients with LMS.

1122 Comprehensive Morphologic Assessment and Clinical Follow-Up of Differentiated Vulvar Intraepithelial Neoplasia and Lichen Sclerosus

Stephanie Skala[1], Shula Schechter[1], May Chan[1], Richard Lieberman[2]
[1]University of Michigan, Ann Arbor, MI, [2]Michigan Medicine, Ann Arbor, MI

Disclosures: Stephanie Skala: None; Shula Schechter: None; May Chan: None; Richard Lieberman: None

Background: Differentiated vulvar intraepithelial neoplasia (dVIN) is a human papillomavirus-independent lesion with potential for rapid progression to invasive squamous cell carcinoma (SCC). The morphologic characteristics of dVIN are often subtle and not all lesions show every feature, hence there is high interobserver variability for its diagnosis. Because dVIN usually does not show diffuse architectural or cytologic atypia, it is often underdiagnosed in cases showing concomitant lichen sclerosus (LS), or misdiagnosed as lichen simplex chronicus (LSC). Here, we assess multiple morphologic features of a large cohort of dVIN and LS cases in order to identify useful differentiating features between dVIN and LS without dVIN which would not require vulvar resection.

Design: Biopsies diagnosed as “differentiated vulvar intraepithelial neoplasia” and “lichen sclerosus” from 2011-2018 were retrieved from the surgical pathology database at a single large academic institution. The control group includes LS cases without prior, concurrent, or subsequent dVIN or SCC based on follow-up ≥2 years; a subset of these cases show superimposed features of LSC. Morphologic features were reviewed and compared between the two groups using Fisher’s exact tests. In the dVIN group, features associated with concurrent or subsequent progression to invasive SCC were identified.

Results: The majority (93%) of dVIN cases had associated LS. Differentiating features between dVIN and LS without dVIN are listed below, in descending order of statistical significance:

Presence of moderate-marked lichenoid inflammation did not show significant association with either group.

37 (54%) cases of dVIN were associated with SCC. Keratin pearl formation was the only discriminator between dVIN associated with SCC (17/37, 46%) and dVIN without progression (7/32, 22%) (p=0.045).

	dVIN (n=69)	LS without dVIN (n=92)	p value
Dyskeratosis	60 (87%)	19 (21%)	<0.0001
Paradoxical maturation	59 (86%)	21 (23%)	<0.0001
Nuclear enlargement	44 (64%)	8 (9%)	<0.0001
Large nucleoli	20 (29%)	3 (3%)	<0.0001
Acanthosis	52 (75%)	22 (24%)	<0.0001
Elongated rete ridges	57 (83%)	28 (30%)	<0.0001
Anastomosing rete ridges	55 (80%)	43 (47%)	<0.0001
Basal pleomorphism	34 (49%)	3 (3%)	<0.0001
Diffuse parakeratosis	24 (35%)	1 (1%)	<0.0001
Keratin pearls	24 (35%)	2 (2%)	<0.0001
Basal layer disarray	60 (87%)	52 (57%)	<0.0001
Mitotic figures above basal layer	23 (33%)	3 (3%)	<0.0001
Intercellular bridges	61 (88%)	57 (62%)	0.0001
Vesicular chromatin	23 (33%)	8 (9%)	0.0001
Blurring of dermoepidermal junction	28 (41%)	13 (14%)	0.0002
Hypergranulosis	14 (20%)	2 (2%)	0.0002
Diffuse orthokeratosis	39 (57%)	36 (39%)	0.0378

Conclusions: The strongest discriminators between dVIN and LS without dVIN were dyskeratosis, paradoxical maturation, nuclear enlargement, large nucleoli, acanthosis, elongated and anastomosing rete ridges, basal pleomorphism, diffuse parakeratosis, keratin pearl formation, basal layer disarray, and mitotic figures above the basal layer. Keratin pearl formation was more frequently seen in dVIN associated with SCC, and may be viewed as an alarming sign of early progression.

1123 Effect of An Alternative Strategy For Measuring Depth of Invasion in Stage I Vulvar Squamous Cell Carcinoma

Stephanie Skala[1], Richard Lieberman[2]
[1]University of Michigan, Ann Arbor, MI, [2]Michigan Medicine, Ann Arbor, MI

Disclosures: Stephanie Skala: None; Richard Lieberman: None

Background: Measurement of depth of invasion can be quite challenging for some cases of vulvar squamous cell carcinoma (SCC). Tumors with ≥1 mm invasion should trigger sentinel lymph node biopsy and/or groin lymph node dissection. However, there is poor interobserver reproducibility in the assessment of presence or absence of invasive carcinoma, as well as where to measure depth of invasion. A previous study including 69 cases of stage IB vulvar SCC demonstrated no change in outcome when depth was measured to the nearest lowest dysplastic rete peg rather than the American Joint Committee on Cancer (AJCC)-recommended nearest highest dermal papilla. We report our institutional experience with depth of invasion in vulvar SCC.

Design: A search of the surgical pathology database of a single large academic institution yielded 75 cases of pT1 invasive vulvar SCC resected from 1998-2018 with lymph node sampling within 1 year. Pathologic staging data and clinical follow-up were recorded. Each invasive SCC was measured by 2 methods: depth from nearest highest dermal papilla (conventional method) and depth from most adjacent dysplastic rete peg (alternative method).

Results: Fifteen cases of invasive SCC were reclassified as pT1a when measured using the alternative method rather than pT1b by the conventional method. Of these 15 reclassified cases, all were pN0 and lacked lymphovascular or perineural invasion. Three of 15 patients (20%) reclassified as pT1a had recurrent invasive carcinoma, as compared to 15/58 (26%) that remained pT1b regardless of measurement method. Of the 58 cases that remained pT1b, 5 (9%) had lymph node involvement, 12 (21%) had lymphovascular invasion, 8 (14%) had perineural invasion. The two cases staged as pT1a regardless of method were pN0 with no lymphovascular invasion, perineural invasion, or recurrent invasive carcinoma.

Conclusions: In 15 cases, the depth of invasion was less than 1 mm when measured using the alternative method rather than the conventional method. None of these cases demonstrated nodal involvement or evidence of lymphovascular or perineural invasion. These results are concordant with previous findings that this alternative method of measuring depth of invasion could safely allow a subset of conventional stage IB vulvar SCC patients to avoid groin surgery, reducing treatment-related morbidity. However, it remains unclear which factors in early vulvar SCC are most associated with nodal metastasis and aggressive clinical course.

1124 Endometrial Tumor Inflammatory Response Is Associated with Tumor Phenotype and Host Exposures in the Nurses' Health Study

Thing Rinda Soong[1], Michael Downing[2], Joy Shi[3], Evan Busch[4], Immaculata De Vivo[5], George Mutter[4]
[1]University of Washington, Seattle, WA, [2]Acton, MA, [3]Harvard T.H. Chan School of Public Health, Cambridge, MA, [4]Brigham and Women's Hospital, Harvard Medical School, Boston, MA, [5]Brigham and Women's Hospital, Harvard Medical School, Belmont, MA

Disclosures: Thing Rinda Soong: None; Michael Downing: None; Joy Shi: None; Evan Busch: None; Immaculata De Vivo: None; George Mutter: None

Background: Inflammation in invasive carcinoma has been proposed as a risk modifier of tumor initiation and progression. Compared to other malignancies, the role of tumor immune response (TIR) in endometrial carcinomas (ECs) is far understudied. We aimed to characterize the associations of EC inflammatory response with tumor phenotype and host non-genetic exposures.

Design: Incident ECs arising in the Nurses' Health Study between 1976 and 2012 were included (n=325). Immune cells within tumors and biomarker expression in tumor epithelium were assessed with tissue microarrays (**Figure 1**). Multivariable logistic regression was used to estimate the associations between inflammatory profiles and tumor features with adjustment for known EC risk factors. Immune marker expression was evaluated at different cut points in increments (5-100 cells/mm^2) to determine appropriate binary categorizations.

Results: Inflammatory cells were present in varying levels in ECs. Increased tumor DNA damage was associated with more leukocyte recruitment (>=200 cells/mm^2)(**Figure 2**). Trends correlated with tumor subtypes included poorly differentiated endometrioid ECs with increased T cells (>=350 cells/mm^2), and non-endometrioid ECs with increased macrophages (>=150 cells/mm^2). History of rheumatoid arthritis conferred 2-fold increased odds of more T helper cells (>=60 cells/mm^2) in ECs. Several immune subpopulations (leukocytes, T cells, T helper cells, FOXP3+ T cells and B cells) were also mildly elevated with longer use of combined estrogen and progesterone hormone therapy. In contrast, former use of aspirin decreased by 3-fold the odds of elevated leukocytes and T cells compared to never aspirin use. Longer oral contraceptive use was correlated with reduced levels of cytotoxic T cells (<25 cells/mm^2) and plasma cells (<7 cells/mm^2). In addition, obesity (body mass index >30 kg/m^2) was associated with decreased leukocytes, FOXP3+ T cells and plasma cells in ECs (**Figure 2**).

Figure 1 - 1124

Inflammatory and tumor biomarkers assessed in endometrial carcinomas	
	Cell populations/processes highlighted by markers
Markers expressed by inflammatory cells* (number of cells per mm^2 of carcinoma)	
CD45	Leukocytes
CD3	T cells (general)
CD4	T helper cells
CD8	Cytotoxic T cells
FOXP3	Regulatory T cells
CD20	B cells (general)
CD163	Macrophages
Kappa and lambda surface light chains	Plasma cells
Markers expressed by tumor epithelium* (number of cells per mm^2 of carcinoma epithelium)	
Gamma-H2AX	DNA damage in cells
Phospho-Histone H3	Mitoses in cells
Estrogen receptor	Estrogen responsiveness
Progesterone receptor	Progesterone responsiveness
* All markers were detected via immunohistochemical studies except kappa and lambda light chains which were detected using in situ hybridization.	

Figure 2 - 1124

Association of pathologic and host characteristics with inflammatory profiles in endometrial carcinomas

Select pathologic and host characteristics	N=325 Col% [b]	Multivariable logistic regression (odds ratios (95% CI)[a]) CD45+ cells ≥200/mm^2	CD3+ cells ≥350/mm^2	CD4+ cells ≥60/mm^2	CD8+ cells ≥25/mm^2	FOXP3+ cells ≥25/mm^2	CD20+ cells ≥5/mm^2	CD163+ cells ≥150/mm^2	Plasma cells ≥7/mm^2
Tumor features									
Tumor histologic type and grade									
Endometrioid (well differentiated)	68	Ref	Ref	Ref	Ref	Ref	Ref	Ref	Ref
Endometrioid (moderately differentiated)	11	1.1 (0.5, 2.5)	1.7 (0.7, 4.3)	0.7 (0.3, 1.7)	0.7 (0.2, 3.6)	1.1 (0.4, 2.6)	0.6 (0.2, 1.6)	1.1 (0.5, 2.7)	1.6 (0.7, 1.3)
Endometrioid (poorly differentiated)	8	0.8 (0.3, 2.8)	**3.3 (1.0, 11.4)	0.5 (0.1, 1.9)	0.3 (0.05, 2.2)	0.8 (0.2, 3.0)	1.0 (0.3, 3.3)	1.5 (0.4, 4.9)	2.1 (0.6, 7.1)
Non-endometrioid	13	0.8 (0.3, 2.3)	0.7 (0.5, 5.3)	1.2 (0.4, 3.8)	1.5 (0.3, 8.0)	3.0 (0.9, 9.2)	1.3 (0.5, 3.8)	**3.0 (1.0, 9.2)	0.5 (0.2, 1.4)
Density of cells with Gamma H2AX signals (every 100 cell increase per mm^2)	97	**1.1 (1.1, 1.3)	1.0 (0.9, 1.1)	1.1 (1.0, 1.2)	1.0 (0.8, 1.1)	1.1 (1.0, 1.2)	1.1 (0.9, 1.1)	1.1 (0.9, 1.1)	1.0 (0.9, 1.1)
Density of cells with Phospho-Histone H3 signals (every 100 cell increase per mm^2)	97	0.9 (0.7, 1.2)	1.0 (0.8, 1.4)	1.1 (0.8, 1.4)	1.3 (0.5, 3.1)	1.3 (0.9, 2.0)	0.8 (0.6, 1.1)	1.4 (0.9, 2.3)	0.8 (0.5, 1.2)
Host exposures at the time of diagnosis of endometrial cancer									
Status of aspirin use									
Never user	10	Ref	Ref	Ref	Ref	Ref	Ref	Ref	Ref
Current user	47	0.6 (0.2, 1.7)	0.8 (0.3, 2.2)	0.9 (0.3, 2.7)	2.7 (0.3, 22.1)	0.6 (0.7, 1.4)	0.6 (0.2, 1.6)	0.7 (0.2, 2.0)	0.8 (0.3, 2.2)
Former user	35	**0.3 (0.1, 0.9)	**0.3 (0.1, 0.9)	0.6 (0.2,1.9)	0.3 (0.05, 2.0)	0.9 (0.2, 1.7)	0.4 (0.1, 1.1)	0.4 (0.1, 1.1)	0.8 (0.3, 2.3)
History of rheumatoid arthritis	15	1.6 (0.1, 1.0)	1.2 (0.5, 2.9)	**2.5 (1.1, 5.6)	1.0 (0.2, 4.3)	0.5 (0.2, 1.1)	2.1 (0.9, 4.6)	0.7 (0.3, 1.6)	0.9 (0.4, 1.9)
Estrogen-only hormone therapy use (every 1 year increase)	100	**0.9 (0.8, 0.9)	**0.8 (0.7, 0.9)	0.9 (0.7, 1.0)	1.4 (0.9, 1.2)	1.0 (0.9, 1.1)	0.9 (0.9, 1.0)	0.9 (0.8, 1.1)	0.9 (0.9, 1.0)
Estrogen and progesterone hormone therapy use (every 1 year increase)	100	**1.1 (1.0, 1.2)	**1.1 (1.0, 1.2)	**1.2 (1.1, 1.3)	1.0 (0.9, 1.2)	**1.1 (1.0, 1.2)	**1.1 (1.0, 1.2)	1.0 (0.9, 1.1)	1.0 (0.9, 1.1)
Other hormone therapy use (every 1 year increase)	100	1.0 (0.9, 1.1)	**1.1 (1.0, 1.2)	**1.1 (1.0, 1.2)	1.1 (0.9, 1.3)	1.0 (0.9, 1.0)	1.0 (0.9, 1.1)	1.0 (0.9, 1.1)	1.0 (0.9, 1.0)
Oral contraceptive use (every 1 year increase)	100	1.0 (0.9, 1.1)	0.9 (0.8, 1.0)	1.0 (0.9, 1.1)	**0.8 (0.7, 0.9)	0.9 (0.8, 1.0)	0.9 (0.8, 1.0)	1.0 (0.9, 1.1)	**0.9 (0.8, 0.9)
Body mass index (kg/m^2)									
<25	28	Ref	Ref	Ref	Ref	Ref	Ref	Ref	Ref
25 to <30	32	1.0 (0.5, 2.0)	**2.3 (1.0, 5.0)	1.5 (0.7, 3.3)	0.2 (0.05, 1.3)	0.7 (0.4, 1.6)	1.0 (0.5, 2.0)	**2.6 (1.2, 5.6)	0.9 (0.5, 1.9)
30+	40	**0.5 (0.2, 1.0)	0.8 (0.3, 1.8)	0.9 (0.4, 1.9)	0.2 (0.04, 1.4)	**0.3 (0.2, 0.7)	0.5 (0.3, 1.1)	0.9 (0.4, 2.0)	**0.5 (0.2, 1.0)

[a] Adjusted for variables in the table as well as tumor ER hormone responsiveness (≥10% staining), tumor PR hormone responsiveness (≥10% staining), current smoking status (yes/no), former smoking status (yes/no), pack-years of cigarettes smoked (continuous variable), diabetes (yes/no), family history of endometrial cancer (yes/no), parity (years as continuous variable), years from menarche to menopause (continuous variable), years since menopause (continuous variable), frequency of aspirin use (continuous variable), and interaction between status and frequency of aspirin use.
[b] Percentages may not add up to 100% due to missing data.
** P<0.05

Conclusions: Our data support the hypothesis that TIR in ECs is co-determined by tumor phenotype as well as host physiologic, hormonal and drug exposures. The differential association patterns seen with different immune cell populations highlight tumor and host risk factors that may promote and suppress TIR in ECs. The findings underscore an interaction between TIR and local environment, and inform follow-up studies to investigate whether and how inflammatory pathways in the endometrium may be manipulated to reduce risk of tumor development and spread.

1125 PDL1 Expression Pattern in Tumor Biopsies of HIV and non-HIV Infected Cervical Cancer Patients in Botswana

Mohan Sopanahalli Narasimhamurthy[1], Keabetswe Rahube[2], Nicola Zetola[3], Erle Robertson[4], Surbhi Grover[5], Hao Shen[5]
[1]Gaborone, Botswana, [2]University of Botswana, Gaborone, Botswana, [3]Botswana UPenn Partnership, Gaborone, Botswana, [4]Hospital of the University of Pennsylvania, Philadelphia, PA, [5]University of Pennsylvania, Philadelphia, PA

Disclosures: Mohan Sopanahalli Narasimhamurthy: None; Keabetswe Rahube: None

Background: Cervical cancer is the 4th most common cancer in women globally, with sub-Saharan Africa (SSA) bearing the highest burden. Botswana has a high burden of cervical cancer due to a limited screening program and high HIV prevalence. About 60% of the cervical cancer patients are HIV positive; most present with advanced cervical disease. Increasing evidence from various studies indicate that Tumor infiltrating lymphocytes (TILs), and the PDL-1/PD1 pathway are important contributors to the development and progression of dysplastic lesions, and cervical cancer. Could enhanced regulatory T-cell activity and T-cell exhaustion in the tumor microenvironment

caused by HIV facilitate carcinogenesis in HIV-infected individuals? This important and high impact question has not been fully explored and is one of our long-term goals. A pilot study was initiated to establish the immunohistochemistry assays at the University of Botswana to examine the tumor infiltrating lymphocytes and associated PDL-1/PD1 expression.

Design: A cross sectional retrospective pilot study evaluating the tumour infiltrating lymphocytes profile and PD-L1 expression in cervical cancer cells using formalin fixed paraffin-embedded (FFPE) biopsy tissue of locally advanced cervical cancer patients with or without HIV infection. FFPE blocks were retrieved, sectioned, processed and stained with antibodies for PDL-1. Stromal cells and histiocytes present in B-cell follicles of reactive lymph node were used as a control for PD-L1 positivity. Tumour cells were designated PD-L1 positive, when more than 1% of the tumour cells were positive for PD-L1. Low <1%, Intermediate >1% and <5%, High>5%

Results: 49 cases out of 50 cases were analysed after excluding one case due to lack of inadequate tissue sections for study on pathological examination. 36/49 cases were HIV infected. The HIV status was not known in 3 cases. In the HIV infected cases 5 out of 36 (14%) cases showed more than 5% PDL-1 positivity compared to none of the 13 cases from HIV negative patients.

Conclusions: 14% of HIV infected cervical cancer patients are PDL-1 positive. Although the statistical significance is not as robust based on the low numbers screened, it is an important observation in HIV infected HPV positive cervical cancer cells. Additional questions as to the levels of PDL-1 signals in the other HIV positive samples and the comparative signals for HPV-encoded antigens will further shed light as the study continues.

1126 The Molecular Pathogenesis of Peritoneal Mesothelial Neoplasia: Distinct Genetic Alterations Underlie Malignant Mesothelioma, Well-Differentiated Papillary Mesothelioma, Benign Multicystic Mesothelioma, and Adenomatoid Tumor of the Genital Tract

Meredith Stevers[1], Sarah Umetsu[1], Nancy Joseph[1], Jessica Van Ziffle[1], Karuna Garg[1], Joseph Rabban[2], Charles Zaloudek[3], David Solomon[1]
[1]University of California, San Francisco, San Francisco, CA, [2]UCSF Pathology, San Francisco, CA, [3]UCSF Medical Center at Mission Bay, San Francisco, CA

Disclosures: Meredith Stevers: None; Sarah Umetsu: None; Nancy Joseph: None; Jessica Van Ziffle: None; Karuna Garg: None; Joseph Rabban: *Employee*, Merck & Co., Inc.; Charles Zaloudek: None; David Solomon: None

Background: Multiple distinct histologic subtypes of mesothelial neoplasms arise in the peritoneal cavity, which include malignant mesothelioma, well-differentiated papillary mesothelioma (WDPM), multilocular peritoneal inclusion cyst (MPIC, also known as benign multicystic mesothelioma), and adenomatoid tumor of the genital tract. Over the past few years, we have studied the genetic basis of these peritoneal mesothelial neoplasms. We identified that malignant mesotheliomas are genetically characterized by a high frequency of inactivation of the *BAP1* tumor suppressor gene (~80% of cases) and also recurrent alterations in the *NF2*, *CDKN2A*, *DDX3X*, and *SETD2* genes (Joseph et al. *Modern Pathology* 2017). Adenomatoid tumors are genetically defined by missense mutations in the *TRAF7* gene (100% of cases), which encodes a TNF-alpha receptor-associated factor (Goode et al. *Modern Pathology* 2018). WDPM is genetically defined by mutually exclusive mutations in *TRAF7* and *CDC42*, indicating a shared molecular pathogenesis between WDPM and adenomatoid tumors (Stevers et al. *Modern Pathology* 2018). Here we report our investigation of the genetic basis of MPIC.

Design: Six cases of MPIC were studied by targeted next-generation DNA sequencing of ~500 cancer-associated genes, whole exome sequencing, and immunohistochemistry for BAP1 and L1CAM.

Results: Targeted next-generation sequencing demonstrated that all MPIC lacked alterations in *TRAF7*, *CDC42*, *BAP1*, *NF2*, *CDKN2A*, *DDX3X*, and *SETD2*, indicating a distinct molecular pathogenesis from malignant mesothelioma, WDPM, and adenomatoid tumors. Additionally, all MPIC had intact BAP1 and lacked L1CAM expression, further differentiating these lesions from other peritoneal mesothelial neoplasms. Assessment of whole exome sequencing data from the six cases of MPIC is currently in progress and will be presented.

Conclusions: These studies demonstrate a distinct molecular pathogenesis of the four different peritoneal mesothelial neoplasms. We are now generating in vitro and mouse models of mesothelial neoplasia in order to investigate the mechanisms by which these recurrent genetic alterations drive mesothelioma development. Our initial functional studies suggest that *TRAF7* mutations drive mesothelial tumorigenesis by activating the NF-kB signaling pathway.

1127 Uterine Adenosarcoma and Low Grade Endometrial Stromal Sarcoma: A Comparative Study Using Novel Immunohistochemical Markers

Irina Stout[1], Sayak Ghatak[1], Heidi Wipf[1], Michelle Dolan[2], Mahmoud Khalifa[1], Paari Murugan[1]
[1]University of Minnesota, Minneapolis, MN, [2]University of Minnesota Medical School, Minneapolis, MN

Disclosures: Irina Stout: None; Sayak Ghatak: None; Heidi Wipf: None; Michelle Dolan: None; Mahmoud Khalifa: None; Paari Murugan: None

Background: In uterine adenosarcoma (UA), recent studies have identified genomic alterations in the sarcomatous but not the glandular components, suggesting that nonneoplastic glands are entrapped by the neoplastic stroma. Because of their stromal origins, we hypothesize that UA and low-grade endometrial stromal sarcoma (LGESS) share similar molecular mechanisms of tumorigenesis and immunohistochemical marker profiles.

Design: After obtaining IRB approval, we identified 24 consecutive cases of UA (10) and LGESS (14) diagnosed at our tertiary care center from 2003-2018. Representative blocks from each case were tested for expression patterns of an immunohistochemical panel selected based on recently published genomic studies. The immunostains were analyzed using the German semi-quantitative scoring system. FISH for JAZF1 rearrangement was also performed.

Results: PTEN immunoreactivity (nuclear and cytoplasmic) was lost in 30% of UA and in 35.7% of LGESS cases. Nuclear MYBL1 was expressed in 10% UA and 7.1% LGESS; nuclear TERT was seen in both UA (90%) and LGESS (64.3%) cases; nuclear PMS2 was expressed in all UA and LGESS cases. Nuclear beta-catenin expression, typically a downstream effect of canonical WNT pathway activation, was seen in 60% of UA and 64.3% of LGESS. FISH testing showed JAZF1 rearrangement in 64.3% LGESS cases, of which 88.9% also had nuclear beta-catenin expression. None of the UA demonstrated JAZF1 rearrangement.

Marker	+ve LGESS cases	+ve UA cases	Technique	Gene Function
PTEN (nuclear, cytoplasmic)	64.3%	70%	IHC	chromatin stability, DNA double-stranded break repair, apoptosis
MYBL1 (nuclear)	7.1%	10%	IHC	maintains germ-line integrity , suppresses transposons
TERT (nuclear)	64.3%	90%	IHC	reverse transcriptase, maintenance of telomeric length
PMS2 (nuclear)	100%	100%	IHC	DNA mismatch repair
beta-catenin (nuclear)	64.3%	60%	IHC	canonical WNT pathway activation
JAZF1 fusion gene	64.3%	0%	FISH	Zinc-finger protein, translocation activates WNT pathway

Figure 1 - 1127

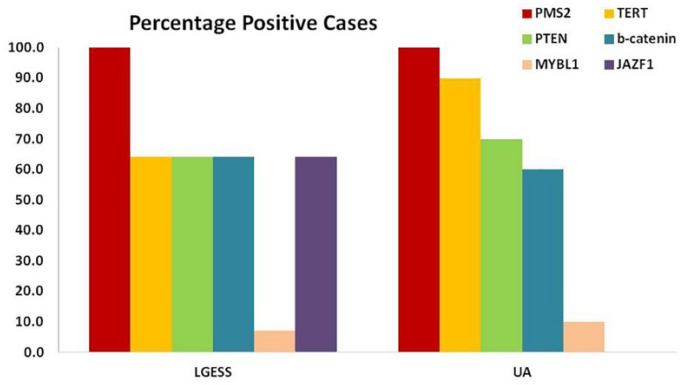

Figure 1 demonstrates the frequency of positive cases. PMS2 was preserved in all the cases. PTEN, TERT and β-catenin was expressed in a sub-set of both UA and LGESS cases. MYBL1 was expressed in one case each of UA and LGESS. JAZF1 fusion gene was present in a subset of only the LGESS cases.

Figure 2 - 1127

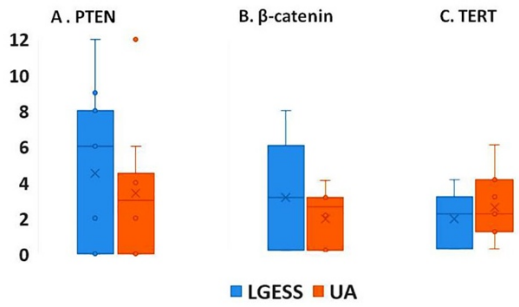

Figure 2 demonstrates the German semi-quantitative score of immunoreactivity for PTEN (Fig. 2A), β-catenin (Fig. 2B) and TERT (Fig. 2C). PTEN expression ranges from 0-12, with median expression of 6 in LGESS and from 0-6 with a median of 4 in UA. β-catenin expression ranges from 0-8 in LGESS with median score of 3, and from 0-4 in UA with median expression of 2.5. TERT expression ranges from 0-4 in LGESS and 0-6 in UA, with median expression of 2 in both. Student T-test p-values were not significant ($\geq$ 0.05) between the two groups.

Conclusions: We documented that UA and LGESS have a similar pattern of PTEN, TERT, PMS2, MYBL1 and beta-catenin expression. Although MYBL1 and TERT expression in UA has been previously reported, this study documents for the first time their expression in LGESS. beta-catenin expression was highly correlated with the presence of JAZF1 rearrangement in LGESS, as previously reported. This correlation suggests that impaired repression of WNT ligand expression by an altered JAZF1 gene product might be implicated in LGESS tumorigenesis. Conversely, beta-catenin nuclear expression in UA in the absence of JAZF1 rearrangement suggests the possibility of an alternate pathway of WNT activation.

1128 Molecular Signature of Aggressive Low Grade Endometrioid Endometrial Adenocarcinomas

Monalisa Sur[1], Martin Hyrcza[2], Priyatharsini Nirmalanantham[3], Mary Anne Brett[4], Yogi Sundaravadanam[5], Ranjan Sur[6], Laurie Elit[6], Alice Lytwyn[7]
[1]McMaster University, Burlington, ON, [2]University of Calgary/Calgary Laboratory Services, Calgary, AB, [3]Brampton, AB, [4]University of Calgary, Calgary, AB, [5]Ontario Institute for Cancer Research, Toronto, ON, [6]McMaster University, Hamilton, ON, [7]Juravinski Hospital, Hamilton, ON

Disclosures: Monalisa Sur: None; Martin Hyrcza: None; Priyatharsini Nirmalanantham: None; Mary Anne Brett: None; Yogi Sundaravadanam: None; Ranjan Sur: None; Laurie Elit: None; Alice Lytwyn: None

Background: Most FIGO grade 1 endometrioid endometrial carcinomas (EEC) are stage 1 at diagnosis, with 98% 5-year survival. Survival is decreased in the 15% of patients with a recurrence or metastasis. 6.4% of FIGO 1 EEC have mutated POL-E , 28.6% are MMR deficient (MMR-D), and 5% are copy number high. The molecular profile of recurrences/metastatic disease has not been reported.

Design: Departmental electronic medical database was searched from 2001-2016 for FIGO1 Stage 1 ECC with recurrent/metastatic disease. Representative tumor sections were cut from formalin fixed paraffin-embedded tissue for MMR and p53 immunohistochemical staining. Five tissue curls of tumour and normal tissue, cut at 10 microns, were submitted for Next Generation Sequencing to determine baseline mutational status. The average coverage of all the samples were 50-100x and 90% of the target regions covering at 18x or more. Paired end reads were mapped to hg19 reference genome using BWA-MEM. Somatic variants were identified using Mutect2. The primary cancers were classified into 4 molecular subgroups, as per the Proactive Molecular Risk Classifier for Endometrial Cancer (ProMisE).

Results: Out of nine cases identified, 8 had sufficient tissue for molecular analysis of both primary and recurrences/metastases. Four primary carcinomas were classified as MMR-D, one as p53 abnormal, three as p53wild type. No POLE mutations in the P286R, S297F, V411L, and A456P hotspots were identified. PIK3CA or PIK3R1 mutations were present in 4 EEC and their recurrences/metastasis, 2 others showed PIK3CA only in the primary, 1 case had PIK3R1 only in the recurrence/ metastasis.

Patient	MMR	POLE mutated	P53/TP53	Recurrence / metastasis	
				Site	Time to recurrence (months)
1	**Abnormal**	-	wild type	Vaginal vault	8
2	**Abnormal**	-	Primary: p53 IHC null Metastasis: TP53 mutation	Upper vagina	84
3	**Abnormal**	-	wild type	Pelvic lymph node	3
4	**Abnormal**	-	Primary: TP53 mutation Vaginal Metastasis: TP53 mutation	Vaginal vault	44
				Lung	99
5	-	-	Primary: p53 IHC null	Abdomen wall at port site	40
6	-	-	wild type	Posterior vagina	10
7	-	-	wild type	Sigmoid colon	36
8	-	-	wild type	Obturator lymph node	Regional metastases at resection

Conclusions: No POLE mutated tumors were identified, consistent with previous data that such EECs have good prognosis. Discordance of PIK3 between the primary and recurrence/metastasis may warrant routine testing of the latter if PIK3 are shown to be actionable mutations.

1129 Evidence That "Precursor Escape" From the Distal Fallopian Tube is an Important Mechanism For High-Grade Serous Carcinogenesis

Nathan Teschan[1], Thing Rinda Soong[2], Andre Pinto[3], Brooke Howitt[4], Marisa Nucci[5], David Kolin[6], Christopher Crum[6]
[1]Brigham and Women's Hospital, Brookline, MA, [2]University of Washington, Seattle, WA, [3]University of Miami, Miami Beach, FL, [4]Stanford University School of Medicine, Stanford, CA, [5]Brigham and Women's Hospital, Harvard Medical School, Boston, MA, [6]Brigham and Women's Hospital, Boston, MA

Disclosures: Nathan Teschan: None; Thing Rinda Soong: None; Andre Pinto: None; Brooke Howitt: None; Marisa Nucci: None; David Kolin: None; Christopher Crum: None

Background: Extra-uterine high-grade serous carcinoma (HGSC) is the most common and lethal form of "ovarian" epithelial cancer, comprising 70% of ovarian tumors, with a ten-year survival near 20%. A carcinogenic sequence in the distal fallopian tube has been implicated in its pathogenesis. Nearly all early HGSCs discovered incidentally during risk reduction surgery manifest in the fimbria as intraepithelial carcinomas (STICs) which share identical *TP53* mutations. However, only ~20-60% of advanced HGSCs are associated with STICs. Recent searches for an alternate HGSC pathogenic pathway revealed *TP53* mutations in less conspicuous precursors or early serous proliferations (ESPs) including p53 signatures and serous tubal intraepithelial lesions (STILs). It has been recently showed that *TP53* mutations in many ESPs are identical with that in concurrent HGSCs in the absence of STICs, indicating lineage identity between ESPs and HGSCs.The unanswered question was the role of ESPs' potential impact on HGSC development in relation to STICs.

Design: We estimated the frequency of STICs in a large cohort of pelvic HGSC resections and fallopian tubes processed with SEE-FIM protocol, and compared it to the frequency of ESPs identified in a subgroup of STIC-negative fallopian tubes using p53 immunohistochemistry. The relative frequencies of occult STICs and ESPs were further computed in a smaller subset of benign appearing fallopian tubes subject to uniform sectioning. ESPs and STICs were classified using current criteria.

Results: Pathology reports from 515 total pelvic HGSC resections for were reviewed, of which 110 (21%) reported an associated STIC. In a subset of 29 cases without STIC, p53 immunohistochemistry disclosed 11 ESPs (38%). On review of a separate cohort of 21 consecutive uniformly but not exhaustively processed fallopian tubes from HGSCs, occult STICs and ESPs were found in isolation in 6 (28%) and 5 (23%) cases respectively and two cases had both ESP and STIC (9%).

Conclusions: Taking into account the recent discovery that ESPs share lineage markers with concurrent HGSCs in the absence of STIC, and the high prevalence of ESPs in fallopian tubes of women with HGSCs, ESPs deserve attention as an important participant in HGSC development. The mechanism of exfoliation ("precursor escape") and eventual intraperitoneal malignant transformation without an intervening STIC supports a dual model of tubal involvement and informs pathogenesis, prevention, and pathologic classification of this lethal disease.

1130 PBRM1 Expression Is Lost in Small Cell Carcinoma of the Ovary Hypercalcemic Type

Basile Tessier-Cloutier[1], Yemin Wang[1], Shane Colborne[2], Jonathan Zhang[1], Dawn Cochrane[3], Anthony Karnezis[4], Friedrich Kommoss[5], Gregg Morin[6], David Huntsman[7]
[1]University of British Columbia, Vancouver, BC, [2]Genome Science Centre, Vancouver, BC, [3]BC Cancer Agency, Vancouver, BC, [4]UC Davis Medical Center, Sacramento, CA, [5]Institute of Pathology, Friedrichshafen, Germany, Friedrichshafen, Germany, [6]British Columbia Cancer Agency, Vancouver, BC, [7]British Columbia Cancer Research Institute, Vancouver, BC

Disclosures: Basile Tessier-Cloutier: None; Yemin Wang: None; Shane Colborne: None; Jonathan Zhang: None; Dawn Cochrane: None; Anthony Karnezis: None; Friedrich Kommoss: None; Gregg Morin: None; David Huntsman: None

Background: Small cell carcinoma of the ovary hypercalcemic type (SCCOHT), is a lethal malignancy affecting young women and children. Little is known about the origin of this type of tumor but loss of SWI/SNF proteins SMARCA4 and SMARCA2 are well established as part of its pathogenesis. In an effort to further define the expression of SWI/SNF proteins in SCCOHT, we performed comprehensive proteomic analysis using mass spectrometry.

Design: Global proteome analysis was performed on formalin fixed tissue from 6 cases of SCCOHT and compared to 12 tubo-ovarian high grade serous carcinomas and Sertoli-Leydig cell tumors with no known SWI/SNF alterations. The SP3-clinical proteomics protocol was used and the samples analyzed on a ThermoFisher Orbitrap Fusion mass spectrometer. The analytic pipeline included batch effect correction (ComBat) and Protein Expression Control Analysis (PECA). An unsupervised cluster analysis was performed to analyze the expression variance of the 28 known SWI/SNF complex proteins between the tumor types. IHC validation of selected candidates was performed on a TMA containing 22 SCCOHT and 140 epithelial ovarian tumors.

Results: The proteomic analysis identified 7329 proteins; 1230 were significantly enriched in the SCCOHT cohort when compared to the tubo-ovarian tumors having no known SWI/SNF alterations. Enrichment analysis further showed that they are highly enriched for proteins involved in development of neuroepithelium. Based on 28 known SWI/SNF proteins, unsupervised clustering predicted the different histologic subtypes. PECA showed decreased expression of SMARCA4, SMARCA2, and PBRM1 in SCCOHT compared to the other ovarian malignancies ($p<<0.0001$).Using IHC, none of the SCCOHT cases expressed PBRM1, whereas all other tested tumors did.

Conclusions: This is the first report of PBRM1 loss in SCCOHT, an important gene required for the stability of the SWI/SNF subcomplexes. PBRM1 loss has shown potential as an immunotherapy biomarker in renal cell carcinoma; suggesting a potential role for immunotherapy for SCCOHT.

1131 A Proteogenomic Analysis of Transitional Cell Carcinoma, the TCC-Like Variant of Tubo-Ovarian High-Grade Serous Carcinoma

Basile Tessier-Cloutier[1], Dawn Cochrane[2], Anthony Karnezis[3], Shane Colborne[4], Jamie Magrill[5], Aline Talhouk[6], Jonathan Zhang[1], Robert Soslow[7], Gregg Morin[8], Christopher Hughes[9], Anna Piskorz[10], Angela Cheng[11], Kendall Greening[12], Sonja Prader[13], Jacobus Pfisterer[14], C. Blake Gilks[15], Stefan Kommoss[16], James Brenton[10], David Huntsman[17], Friedrich Kommoss[18]
[1]University of British Columbia, Vancouver, BC, [2]BC Cancer Agency, Vancouver, BC, [3]UC Davis Medical Center, Sacramento, CA, [4]Genome Science Centre, Vancouver, BC, [5]OVCARE, Richmond, BC, [6]University of British Columbia and British Columbia Cancer Agency, Vancouver, BC, [7]Memorial Sloan Kettering Cancer Center, New York, NY, [8]British Columbia Cancer Agency, Vancouver, BC, [9]British Columbia Genome Sciences Center, Vancouver, BC, [10]University of Cambridge, Cambridge, United Kingdom, [11]Genetic Pathology Evaluation Centre, Vancouver, BC, [12]Vancouver, BC, [13]Kliniken Essen Mitte, Essen, Germany, [14]Gynecologic Oncology Center, Kiel, Germany, [15]Vancouver General Hospital, Vancouver, BC,[16]Tuebingen University Hospital, Tuebingen, Germany, [17]British Columbia Cancer Research Institute, Vancouver, BC, [18]Institute of Pathology, Friedrichshafen, Germany, Friedrichshafen, Germany

Disclosures: Basile Tessier-Cloutier: None; Dawn Cochrane: None; Anthony Karnezis: None; Shane Colborne: None; Jamie Magrill: None; Aline Talhouk: None; Jonathan Zhang: None; Robert Soslow: *Speaker*, Ebix/Oakstone; Gregg Morin: None; Christopher Hughes: None; Anna Piskorz: None; Angela Cheng: None; Kendall Greening: None; Sonja Prader: None; Jacobus Pfisterer: None; C. Blake Gilks: None; Stefan Kommoss: None; James Brenton: None; David Huntsman: None; Friedrich Kommoss: None

Background: The current WHO classification does not separate transitional carcinoma of the ovary (TCC) from conventional tubo-ovarian high-grade serous carcinoma (HGSC), although some evidence supports better prognosis for TCC. Since the two subtypes show only subtly different immunoprofiles, we sought to compare the global proteomic profiles of conventional HGSC and TCC to identify candidate prognostic proteins enriched in TCC.

Design: Full proteome analysis was performed on archival material from 12 cases each of TCC and HGSC using SP3-proteomics, run on a ThermoFisher Orbitrap Fusion mass spectrometer. The protein expression was clustered and used for pathway analysis. For comparison, a mutation panel was performed on 71 TCC. Validation of single biomarker candidates was performed using tissue microarrays of TCC (n=130) and HGSC (n=277). Survival analysis was performed with a series of 14 pure and mixed TCC.

Results: We identified 1220 proteins that were significantly enriched in TCC versus HGSC. Unsupervised co-clustering successfully separated TCC from HGSC based on protein expression while, based on DNA sequencing analysis, mutation profiles were similar. Pathway analysis showed that cell death, necrosis, and apoptosis were upregulated in TCCs, while DNA homologous recombination, cell mitosis, proliferation and survival, and cell cycle progression were upregulated in HGSC. Survival analysis trended towards better prognosis in pure TCCs (p=0.089) compared to mixed TCC. From the proteomic analysis two biomarkers were selected for validation by IHC, claudin-4 and ubiquitin carboxyl-terminal esterase L1 (UCHL1). As predicted, the IHC expression for those proteins was stronger in TCC (p<0.0001) compared to HGSC.

Conclusions: Proteomic analysis showed differing protein profiles for TCC and HGSC, despite having similar mutation spectrums. The prognostic value of the TCC morphology is still unclear but the potential to predict homologous recombination status would be extremely valuable to help plan management. This study demonstrates that global proteomic analysis on archival pathology tissue is a valid approach to identify potential prognostic biomarkers.

1132 Aggressive Uterine Inflammatory Myofibroblastic Tumors Have Pathogenic Molecular Alterations in Addition to ALK Fusions

Nicole Therrien[1], Nicholas Ladwig[1], Walter Devine[2], Gregory Bean[3], Karuna Garg[4], Sarah Umetsu[4]
[1]San Francisco, CA, [2]University of California, San Francisco, Berkeley, CA, [3]Stanford University School of Medicine, Stanford, CA, [4]University of California, San Francisco, San Francisco, CA

Disclosures: Nicole Therrien: None; Nicholas Ladwig: None; Walter Devine: None; Gregory Bean: None; Karuna Garg: None; Sarah Umetsu: None

Background: Inflammatory myofibroblastic tumor (IMT) of the uterus is a rare and under-recognized mesenchymal tumor which frequently contains *ALK* gene fusions. IMTs generally behave as benign or locally recurrent tumors. However, a subset of uterine IMTs demonstrate an aggressive clinical course with a high stage at presentation including multiple metastases. Although the morphologic features of clinically aggressive IMT have been reported in the literature, no molecular underpinnings have been identified in these cases. The aim of this study is to analyze the clinical and histopathologic findings in aggressive uterine IMTs and to identify additional pathogenic molecular alterations in these cases which may help to predict outcome.

Design: Review of our archives identified 3 cases of aggressive uterine IMT with metastases. Histologic features were reviewed and clinical data was obtained from the electronic medical record and the California cancer registry database. Immunohistochemistry (IHC) for ALK was performed on all cases. Genomic DNA was purified from formalin-fixed, paraffin-embedded tumor and normal tissue from 3 patients and capture based next-generation sequencing targeting 479 cancer genes was performed.

Results: All patients had widely metastatic IMT, underwent multiple surgeries with adjuvant chemotherapy, and continued to have persistent disease post-therapy (Table 1). ALK IHC was positive in all cases. In addition to ALK fusions, one or more pathogenic mutations were identified in all three cases. Case 1 showed a *TP53* missense mutation, Case 2 showed nonsense mutations in *NF2* and *RAD50*, and Case 3 contained deep deletions in *NF1, CDKN2A/B* and *CDKN2C*. In Case 3, both the primary uterine tumor and the metastasis (identified 6 years after initial diagnosis) were sequenced, and both showed deep deletions in *CDKN2A/B* and *CDKN2C.* The metastasis additionally contained a deep deletion in *NF1.*

	Case No. 1	Case No. 2	Case No. 3
Age at diagnosis (yr)	50	55	57
Uterine tumor size (cm)	12	-- (morcellated)	12 (from imaging)
Histologic pattern	Fascicular	Fascicular	Fascicular and hyalinized
Myxoid background	Not present (present in metastases)	Present	Present
Nuclear atypia	Moderate	Mild-to-marked	Moderate
Necrosis	Present (tumor-type)	Present (tumor-type)	Present (tumor-type)
Mitoses per 10 HPF	5	11	5
Tumor border	Infiltrative	Infiltrative	Infiltrative
Treatment	Multiple surgeries, chemotherapy, radiation	Multiple surgeries, chemotherapy	Multiple surgeries, chemotherapy, ALK-inhibitor (first crizotinib, now brigatinib),VEGF-A inhibitor (bevacizumab)
Metastasis (number and location)	4 (Paraspinal, left lung, right lung, and hilum)	8 (7 intraperitoneal and 1 lung)	At least 21: All intraperitoneal
Time from diagnosis to metastasis	Present at diagnosis (paraspinal)	Two months (intraperitoneal)	Three months (intraperitoneal)
Clinical follow-up	Alive with disease (stable partially necrotic paraspinal mass) 8 years and seven months after diagnosis No current treatment	Died with widely metastatic disease 12 months after diagnosis	Alive with disease 7 years and 3 months after diagnosis Currently receiving treatment
Pathogenic Molecular Alterations	*ALK1-IGFBP5*fusion *TP53* missense mutation	*ALK1-FN1* fusion *NF2* and *RAD50*nonsense mutations	*ALK1-NRP2* fusion *CDKN2A/B*, *CDKN2C*, and *NF1* deep deletions

Conclusions: In our study, aggressive uterine IMTs contained pathogenic molecular alterations in addition to *ALK* fusions. These findings may explain the malignant histologic features and aggressive clinical behavior seen in this subset of uterine IMTs. Knowledge of additional pathogenic mutations in IMT at time of resection may identify tumors with metastatic potential and help guide clinical management.

1133 Use of p53 as an Ancillary Tool for the Assessment of Margin Status in Cases of Differentiated Vulvar Intraepithelial Neoplasia (dVIN) and HPV (human papillomavirus)-independent Squamous Cell Carcinoma (SCC) of the Vulva

Emily Thompson[1], Giorgia Trevisan[2], Richard Wong[3], Basile Tessier-Cloutier[4], Anthony Karnezis[5], Naveena Singh[2], C. Blake Gilks[6], Lynn Hoang[4]

[1]Vancouver General Hospital/University of British Columbia, Vancouver, BC, [2]Barts Health NHS Trust, London, United Kingdom, [3]Pamela Youde Nethersole Eastern Hospital, Hong Kong, Hong Kong SAR, [4]University of British Columbia, Vancouver, BC, [5]UC Davis Medical Center, Sacramento, CA, [6]Vancouver General Hospital, Vancouver, BC

Disclosures: Emily Thompson: None; Giorgia Trevisan: None; Richard Wong: None; Basile Tessier-Cloutier: None; Anthony Karnezis: None; Naveena Singh: None; C. Blake Gilks: None; Lynn Hoang: None

Background: Our group has previously found that p53 immunohistochemistry (IHC) is a useful tool for detecting histologically under-recognized dVIN and can change margin status from negative to positive in 31% of cases (PMID: 25025443). Abnormal p53 is typically found in dVIN, but can also be found in the adjacent histologically normal skin (akin to a p53 signature). The clinical significance of finding a p53 signature at the margins of a vulvectomy is uncertain. The goals of this study were to 1) reaffirm the rates of margin status change using p53 IHC in a larger cohort and 2) determine the impact of abnormal p53 at margins on disease recurrence.

Design: Vulvectomy specimens containing p16-negative SCC +/- adjacent dVIN and margins originally reported as negative by at least 5 mm (for both invasive and in-situ disease) were included. Selected sections of closest margins were stained with p53 and scored as wild-type, overexpression or null. Abnormal p53 at margin was then compared to recurrence rates.

Results: Forty cases of vulvar SCC were included, 29 had adjacent dVIN. Patients were on average 76 years of age (range: 46-95 years) and were predominantly FIGO stage IB (IA=1, IB=24, II=0, III=13, unknown=2). Abnormal p53 staining was seen in 35/40 (88%) vulvar SCC (Table 1). One vulvar SCC had overexpression of p53 and two adjacent areas of dVIN (one showing overexpression and the other showing a null-pattern).

Table 1. Patterns of p53 expression in vulvar SCC and dVIN.

	Overexpressed	Null	Null & overexpressed	Wild type
SCC n=40	30 (75%)	5 (12.5%)	0 (0%)	5 (12.5%)
dVIN n=29	19 (65.5%)	4 (13.7%)	1 (0.3%)	5 (17.2%)

Figure 1 - 1133

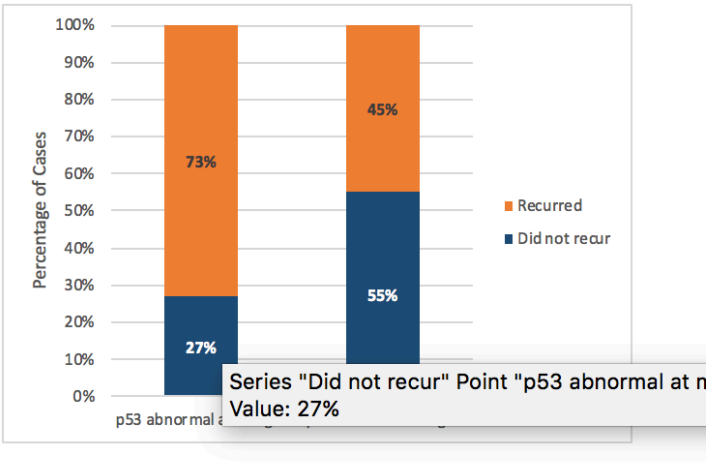

Figure 1. p53 Status at Vulvectomy Margin and Risk of Recurrence (p=0.16).

Conclusions: p53 is a useful adjunct for detecting histologically under-recognized dVIN and changes margin status in 28% of cases. The finding of a p53 abnormality at the margins of a vulvectomy (either in dVIN or as a p53 signature) correlated with worse local recurrence rates, but this was not statistically significant in our series. Patients diagnosed before the age of 55 did have higher recurrence rates, which was statistically significant.

1134 Trends in the Diagnosis of Vulvar Intraepithelial Neoplasia (VIN) over Time

Emily Thompson[1], Evan Gibbard[2], Ardalan Akbari[3], C. Blake Gilks[4], Lynn Hoang[3]
[1]Vancouver General Hospital/University of British Columbia, Vancouver, BC, [2]BC Cancer, Vancouver, BC, [3]University of British Columbia, Vancouver, BC, [4]Vancouver General Hospital, Vancouver, BC

Disclosures: Emily Thompson: None; Evan Gibbard: None; Ardalan Akbari: None; C. Blake Gilks: None; Lynn Hoang: None

Background: Vulvar squamous cell carcinoma (VSCC) arises from two main etiopathologic pathways, one path is driven by human papillomavirus (HPV) infection and the path occurs independently of HPV. The precursor lesions to VSCC corresponding to these two main pathways are termed usual-type VIN (uVIN) and differentiated-type VIN (dVIN), respectively. The diagnosis of dVIN is notoriously difficult, but increased awareness has been brought to this entity. Our main goal was to explore the trends of dVIN diagnosis over time at our large tertiary-care center.

Design: The institutional pathology archive was searched for first time diagnoses of invasive SCC of the vulva made between the years 2013-2017. The presence of adjacent vulvar intraepithelial neoplasia and its type (uVIN, dVIN, not otherwise specified (NOS) and not present) were recorded. Trends in VIN diagnoses were examined over the 5 year period. In addition, various clinicopathologic parameters were compared between patients with VSCC associated with dVIN to those with VSCC associated with uVIN.

Results: A total of 103 patients were identified; 36 (34.9%) were associated with uVIN, 49 (47.6%) were associated with dVIN, 3 (2.9%) were associated with VIN NOS and 15 (14.6%) did not have any adjacent in-situ lesion (Figure 1). The diagnosis of dVIN was made increasingly over time, while the diagnosis of VIN NOS and no in situ lesion both decreased over the same period (Figure 1). The categorization of VIN was based mostly on histologic examination. In 51.4% of cases ancillary immunohistochemistry (IHC, either p16 or p53) was performed. The use of IHC did increase over the 5 year period (Table 1).

When comparing, dVIN associated VSCC to uVIN associated VSCC, the former presented at an older age (72 vs 65 years, p=0.010), presented at higher stage (p=0.05), were more likely to have lichen sclerosus (67% vs 6%, p=0.0001) and more likely to have lymph node metastases (50% vs 7%, p=0.0003). There was no difference in lymphovascular invasion (11% vs 13%, p=0.74), perineural invasion (11% vs 8%, p=0.73), margin involvement (28% vs 20%, p=0.44) or recurrence (31% vs 25%, p=0.62).

	Use of p16 IHC	Use of p53 IHC	Cases with ICH use (%)
2013	1	0	1/11 (9%)
2014	9	2	9/22 (41%)
2015	9	1	9/25 (36%)
2016	16	0	16/23 (70%)
2017	17	6	18/23 (78%)

Table 1. VSCC and use of ancillary IHC testing with p16 and p53 over time.

Figure 1 - 1134

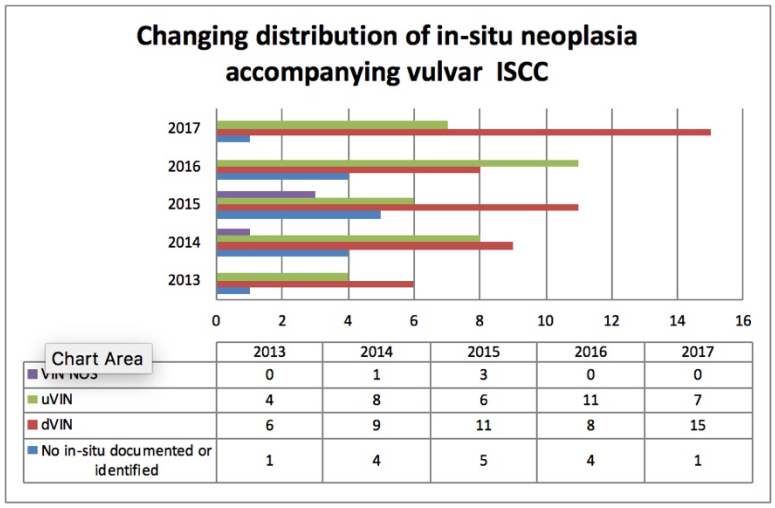

Figure 1. Distribution of VIN diagnoses accompanying vulvar invasive squamous cell carcinoma (ISCC) over time.

Conclusions: Over a 5 year period, there was increased awareness and diagnosis of dVIN at our institution and a correspondingly reduced number of unclassified and under-recognized VIN. dVIN associated VSCC also correlated with older age at presentation, higher stage and metastatic disease to lymph nodes.

1135 Histopathologic Findings in Placentas from Women with Advanced Maternal Age

Vanda Torous[1], Drucilla Roberts[1]
[1]Massachusetts General Hospital, Boston, MA

Disclosures: Vanda Torous: None; Drucilla Roberts: None

Background: Advanced maternal age (AMA), defined as maternal age greater or equal to 35 years at childbirth, has been increasing. It has been associated with a number of adverse maternal and fetal outcomes, including low birth weight, pre-term birth, and stillbirth/unexplained fetal death. While studies have investigated the impact of AMA on pregnancy outcomes, to date few studies have detailed the histopathologic findings in the placentas from these women.

Design: A retrospective review of our institutional pathology archives was conducted to identify placenta specimens from women with a clinical history of advanced maternal age. A total of 127 cases were identified between August 2008 and August 2018. The findings were evaluated overall, as well as subdivided further into two subgroups: age 35-39 years and age > 40 years.

Results: The median patient age was 39 years (range 35-51). Overall, 6% of cases had no histologic findings and 28% had no or only one minor histologic finding; this was not statistically significant between the two subgroups. There were 3 cases of fetal demise. 11% (14/127) had preterm pregnancies (delivering before 37 weeks gestational age). About 30% of placentas from AMA women were found to weigh less than the 10th percentile for gestational age, which was similar for both subgroups. The most common histologic finding for both subgroups was the presence of meconium (44% overall); however, this was only minimal to mild in most cases. Another frequent finding was chorangiosis, which was found in about a third of cases overall. Chorioamnionitis was identified in 27% of cases overall, and notably was found more significantly in those of the 35-39 age group (38.5% vs 14.5%, p=0.02). Additional histologic findings included villitis of unknown etiology (VUE) in 21% of cases, intervillous thrombi in 20.5%, infarcts in 14%, fetal vascular malperfusion in 9%, chronic deciduitis in 8%, and decidual arteriopathy in 3% (Table 1).

	Overall	35-39 years	>40 years	P-value
	N=127	N=65	N=62	
Preterm pregnancy	14 (11.0%)	9 (13.8%)	5 (8.1%)	NS
Placenta Size				NS
<10th percentile	38 (29.9%)	20 (30.7%)	18 (29.0%)	
11-25th percentile	29 (22.8%)	11 (16.9%)	18 (29.0%)	
26-50th percentile	25 (19.7%)	18 (27.7%)	7 (11.3%)	
>51st percentile	35 (27.6%)	16 (24.6%)	19 (30.6%)	
Meconium	56 (44.1%)	29 (44.6%)	27 (43.5%)	NS
Minimal to Mild	53 (41.7%)	27 (41.5%)	26 (41.9%)	
Moderate to Severe	3 (2.4%)	2 (3.1%)	1 (1.6%)	
Chorangiosis	41 (32.2%)	19 (29.2%)	22 (35.5%)	NS
Acute Chorioamnionitis				p=0.02
Maternal response	34 (26.8%)	25 (38.5%)	9 (14.5%)	
Minimal to Mild	21 (16.5%)	17 (26.2%)	4 (6.5%)	
Moderate to Severe	13 (10.2%)	8 (12.3%)	5 (8.0%)	
Acute Chorioamnionitis				NS
Fetal response	14 (11.0%)	9 (13.8%)	5 (8.1%)	
Minimal to Mild	9 (7.1%)	8 (12.3%)	1 (1.6%)	
Moderate to Severe	5 (3.9%)	1 (1.5%)	4 (6.5%)	
Villitis of unknown etiology	27 (21.3%)	13 (20.0%)	14 (22.6%)	NS
Minimal to Mild	18 (14.2%)	9 (13.8%)	9 (14.5%)	
Moderate to Severe	9 (7.1%)	4 (6.2%)	5 (8.1%)	
Intervillous Thrombi	26 (20.5%)	10 (15.4%)	16 (25.8%)	NS
Single	19 (15.0%)	6 (9.2%)	13 (21.0%)	
Multiple	7 (5.5%)	4 (6.2%)	3 (4.8%)	
Infarct	18 (14.2%)	11 (16.9%)	7 (11.3%)	NS
Single	11 (8.7%)	8 (12.3%)	3 (4.8%)	
Multiple	7 (5.5%)	3 (4.6%)	4 (6.5%)	
Fetal vascular malperfusion	12 (9.4%)	4 (6.2%)	8 (12.9%)	NS
Low-grade/Avascular villi only	10 (7.9%)	2 (3.1%)	8 (12.9%)	
High-grade	2 (1.5%)	2 (3.1%)	0 (0%)	
Deciduitis	10 (7.9%)	6 (9.2%)	4 (6.5%)	NS
Decidual Arteriopathy	4 (3.1%)	1 (1.5%)	3 (4.8%)	NS

Conclusions: The aim of this study was to perform an in-depth assessment of the histopathologic findings in the placentas of AMA women to investigate if there are any underlying trends in placentas from these women. The rate of meconium deposition, chorangiosis, and VUE were all higher than those published in the literature for term pregnancies overall (10-15%, 1-2%, and 5-15%, respectively). Thus, there appear to be histopathologic findings in the placentas of AMA women which could correlate with the reported increased adverse maternal and perinatal outcomes.

1136 PNL2 is a Superior Biomarker to MelanA and CathepsinK in the Diagnosis of Uterine PEComa

Aida Valencia-Guerrero[1], Andre Pinto[2], Giorgia Trevisan[3], William Anderson[4], Marisa Nucci[4], Michelle Hirsch[1]
[1]Brigham and Women's Hospital, Boston, MA, [2]University of Miami, Miami Beach, FL, [3]Barts Health NHS Trust, London, United Kingdom, [4]Brigham and Women's Hospital, Harvard Medical School, Boston, MA

Disclosures: Aida Valencia-Guerrero: None; Andre Pinto: None; Giorgia Trevisan: None; William Anderson: None; Marisa Nucci: None; Michelle Hirsch: None

Background: Perivascular epithelioid cell tumors (PEComa) are rare mesenchymal neoplasms characterized by co-expression of melanocytic and muscle markers. Traditionally, HMB45 and Melan-A are the melanocytic markers employed to confirm the diagnosis; however, both markers may only show focal expression, and sensitivity is low for Melan-A. PNL2 is a sensitive biomarker for epithelioid melanoma and has been shown to be a more reliable marker in recognizing AMLs and PEComas of the kidney. The objective of this study was to determine the utility of PNL2 in distinguishing uterine PEComa and its potential mimics, most notably smooth muscle tumors.

Design: A total of 17 uterine PEComas (8 malignant) and 31 smooth muscle tumors (SMTs), including 8 leiomyomas, 20 leiomyosarcomas (LMS; 13 spindled, 7 epithelioid), and 3 SMTs of uncertain malignant potential (STUMP), were analyzed for PNL2, HMB45, Melan-A, CathepsinK, Desmin and Caldesmon expression. Cases were scored as negative (0), focal (1+, <10%), patchy (2+, 10-50%), or diffuse (3+, >50%). P values were calculated using Fisher's Exact test.

Results: PEComas were positive for HMB45, Melan-A, PNL2 and CathepsinK in 100%, 60%, 82% and 100% of cases, respectively. 9/14 (64%) PNL2 positive PEComas showed patchy to diffuse (2+/3+) PNL2 staining, whereas only 2 of all 31 (6.5%) SMTs (2 LMSs) showed focal (1+) reactivity for this marker (p=<0.0001). In 56% of PEComas, PNL2 stained more extensively when compared to Melan-A. CathepsinK was strongly and diffusely positive in 91% of SMTs, particularly in epithelioid LMSs. HMB45 was focally (1+) positive in one SMT; all SMTs were negative for Melan-A. Desmin was positive in 87% of PEComas and 95% of SMTs, while Caldesmon was positive in 72% and 78% of these cases, respectively.

Conclusions: PNL2 appears to be a useful biomarker for the diagnosis of uterine PEComas, with comparable sensitivity and specificity to HMB45. PNL2 is superior to Melan-A in sensitivity and ease of interpretation as it typically demonstrates more extensive staining. CathepsinK appears to be of little utility excluding PEComa's potential mimics; however, it is highly sensitive, and lack of staining argues against PEComa. Desmin and Caldesmon stain both PEComas and SMTs similarly. PNL2 should be used in conjunction with HMB45 instead of Melan A in the diagnosis of PEComas of the uterine corpus.

1137 The Potential Role of CDKN2A gene in Invasive Serous Carcinoma Arising from Serous Borderline Tumor

Sonia Veran-Taguibao[1], Nahideh Haghighu[2], Ifegwu Ibe[3], Di Lu[4], Nicolas Gallegos[4]
[1]University of California Irvine Medical Center, Orange, CA, [2]University of California, Irvine, Mission Viejo, CA, [3]University of California, Irvine, Santa Ana, CA, [4]University of California, Irvine, Orange, CA

Disclosures: Sonia Veran-Taguibao: None' Nahideh Haghighu: None; Ifegwu Ibe: None; Di Lu: None; Nicolas Gallegos: None

Background: Chromosome 9p21.3 houses Cyclin-dependent kinase Inhibitor 2A gene (CDKN2A), a tumor suppressor gene linked to multiple tumor types including ovarian carcinoma. This gene acts as a checkpoint and maintains tumor cell senescence while the deletion of this gene will assist tumor cells in entering an oncogenic state through the mutated KRAS/BRAF pathway leading to tumor immortality. In this study, we aimed to evaluate the CDKN2A gene and its role in invasive serous carcinoma arising from serous borderline tumor (SBT).

Design: We have gathered 47 SBT cases from 2014 to 2018 from the medical center archives. Eight cases of SBT with an invasive component were used in the study. DNA was isolated from the formalin-fixed paraffin-embedded (FFPE) tissues using a GeneRead DNA FFPE Kit (Qiagen, GmbH). The targeted NGS libraries were prepared from 400 ng of DNA per sample, using the ArcherDX VariantPlex 65 Solid Tumor (SK0111) panel. The resulting libraries were sequenced on an Illumina MiSeq instrument using v2 chemistry. The FASTQ data files were analyzed on ArcherDX Suite Analysis software (v. 6.0) to identify SNPs, Indels, structural rearrangements, and Copy Number Variations.

Results: Our study yielded no deletion or mutation in the CDKN2A gene region spanning from 21,967,751 to 21,994,490 bp in contrast to our control (Figure 1). Four samples showed KRAS/BRAF mutations. Other mutations detected were TP53, KDR, and APC.

Figure 1 - 1137

Figure 2 - 1137

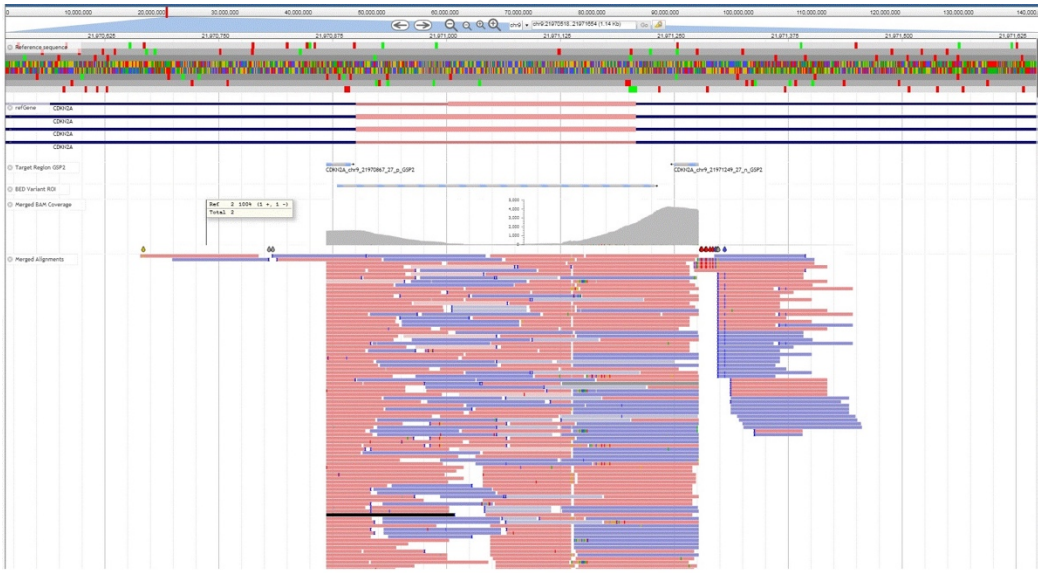

Conclusions: Review of literature suggests that retained CDKN2A gene may suppress the development of SBT to invasive serous carcinoma. In our study, the retained CDKN2A gene (Figure 2) did not interfere with the evolution of SBT to an invasive carcinoma. This suggests that there might be other genes that are involved in this transformation. Also, possible recruitment of more cases might provide more statistical significance. Future exploration of the mechanism of transformation from SBT to invasive serous carcinoma should be pursued.

1138 Identification of Possible Lynch Syndrome in Endometrial Carcinomas at a Public Hospital in South Africa

Reubina Wadee[1], Wayne Grayson[1]
[1]*University of the Witwatersrand, Johannesburg, South Africa*

Disclosures: Reubina Wadee: None; Wayne Grayson: None

Background: Endometrial carcinoma is a common malignancy with an increasing occurrence noted worldwide. Microsatellite instability (MSI) is commonly identified in endometrioid endometrial carcinomas (EECs) and in most Lynch Syndrome (LS) associated tumors. We aimed to identify the number of EECs seen in at a public hospital in South Africa, diagnosed by immunohistochemistry for the 4 mismatch repair stains, which may suggest possible LS, for the period 2009-2015.

Design: Once ethical clearance was obtained, 145 cases of archived EEC were identified and retrieved at our institution, all of which underwent immunohistochemical mismatch repair testing for 4 antibodies, namely MLH1, MSH2, MSH6 and PMS2. The cases that were negative for MLH1 were subjected to EpiTYPER for quantitative methylation of the MLH1 promoter region using the Agena MassARRAY® platform.

Results: A total of 41 (28.28%) cases showed complete negativity of tumor nuclei for one or more immunohistochemical stains in the presence of adequate internal controls such as positive staining of endothelial cells. Twenty cases (13.79%) showed negativity for MLH1 and PMS2, 16 cases (11.03%) demonstrated isolated MLH1 negativity and a single case (0.69%) was negative for MLH1, PMS2 and MSH6. Two cases showed isolated MSH6 negativity and 2 cases were negative for both MSH2 and MSH6. Of the 37 MLH1 negative cases that underwent hypermethylation analysis, 1 case had insufficient DNA for further analysis, 30 (83.33%) cases demonstrated methylation levels of more than 10% whilst 6 cases (16.67%) had very low levels of methylation and were not regarded as being methylated.

Conclusions: A total of 41 cases demonstrated microsatellite instability by immunohistochemistry, of which 37 (90.24%) showed loss of MLH1. The majority (83.33%) of the MLH1 negative cases showed evidence of promoter hypermethylation, thus pointing toward a sporadic occurrence of carcinogenesis. The patients from whom the 2 cases with isolated MSH6 mutation, 2 cases with MSH2 and MSH6 mutation, in addition to the 6 cases whereby MLH1 negativity was not explained by methylation will be identified and offered genetic counselling with the view to possible germline mutational analysis as these patients are suspected of having Lynch Syndrome. Thus, our study demonstrates a possible 10 out of 145 (6.90%) of patients who may have Lynch Syndrome and require further testing.

1139 SATB2 Demonstrates Superior Accuracy and PAX8 Superior Specificity in Differentiating Primary Ovarian Mucinous Neoplasm from Lower Gastrointestinal Metastasis Comparing to Traditional Markers

Linyuan Wang[1], Nicola Meagher[2], Oliver Bathe[1], Xianyong Gui[3], Susan Ramus[4], Martin Kobel[1]
[1]University of Calgary, Calgary, AB, [2]University of NSW Sydney, Sydney, NSW, Australia, [3]University of Washington Medical Center, Seattle, WA, [4]University of New South Wales, Sydney, NSW, Australia

Disclosures: Linyuan Wang: None; Nicola Meagher: None; Oliver Bathe: None; Xianyong Gui: None; Susan Ramus: None; Martin Kobel: None

Background: Primary ovarian mucinous tumors can be difficult to distinguish from metastatic gastrointestinal neoplasms by histology alone. This study aimed to refine the classification of mucinous tumors within the Ovarian Tumor Tissue Analysis (OTTA) using novel immunohistochemical markers SATB2 and PAX8, and compare them to the conventional markers (CK7, CK20 and CDX2).

Design: The cohort included 144 ovarian mucinous tumors (77 mucinous carcinomas and 67 mucinous borderline tumors) and 245 lower gastrointestinal neoplasms (133 stage II colorectal adenocarcinomas, 40 appendiceal goblet cell carcinoids, 24 low-grade appendiceal mucinous neoplasms/LAMNs, 22 appendiceal carcinoids, 14 high-grade appendiceal mucinous neoplasms/carcinomas and 12 non-mucinous appendiceal adenocarcinomas). All were assessed for SATB2, PAX8, CK7, CK20 and CDX2 immunohistochemistry on tissue microarrays. Positivity was defined as expression in 1% of tumor cells.

Results: The sensitivity, specificity and accuracy for distinguishing ovarian mucinous tumors from lower gastrointestinal neoplasms are 97.1%, 80.7% and 86.7% for CK7; and 36.8%, 97.9%, 75.1% for PAX8. The sensitivity, specificity and accuracy for distinguishing lower gastrointestinal neoplasms from ovarian mucinous tumors are 90.1%, 86.7% and 88.8% for SATB2; 97.9%, 16.6%, and 68.2% for CDX2; 86.9%, 20.1% and 63.0% for CK20.

Conclusions: CDX2 and CK20 have limited specificity for identifying lower gastrointestinal neoplasms and should not be used. SATB2 and CK7 show the highest accuracy in the distinguishing primary ovarian mucinous tumors from lower gastrointestinal neoplasms. The addition of PAX8 is recommended due to its high specificity for ovarian mucinous tumors.

1140 Metal Regulatory Transcription Factor 1 (MTF1): Essential Role in Ovarian Cancer Metastasis and A Poor Clinical Prognostic Molecular Marker

Yaohong Wang[1], Guannan Zhao[1], Yongchao Li[1], Shuyu E[1], Jatin Gandhi[1], Adel Abdallah[1], Jacob Abel[1], Ali Saad[2], Jie Zhang[1], Ian Clark[1], Robins David[3], Junming Yue[1], Mahul Amin[3]
[1]University of Tennessee Health Science Center, Memphis, TN, [2]Methodist/LeBonheur Health System, Memphis, TN, [3]Methodist University Hospital, Memphis, TN

Disclosures: Yaohong Wang: None; Guannan Zhao: None; Yongchao Li: None; Shuyu E: None; Jatin Gandhi: None; Adel Abdallah: None; Jacob Abel: None; Ali Saad: None; Jie Zhang: None; Ian Clark: None; Robins David: None; Junming Yue: None

Background: High-grade ovarian cancer has one of the worst prognoses among gynecological tumors due to the high frequency of peritoneal metastasis and recurrence. Metal regulatory transcription factor 1 (MTF1) is a zinc finger transcription factor which is activated

by zinc and promotes cell survival and migration by further activating downstream target genes. Ratio of serum copper versus zinc have been long-used as a biomarker for ovarian cancer diagnosis together with CA125. MTF1 is upregulated in certain human cancers, including breast, lung and cervical cancers. However, role of MTF1 in ovarian cancer is largely unknown.

Design: Oncomine database and Human Protein Atlas Program were used for gene expression profiling of human MTF1 expression. An orthotopic ovarian cancer mouse model was used for assessment of in-vivo primary tumor growth and metastasis. MTF 1 knockout SKOV3 ovarian carcinoma cells were generated by lentiviral CRISPR/Cas9 nickase vector. A cell invasion assay was performed by the matrigel transwell system. Immunodeficient NSG female mice were intra-bursally xenografted with MTF1 knockout SKOV3 and control cells. Tissue selections of patients with ovarian serous carcinoma from Methodist University Hospital and West Cancer Center were stained with MTF1, PCNA, CA-125, WT-1, P53 and Pax 8.

Results: Gene expression profiling from Oncomine database shows MTF1 mRNA expression was significantly increased ($p < 0.01$) in ovarian serous carcinoma ($n = 185$) compared with control normal ovary surface epithelium ($n = 10$). High MTF1 mRNA expression is correlated with poor patient survival based on Human Protein Atlas Program ($p < 0.01$). Knockout of MTF1 resulted in the inhibition of primary tumor growth and metastasis in an orthotopic ovarian cancer mouse model. Immunostaining showed increased MTF1 expression in ovarian cancer patients. Further clinical data analysis showed that high MTF1 expression was associated with advanced surgical stage, higher tumor grade, deeper invasion, increased lymph node metastases, more disease relapse and poor patient survival.

Conclusions: In current study, we report for the first time that MTF1 expression is significantly upregulated in ovarian cancer, and its high expression is an overall poor prognostic indicator. Our studies further demonstrate that MTF1 plays an essential role on ovarian tumor invasion and metastasis. MTF1 may be a novel biomarker for early diagnosis, risk stratification, prognostic evaluation as well as a drug target for clinical therapy.

1141 Next Generation Sequencing in Endometrial Hyperplasia: Profiles of Cases that Resolve vs Those that Progress to Endometrioid Adenocarcinoma

Joshua Warrick[1], Mariano Russo[2], James Broach[2], Joshua Kesterson[3], Carrie Hossler[3], Jennifer Rosenberg[2], Jordan Newell[3]
[1]Hershey, PA, [2]Penn State Health Hershey Medical Center, Hershey, PA, [3]Penn State Health, Hershey, PA

Disclosures: Joshua Warrick: None; Mariano Russo: None; James Broach: None; Joshua Kesterson: None; Carrie Hossler: None; Jennifer Rosenberg: None; Jordan Newell: None

Background: The endometrioid type of endometrial adenocarcinoma arises from endometrial intraepithelial neoplasia (EIN; synonymous with atypical hyperplasia per current WHO manual). This arises from non-atypical endometrial hyperplasia, a process driven by unopposed estrogens. We set out to determine if DNA sequencing can gauge cancer risk in endometrial hyperplasia.

Design: The study employed a retrospective, case-control design. Cases included 15 samples of hyperplasia (all atypical hyperplasia/EIN), diagnosed on biopsy, in women subsequently diagnosed with endometrioid adenocarcinoma, hereafter termed "progressing hyperplasia." Controls included 14 cases of hyperplasia (3 atypical hyperplasia/EIN, 11 non-atypical hyperplasia), diagnosed on biopsy, treated conservatively, and followed for at least two years, hereafter termed "resolving hyperplasia." DNA was extracted from biopsy material (formalin fixed, paraffin embedded), after macrodissecting areas of interest, using the Ion Torrent platform and targeted sequencing libraries generated from the Ion Ampliseq Comprehensive Cancer Panel, along with a small custom panel. All samples were resequenced with the same approach for validation.

Results: Mutational burden was greater in progressing hyperplasia than resolving hyperplasia (mean 15 vs 5; Figure 1). Mutational profiles differed between progressing and resolving hyperplasias, but there was great overlap. Progressing hyperplasias demonstrated mutational profiles similar to endometrioid adenocarcinoma, with frequent mutatations in PIK3CA (53% of cases), ARID1A (33%), KRAS (20%), PIK3R1 (13%), FGFR2 (40%), and PTEN (60%). Resolving hyperplasias similarly demonstrated frequent mutations in PTEN (36% of cases) and FGFR2 (21%). One resolving hyperplasia, morphologically considered non-atypical hyperplasia, harbored an activating PIK3CA mutation, and another an activating KRAS mutation. No resolving hyperplasia had an ARID1A mutation.

Figure 1 - 1141

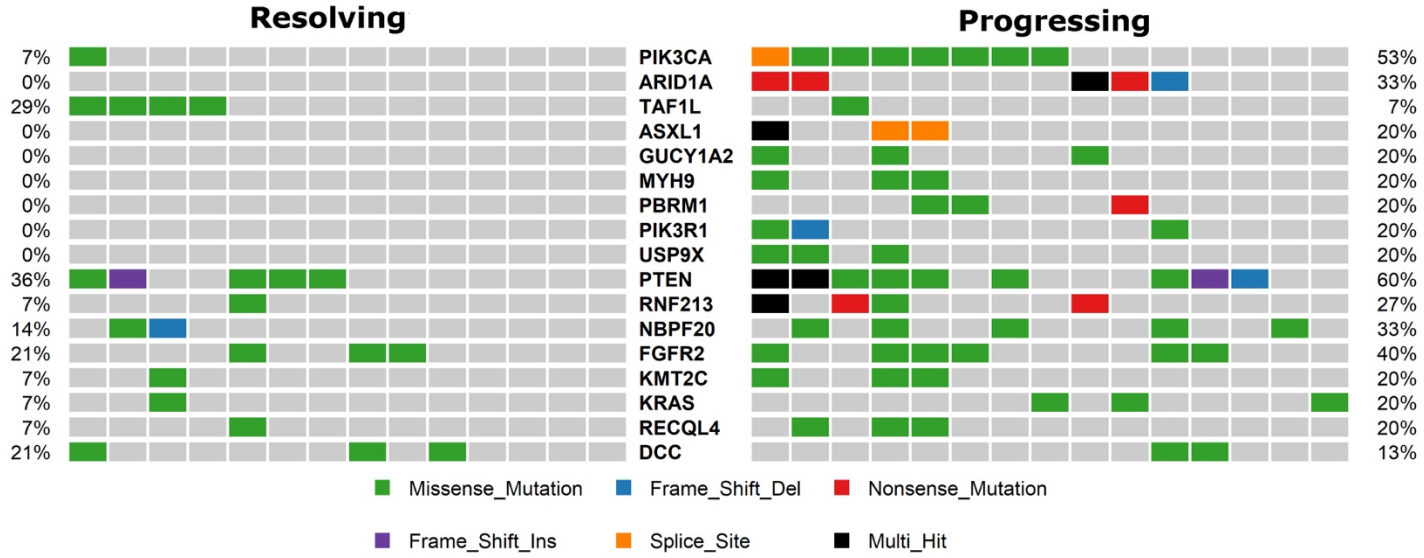

Conclusions: While mutational burden tended to be higher in progressing hyperplasia compared to resolving hyperplasia, the overlap in specific genes mutated, and the overlap in mutational burden, indicate next generation sequencing lacks sufficient predictive power to gauge cancer risk in endometrial hyperplasia. However, the findings provide insight into the evolution of endometrial hyperplasia to adenocarcinoma, by indicating oncogenes and tumor suppressor genes are mutated early in endometrial hyperplasia, before atypical hyperplasia/EIN is identifiable.

1142 Beta Catenin Expression in Benign and Premalignant Lesions of the Endometrium

Jaclyn Watkins[1], Mirna Podoll[1], Charles Quick[2], Sarah Fitzlaff[3], Martha Wright[1]
[1]Vanderbilt University Medical Center, Nashville, TN, [2]University of Arkansas for Medical Sciences, Little Rock, AR, [3]Vanderbilt University School of Medicine, Nashville, TN

Disclosures: Jaclyn Watkins: None; Mirna Podoll: None; Charles Quick: None; Sarah Fitzlaff: None; Martha Wright: None

Background: Beta catenin mutations in endometrial cancer have been linked to poorer outcomes. However, beta catenin expression has only been minimally explored in benign endometrial lesions (e.g., squamous morular metaplasia (SMM)), benign hyperplasia (BH), and precancerous lesions (e.g., endometrial intraepithelial neoplasia (EIN), focal glandular crowding (FCG) sub-diagnostic of EIN, and atypical polypoid adenomyoma (APA)).

Design: The Vanderbilt University Medical Center pathology archives were searched for cases of SMM, APA, and FGC (biopsy or hysterectomy) occurring between 1999 and 2014. Cases were re-reviewed for diagnosis on H&E and re-classified as either SMM in a benign background, SMM with BH, SM with FGC, or APA. A few cases of EIN were included in this preliminary study and additional cases of EIN will be incorporated in the future. Representative blocks were stained for beta catenin, and expression patterns were recorded. Subsequent pathology as available, BMI, and age were extrapolated from the medical record.

Results: 28 cases were included (26 endometrial biopsies, 2 hysterectomies): 11 SMM in a benign background, 1 SMM with BH, 7 SMM with FGC, 7 APAs, and 2 EIN with SMM. All demonstrated glandular membranous beta catenin staining and nuclear staining in the SMM components. Scattered to diffuse nuclear positivity in glands immediately associated with SMM was seen in 16/28 cases (57%). Twelve cases (12/28, 43%) showed nuclear glandular positivity in foci away from SMM, including 2/11 SMM in a benign background, 5/7 SMM with FGC, 3/5 APAs, and 2/2 EIN with SMM. 9/26 endometrial biopsy cases had a subsequent hysterectomy, with two demonstrating endometrioid adenocarcinoma (1 SMM in benign background, 1 APA).

Conclusions: Beta catenin mutations confer worse prognosis in even low FIGO stage endometrioid adenocarcinomas. However, expression in SMM and APAs is of uncertain significance. Here we present cases with beta catenin expression both in association with SMM but also in non-morular glandular foci and in EIN. While additional cases of EIN will be evaluated to draw conclusions regarding prognostic significance of beta catenin expression, our preliminary study demonstrates potential patterns of expression in biopsies with SMM and APA. Further, it demonstrates progression to endometrioid adenocarcinoma in at least one case of APA with extensive beta catenin staining.

1143 Diagnostic Utility of SF1 in Comparison with Inhibin and Calretinin in Ovarian Neoplasms

Marissa White[1], Mark Hopkins[1], Alexander Berrebi[2], Lee Wu[3], Jane Morrison[4], Allen Gown[5], Russell Vang[6]
[1]Johns Hopkins Hospital, Baltimore, MD, [2]Johns Hopkins, Baltimore, MD, [3]Johns Hopkins University School of Public Health, Baltimore, MD, [4]Michigan Pathology Specialists, Grand Rapids, MI, [5]PhenoPath Laboratories, PLLC, Seattle, WA, [6]Johns Hopkins Hospital, Ellicott City, MD

Disclosures: Marissa White: None; Mark Hopkins: None; Alexander Berrebi: None; Lee Wu: None; Jane Morrison: None; Allen Gown: None; Russell Vang: None

Background: Commonly used immunohistochemical markers for the differential diagnosis of ovarian sex cord-stromal neoplasms are inhibin and calretinin. While some data suggest SF1 may have comparable diagnostic utility, a comprehensive evaluation with inhibin and calretinin in order to determine the diagnostic value of SF1 among sex cord-stromal and non-sex cord-stromal tumors of the ovary would help refine the choice of immunohistochemical markers in this setting.

Design: 389 ovarian tumors/tumor-like lesions were studied, which consisted of 188 sex cord-stromal lesions (including fibroma/fibrothecoma, cellular fibroma/fibrothecoma, fibromatous nodule, adult granulosa cell tumor, juvenile granulosa cell tumor, granulosa-theca cell tumor, Sertoli-Leydig cell tumor, sclerosing stromal tumor, and various benign non-neoplastic proliferations) and 201 non-sex cord-stromal lesions (including germ cell tumors, adnexal mesenchymal tumors, metastatic carcinoma, primary ovarian carcinoma, primary ovarian benign tumors, and various benign rests). Whole tissue sections and tissue microarrays were stained with SF1, calretinin, and inhibin. The overall distribution (0, <5% positive cells; 1+, 5% to 24%; 2+, 25% to 49%; 3+, 50% to 74%; 4+, 75% to 100%) and intensity (1, weak; 2, moderate; 3, strong) of expression for each immunohistochemical stain was recorded. Composite immunohistochemical scores (distribution x intensity) were determined with a maximum possible composite score of 12 for each stain.

Results: 99% (n = 188) of sex cord-stromal neoplasms were positive for SF1 (mean composite score 7.5). In contrast, calretinin and inhibin were expressed in 59% (n = 182, mean composite score 4) and 49% (n = 188, mean composite score 4.3), respectively, of sex cord-stromal neoplasms. Staining was more frequent in the sex cord (e.g., adult granulosa cell tumor) rather than stromal (e.g., fibroma) subgroups. The specificities for SF1, calretinin, and inhibin were 90%, 74%, 95%, respectively, with 59% of primary ovarian epithelial tumors (n = 125) expressing calretinin.

Conclusions: SF1 is sensitive and specific for ovarian sex cord-stromal neoplasms and demonstrates superior utility (combined sensitivity/specificity) compared with inhibin and calretinin in the distinction of sex cord-stromal from non-sex cord-stromal tumors. Instead of the commonly used combination of inhibin/calretinin for this differential diagnosis, we recommend abandoning calretinin and replacing this panel with SF1/inhibin.

1144 Expression of the Immune Checkpoint LAG-3 and its Ligand Gal-3 in High-Grade Serous Ovarian Carcinoma

Rachel Whitehair[1], Lauren Peres[2], Anne Mills[1]
[1]University of Virginia, Charlottesville, VA, [2]Moffitt Cancer Center, Tampa, FL

Disclosures: Rachel Whitehair: None; Lauren Peres: None; Anne Mills: None

Background: High-grade serous ovarian carcinomas (HGSOC) have shown lackluster responses to immunotherapies targeting the PD-1/PD-L1 axis, perhaps due to the presence of other mechanisms of immune evasion in this tumor type. Lymphocyte activation gene-3 (LAG-3) is another inhibitory checkpoint which can be expressed on tumor-associated lymphocytes and is targeted by drugs currently in clinical trials. Galectin-3 (GAL3), one of LAG3s binding partners, is also an emerging drug target that represents a potential mechanism of tumoral immune evasion both through its interaction with LAG-3 and through independent immunosuppressive effects. LAG-3 and GAL3 expression have both been identified in a variety of tumor types, but they have not been well-studied in HGSOC.

Design: 48 cases of HGSOC with known germline BRCA mutation status were stained for LAG-3 and GAL-3 on whole section slides. LAG-3-positive lymphocytes were enumerated and averaged over 10 high-power field (HPF). Tumoral GAL-3 was scored based on cytoplasmic tumor staining extent as 0=<1; 1=1-5%; 2=6-10%; 3=11-25%; 4=25-50%; 5=>50%. Statistics were performed using ANOVA, Wilcoxon rank-sum test, and Fisher's Exact test.

Results: The average number of LAG-3-posiitve tumor-associated lymphocytes was 6/HPF (range of 1-13). (Figure 1) Tumoral GAL-3 expression was identified in 48% (23/48) of all HGSOC, however most positive cases (10/23, 52%) showed only 1-5% expression. Only four cases showed >50% staining. (Figure 1) There was no significant correlation between LAG3+ lymphocytes and GAL3 expression. Neither LAG-3-positive lymphocyte counts nor tumoral GAL3 expression was significantly associated with germline BRCA status, and neither variable was correlated with survival.

Figure 1 - 1144

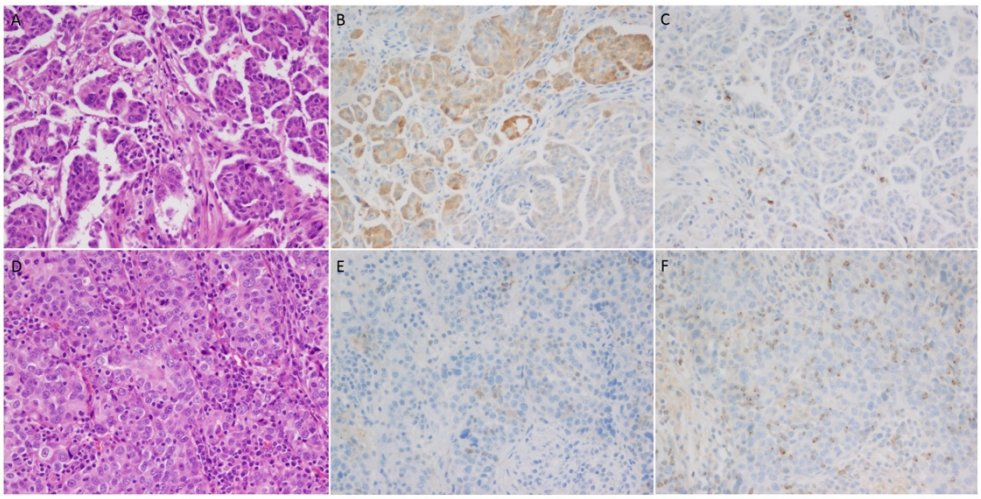

Figure 1: HGSOC showed variable expression of LAG3 and GAL3. The case depicted in A-C demonstrated GAL3 expression in the majority of tumor cells (B) with scattered tumor-associated LAG-3-positive lymphocytes (C). In contrast, the case depicted in D-F was largely GAL3-negative (E) with a more robust infiltrate of LAG3-positive lymphocytes.

Conclusions: The immune modulatory molecules LAG-3 and GAL-3 are expressed in a subset of HGSOC. This suggests that immunotherapies targeting these molecules may benefit some HGSOC patients, either alone or in combination with other approaches. However, even when positive expression is typically limited, invoking caution against the role these immunomodulatory molecules play for most examples of this tumor type.

1145 Mutations are common in complex endometrial hyperplasia

Todd Williams[1], Sung Eun Yang[2], Terry Morgan[2], Christopher Corless[1], Corinne Gardner[2]
[1]Portland, OR, [2]Oregon Health & Science University, Portland, OR

Disclosures: Todd Williams: None; Sung Eun Yang: None; Christopher Corless: None; Corinne Gardner: None

Background: The current obesity epidemic is dramatically increasing the incidence of endometrial hyperplasia in reproductive age women. This is significant because a subset of these cases do not adequately respond to progestin therapy and require a hysterectomy. Simple hyperplasia is unlikely to be associated with cancer, but complex atypical hyperplasia (CAH) has a relatively high risk and may be treated by hysterectomy if progestin therapy fails. Recent genetic studies suggest that 30% of complex hyperplasia cases may harbor mutations commonly observed in endometrial adenocarcinoma. Our objective was to determine whether molecular profiling of complex hyperplasia (CH) and CAH could identify a subset of cases with mutations more likely to be associated with progression to adenocarcinoma.

Design: Retrospective cross-sectional study of *de novo* endometrial biopsies diagnosed with CH or CAH by general surgical pathologists at our university hospital within the past 4 years. Cases were separately reviewed by two gynecologic pathologists to confirm classification, and categorized as benign, simple hyperplasia, complex hyperplasia (CH), complex atypical hyperplasia (CAH), or adenocarcinoma (ACA). A pilot study of reproducible diagnoses from each available category was then performed using next generation sequencing of FFPE archived tissue to screen for mutations in PIK3CA, PIK3R1, AKT1, mTOR, PTEN, CTNBB1, KRAS, ARID1A, and loss of PMS2 or MSH6 .

Results: In this pilot study of 16 cases originally diagnosed as complex hyperplasia, four were upgraded to grade 1 adenocarcinoma (ACA) by more specialized gynecologic pathologists in our group. Surprisingly, 11/12 (92%) of the complex hyperplasia cases had at least one mutation (Table). The majority of cases in each diagnostic group had multiple mutations. Sample size was not sufficiently powered to identify statistically significant differences between diagnostic groups.

	TOTAL	CH	CAH	ACA
Total	16	9	3	4
Mutated	15 (94%)	9 (100%)	2 (67%)	4 (100%)
Multiple Mutations	11 (65%)	6 (67%)	2 (67%)	3 (75%)
PIK3CA	4 (24%)	3 (33%)	0	1 (25%)
PIK3R1	5 (29%)	3 (33%)	2 (67%)	0
AKT1	3 (18%)	2 (22%)	0	1 (25%)
MTOR	2 (12%)	2 (22%)	0	0
PTEN	6 (35%)	3 (33%)	2 (67%)	1 (25%)
CTNBB1	7 (41%)	4 (44%)	1 (33%)	2 (50%)
KRAS	4 (29%)	2 (22%)	0	2 (50%)
ARID1A	2 (12%)	0	1 (33%)	1 (25%)
MSI	2 (12%)	1 (11%)	0	1 (25%)

Conclusions: Our preliminary data suggest that oncogenic mutations may be more common in endometrial complex hyperplasia than previously appreciated. It is possible we have identified a higher frequency of mutations because we evaluated more genes than has previously been studied. Additional samples of simple hyperplasia, CH and CAH are being analyzed.

1146 Loss of Mutation Specific MMR protein expression in non-neoplastic endometrium of Lynch syndrome patients

Serena Wong[1], Pei Hui[2], Natalia Buza[3]
[1]Yale New Haven Hospital, New Haven, CT, [2]Yale University School of Medicine, New Haven, CT, [3]Yale University, New Haven, CT

Disclosures: Serena Wong: None; Pei Hui: None; Natalia Buza: None

Background: Lynch syndrome is a hereditary cancer syndrome that increases the risk of developing colorectal and endometrial carcinomas. It is most often caused by a germline mutation in one of four DNA mismatch repair (MMR) genes: MLH1, PMS2, MSH2 or MSH6. Establishing the diagnosis of Lynch syndrome can be challenging, and ancillary studies that help to differentiate sporadic MMR protein deficiency from true germline mutations are needed. A recent study has shown loss of MMR expression in non-neoplastic colonic crypts in patients with Lynch syndrome. The aim of this study is to evaluate MMR protein expression in non-neoplastic endometrium of patients with known Lynch syndrome.

Design: Prophylactic hysterectomies and endometrial curettings were retrieved from our departmental archives from 18 patients with known Lynch syndrome, confirmed by a germline mutation in one of the MMR genes: MLH1 (n=3), PMS2 (n=3), MSH2 (n=7) and MSH6 (n=5). H&E slides were reviewed to confirm absence of endometrial malignancy. One tissue block with the highest number of benign endometrial glands was selected from each case and stained for MLH1, PMS2, MSH2, and MSH6 by immunohistochemistry. For control groups, MMR immunostains were performed on benign endometrium adjacent to sporadic, MMR proficient endometrial cancer (n=10) and proliferative endometrium from hysterectomy specimens for benign indications (n=10).

Results: Microscopic foci of MMR protein deficient non-neoplastic endometrial glands were identified in 10 cases, all of which were in the Lynch syndrome group (56%, 10/18). In all 10 cases the protein expression loss matched with the known germline mutation (MLH1=2, PMS2=1, MSH2=6, MSH6=1). In the cases with loss of MMR protein expression and MLH1 or MSH2 mutation, loss of staining was also seen in the paired heterodimers, PMS2 and MSH6, respectively. In two of these ten cases, focal atypical hyperplasia was identified which also showed loss of MMR protein expression. No loss of expression of any MMR proteins was seen in the control groups.

Conclusions: Our findings suggest that, similar to the previously described phenomenon in the colon, MMR protein deficient non-neoplastic endometrial glands may be a unique marker of Lynch syndrome. Evaluation of MMR protein expression of benign endometrium in endometrial cancer patients may provide additional critical information in the screening algorithm for Lynch syndrome.

1147 Discordant Status of DNA Mismatch Repair Deficiency between Endometrioid Carcinoma and Adjacent Atypical Endometrial Hyperplasia

Serena Wong[1], Natalia Buza[2], Pei Hui[3]
[1]Yale New Haven Hospital, New Haven, CT, [2]Yale University, New Haven, CT, [3]Yale University School of Medicine, New Haven, CT

Disclosures: Serena Wong: None; Natalia Buza: None; Pei Hui: None

Background: Reflex testing of endometrial cancer by mismatch repair (MMR) IHC and MSI PCR has been integrated into the routine screening algorithm for Lynch syndrome. It is unclear whether endometrial complex atypical hyperplasia (CAH), a precursor lesion to endometrioid carcinoma, may have acquired similar MMR deficiencies identical to their corresponding carcinomas. The aim of this study

is to investigate the MMR protein expression and MSI status of CAH associated with endometrial endometrioid carcinoma with known MMR deficiency.

Design: A total of 12 hysterectomies with MMR deficient endometrial carcinoma were included. H&E slides were reviewed to select foci of CAH for immunostaining by four MMR proteins and MSI PCR testing. The staining patterns of MMR proteins and the MSI results were compared between the carcinoma and adjacent CAH.

Results: The twelve study cases had abnormal MMR protein expression in the carcinomas, including 9 cases with loss of MLH1 and PMS2, 2 cases with loss of PMS2 and 1 case with loss of MSH6 (Table 1). Of the 9 cases with loss of MLH1 and PMS2, 7 showed identical loss in the background CAH. Of the 2 cases with PMS2 loss, 1 case had the same loss in the CAH. The one case with loss of MSH6 showed the same loss in the CAH. Among the 9 cases with loss of MLH1 and PMS2, all carcinomas were MSI high by PCR, which was observed in only 2 of 9 cases in the corresponding CAH. The remaining 7 cases were MSI stable in the CAH. Of the 2 carcinomas with loss of PMS2, one was MSI high while the other was MSI low, and the corresponding CAH was MSI stable and MSI low, respectively. In the one carcinoma with MSH6 loss, MSI was high in the carcinoma but stable in the corresponding CAH.

Patient	MMR staining in tumor	MMR Staining in CAH	MSI-Tumor	MSI-CAH
1	Loss of PMS2	Loss of PMS2	MSI low	MSI low
2	Loss of MLH1 and PMS2	Loss of MLH1 and PMS2	MSI high	MSI stable
3	Loss of MLH1 and PMS2	Loss of MLH1 and PMS2	MSI high	MSI stable
4	Loss of MLH1 and PMS2	MLH1 and PMS2 retained	MSI high	MSI stable
5	Loss of MLH1 and PMS2	Loss of MLH1 and PMS2	MSI high	MSI high
6	Loss of MLH1 and PMS2	Loss of MLH1 and PMS2	MSI high	MSI stable
7 *	Loss of MLH1 and PMS2	Loss of MLH1 and PMS2	MSI high	MSI stable
8	Loss of PMS2	PMS2 retained	MSI high	MSI stable
9	Loss of MLH1 and PMS2	Loss of MLH1 and PMS2	MSI high	MSI high
10	Loss of MLH1 and PMS2	Loss of MLH1 and PMS2	MSI high	MSI stable
11	Loss of MLH1 and PMS2	MLH1 and PMS2 retained	MSI high	MSI stable
12	Loss of MSH6	Loss of MSH6	MSI high	MSI stable

* The focus of CAH in this case was very closely intermixed with normal endometrial glands

Conclusions: MMR deficient endometrial endometrioid carcinomas have identical abnormal MMR protein expression in their corresponding CAH in the majority but not all of the cases. However, their corresponding CAH fails to have fully developed microsatellite instability in the majority of the cases, suggesting that CAH may not be an ideal lesion for the screening of Lynch syndrome.

1148 Pathologic analysis and accurate diagnosis of hydatidiform moles based on a large volume (54,289) of gestational lesions of Chinese women

Tao Wu[1], Pifu Luo[2], Xuefeng Li[1], Zhikui Zhang[1]
[1]KingMed Diagnostics, Guangzhou, China, [2]KingMed Diagnostics, Central Point, OR

Disclosures: Tao Wu: None; Pifu Luo: None

Background: Hydatidiform mole (HM) is seen more often in Chinese population. Accurate diagnosis is critical for the patients' managements. This study retrieved a large number of gestational lesions in China's largest CAP certified clinical laboratory to investigate HM incidence, age distribution and diagnostic approaches.

Design: A total of 54,289 gestational lesions were collected from January 2013 to March 2018 from pathology department records in KingMed Diagnostics Guangzhou. All cases were histologically reviewed and p57kip2 protein immunostain was added. Short tandem repeat (STR) genotyping was performed for further confirmation on equivocal or uncertain cases.

Results: A total of 1790 cases of HM and other significant gestational lesions were diagnosed, including 1641 complete moles (CMs), 144 partial moles (PMs), 3 invasive moles (IMs), 1 placental mesenchymal dysplasia (PMD) and 1 trisomy 16q. HM rate is 3.02% in these gestational specimens (1790/54289). Usually CMs are diagnosed based on morphology. With p57kip2 stain, early CMs can be distinguished from PMs and other gestational lesions by absence of nuclear staining in cytotrophoblasts and villous stromal cells. In 103 uncertain cases, STR was performed to facilitate the final diagnosis. Of the CMs, 1425 (86.83%) were diagnosed in patients between 15 to 40 years, 212 (12.93%) were above 40 years and only 4 (0.24%) were seen in patients younger than 15 years. 2 gemellary pregnancies (normal fetus with molar placenta) and 1 recurrent mole were identified within CMs. Among the PMs, 131 (90.97%) were seen in patients between 15 to 40 years and 13 (9.08%) were above 40 years (See table 1).

Table 1. 1790 cases of HMs and related gestational lesions

Pathological types	Total	Ages (Years)		
		Less than 15	15 to 40	More than 40
CMs	1641 (3.02%)	4 (0.24%)	1425 (86.83%)	212 (12.93%)
PMs	144 (0.27%)	0	131 (90.97%)	13 (9.03%)
HAs	52,499 (96.70%)	14 to 51		
IMs	3	26, 30, 44		
PMD	1	27		
Trisomy 16q	1	38		

Conclusions: HM is one of gestational trophoblastic diseases (GTDs) with distinct clinicopathological and genetic characteristics. HMs can develop persistent GTDs and choriocarcinoma. CMs have higher risk of developing to malignancy in comparison to PMs. In addition, the risk of persistent GTDs may be higher for heterozygous CMs than for homozygous ones. It is very critical to differentiate HMs from hydropic abortions (HAs), and classify accurate genetic subtypes in CMs. Our study indicates the majority of patients with HMs are between 15 to 40 years which is different from WHO's description (2014) demonstrating the significant risk-factors of molar pregnancy include maternal age less than 15 years and more than 40 years. Our analysis encourages a combination of morphology, p57kip2 immunostain and STR genotyping in a precision diagnosis of molar pregnancies.

1149 Recurrent BCOR hotspot mutations in endometrial carcinoma

Xinyu Wu[1], Douglas Rottmann[2], Padmini Manrai[1], Pei Hui[3], Natalia Buza[4]
[1]New Haven, CT, [2]Yale University School of Medicine, Hamden, CT, [3]Yale University School of Medicine, New Haven, CT, [4]Yale University, New Haven, CT

Disclosures: Xinyu Wu: None; Douglas Rottmann: None; Padmini Manrai: None; Pei Hui: None; Natalia Buza: None

Background: BCOR is a transcription regulatory factor, originally identified as a corepressor of BCL6. BCOR genetic aberrations (internal tandem duplications and translocations) have been recently reported in soft tissue sarcomas, clear cell sarcoma of the kidney, and in a subset of high grade endometrial stromal sarcomas. In addition, somatic BCOR mutations have been identified by The Cancer Genome Atlas (TCGA) project in various different tumor types, including 18% of endometrial carcinomas. We aimed to investigate the clinicopathological and molecular characteristics of endometrial carcinomas with BCOR mutations.

Design: A total of 88 cases of endometrial carcinomas with available next generation sequencing (NGS) results in their medical records were retrieved from our departmental archives. Cases with BCOR mutations were identified and reviewed in detail to evaluate their clinico-pathological features and outcome.

Results: Seven of 88 cases (7/88, 8%) harbored BCOR mutations. The most common mutation, a missense mutation at N1425S (COSMIC 403987), was present in 6 cases (6/7, 86%), and one case showed a frameshift mutation S336fs42 (1/7, 14%). The patients' age at diagnosis ranged from 55 to 81 years (mean: 71 years). Majority (4/7, 57%) of BCOR mutant tumors were of endometrioid type, one tumor was serous (1/7, 14%), and one was an undifferentiated carcinoma (1/7, 14%). All but one case were stage I at the time of the initial surgery. Five patients demonstrated microsatellite instability (MSI-high) (5/7, 71%), one case was MSI-low and one was microsatellite stable by PCR. Conversely, the proportion of MSI-high tumors among cases with no BCOR mutation was only 20% (16/81). (Additional relevant molecular results are listed in Table 1.) The clinical follow-up period ranged from 16 to 88 months (mean: 57 months), during which five patients (5/7, 71%) developed metastatic disease. All patients were alive at last follow up. [Table 1].

Case #, BCOR mutation type	Patient age (at diagnosis)	Tumor histologic subtype	FIGO grade	Initial Tumor Stage (AJCC 7TH ed.)	MSI status (by PCR)	Other relevant mutations (by NGS)	Follow-up (months)	Outcome
1 (S336fs*42)	74	Endometrioid	2	IB	MSI-H	CTNNB1, PIK3CA, PTEN, ARID1A	58	AWD (Lung mets)
2 (N1425S)	74	Endometrioid	3	IA	MSI-H	CTNNB1, PTEN, ARID1A	75	AWD (Lung mets)
3 (N1425S)	55	Endometrioid	2	IA	MSS	KRAS, PTEN	88	AWD (Colon mets)
4 (N1425S)	67	Serous	NA	IB	MSI-L	PIK3CA, PTEN, ARID1A, TP53	53	AWD (mets to supraclavicular and para-aortic lymph nodes)
5 (N1425S)	81	Endometrioid	2	IB	MSI-H	PTEN, ARID1A, TP53	58	AWD (mets to peritoneum, abdominal soft tissue)
6 (N1425S)	65	Dedifferentiated	NA	IIIC2	MSI-H	KRAS, CTNNB1, PTEN, ARID1A, TP53, CDKN2A	48	NED
7 (N1425S)	79	Endometrioid	3	IA	MSI-H	BRCA2, MSH6, PIK3CA, PTEN, ARID1A	16	NED

Table 1. Clinicopathological characteristics of endometrial carcinomas with BCOR mutations.

Conclusions: BCOR mutations were identified in 8% of endometrial carcinomas in our series, a lower prevalence compared to the 18% in the endometrial TCGA dataset. Majority of BCOR-mutant tumors showed an endometrioid histology and high microsatellite instability. A large proportion of patients with BCOR mutant tumors developed metastases; however, none of the patients died of the disease. The potential associations between BCOR mutations, MSI status, and disease recurrence/ progression warrant additional studies in larger patient cohorts.

1150 Recurrent genetic alterations in primary and metastatic invasive squamous cell carcinoma of the vulva

Deyin Xing[1], Wei Song[2]
[1]Johns Hopkins Medical Institutions, Ellicott City, MD, [2]Weill Cornell Medical College, Short Hills, NJ

Disclosures: Deyin Xing: None; Wei Song: None

Background: While nearly all squamous cell carcinoma (SCC) of the uterine cervix are caused by high-risk human papillomavirus (HPV), two different pathways in the development of vulvar SCC has been proposed: one occurred in younger women with HPV involvement and another occurring in elderly women with unknown pathogenic mechanism. The latter, usually originating from the precursor lesion, differentiated-type vulvar intraepithelial neoplasia (dVIN), tends to recur and progress. Thus, there is a need for novel approaches to understand and treat this tumor.

Design: Using a comprehensive next generation sequencing (NGS) pipeline (143 genes), Oncomine, we have performed both DNASeq and RNASeq, in search of potential recurrent variants, including single nucleic variant (SNV), copy number change and translocation fusion. Clinicopathologic features of 22 cases are reported. Genomic DNA was extracted from paraffin-embedded 32 tumor tissues of 22 cases. Immunohistochemical analysis of p16 and in situ hybridizations for high-risk HPV were performed in a subset of cases.

Results: 4 (18%) of 22 cases with vulvar SCC showed concurrent usual type high grade squamous intraepithelial lesion (VIN3) or a “block” pattern p16 immunostaining, indicating a high-risk HPV related process. Interestingly, 3 cases harbored PIK3CA gain-of-function mutations which correlated with high-risk HPV associated oncogenesis. One case contained both PIK3CA and TP53 mutations. 18 cases

demonstrated morphology of well differentiated keratinizing SCC unrelated to usual VIN. The patients in this group ranged in age from 25 to 92 years old (mean 67, median 71). The most common somatic mutation in HPV-unrelated SCC was TP53, present in 17 (94%) of 18 cases. Recurrent somatic mutations of CDKN2A, BAP1, HRAS, NOTCH1 were also detected. Importantly, 9 of 10 cases displayed identical mutational profile in the primary and metastatic tumors, supporting a clonal evolution. However, additional genetic alterations that may confer metastatic potential were not identified.

Conclusions: Targeted next-generation gene sequencing identified recurrent genetic alterations that co-operate with TP53 pathways in the development of HPV-unrelated SCC of the vulva. The presence of genetic alterations that are amenable to targeted therapy offers the potential for individualized management strategies for treatment of this aggressive tumor.

1151 Identification of Novel ALK Translocation in Gynecologic Clear Cell Carcinoma

Chen Yang[1], Latisha Love-Gregory[2], Lingxin Zhang[3], Ian Hagemann[2], Dengfeng Cao[4]
[1]Yale University School of Medicine, New Haven, CT, [2]Washington University School of Medicine, St. Louis, MO, [3]Hospital for Special Surgery, New York, NY, [4]Barnes Jewish Hospital/Washington University, St. Louis, MO

Disclosures: Chen Yang: None; Latisha Love-Gregory: None; Lingxin Zhang: None; Ian Hagemann: None; Dengfeng Cao: None

Background: Clear cell carcinomas of the gynecologic tract are aggressive tumors with poor long-term survival that show high resistance rate to conventional platinum-based chemotherapies. Currently, there is no targeted therapy available, and the molecular features for these tumors remain largely unknown. The aim of the present study was to identify novel anaplastic lymphoma kinase (*ALK*) translocation, a potential molecular target for therapy.

Design: The archives of a single institution between 1987 and 2017 were searched. A total of 97 consecutive patients (median age 63, range 30-90) with gynecologic clear cell carcinoma (ovary 62, endometrium 27, and cervix 8) were identified. All cases were screened for *ALK* rearrangement and *ALK* copy number gain using *ALK* break-apart fluorescence in-situ hybridization (FISH) probe. The genomic landscape of all cases with *ALK* rearrangements and 10 cases with *ALK*copy number gain was further characterized using a hybrid capture based next-generation sequencing assay to interrogate 122 genes for multiple variant types including *ALK* fusion partners. Finally, the results were correlated with ALK (clone D5F3) immunohistochemistry (IHC) expression and clinicopathologic parameters.

Results: *ALK* rearrangement was detected by FISH in 5% (5/97) of gynecologic clear cell carcinomas (ovary 2, endometrium 2, cervix 1) and *ALK* copy number gain was detected in 79.4% (77/97) of cases. Next-generation sequencing in *ALK*-rearranged clear cell carcinomas identified a novel fusion *BRE-ALK* in one case. *ALK* translocation partners were not identified in the remaining 4 *ALK*-rearranged or any *ALK*-copy number gain cases. Other variants including PIK3CA (2), FLT3(2), KMT2D (2), AR (4), ROS1 (4) were identified in *ALK*-rearranged cases. The case with *BRE-ALK* fusion showed 2+ staining of ALK by IHC. Cases of clear cell carcinoma with *ALK* aberrances by FISH showed worse disease-free survival and long-term survival when compared with cases without *ALK* aberrances (both $p<0.05$).

Conclusions: We systematically investigated the *ALK* gene in a large series of gynecologic clear cell carcinomas. A novel *BRE-ALK* translocation was identified along with 4 other cases harboring *ALK* rearrangement by FISH. Our findings show that *ALK*, which is targetable in other cancers, may be a pathogenetic mechanism in gynecologic clear cell carcinoma.

1152 Clinicopathological correlation of ARID1A status with HDAC6 and its related factors in ovarian clear cell carcinoma

Mitsutake Yano[1], Tomomi Katoh[1], Mariko Miyazawa[2], Masaki Miyazawa[2], Naoki Ogane[3], Maiko Miwa[1], Kosei Hasegawa[1], Hisashi Narahara[4], Masanori Yasuda[1]
[1]Saitama Medical University International Medical Center, Hidaka, Japan, [2]Tokai University School of Medicine, Isehara, Japan, [3]Kanagawa Prefectural Ashigarakami Hospital, Ashigarakami, Japan, [4]Oita University Faculty of Medicine, Yufu, Japan

Disclosures: Mitsutake Yano: None; Tomomi Katoh: None; Mariko Miyazawa: None; Masaki Miyazawa: None; Naoki Ogane: None; Maiko Miwa: None; Kosei Hasegawa: *Grant or Research Support*, Pfizer Inc.; *Grant or Research Support*, Yakult Honsha Co.; *Grant or Research Support*, OncoThreapy Science Inc.; *Speaker*, Chugai Pharmaceutical Co.; *Speaker*, Daiichi-Sankyo Co., Ltd.; Hisashi Narahara: None; Masanori Yasuda: None

Background: Ovarian clear cell carcinoma (OCCC) is well known for having a close association with a frequent ARID1A function loss. Aside from this, a recent study has reported that ARID1A directly suppresses histone deacetylase (HDAC) 6 in OCCC cell lines. The present study was aimed at evaluation of the clinical significance of HDAC6 and its related factors expression in terms of ARID1A status.

Design: Immunohistochemical expressions of HDAC6, hypoxia inducible factors-1α (HIF-1α), programmed death-1 ligand (PD-L1), cancer stem cell marker (CD44), and ARID1A were analyzed for 106 patients with OCCC to assess if these markers may be associated with their prognosis.

Results: The nuclear high expression of HDAC6 was correlated with death (p = 0.038) and overall survival (p = 0.054) of OCCC patients in univariate analysis. In multivariate analysis of overall survival, surgical residual tumor, high expressions of PD-L1, and HDAC6 (hazard ratio = 1.68; p = 0.034) were found to become the independent prognostic factors. High expressions of HDAC6 and HIF-1α were associated with a poor prognosis in OCCC with ARID1A loss, but were not associated with a poor prognosis without ARID1A loss. HDAC6 expression showed a significantly positive correlation with HIF-1α, PD-L1, and CD44.

Conclusions: HDAC6 involvement in prognosis was demonstrated to depend on ARID1A status in OCCCs. HDAC6 may be a promising therapeutic target for OCCCs with ARID1A loss via immuno-modulation, response to hypoxia, and cancer stem cell phenotype. Immunohistochemical status of ARID1A would be expected to become an indicator to predict its usefulness.

1153 Stratification of endometrial endometrioid carcinoma with a support of p53 immunohistochemical status

Mitsutake Yano[1], Kozue Ito[1], Akira Yabuno[1], Tomomi Katoh[1], Naoki Ogane[2], Mariko Miyazawa[3], Masaki Miyazawa[3], Kosei Hasegawa[1], Hisashi Narahara[4], Masanori Yasuda[1]
[1]Saitama Medical University International Medical Center, Hidaka, Japan, [2]Kanagawa Prefectural Ashigarakami Hospital, Ashigarakami, Japan, [3]Tokai University School of Medicine, Isehara, Japan, [4]Oita University Faculty of Medicine, Yufu, Japan

Disclosures: Mitsutake Yano: None; Kozue Ito: None; Akira Yabuno: None; Tomomi Katoh: None; Naoki Ogane: None; Mariko Miyazawa: None; Masaki Miyazawa: None; Kosei Hasegawa: *Grant or Research Support*, Pfizer Inc.; *Grant or Research Support*, Yakult Honsha Co.; *Grant or Research Support*, OncoThreapy Science Inc.; *Speaker*, Chugai Pharmaceutical Co., Ltd.; *Speaker*, Daiichi-Sankyo Co., Ltd.; Hisashi Narahara: None; Masanori Yasuda: None

Background: Endometrial endometrioid carcinoma (EEC), the major histotype of the uterine body cancer through the entire patient age spectrum, is usually graded into 3-tiered histological subgroups (Grade 1/2/3) based on the architectural and cytological atypia/abnormality. But, well differentiated EEC, i.e. G1/2, are in part unfavorable in their prognosis especially in elderly patients, showing a similarity to type-2 carcinomas such as EEC G3 and serous carcinoma. This study was conducted to examine whether the abnormal expression of p53 in EEC would contribute to reconsideration of the current grading system.

Design: A total of 475 patients with EEC, whose tumors were pathologically confirmed, were recruited from our hospital during 10 years from 2007 to 2016. Immunohistochemical expression of p53 (clone DO7, monoclonal mouse, Dako) was analyzed using tissue microarray. The weak and moderate expression cases were regarded as wild-type/normal, whereas the completely negative and markedly positive cases were considered as mutated-type (MT)/abnormal. The relationship between p53 expression and clinical outcome (progression free survival, PFS; overall survival, OS) was analyzed. This study was performed under the approval of our Institutional Research Board.

Results: EECs were divided into 327 cases (68%) for G1, 88 cases (19%) for G2, and 60 cases (13%) for G3. Univariate survival analysis showed that p53-MT was significantly associated with inferior PFS in G1 (median PFS; 63 vs 103 months, p < 0.001) and G2 (63 vs 100 months, p = 0.010), but not in G3 (51 vs 55 months, p = 0.616). p53-MT EEC had a significantly adverse prognosis (PFS and OS) regardless of the histological grade. Additionally, there was a positive correlation between age (≥ 60 vs < 60 years) and p53-MT in G1 (4 % vs 16 %, p = 0.001), but not in G2 (15 % vs 28 %, p = 0.126) and G3 (58 % vs 47 %, p = 0.281).

Conclusions: A subgroup of type-1 EEC G1/2, which showed p53-MT, was found to mimic type-2 carcinoma in terms of the prognosis especially in the elderly patients. Therefore, using only the histological grading system has a limitation in prediction of type-1 ECC carcinoma with potentially unfavorable prognosis. Therefore, application of p53 immunohistochemistry in the routine practice is thought to be useful for all EEC G2 cases and elderly EEC G1 cases. In conclusion, with the combination of p53 immunohistochemistry the traditional histological grading system for ECC is believed to improve the accuracy in terms of the consisten

1154 Endometrial stem/progenitor cell (ES/PC) markers in endometrial stromal sarcoma: Implications on histogenesis and prognosis

Ju-Yoon Yoon[1], Blaise Clarke[1], Marjan Rouzbahman[2]
[1]University of Toronto, Toronto, ON, [2]Toronto, ON

Disclosures: Ju-Yoon Yoon: None; Marjan Rouzbahman: None

Background: The classification of endometrial stromal sarcoma (ESS) has become increasingly complex with the identification of driver gene fusions, including *JAZF1-SUZ12* among many other genetic alterations. Previously, we had characterized our ESS cohort with respect to the frequency of the *JAZF1-SUZ12* fusion. Since our report, the role of Suz12 in embryonic stem cell biology has been better defined. The uterus is one of the most dynamic organs in the human body, and this dynamic homeostasis is supported by endometrial stem/progenitor cells (ES/PCs). ES/PCs are a group of progenitor/stem cells isolated from the uterus, representing a spectrum ranging

from multipotent endometrial mesenchymal stem cells (eMSCs) to more differentiated precursor/progenitor cells. In the context of these advances, we looked to examine the expression pattern of eleven ES/PC markers in our cohort ESS.

Design: We began with a literature review for available ES/PC markers. We chose and examined the expression levels of eleven ES/PC markers, along with three differentiation markers (ER, PR, CD10), by immunohistochemistry (IHC) in our cohort of 36 ESS cases. We compared the observed IHC patterns and compared the patterns with respect to the known ESS grade, presence/absence of *JAZF1-SUZ12* fusion and to known expression patterns in ES/PCs. Kaplan-Meier method was employed to examine the prognostic significance of ES/PC markers.

Results: In general, ESSs exhibited variable and limited immunophenotypic resemblance to eMSCs, and resemblance was observed across the different grades. Among the eleven ES/PC markers, the expression levels of SUSD2 and CD90, two of the more specific eMSC markers, correlated positively with each other. Unsupervised clustering of the fourteen protein levels resulted in three clusters. Cluster 1 was comprised mostly of high-grade ESS and was notable for low expression of differentiation markers and Msi1. Cluster 2 and 3 comprised mostly of low-grade ESS, with most tumors with *JAZF1-SUZ12* fusion falling into cluster 3. Interestingly, high expression of MSI1, CD90 or SUSD2 was associated with better overall survival, regardless of the tumour grade. The ES/PC marker clusters were also of high prognostic significance for both overall and disease-free survival.

Conclusions: Differential IHC patterns of ES/PC markers observed among the low- and high-grade ESSs are likely reflective of the known biological differences between the ESSs, part of which may be related to their histogenesis.

1155 Increased CRM-1 in Metastatic Ovarian Cancers Compared With Primary Tumors

Lorene Yoxtheimer[1], Dan Lu[2], Tamara Kalir[3]
[1]Mt. Sinai Hospital, New York, NY, [2]New York, NY, [3]Mount Sinai Health System, New York, NY

Disclosures: Lorene Yoxtheimer: None; Dan Lu: None; Tamara Kalir: None

Background: Ovarian cancer is the most lethal gynecologic cancer in the United States with over 22,000 new cases and over 14,000 deaths per year. The standard treatment is surgery and platinum-based chemotherapy. This, unfortunately, has not improved survival over the past few decades. Hence, a better understanding of the molecular pathogenesis is needed. In this age of personalized medicine, it is essential to identify new biomarkers as therapeutic targets. Chromosomal Maintenance 1 (CRM-1), also known as Exportin 1, facilitates the transport of RNA and proteins from the nucleus to the cytoplasm. The aim of this study is to compare CRM-1 protein distribution among subcellular compartments (nucleus, nucleolus, nuclear membrane, and cytoplasm) between primary and metastatic ovarian high-grade serous carcinoma using electron microscopy.

Design: Paired samples of primary ovarian high-grade serous carcinoma and omental metastases were collected from three patients. They were submitted for electron microscopic examination (Hitachi 7000 Transmission Electron Microscope equipped with an AMT 2Kx2K side-mount digital camera) to analyze CRM-1 protein expression and distribution among 4 subcellular compartments (nucleus, nucleolus, nuclear membrane, and cytoplasm) using a CRM-1 antibody (H-300; Santa Cruz Biotechnology, Inc.) and gold-tagged secondary antibody. CRM-1 proteins were counted, and the diameters of the nucleoli were measured. The area of each nucleolus was calculated. Data were analyzed using the Student's T-test.

Results: CRM-1 particles were increased in metastases compared with the same patient's primary in all four subcellular compartments investigated. This was reflected by the group's increased quantity and concentration of CRM-1 particles in the metastatic tumor's nucleoli compared the primary (Table 1). Interestingly, nucleoli were smaller in metastases compared to primary ovarian cancers. The cytoplasmic compartment showed 50.7 CRM-1 particles in metastases compared to 39.7 in primaries. The nuclei of metastatic tumors had twice as many CRM-1 particles as primaries (226.9 vs. 117.3), and the nuclear membrane displayed over 3 times as many CRM-1 particles in metastases versus primaries (175 vs. 50.8).

	Primary	Metastasis	T-Test
CRM1 proteins	61.61 +/- 48.51	206.89 +/- 81.43	P < 0.0001
Nucleolar Area (nm2)	2,088,091 +/- 1,574,061	870,728 +/- 613,987	P < 0.0001
CRM1 proteins standardized per Nucleolar Areas ($x10^5$)	4.10 +/- 3.64	34.08 +/- 28.35	P < 0.0001

Conclusions: CRM-1 protein is found in greater number and concentration in ovarian cancer metastases compared with primaries. These results suggest, among other things, higher metabolic activity in the metastases. CRM-1 has the potential to become an important biomarker for targeted therapy.

1156 Evaluation of potential immunotherapy biomarkers in female genital tract malignant melanomas

Ying Yu[1], Tse Ka-Yu[2], Kin Long Chow[3], Horace Hok-Yeung Lee[1], Wah Cheuk[4], Elaine Cheung[4], Richard Wong[5], Wai-Kong Chan[6], Victor Wai-Kwan Lee[3], Annie NY Cheung[7], Philip Ip[7]
[1]University of Hong Kong, Hong Kong, Hong Kong SAR, [2]Obstetrics and Gynaecology, The University of Hong Kong, Hong Kong, Hong Kong SAR, [3]Hong Kong, Hong Kong SAR, [4]Queen Elizabeth Hospital, Hong Kong, Hong Kong SAR, [5]Pamela Youde Nethersole Eastern Hospital, Hong Kong, Hong Kong SAR, [6]Hong Kong Sanatorium and Hospitals, Hong Kong, China, [7]The University of Hong Kong, Hong Kong, Hong Kong SAR

Disclosures: Ying Yu: None; Tse Ka-Yu: None; Kin Long Chow: None; Horace Hok-Yeung Lee: None; Wah Cheuk: None; Elaine Cheung: None; Richard Wong: None; Wai-Kong Chan: None; Victor Wai-Kwan Lee: None; Annie NY Cheung: None; Philip Ip: None

Background: Female genital tract malignant melanomas may response to immune checkpoint inhibitors. However, immunohistochemical assessment of the biomarker PD-L1 is difficult due to interobserver variation and intra-tumoral and temporal heterogeneity. Other predictive biomarkers are needed. The FDA has recently approved the use of pembrolizumab for mismatch repair (MMR) deficient solid tumors but the MMR status in genital melanomas has not been explored.

Design: Immunohistochemical evaluation of CD8+ tumor infiltrating lymphocytes (TIL) density and MMR proteins status was done on 55 genital tract melanomas. Anti-CD8 antibody (clone C8/144B. Dako) was used. Assessment of TIL density was made in an area with highest lymphoid cells density identified on low-magnification. An absolute count of CD8+ cells per high power field (x40 objective, 0.55 mm field diameter) was made. Survival analysis was performed by using a Cox proportional hazard model. Using receiver operating characteristic analysis, the optimal cut-off value for TIL count was determined by choosing the maximum value of Youden's index. The relationship between TIL count and PD-L1 expression (previously performed on the same patients by using Roche Ventana SP263 antibody) was done with Pearson's Product-moment correlation analysis. MMR protein (Roche Ventana) antibodies used were anti-MLH1 (clone M1), anti-MSH2 (clone G219-1129), anti-MSH6 (clone SP93) and anti-PMS2 (clone A16-4). A tumor was considered to have abnormal MMR expression when nuclear staining was absent.

Results: There were 20 vulvar, 32 vaginal and 3 cervical melanomas. The median counts of CD8+ TILs in vulvar, vaginal and cervical melanomas were 158, 65.5 and 150 per high power field, respectively. CD8+ TILs density was significantly higher among vulvar melanomas compared with non-vulvar melanomas ($p<0.05$) and showed a positive correlation with the PD-L1 score with a coefficient of 0.355 ($p = 0.01$). Univariable analysis showed that a CD8+ TIL count <93 per high power field was significantly associated with an adverse outcome. Loss of MLH1 and PMS2 staining was observed in 4 vulvar melanomas (21.1%) and 3 vaginal melanomas (9.38%). All 3 cervical melanomas had intact staining for all 4 proteins.

Conclusions: CD8+ TIL count showed a positive correlation with PD-L1 immunohistochemistry and interpretation of staining was easier. The combined evaluation of CD8+ TIL and MMR protein status in genital melanomas may be useful predictive biomarkers for immunotherapy.

1157 Predicting Responses to Neoadjuvant Chemotherapy in Patients with High Grade Tubo-Ovarian Serous Carcinoma Using A Proteomic Approach

Somaye Zare[1], Katy Smoot[2], Vinita Parkash[3], Charles Quick[4], Erin Seeley[2], Oluwole Fadare[1]
[1]University of California, San Diego, La Jolla, CA, [2]New River Labs, LLC, Morgantown, WV, [3]Yale University School of Medicine, New Haven, CT, [4]University of Arkansas for Medical Sciences, Little Rock, AR

Disclosures: Somaye Zare: None; Katy Smoot: *Employee*, New River Labs; Vinita Parkash: None; Charles Quick: None; Erin Seeley: *Employee*, New River Labs; Oluwole Fadare: None

Background: Interval debulking surgery after a few cycles of neoadjuvant chemotherapy (NACT) is a commonly utilized approach in the management of patients with high grade serous carcinoma of tubo-ovarian origin (HGSC). Previously reported analyses of the removed post-NACT samples have shown varying response rates to the NACT, and the optimal selection criteria for patients that are most likely to benefit from NACT remains elusive. We sought to determine whether analysis of the pre-NACT biopsies, using a proteomic approach, can uncover a signature that can be used to predict the response to NACT in patients with advanced stage HGSC.

Design: Diagnostic pre-NACT samples (16 biopsies, 16 effusion fluid samples, 1 lymph node FNA) from 33 patients diagnosed with HGSC, and all of whom were subsequently treated with platinum-based NACT, were assessed using histology guided mass spectrometry. Briefly, 5 µm sections were deparaffinized, antigen retrieved, and subjected to on tissue tryptic digestion and matrix applications. Mass spectrometry data were collected from approximately twenty 100 µm areas per sample as designated in an H&E stained serial section . Response rates for all 33 post-NACT samples were determined using a modified three-tiered chemotherapy response scoring system (CRS) on H&E stained sections. We assessed for a classification model that significantly stratified the samples into the three CRS groups, followed by an internal cross validation

Results: We detected 437 spectral peaks in the combined pre-NACT dataset, 267 of which were significantly different (p-value <0.0001) between the CRS subgroups when applying a Kruskal-Wallis test. In a 3-group classification model, an internal cross validation accuracy of 91.9% in correctly assigning the pre-NACT spectra to each post-NACT CRS group was achieved. In a 2-group classification model (CRS 1 and 3 only), a 96.9% internal cross validation accuracy was achieved. At the morphologic level, the pre-NACT samples that corresponded to the three post-NACT CRS groups showed no significant differences.

Conclusions: Our findings suggest that there are proteomic signatures that can distinguish between NACT responders and non-responders in patients with tubo-ovarian HGSC. Additional validation of these findings in larger cohorts may ultimately allow for a better prediction of patients that are most likely to benefit from NACT.

1158 Mutational Profile of Vulvar, Vaginal and Urethral Melanomas, Review of 37 Cases with Focus on Tumor Site

Shabnam Zarei[1], Jesse Voss[2], Long Jin[2], Debra Bell[3], Benjamin Kipp[3], Thomas Flotte[3]
[1]Cleveland Clinic, Cleveland, OH, [2]Rochester, MN, [3]Mayo Clinic, Rochester, MN

Disclosures: Shabnam Zarei: None; Jesse Voss: None; Long Jin: None; Debra Bell: None; Benjamin Kipp: None; Thomas Flotte: None

Background: *BRAF-V600E* is the most common mutation seen in dermal melanomas whereas mucosal melanomas lack *BRAF* and instead show *KIT* mutations. The updated staging guideline by the American Joint Committee on Cancer (AJCC 8th edition) recommends using cutaneous melanoma guidelines for vulvar melanoma staging and removed any recommendation for staging vaginal melanoma. We aimed to investigate the mutational status of vulvovaginal melanomas with focus on their site (hair-bearing, glabrous skin, vagina and urethra) in 37 patients with primary urogenital melanomas.

Design: After Institutional Review Board (IRB) approval, 109 patients diagnosed with urogenital melanoma in our institution from 2006-2016 were reviewed. A subset of 37 primary melanoma cases with at least 20% tumor volume and known primary site were selected. These included cases from labia majora (11), labia majora/minora junction (3), labia minora (6), vagina (8), urethra (7) and rectum/rectovagina (2). DNA was extracted from formalin-fixed paraffin-embedded tissue using the QIAamp DNA FFPE kit. The DNA samples were run on a targeted Next Generation Sequencing (NGS) panel covering 21 most common genes and hotspots in melanoma. Survival data was correlated with tumor site and molecular alterations, using Kaplan-Meier plots.

Results: Overall the most common mutated genes were *KIT* (35.1%), *NF1* (21.6%) and *TP53* (18.9%). A minority (5/37) did not have any alterations. The most common mutated genes in hair-bearing vulva were *KIT* (36.4%), *NF1* (18.2%) and *NRAS* (18.2%). This was similar to glabrous skin vulva with *KIT* (66.7%) and *NF1* (33.3%), vagina with *KIT*, *NF1* and *TP53* (25% each) and urethra with *KIT* and *TP53* (28% each). The only BRAF mutation was a non-V600 mutation in a urethral tumor. There was no statistical significance between tumor sites and molecular alterations or survival.

Conclusions: We found high frequency of *KIT* and *NF1* mutations and an overall high frequency of MAPK pathway alterations in female lower genital tract melanomas irrespective of tumor site (hair-bearing, glabrous skin vulva or vagina), suggesting a similar pathogenesis pathway. Revision of the current AJCC staging guideline is recommended to include female lower genital tract melanomas in a single group, similar to mucosal melanomas for staging purposes.

1159 HER2 Amplification Status in Extramammary Paget Disease (EMPD) Evaluated by IHC, FISH and Chromosomal Microarray. Review of 78 Cases

Shabnam Zarei[1], Toni Kilts[2], John Schoolmeester[3], Jamie Bakkum[2], Kevin Halling[3], Benjamin Kipp[2], William Cliby[2], William Sukov[3]
[1]Cleveland Clinic, Cleveland, OH, [2]Mayo Clinic, Rochester, MN, [3]Rochester, MN

Disclosures: Shabnam Zarei: None; Toni Kilts: None; John Schoolmeester: None; Jamie Bakkum: None; Kevin Halling: None; Benjamin Kipp: None; William Cliby: None; William Sukov: None

Background: EMPD is a rare neoplasm that can involve the anogenital and axillary skin. It often has an indolent course; however aggressive behavior and death from disease have been reported. Additionally, surgical excision is often extensive, recurrence rates are high, and novel therapies are needed. We investigated *HER2 (ERRB2)* as a potential therapeutic target using three different methods.

Design: After Institutional Review Board (IRB) approval, 78 EMPD with first time diagnostic material available for review were selected. Immunohistochemistry (IHC) was performed on paraffin-embedded tissue on all cases and DNA was extracted using Qiagen FFPE extraction kit in 38 cases with at least 20% tumor percentage. Chromosomal microarray (CMA) was used to evaluate copy number alterations. FISH was performed in cases lacking enough DNA for microarray studies (11 cases). Skin punch biopsy specimens were evaluated by IHC only (29 cases). Clinical data were abstracted from medical records.

Results: Overall 64/78 (82%) patients had in situ, 6/78 (7.7%) had microinvasive and 8/78 (10.3%) had invasive EMPD. 28/78 (36%) patients had disease recurrence, 39/78 (50%) did not have recurrence and 11/78 (14%) had unknown recurrence status. 65/78 (83.3%) had primary EMPD, 1/78 (1.3%) had secondary Paget and 12/78 (15.4%) had unknown status. The overall *HER2* amplification was positive by IHC (17/78, 21.8%) and FISH (4/11, 36.4%), negative by IHC (40/78, 51.3%) and FISH (6/11, 54.5%) and equivocal by IHC (21/78, 26.9%) and FISH (1/11, 9.1%). CMA results from 29 cases were of sufficient quality. A total of 4 (4/29, 13.8%) cases showed copy number gain of the *HER2* region (17q12) compatible with amplification (copy number > 4). *HER2* amplification status did not correlate with tumor invasiveness or recurrence rate.

Conclusions: *HER2* amplification was identified in between 13.8 and 36.4% of cases as assessed by IHC, FISH and CMA. FISH and CMA showed similar rates of amplification, although the comparison is difficult due to the absence of strict amplification criteria in CMA. These results suggest that *HER2* amplification is a relatively common abnormality and testing combined with targeted therapy should be studied.

1160 Utility of HPV E6 and E7 mRNA in situ Hybridization in Diagnosing Cervical Low-Grade Squamous Intraepithelial Lesion (LSIL)

Bin Zhang[1], Jianhui Shi[1], Haiyan Liu[1], Robert Monroe[2], Fan Lin[1]
[1]Geisinger Medical Center, Danville, PA, [2]Advanced Cell Diagnostics, San Mateo, CA

Disclosures: Bin Zhang: None; Jianhui Shi: None; Haiyan Liu: None; Robert Monroe: *Employee*, Bio-Techne; Fan Lin: None

Background: Overdiagnosis of LSIL is a common problem encountered in many surgical pathology laboratories. p16, a highly sensitive immunohistochemical marker in confirming a diagnosis of cervical high-grade squamous intraepithelial lesion (HSIL), lacks sensitivity in diagnosing LSIL. A similar issue has been reported with human papilloma virus (HPV) deoxyribonucleic acid (DNA) in situ hybridization (ISH). Limited data in the literature demonstrate that detection of HPV on cervical biopsies using a new generation of messenger ribonucleic acid (mRNA) ISH is promising (AJ Mills, AJSP, 2017). In this study, we investigated the utility of HPV mRNA ISH in the diagnosis of LSIL.

Design: Seventy-nine consecutive cervical biopsy cases were retrieved from the surgical pathology archives, including LSIL (N=48), HSIL (N=10), and benign/reactive (N=21). Available Pap smears and HPV DNA testing results for these cases were reviewed. RNA ISH using a cocktail of 18 high-risk (HR) HPV (16, 18, 26, 31, 33, 35, 39, 45, 51, 52, 53, 56, 58, 59, 66, 68, 73, and 82) and 6 low-risk (LR) HPV (6, 11, 40, 42, 43, and 44) mRNA probes (Advanced Cell Diagnostics) was performed on these cases using a Leica Bond III staining platform. The staining results were recorded as negative (no staining) or positive (nuclear and cytoplasmic dot-like staining). The positive staining results were further classified into 1) proliferative pattern (full-thickness staining of atypical squamous epithelium); and 2) non-proliferative pattern (limited to the basal half of atypical squamous epithelium).

Results: Twenty-five of 48 LSIL cases (52%) were positive for HPV mRNA ISH, 13 cases with proliferative pattern and 13 cases with non-proliferative pattern (Fig). Of the 25 HPV ISH-positive cases, one case was positive for both HR and LR HPV, and two cases were positive LR HPV only. Three of 21 benign/reactive cases (14%) were positive for HR HPV, 2 cases with proliferative pattern and 1 case with non-proliferative pattern. Ten of 10 HSIL cases (100%) were positive for HR HPV, 9 cases with proliferative pattern and 1 with non-proliferative pattern. The results of HPV DNA testing and HPV mRNA ISH for the LSIL group are summarized in Table 1.

Table 1. HPV mRNA ISH and HPV DNA Testing Results on the LSIL Group

LSIL Group	No Cases	HPV DNA Testing Results			HPV RNA ISH Positive	
		Positive	Negative	N/D	18 HR	6 LR
RNA ISH - Positive	25	20	2	3	23*	3*
RNA ISH - Negative	23	15	5	3	0	0
Total Cases	48	35	7	6	23	3

*One case was positive for both HR and LR HPV by RNA ISH; N/D – Not done

Figure 1 - 1160

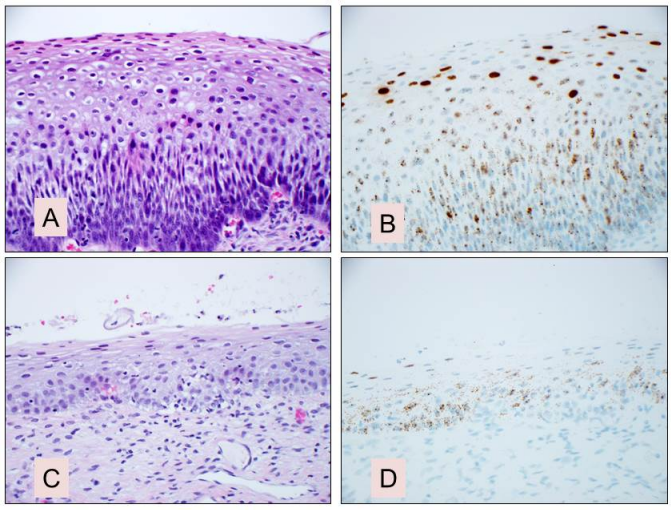

Figure A-D showing a typical LSIL (A) positive for HR HPV mRNA ISH with proliferative pattern (B); and squamous atypia/LSIL (C) also positive for HR HPV mRNA ISH with non-proliferative pattern (D).

Conclusions: These data demonstrate 1) HPV mRNA ISH is a highly sensitive method of detecting HPV; 2) a significant percentage of LSILs were over-diagnosed; 3) a small portion of LSILs were under-diagnosed; and 4) HPV mRNA ISH should be routinely performed when a morphological diagnosis of LSIL is questionable.

1161 Histological Features not Included in the Chemotherapy Response Score for Ovarian/Fallopian Tube/Peritoneal High Grade Serous Carcinoma, Are They Relevant?

Yanping Zhong[1], Barrett Lawson[1], Anais Malpica[1], Elizabeth Euscher[1], Preetha Ramalingam[2], Nicole Fleming[1], Anil Sood[1], Jinsong Liu[1]
[1]The University of Texas MD Anderson Cancer Center, Houston, TX, [2]Houston, TX

Disclosures: Yanping Zhong: None; Barrett Lawson: None; Anais Malpica: None; Elizabeth Euscher: None; Preetha Ramalingam: None; Nicole Fleming: None; Anil Sood: *Grant or Research Support*, M-Trap; *Major Shareholder*, Biopath; *Advisory Board Member*, Kiyatec; Jinsong Liu: None

Background: The chemotherapy response score (CRS) for reporting on post neoadjuvant chemotherapy (NACT) ovary/fallopian tube/peritoneal high grade serous carcinoma (HGSCa) mainly focuses on fibroinflammatory changes, pattern of invasion and size of largest focus of residual tu (tu). However, there are other histological features (HF) that are not included in the three-tier CRS. The aim of this study was to assess if these HFs correlated with CR in post NACT HGSCa.

Design: 103 cases of advanced stage HGSCa (2005- 2017) status post NACT were retrieved. The HFs listed in Table 1 and the three-tier CRS were evaluated in omental (OM) and adnexal (AD) sections independently by two pathologists. A semiquantitative score was used for the HFs, except for pattern of tu infiltration: 0-1, no or minimal presence (<5%); 2, focal occurrence (5-50%); 3, widespread occurrence (>50%). Pattern of tu infiltration was scored as 1+, large confluent tu mass(es); 2+, multiple small tu foci; 3+, scattered tu cells or complete absence of tu. HFs and CRS were compared by the Kruskal-Wallis test.

Results: Of the 103 cases, 26 (25.24%), 63 (61.17%), and 14 (13.59%) had a CRS of 1, 2, and 3, respectively. Table 1 shows the HFs and their correlation with CRS. Giant tu cells (mononuclear or polyploid giant cells), the pattern of tu infiltration, and tu necrosis showed significant correlation with CRS (p=0.0125, p<0.0001, and p=0.0237, respectively). CRS showed no significant correlation with eosinophilic cytoplasm with vacuolization (p=0.2966); oncocytic change (p=0.1723); fibrosis (p=0.07); foamy histiocytes (p=0.1423), and inflammatory cells (p=0.4712).

Table1. Histological Features and Their Correlation with CRS

Histological Features	HF Score	CRS 1	CRS 2	CRS 3	*p* value
Giant tu cells	0-1	19 (27.1)	41 (58.6)	10 (14.3)	0.0125
	2	7 (31.8)	15 (68.2)		
	3		7 (63.6)	4 (36.4)	
Pattern of tu infiltration	1+	25 (62.5)	26 (62.5)	4 (10.0)	<.0001
	2+	1 (1.7)	52 (88.1)	6 (10.2)	
	3+			3 (100)	
Necrosis	0-1	17 (20.2)	54 (64.3)	13 (15.5)	0.0237
	2	4 (36.4)	6 (54.5)	1 (9.1)	
	3	5 (62.5)	3 (37.5)		
Eosinophilic cytoplasm with vacuolization	0-1	21 (24.7)	51 (60.0)	13 (15.3)	0.2966
	2	4 (23.5)	12 (70.6)	1 (5.9)	
	3	1 (100)			
Oncocytic change	0-1	20 (25.3)	47 (59.5)	12 (15.2)	0.1723
	2	6 (26.1)	16 (69.6)	1 (4.3)	
	3			1 (100)	
Foamy histiocytes	0-1	16 (31.4)	30 (58.8)	5 (9.8)	0.1423
	2	8 (19.5)	28 (68.3)	5 (12.2)	
	3	2 (18.2)	5 (45.5)	4 (36.4)	
Fibrosis	0-1	21 (26.6)	50 (63.3)	8 (10.1)	0.07
	2	4 (23.5)	11 (64.7)	2 (11.8)	
	3	1 (14.3)	2 (28.6)	4 (57.1)	
Inflammatory cells	0-1	10 (26.3)	24 (63.2)	4 (10.5)	0.4712
	2	13 (26.5)	30 (61.2)	6 (12.2)	
	3	3 (18.8)	9 (56.3)	4 (25.0)	
Calcification/psammoma bodies	0-1	22 (31.0)	41 (57.7)	8 (11.3)	0.1274
	2	3 (13.0)	16 (69.6)	4 (17.4)	
	3	1 (11.1)	6 (66.7)	2 (22.2)	
Desmoplasia	0-1	14 (26.9)	26 (50.0)	12 (23.1)	0.1383
	2	9 (32.1)	19 (67.9)		
	3	3 (13.0)	18 (78.3)	2 (8.7)	
Hemosiderin deposition	0-1	22 (28.2)	44 (56.4)	12 (15.4)	0.3784
	2	4 (17.4)	18 (78.3)	1 (4.3)	
	3		1 (50.0)	1 (50.0)	

Conclusions: Increased giant tu cells, pattern of tu infiltration, and absence/minimal necrosis correlated with a better CRS in post NACT ovarian/fallopian tube/peritoneal HGSCas. The amount of giant tu cells and necrosis should be considered when grading chemotherapy response.